THE DESIGN AND CHARACTERISATION OF BIOMIMETIC ARTIFICIAL RECEPTORS BASED ON MOLECULAR IMPRINTING TECHNOLOGY

Keith Farrington

School of Chemical Sciences,
Dublin City University

Thesis submitted for the award of

PhD

May 2007

Declaration

I hereby certify that this material, which I now submit for assessment on the programme of study leading to the award of PhD is entirely my own work and has not been taken from the work of others save and to the extent that that such work has been cited and acknowledged within the text of my own work.

Signed: Keith Farrington

ID No: 96063483

Date: 17-09-2007

Acknowledgements

Firstly, I would like to thank my supervisor Dr. Fiona Regan for all her help and encouragement and for the travel opportunities afforded to me which was an integral part of this work.

I would like to express my gratitude to Prof. Boris Mizaikoff who allowed me to spend time with his group in Georgia Tech and to the members of his group for their friendship and for making my time in Atlanta so enjoyable, in particular thanks to Dan Menasha who helped with the Amber studies.

I would also like to thank Dr Andrew Mayes UEA, Norwich for lending his expertise regarding the suspension polymerisation and Dr. Edmond Magner, University of Limerick for allowing me to use equipment in his lab.

I also appreciate the help given to me by all members of the technical staff in the School of Chemical Sciences at DCU.

Finally I would like to thank my co-workers and friends from DCU who helped in so many ways both academic and non-academic and made my time what it was. Thanks to Yuliya, Gill, Michael, Frank, Li, Emma, Áine and everyone else I met in DCU 2003-2007.

And thanks to Steph for being there.

TABLE OF CONTENTS

Glossary

α	Selectivity factor
Å	Angstrom
AA	Acrylamide
ACN	Acetonitrile
AIBN	2,2-Azobisiosbutyronitrile
AMBER	Assisted model building with energy refinement
APTES	Aminopropyl triethyl silane
BET	Brunauer-Emmet-Teller
$CDCl_3$	Deuterated chloroform
CD_3CN	Deuterated Acetonitrile
$CHCl_3$	Chloroform
CEC	Capillary Electrochromatography
CS	Computer simulation
CTL	Control
DMF	Dimethylformamide
DMSO	Dimethylsulfoxide
EGDMA	Ethylene Glycol Dimethacrylate
FLD	Fluorescence detector
FTIR	Fourier Transform Infrared
GC	Gas Chromatography
HEMA	Hydroxymethacrylate
HOAc	Acetic Acid
HPLC	High Performance Liquid chromatography
k'	Capacity factor
MAA	Methacrylic acid
MAM	Methacrylamide
MeOH	Methanol
MC	Monte Carlo simulation method
MD	Molecular Dynamics
MIP	Molecularly Imprinted Polymer
MISPE	Molecularly Imprinted Solid phase Extraction
MHz	MegaHertz
MS	Mass Spectrometry/Spectrometer

MTX	Methotrexate
NMR	Nuclear magnetic Resonance
nm	nanometers
NMP	1-methyl-2-pyrrolidone
ns	nanosecond ($1x10^{-9}$ s)
NSAID	Non-steroidal anti-inflammatory drug
NZL-Glu-OH	N Protected Glutamic acid
pH	$-\log_{10}$(concentration of H^+ ions)
p*K*a	$-\log_{10}$(acid dissociation constant)
PDB	Protein Data Bank
ppb	Part per billion
PTMOS	Phenyltrimethoxysilane
PFDMC	Perfluoro-(1,3-dimethylcyclohexane)
ppm	Part per million
PPC	Pre-Polymerisation Complex
ps	Picosecond ($1x10^{-12}$ s)
RI	Retention Index
SEM	Scanning Electron Microscopy
SPE	Solid Phase Extraction
TEOS	Tetraethoxysilane
TFMAA	trifluoromethacrylic acid
TMOS	Tetramethoxysilane
THF	Tetrahydrofuran
t_r	Retention time
TRIM	Trimethylolpropane trimethacrylate
µm	Micrometer
UV	Ultra violet
2VP	2-Vinylpyridine
4VP	4-Vinylpyridine
VWD	Variable Wavelength Detector

Chapter 1

Literature survey

1.1 Biomimetics, synthetic receptors and MIPs

Within the field of synthetic receptors, biomimetic (or biologically inspired) properties are engineered by mimicking motifs found in nature. The ability of many biomolecular receptors to selectively recognise and bind specific substrates is a key process essential to every biological system. For biological systems, specific recognition by molecular receptors usually occurs via the formation of non-covalent bonds. Subsequently, selective recognition of a guest molecule is the highest desirable property of receptor mimics and artificial antibodies. The synthesis of artificial recognition systems does have advantages over antibodies. While antibodies are used in a wide variety of analytical applications, they are costly and have a comparatively short shelf life. The highest aim of molecular imprinting is the generation of biomimetic recognition elements containing synthetic receptor sites capable of selective template binding with similar affinity to enzyme-substrate or antibody antigen interactions.

1.2 The scope of this work

Molecularly imprinted non-covalent templating techniques rely on the nature and stability of the complex formed between the template and functional monomer building blocks prior to radical polymerisation. Essentially this controls the amount of high affinity binding sites and binding site distribution obtained within the resultant imprinted polymer. Hence, a molecular level understanding of the types of interactions responsible for complex formation and complex stability during the formation of the PPC are critical for rational understanding and development of designed biomimetic recognition materials. Furthermore, knowledge of the strength of interaction and complex stoichiometry can be used for further development of components involved in imprinting as well as selection of the optimum monomers for a given template molecule. The aim of this thesis is to evaluate the events required for successful molecular imprinting. It is the objective of this work to assess the applicability and feasibility of using molecular modelling and ^{1}H NMR spectroscopy to characterise the pre-polymerisation solution inter-molecular processes at a molecular level for the pre-screening of components involved in the molecular

imprinting of a particular template analyte. Furthermore, resultant polymers are characterised physically to determine the effect of the chosen conditions on the morphology and capacity of the MIPs.

1.3 Molecularly imprinted polymers

There is always a need for more sensitive and selective analytical procedures. This is especially true in the pharmaceutical and environmental industries and in biomedical analysis, with an increasing number of analytes fast method development is required along with methods amenable to online utilisation. Presently, the majority of analytical methods for trace complex matrices are based on efficient sample enrichment and selective assays. One of the most promising and potential areas of analytical endeavour is that of molecular imprinting. Molecularly Imprinted Polymers (MIP's) have gained interest both as a novel type of sorbent with attractive properties and as chemical agents of high sensitivity and affinity, which are of considerable use in assay development [1].

As applied in the present work, the molecular imprinting is based on non-covalent self-assembly of the template with the functional monomer(s) prior to polymerisation. Imprinting of template molecules typically occurs by the polymerisation of functional and cross-linking monomers in the presence of a templating ligand [2]. The template-monomer system is chosen such that in solution, the imprint molecule complexes one or several functional monomers which then become spatially fixed in a solid polymer by the polymerisation reaction. The resultant imprints possess steric and chemical (spatial arrangement of complementary functionality) "memory" for the template. Hence, following removal of the imprint molecules, these imprints enable the polymer to selectively rebind the imprint molecule from a mixture. Figure 1.1 (below) shows a depiction of the basic principles of molecular imprinting.

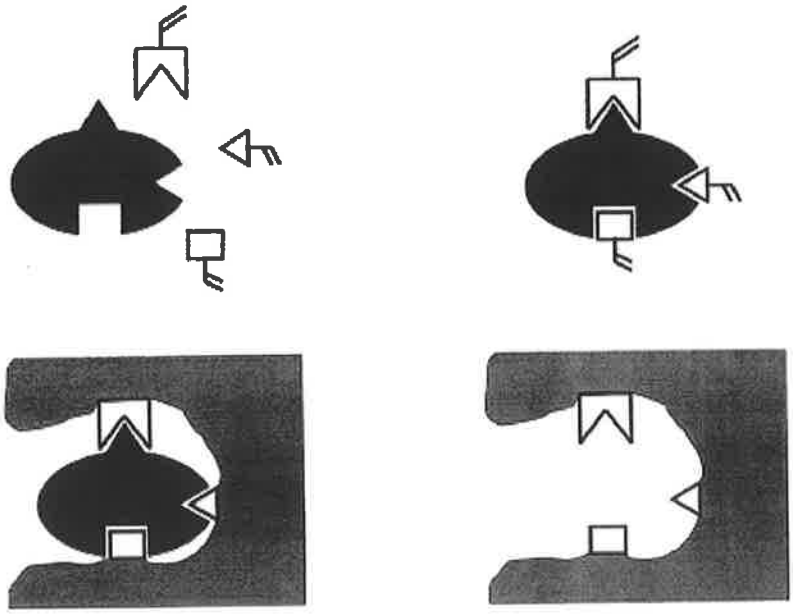

Figure 1.1: shows the schematic depiction of the preparation of molecular imprints. Reproduced from Andersson., [3]

Molecularly imprinted polymers then are synthetic polymers prepared in the presence of a template and the latter serves as a structure-directing agent for the formation of template-complementary binding sites. The ability of MIPs to rebind the template with high fidelity distinguishes them from the broader class of template synthesised nanostructured materials. Thus they can be programmed to recognise a large variety of target structures with antibody-like affinities and selectivities [4]. Mainly because of their robustness and ease of preparation, the materials are being studied in widely differing contexts encompassing solid phase extraction [5], sensors [6], enantiomer separations [7], ligand binding assays [8], drug discovery [9], drug delivery [10] and catalysis [11].

While the imprinting strategy appears simple and straightforward, application of imprinted polymers in analytical chemistry is still limited as in reality it offers templated materials with low yields of high affinity binding sites. Trial and error approaches for synthesis of MIPs for new target molecules follow already established imprinting protocols. More importantly however, a lack of rational understanding and tailoring of the molecular imprinting strategy has restricted the universal acceptance of MIPs [12]. An ever increasing volume of successful imprints reported in the

literature contrasts these considerations. In particular, ease of preparation along with superior chemical and mechanical properties render molecularly imprinted polymers an appealing alternative to natural receptors for a variety of applications. These range from analytical measurements to environmental clean up [13], toxin removal [14] and selective filtration [15]. Taking into account the above considerations, an in depth understanding of how MIPs work or why they might not work in certain applications appears vital to the future development and more widespread use of molecular imprinting techniques.

1.3.1 Approaches to molecular imprinting

Two principally different approaches to molecular imprinting can be distinguished. Briefly, these consist of the non-covalent, or self-assembly approach, where complex formation is the result of non-covalent or metal ion coordination interactions [16]. Secondly, there is the covalent, or pre-organised approach, which employs reversible covalent bonds, usually, involving a prior chemical synthesis step to link the monomers to the template [17]. It is generally perceived that non-covalent imprinting is more flexible in the range of chemical functionalities, which can be targeted, and thus the range of template that can be used. Covalent imprinting however yields better-defined and more homogenous binding sites [17]. The former though is much easier practically, since complex formation occurs on mixing template and monomers in solution prior to polymerisation.

1.3.2 Background to the theory of MIP binding

The most common procedures for the synthesis of MIP's have been reviewed in detail [18-20] (and references contained therein). Single or multiple interactions of functional groups with template functionalities can describe the interaction between the analytes/template molecules and the monomers. The types of interaction can include hydrogen bonds, ion pairing, π-π interactions or can be based on hydrophobic interaction. The selection of the monomer(s) is based on the generation of these particular interactions. This implies that polymers will always interact with the analyte or template molecule as well as with compounds that contain functional

groups similar to those of the template. The analyte affinity increases with the number of interacting groups [21]. However, each individual interaction may be strongly dependent on the properties of the solvent e.g. protic or aprotic, polarity, dielectric constant or the presence of complex forming agents [22,23]. These effects can occur through interaction with the polymer, the analyte or both. This implies that affinities can vary from zero to nanomolar equilibrium dissociation constants. Therefore the application of MIPs appears to have potential for the range of analytical applications noted above.

It is assumed that a change in selectivity of MIPs in comparison to non-imprinted polymers can only occur when the analyte and/or the matrix components of the sample have an increased number of two or more points of interaction [24]. Therefore (individual and) dual point interactions that take place between the analyte and the polymer will affect the selectivity. In other cases the interactions of analytes and matrix components with non-imprinted parts of a polymer may overshadow the interactions of the analyte with the true imprint so that the selectivity is not as good as required for the application, irrespective of the imprinting efficacy. The number of binding sites present in the polymer that play a role in the selective interaction of the analyte with the imprint (cavity) is typically less than 1% but can rise to 35% of the theoretical maximum number of binding sites [20]. Therefore the impact of both the selective (imprinted part of the polymer) and the non-selective (non-imprinted part of the polymer) interactions on the applicability of imprinted polymers in different analytical techniques is vital to their design and success.

1.3.3 Imprinting Matrices and Target Molecules

Presently, the majority of papers on MIPs describe organic polymers synthesised from vinyl or acrylic functional monomers by radical polymerisation and using non-covalent interactions. This can be attributed to the straightforward synthesis of these materials and to the vast choice of available monomers with different functional groups. They can be basic e.g. vinylpyridine or acidic e.g. methacrylic acid, permanently charged e.g. 3-acrylamidopropyltrimethylammonium chloride, hydrogen bonding e.g. acrylamide, hydrophobic e.g. styrene metal containing etc. These

functional monomers are sometimes considered analogues to the twenty amino acids that constitute the building blocks of proteins. These simple monomers have association constants with the template that are too low for the formation of a stable complex. In the final polymer though, the formation of several simultaneous interactions and a favourable entropy term normally ensure tight binding of the target molecule. During non-covalent imprinting, functional monomers are generally used in excess to shift the equilibrium towards complex formation [25]. This results in some functional groups being randomly distributed throughout the polymer – one of the reasons for non-specific binding. Compared to proteins selected for the required recognition and binding properties through evolution, or, in the case of antibodies, clonal selection, this is a considerable drawback. Therefore somewhat more sophisticated monomers are being designed that form more stable interactions with the template molecule or substructures thereof or that can be used in stoichiometric ratios [25,26]. Sometimes it is seen as advantageous to prepare monomers that specifically target structural features of the template. In particular multiple hydrogen bonding regimes can enhance association constants and lead to more selective recognition sites. Tanabe *et al.* [27] prepared 2,6-*bis*-acrylamidopyridine as a complement to the cyclic imide functionality of the barbiturates, the concave H-bond donor–acceptor–donor configuration of the monomer matching the convex acceptor–donor–acceptor structure of the template. The related 2-(meth)acrylamidopyridines have also been prepared as complements to carboxylic acids [28] and [29]. Spivak and Shea [28] prepared a monomer based on the nucleotide base adenine as a complement to carboxylic acids.

Other organic polymers are sometimes used for imprinting that are better suited for a specific application or easier to synthesise in the desired form, for example, poly(phenylene) diamine [30] and overoxidised polypyrrole [31]. Imprinting is also possible in inorganic matrices e.g. sol-gels of silica [32]. The molecular imprinting technique can be applied to different kinds of target molecules ranging from small organic molecules e.g. pharmaceuticals [33], pesticides [34], amino acids [35] and peptides [36], nucleotide bases [37], steroids [38], sugars [39] to larger peptides [40] and some proteins [41,42]. However, the imprinting of large molecules such as polypeptides and proteins is still a challenge, necessitating specially adapted protocols. There have also been reports on imprinting using whole bacteria or yeast

cells [43] as templates. Figure 1.2 shows the most commonly used functional monomers used in molecular imprinting:

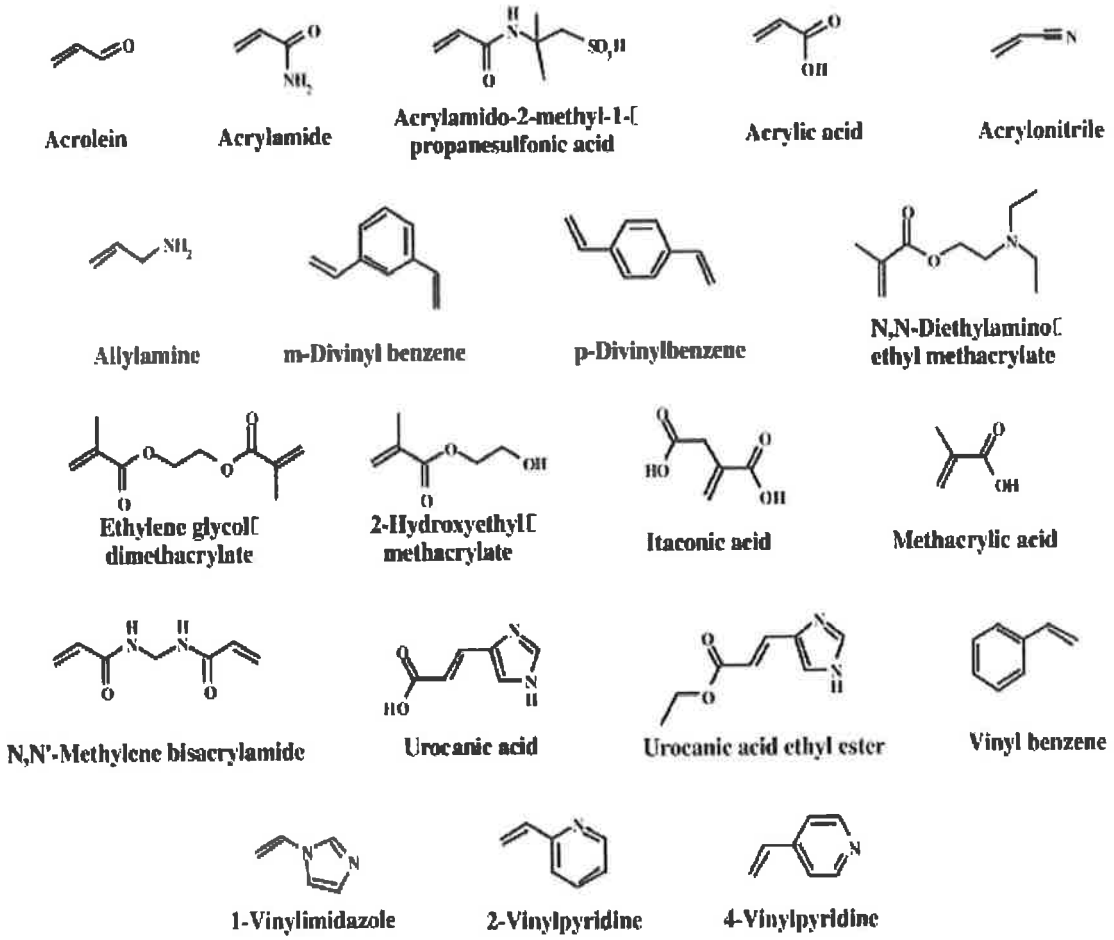

Figure 1.2 Structure of the functional monomers used in modelling and in polymer preparation. Reproduced from Karim *et al.*, [44]

Factors such as the polarity and hydrogen-bonding strength of the solvent and the polymerisation temperature will affect some interactions more strongly than others. In general, H-bonding interactions are favoured by low polarity solvents and lower temperatures whereas ion pair and other strong dipolar interactions are favoured by polar solvents. In practice a compromise between solvent polarity and solubility of the template usually needs to be made and the solvent also determines the structure and porosity of the imprinted resin [45]. This also places some constraints on the system. While there are many exceptions this usually limits the choice of solvent to a small list comprising chloroform, dichloromethane, acetonitrile, toluene and perhaps

tetrahydrofuran for predominantly hydrogen-bonded complexes. The potential for multiple sites of interaction between functional monomers and template in the pre-polymerisation complexes with multifunctional templates (see Figure 1.3 for some examples proposed in the literature) demonstrates the complexity of the system.

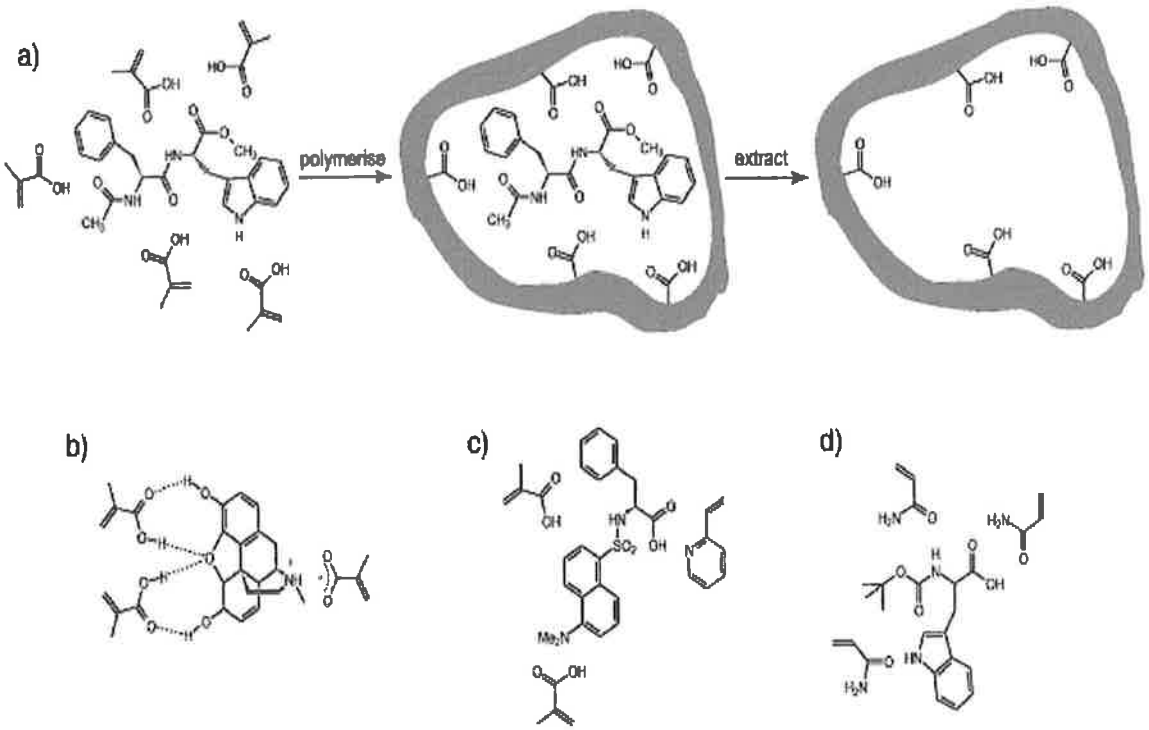

Fig. 1.3 (a) Non-covalent imprinting of a dipeptide derivative by multiple non-covalent interactions with methacrylic acid and the structure of some proposed non-covalent pre-polymerisation complexes for the imprinting of (b) morphine with methacrylic acid, showing H-bonding and ion pair interact (c) dansyl phenylalanine complexed with a mixture of 2-vinylpyridine and methacrylic acid, evidence from the recognition properties of the polymer suggest that the 2-vinylpyridine complexes with the template despite the presence of an acidic monomer and (d) t-Boc tryptophan with acrylamide, this monomer is electrostatically neutral and possesses H-bond donor and acceptor sites, its complexation properties are therefore similar to methacrylic acid but without the possibility of ion pair formation.

Reproduced from Mayes and Whticombe, [46] and references contained herein

1.3.4 Physical forms of MIPs

Traditionally, MIPs have been prepared as bulk polymer monoliths, a solid state macroporous material with large through pores, followed by mechanical grinding to obtain small micrometer sized particles [47]. The materials obtained through this method are still useful for certain applications; others require MIPs in defined physical forms for which specially adapted synthetic methods are required. For binding assays, small spherical particles of below μm size are particularly well suited, whereas in sensors the MIPs are often used in the form of thin layers or membranes. Another aspect is the synthesis of binding sites close to the polymer surface to avoid long response times and improve the steric accessibility of the sites. A method for the synthesis of MIP nanobeads by precipitation polymerisation [48] has been developed. This is performed with similar monomer mixtures as for bulk polymers, except that the relative amount of solvent present in the mixture is much higher. When polymerisation progresses, imprinted nanospheres or microspheres precipitate instead of polymerising together to form a polymer monolith. The method has the drawback that because of the dilution factor, higher amounts of imprint molecule are needed. The latter may be compensated for by the typically higher yields obtained. In these materials a statistically higher percentage of the binding sites should be accessible at the binding surface.

Approaches somewhat similar to the precipitation polymerisation mentioned above have also been employed [49,50]. However, instead of precipitated particles, soluble polymer microgels were produced. These had a molecular weight in the range of 10^6 g mol^{-1} that is in the same order of magnitude as proteins. Although microgels were readily obtained with optimised protocols, selectivity proved to be more difficult to achieve with this technique even though a covalent imprinting complex was used. Molecular imprinting is also possible inside dendrimers [51,52]. The method involved covalent attachment of dendrons to a porphyrin (the template) core, cross-linking of the end groups of the dendrons and removal of the porphyrin template by hydrolysis. This approach ensures nearly homogenous binding sites, quantitative template removal, the presence of only one binding site per molecule and solubility in common organic solvents. Figure 1.4 demonstrates the structure:

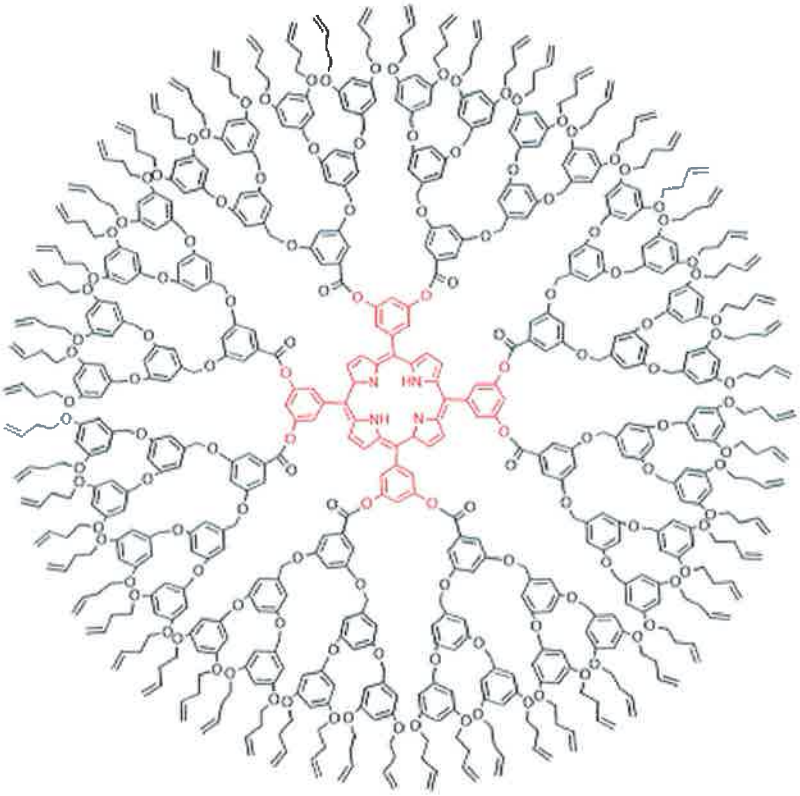

Figure 1.4: A dendrimer with cross-linkable double bonds at the outer shell and the covalently attached porphyrin template in the core. Reproduced from Zimmermann *et al* [52].

An interesting method of producing MIP beads is by suspension polymerisation [53-55]. Small imprinted beads are created based on emulsion polymerisation i.e. small beads are created from an oil in water biphasic system stabilised by a surfactant. The particularity of their protocol is that the template molecule (cholesterol) is part of the surfactant (pyridinium 12-(cholesteroloxycarbonyloxy)dodecane sulfate. This results in all binding sites being situated at the particle surface, which was demonstrated by flocculation experiments using PEG-bis-cholesterol. A procedure for producing surface binding sites in MIPs has also been produced. The imprint molecule is immobilised onto a solid support such as porous silica beads. Following polymerisation in the pores, the silica is removed by chemical dissolution. This leaves behind a porous polymeric structure. The binding sites are located at the surface of the polymer and are uniformly orientated.

1.3.5 Morphological considerations

Molecular level design of imprinted polymers can be made by establishing "tailor made" binding sites. Such design of imprinted polymers can mostly be done by selection of functional monomers. Basically the functional monomers are selected according to the functionality of a template molecule. They are bound with the template during the polymerisation process and a complementary binding site can be formed in the resultant polymer. MIPs can also be designed according to the environments of their use. A notable difference between antibodies and MIPs lies in the fact that MIPs are classified as cross-linked organic polymers generally insoluble in common solvents and for practical use, MIPs need to be prepared in a desirable form for applications. Here, a macro-morphology design appears to be an important matter in terms of the eventual application of the MIP. *In situ* molecular imprinting can be defined as a technique for preparing imprinted polymers in a place where the polymers are subsequently utilised. They therefore require no subsequent treatment of the resultant polymer, except washing to extract the template and can be directly used for subsequent analyses. There are three major areas of this approach:

(i) Preparation in a column tube for chromatographic or SPE use;
(ii) Preparation in a capillary for capillary electrophoresis and
(iii) Preparation in a vial for batch use. These *in situ* approaches utilise polymer rods, dispersion polymers and polymer coats respectively.
(iv) Thin films on sensor surfaces

It is also likely that the *in situ* method would be useful for designing a molecular imprinting system (optimum morphology) and helpful for mechanistic studies of molecular imprinting and recognition. Thus advances in the basics and applications of molecular imprinting can be expected by the utilisation of this technique. Recently, new synthetic conditions to obtain MIP beads with controllable size in the nano- to micro-meter range, using racemic propranolol as a model template have been employed by Haginaka *et al.*, [56]. Variation of the composition of the cross-linking monomer allowed the particle size of the MIP beads to be altered in the range of 130 nm to 2.4 μm, whereas the favourable binding property of the imprinted beads

remained intact. The chiral recognition sites were further characterized with equilibrium binding analysis. Compared to previously reported irregular particles, the chiral selectivity of competitive radioligand binding assays developed was increased by six to seven folds in an optimized aqueous solvent. Figure 1.5 shows examples of the beads obtained by the method of Yoshimatsu *et al.* [57]. This study shows the system specific nature of imprinted polymers however as there is no functional reason as to why speerical or beaded polymers should outperform irregularly shaped particles in this regard. Contrast [57] with references [88,89] on page 25 of this thesis where the irregularly shaped particles are shown to be superior. Indeed this points to the morphology of the polymer itself and its resultant "template access characteristics" being critical in MIP performance.

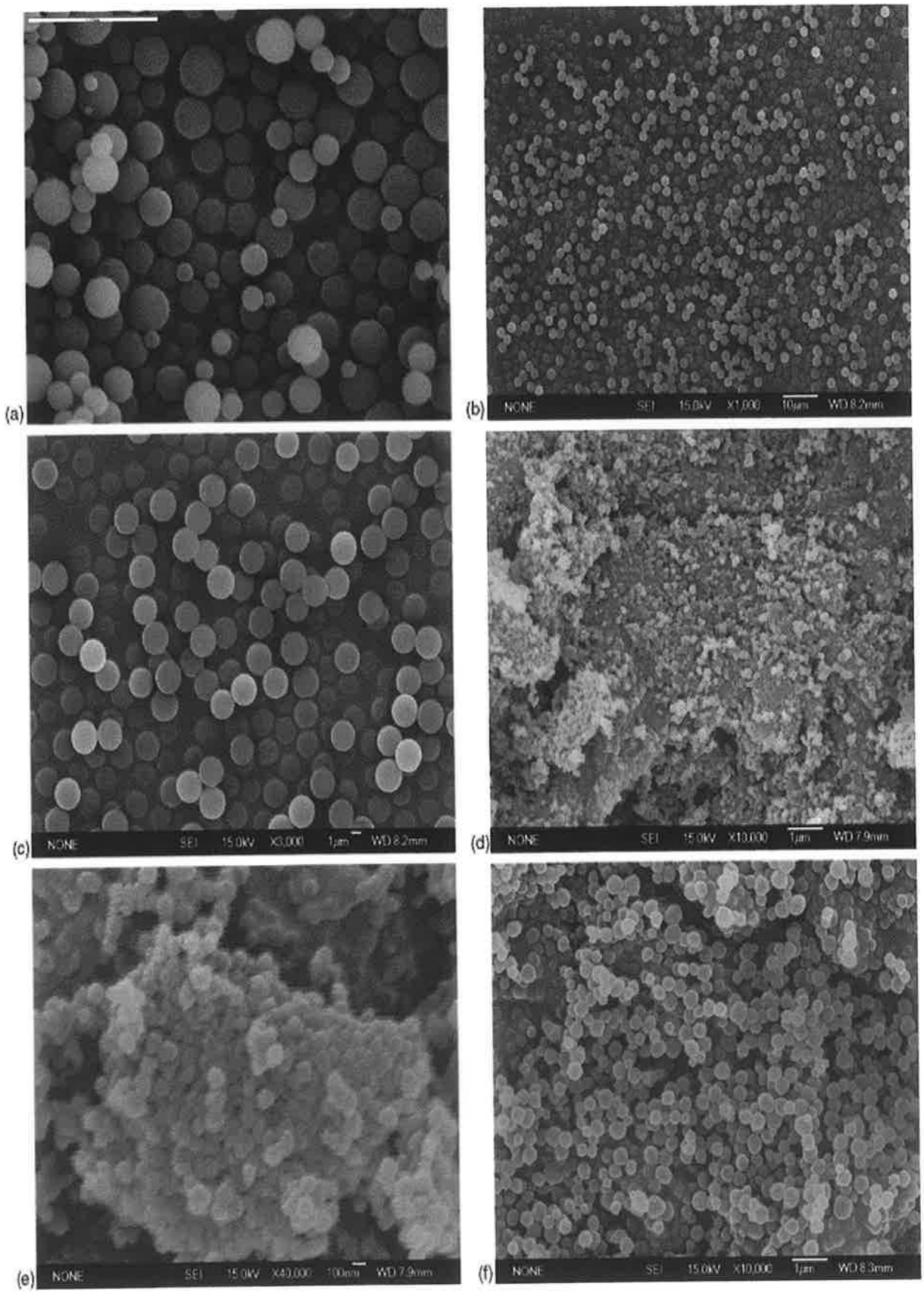

Figure1.5 Beads obtained by the method of Yoshimatsu. Reproduced from [57]

1.4 Non-covalent molecular imprinting

1.4.1 Covalent versus non-covalent

The covalent approach to molecular imprinting promises the most homogenous binding site distribution with largely identical binding pockets. The binding constants for the template molecule are high, since the interaction between the template and functional monomer is based on covalent interactions that can withstand polymerisation conditions [46]. A chemical synthesis step is necessary to bind the template to the functional monomer with bond types such as Schiff bases, boronates, ketals, carboxylic amides and esters. However, despite the high affinities of the polymeric material, the range of functional groups that can be targeted is restricted and removal of the template molecules is not straightforward (chemical cleavage). This limits the application of covalently prepared MIPs. Furthermore, slow binding kinetics restricts the analytical application of covalent MIPs, if rebinding is based on reversible covalent bonds. Alternatively, in the semi-covalent approach rebinding occurs via non-covalent interactions taking advantage of faster rebinding kinetics.

In non-covalent molecular imprinting, complexes assembled by non-covalent interactions are formed in the pre-polymerisation mixture. Complexation is achieved by mixing template, functional monomer and cross-linker in a porogenic solvent matrix. As a consequence, sufficient complex stability is required to enable binding pocket formation during the polymerisation process. In contrast to covalent imprinting, the self-assembly approach is characterised by a more heterogeneous binding site distribution. Resulting sample overload may occur due to rapid saturation of the comparatively low amount of high affinity binding sites causing decreased overall polymer performance [58]. Despite this drawback, simple preparation procedures, the wide range of imprintable compounds and reversible host guest binding based on non-covalent interactions (biomimetic binding) render the non-covalent approach the most widely employed method for MIP preparation. Given its versatility and closest resemblance to naturally occurring recognition mechanisms, the discussion for the remainder of this study will focus on non-covalent imprinting. It has been stated [59], that the extent of complexation governs the recognition

properties of the imprinted polymer. It has also been reported by Andersson *et al.*, [60], that that approximately 0.3% of template molecules and 0.6% of functional monomer successfully form complexes in pre-polymerisation mixtures. The systems studied in this work were three MIP-template systems, namely, *N*-acetyl-L-phenylalaninyl-L-tryptophanyl methyl ester, yohimbine and cinchonidine. These templates were imprinted with MAA as functional monomer and EGDMA as cross linker. Evidently the above statements summarise conditions that would appear to be less favourable for the development of a successful imprint by non-covalent means. Again this demonstrates the system specific nature of MIP recognition and not all systems an be generalised.

1.4.2 Problems associated with non-covalent molecular imprinting

When a suitable guest molecule fits the internal cavity of a spatially complementary host structure numerous events occur leading to optimal binding conditions. Bond spatial fixation, coordination (self-assembly involving coordination chemistry) and molecular recognition are the main factors in this process. In the molecular recognition event, spatial (size/shape) and chemical (functional groups) factors play a crucial role. Similar to host-guest interactions, molecularly imprinted polymers provide receptor sites that selectively recognise and rebind the analyte of interest (template). The performance of the MIP will depend on both the quality and quantity of the spatial arrangement of the binding cavities and the binding sites [61]. Therefore, a higher amount of interaction sites involved in recognition will enhance the selectivity of a receptor between similar substrates [62]. Additionally, a 3-dimensional cavity with multiple interaction sites will show enhanced binding to its template. Figure 1.6 shows the postulated representation of binding sites in heterogeneous imprinted polymers

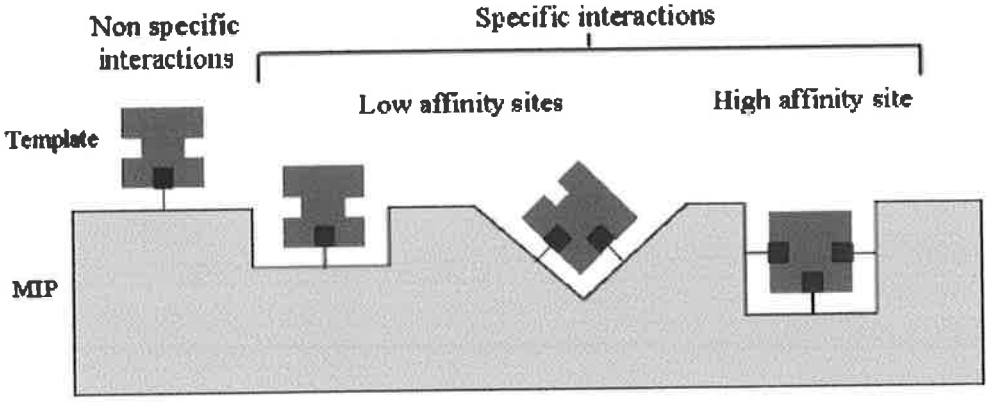

Figure 1.6 Postulated representation of binding sites in heterogeneous imprinted polymers. Reproduced from Karim *et al.*, [44]

A serious drawback with the non-covalent self-assembly approach is the formation of a heterogeneous distribution of binding site affinities. A very small number of these will exhibit high affinity for the analyte. Therefore, two issues need to be considered. Firstly, if the binding constant is too high, the guest molecule will block the binding site and will prevent further binding of other molecules to the binding site. Secondly, if the binding constant is too low, the MIP will not demonstrate selective recognition. A simple analysis of these considerations leads to the conclusion that without a knowledge of and control over the intermolecular forces involved in the self-assembly process, no reliable indications on structure and properties of the pre-polymerisation complex and hence the recognition properties of the MIP can be made.

Studies by both Baggiani *et al.*, [63] and Spivak *et al.*, [64] have shown evidence for shape selectivity in rebinding MIPs generated by non-covalent methods. This has been performed using probes analogous to the template but differing in size or spatial distribution. In the self-assembly approach, the cross linker may be a third component influencing the properties of the formed pre-polymerisation complex. Ultimately, it is the strength of the different possible configurations of each complex that will determine the ability of the complex to withstand the polymerisation process, particularly at elevated temperatures. The polymerisation process itself will result in the formation of the binding cavities and the arrangement of the functional groups within the cavities. Subsequently, it is expected that polymers will be formed that contain a heterogeneous binding site distribution will be formed with affinity

distributions ranging from high affinity for the template to weak non-specific binding to the cross linked polymer matrix. Reports on the nature of MIP recognition range from binding that occurs in vacant cavities to interaction with residual template molecules [65,66] (co-operative molecules).

1.4.3 Molecular interactions in non-covalent imprinting

Hwang *et al.*, [67] have investigated the chromatographic characteristics of cholesterol-imprinted polymers prepared by semi-covalent(generation of MIP by covalent chemistry but rebinding under non-covalent conditions) and non-covalent imprinting methods. The covalently prepared MIP was found to have a higher adsorption capacity for cholesterol and about five-fold higher chromatographic efficiency for cholesterol separation, in comparison with the non-covalently prepared MIP. The use of covalent imprinting significantly reduced the peak broadening and tailing. This advantage along with constant retention suggests that the covalently prepared MIP has potential for quantitative analysis. Two important drawbacks of the non-covalent method are lower adsorption capacity and heterogeneous binding site affinity distributions [68].

Numerous intermolecular forces can contribute to non-covalent formation of the PPC. The major elements are hydrogen bonding with energies in the range of 4-60 kJ/mol [69, 70, 71]. This is classed as a weak to medium interaction. Hydrophobic effects can also play significant roles in imprinting, particularly when imprinting in aqueous systems. Weaker than hydrogen bonding, typical energies are 1-3 kJ/mol [69]. One of the strongest types of interaction is ion-ion with energies greater than 250kJ/mol [69,70]. π-π stacking interactions energies can vary significantly from 1-50 kJ/mol [70]. Other interactions include dipole-dipole and attractive van der Waals forces. Both of these interactions are considered weak with interaction energies less than 10-15 kJ/mol [69,70,71].

In addition, Coulombic attraction, charge transfer induction, dispersion and exchange-repulsion contribute to complex formation. Hydrogen bonding then is a relatively strong interaction that participates in naturally occurring non-covalent interactions [72] such as occur between molecules that have a permanent net dipole resulting from

hydrogen being covalently bonded to fluorine, oxygen or nitrogen. For example, hydrogen bonds operate between water (H_2O) molecules, ammonia (NH_3) molecules, hydrogen fluoride (HF) molecules, hydrogen peroxide (H_2O_2) molecules, alkanols (alcohols) such as methanol (CH_3OH) molecules, and between alkanoic (carboxylic) acids such as ethanoic (acetic) acid (CH_3COOH) and between organic amines such as methanamine (methyl amine, CH_3NH_2). Hydrogen bonds are a stronger intermolecular force than either Dispersion forces or dipole-dipole interactions since the hydrogen nucleus is extremely small and positively charged and fluorine, oxygen and nitrogen being very electronegative so that the electron on the hydrogen atom is strongly attracted to the fluorine, oxygen or nitrogen atom, leaving a highly localised positive charge on the hydrogen atom and highly negative localised charge on the fluorine, oxygen or nitrogen atom. This means the electrostatic attraction between these molecules will be greater than for the polar molecules that do not have hydrogen covalently bonded to fluorine, oxygen or nitrogen.

In general, these interactions are favoured in weakly polar aprotic solvents such as acetonitrile or DMF. In contrast, polar protic solvents support interactions such as metal ion co-ordination of the template molecule. Comparatively weak interactions such as π-π stacking may occur in polar aprotic solvents and in water. Hydrophobic interactions are facilitated in highly polar solvents or solvent mixtures such as water/methanol. The molecular modelling study by Liu *et al.*, [73] has indicated possible conformations for hydrogen bonded arrangements of template and functional monomer. One such arrangement is depicted below in figure 1.7.

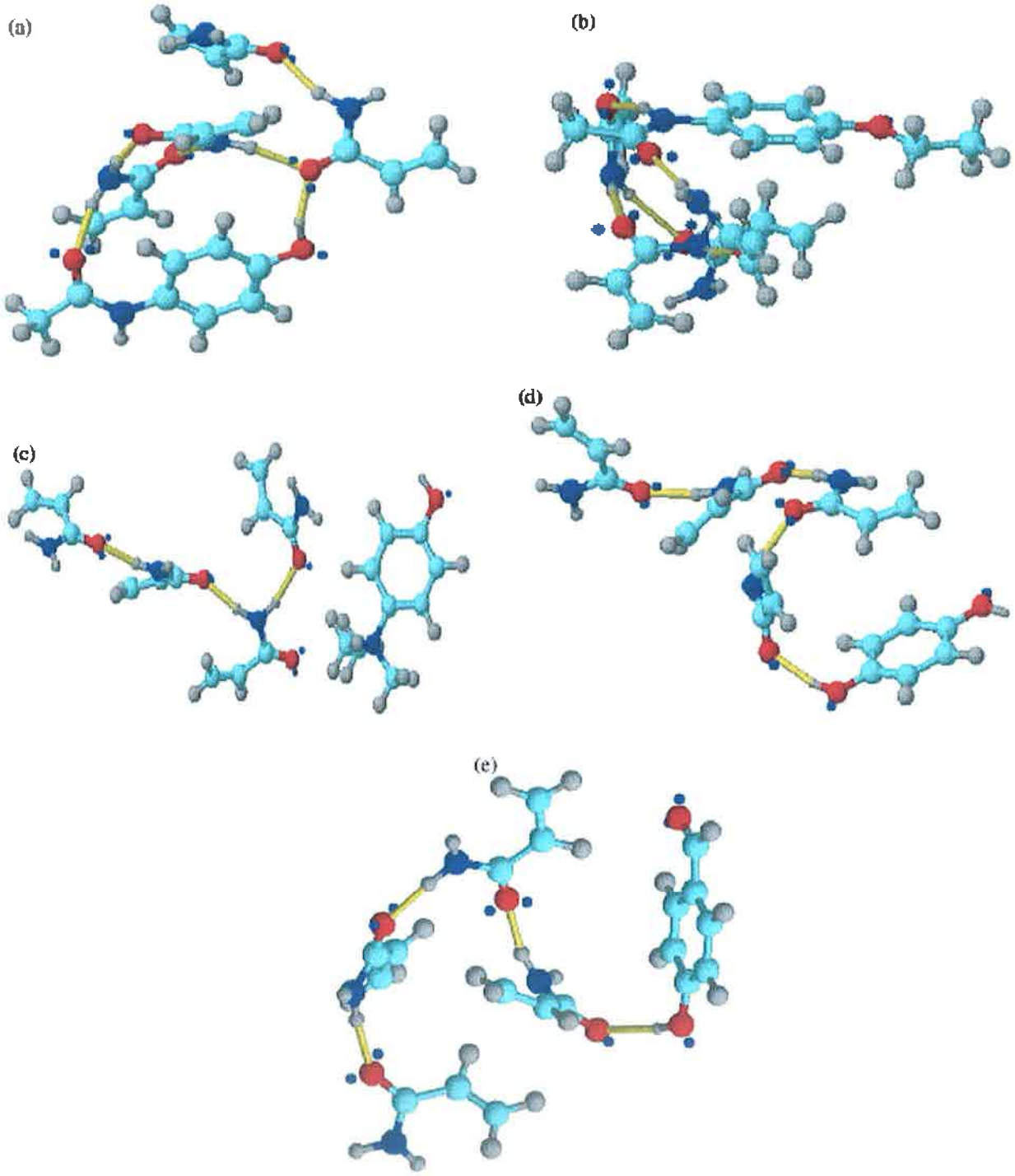

Figure 1.7 some typical conformations of paracetamol or analogues interacting with AAM: (a) paracetamol; (b) phenacetin; (c) *p*-tertiary butylphenol; (d) *p*-benzenediol; (e) 4-hydroxybenzaldehyde. Reproduced from Liu *et al.*, [73].

1.4.4 Solvating the pre-polymerisation complex

Three major characteristics regulate the choice of the solvent (porogen) to be used in conjunction with the polymerisation process:

(i) The ability to solubilise the constituents;
(ii) The effects on complex formation between the template and monomer(s) and
(iii) The effects on porosity and surface area of the resultant polymer.

Besides affecting the morphology of the polymer produced, the solvent properties control the type and strength of the non-covalent interactions. An enhanced appreciation of these processes enables control of the recognition efficiency of the resulting MIP by appropriate selection of the solvent matrix and tuning of its dielectric properties. In general, optimum recognition occurs in the same solvent that was used as the porogen. However, MIPs prepared in aprotic solvents have also demonstrated recognition in aqueous conditions [74,75]. Jodlbauer *et al.*, [76], observed complementary substrate selectivities/affinities in aprotic and polar solvents. The possibility of solvent-dependent tuning of substrate selectivity/affinity and the high binding capacity recommend the developed MIPs as promising solid-phase extraction adsorbents for clean-up and pre-concentration of Ochratoxin A (OTA) from various biologically relevant matrices. A MIP has bee prepared using the polar aprotic solvent DMSO [77] for the recognition of enalapril and lisinopril. Here it was shown that imprinting in DMSO rather than methanol produced a higher imprinting efficiency.

The capability of operating in aqueous environments and organic solvents is an advantage of MIPs compared to natural receptors. Despite this fact, exchanging the non-polar organic solvent environment used during the polymerisation process for a polar aqueous environment during rebinding usually leads to a loss of the interactions favoured in the non-polar solvents. Subsequently this leads to deterioration in MIP performance. Efforts at imprinting in highly polar and aqueous conditions have been performed [78,79]. Imprinting under aqueous conditions would allow maintaining the

same conditions during the rebinding step and most importantly, operating in aqueous environments allows the imprinting of biomolecules. Typically, when the intended use of the polymer is under aqueous conditions polar aprotic solvents such as DMF have been shown to be the most compatible with the intended application [80].

1.4.5 Polyclonal nature of MIPs

The binding of ligand to MIP is analogous to antibody binding to antigen [81]. There are two distinct types of antibody production processes, monoclonal and polyclonal. Antibodies however, are not synthesised to a template (although formerly this was believed to be the case and was known as the "Instructive theory") but are generated at the molecular genetic level by the combination of different gene segments, which produces a huge library of molecules which are screened against an antigen until a "fit" is found. This library has been constructed over millions of years of evolution. Figure 1.8 demonstrates this.

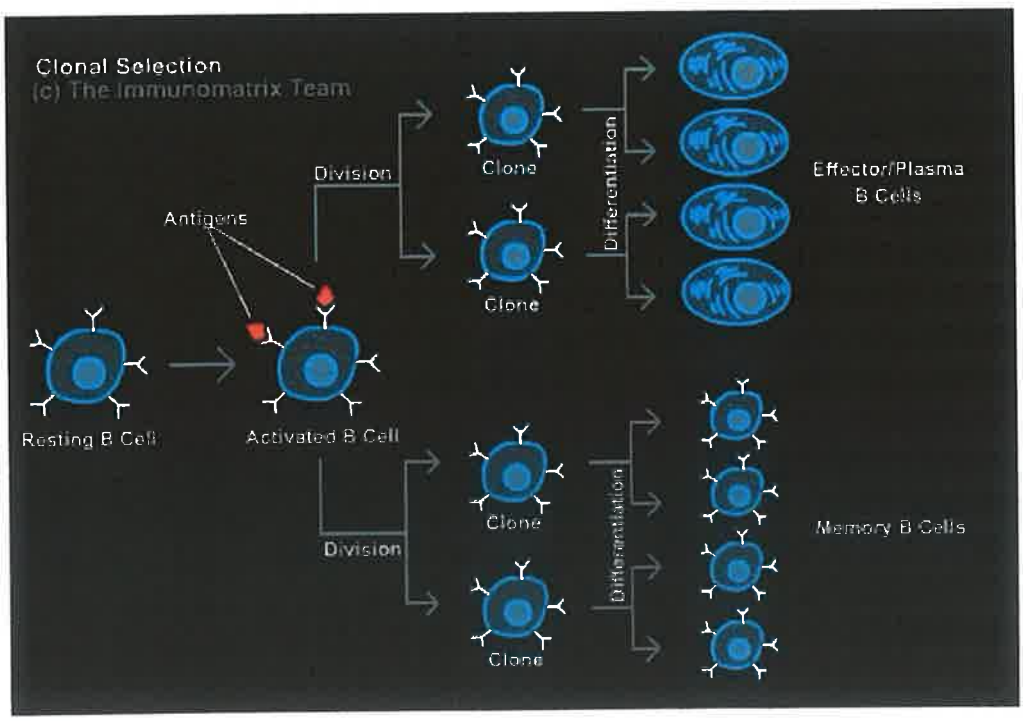

Figure 1.8 – clonal selection of antibody producing B cells

Reproduced from [82]

MIP's however, do possess a similar binding nature to polyclonal antibodies i.e. they contain binding sites of differing affinities. The outstanding difference is that antibodies work in a naturally aqueous environment whereas MIPs generally function in a non-polar organic environment. Researchers have attempted to engineer antibodies to allow detection of analytes under organic conditions, whereas there is now a drive to synthesise MIPs capable of recognition in aqueous conditions [83,84]. This is particularly applicable to solid phase extraction where selective clean up of aqueous samples is required. Some advantages that MIPs do possess over antibodies are that they are capable of withstanding temperatures of 120^{o}C plus [85]. Furthermore, MIPs do not need to be stored at low temperatures, unlike antibodies and are capable of regeneration and reuse – again unlike antibodies, which are not capable of prolonged use and ideally should not be used more than once. Antibody preparation against low molecular weight compounds such as drugs involves the conjugation of the hapten to a carrier protein such as BSA before introduction to the animal. Conjugation however, can present a synthetic challenge and often changes in the structural properties of the antigen. Provided the molecule (analyte) is soluble in the polymerisation mixture, MIP preparation generally does not include derivatisation of small (hapten) molecules.

As mentioned earlier, non-covalently produced MIP's are generally polyclonal in nature meaning that they have subpopulations of binding site densities. This could potentially upset their use in situations or assays that require a high degree of selectivity. Essentially, with a large population of weakly interacting binding sites, analogous molecules (or unrelated molecules of similar shape and/or functionality) could non-specifically bind to these sites. This does have the advantage however of enabling dummy imprinting i.e. imprinting an analogue of the template of interest. One positive outcome of this is the potential for removing the possibility of template bleeding. Production of polyclonal antibodies suffers from the fact that different individuals elicit antibodies with different properties and to generate an antiserum with the desired selectivity immunisation of several animals is strongly desired. MIP preparation can be reproduced with each batch having close to identical properties. The preparation of monoclonal antibodies however, offers scale up possibilities and long-term production of antibodies of consistent quality.

1.4.6 The cross –linker, porogen and flexibility

Studies such as that of Zhang *et al.*, [86] and Lu *et al.*, [87] have investigated the effect of changing the concentration of cross-linker on the morphology and performance of MIPs. It was found [86] that when the ratio of EDMA to MAA was in the range of 5:1–10:1, molecularly imprinted polymers with the optimal uniform size are obtained. Scatchard analysis suggests that there exist two classes of distinct binding sites in the MIPs for niacinamide and the affinity of these polymers increase with the increment of the amount of cross-linker until the ratio reaches up to 20:1. It was also shown that the selectivity of the sensors increases with an increase of the amount of cross-linker. This is displayed in figure 1.9 below:

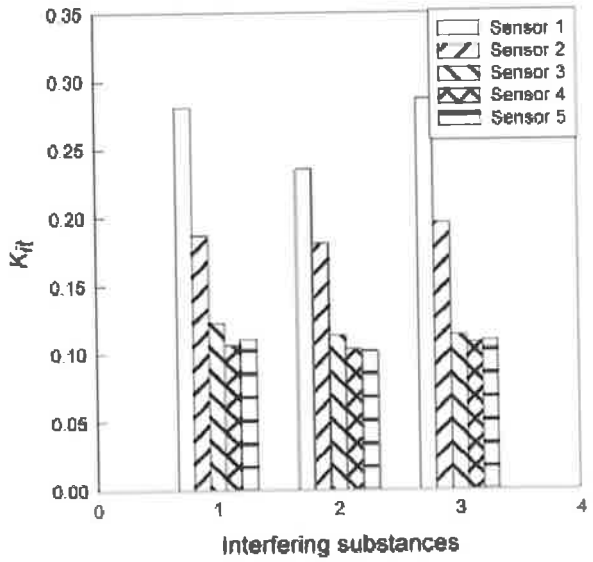

Figure 1.9: The selectivity of the different sensors (1-5 decreasing cross-linker concentration) modified with different MIPs: (1) nicotinic acid; (2) nicotine; (3) nicotinic alcohol. Reproduced from Zhang *et al.*, [86]

The main driving force for a molecule to diffuse into and migrate through a polymer is its affinity to the matrix/binding pockets. While the diffusion is related to dipole-dipole interactions and Van der Waals forces, the friction forces within the cross-linked polymer will determine the rate at which the molecules permeate. The initial friction force (diffusion coefficient) is determined by the size of the permeant and the dimensions of the void spaces of the highly cross linked polymer matrix. Furthermore,

with an increasing permeant volume, the internal stress imposed onto the polymer chains will cause the dimensions of the polymer to change resulting in polymer swelling effects that may affect the integrity of the binding pockets [88,89].

Besides the structural flexibility of the polymer matrix, tuning of the void volume i.e. porosity is another parameter affecting access to embedded binding pockets. Selecting the appropriate polymerisation method allows preparation of MIPs in different formats ranging from monolithic block polymers to micro- and nanospheres and polymer films. In the former case a rigid polymer monolith is obtained which is usually characterised by a multitude of micro- (<2 nm), meso- (2-50 nm) and macropores (>50 nm) [20]. The polymer monolith is then crushed ground and sieved to obtain particles with a well-defined particle size distribution.

Two types of trimethoprim imprinted polymers in bulk and sphere (by suspension polymerisation) were prepared and used as sorbents for solid-phase extraction [90]. By comparing adsorption of trimethoprim in different solvents, desorption with ratios of ethanol and *N,N*-dimethylformamide, acetic acid and ratios of methanol and trifluoroacetic acid, it was found that MIPs in bulk form were more selective and possessed a higher adsorptive capacity than in sphere form. Moreover specific surface area and pore volume of the polymers in bulk form were about twice than in sphere form. But these two types of polymers both enriched and separated trimethoprim from human urine and a pharmaceutical tablet successfully. The linear range of trimethoprim was 1–100 nmol ml^{-1} and the limit of detection was 0.1 nmol ml^{-1}. The differences in morphology as reported by BET in the study are shown in table 1.1:

Table 1.1 Data of specific surface area, pore volume and pore width of MIPs and MIPs-S (spheres). Adapted from Hu *et al.*, [90]

Measurement	MIP-s	MIP-sS
Multipoint BET (m^2/g)	1.780E+2	0.8289E+2
Langmuir surface area (m^2/g)	2.788E+2	1.318E+2
DR method micropore area (m^2/g)	2.443E+2	1.134E+2
DR method micropore volume (cm^3/g)	8.683E−2	4.028E−2
HK method cumulative pore volume (cm^3/g)	7.146E−2	3.258E−2
SF method cumulative pore volume (cm^3/g)	7.315E−2	3.347E−2
DR method micropore width (Å)	5.784E+1	5.953E+1
DA method pore diameter (Å)	1.840E+1	1.840E+1
HK method pore width (Å)	1.392E+1	1.373E+1
SF method pore diameter (Å)	2.611E+1	2.574E

The physical crushing of the monolith results in material loss and induces problems such as decreased interparticular volume and reduced mass transfer after packing into columns or cartridges [91]. Nevertheless, this method of preparation is among the most commonly used for molecularly imprinted polymers. The porous MIP structure provides a high surface area and facilitates access to the binding pockets. Therefore, in case of a block polymer the pore size distribution is the key quality factor, which, can be tuned by variables such as temperature, the nature of the porogenic solvent and the amount and type of cross linker [92,93]. The effect of these variables on co-polymer porosity can be directly investigated by methods such as the BET method for surface area determination. However, the generation of selective binding sites within the polymer matrix depends on the same variables and hence, does not necessarily allow for concurrent tuning of the pore size.

1.4.7 Monomer-template solution structures

The extent to which solution complexes are formed between the monomer and the template in solution reflects the architecture of the polymeric binding sites. This is significant since, characterisation of the monomer-template assemblies is important in deducing the structure of the binding sites in the polymer and as such may have a role in prediction. The potential for a complex to produce templated sites can be predicted by measuring the stability constants in a homogenous solution mimicking the monomer mixture prior to polymerisation. This can ultimately be used as a preliminary screening procedure to search for suitable functional monomers. Thus, estimated solution association constants can be compared and contrasted with the heterogeneous binding constants determined in the rebinding step to the imprinted sites. Figure 1.10 below shows a postulated monomer template structure for a 2,4-dichlorophenoxyacetic acid/4-vinylpyridine complex [23].

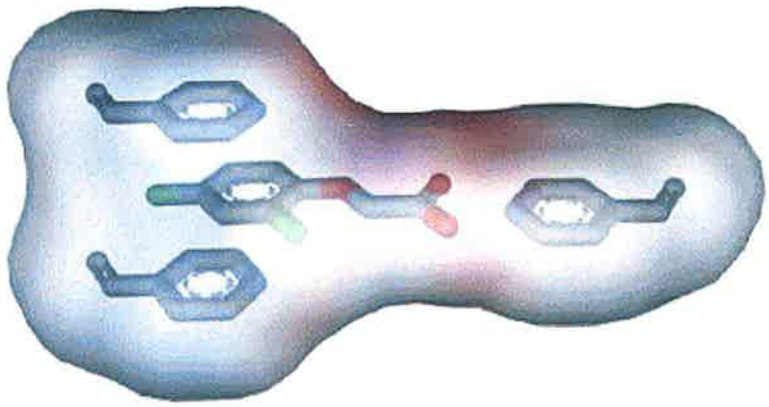

Figure 1.10 Model of the 2,4-D/4-VP pre-polymerization complex established from NMR titration and molecular modelling data. Reproduced from O'Mahony *et al.*, [23]

From figure 1.10, it can be seen how both chemical functionality and spatial organisation can play equally important roles in molecular recognition.

Rebinding to sites formed from residual non-extracted template has also been proposed as a contributing factor to the observed recognition. A study by Lavignac et *al.*, [66] observed that both selectivity and affinity were dependent on the concentration of the ligand and that unusually selectivity and affinity were better at higher atrazine concentrations. It was concluded that this phenomenon resulted from the formation of atrazine–atrazine complexes during the pre-polymerisation stage and during rebinding and that the polymer demonstrated improved atrazine affinity when the conditions favoured complex formation. This phenomenon is demonstrated in figure 1.11

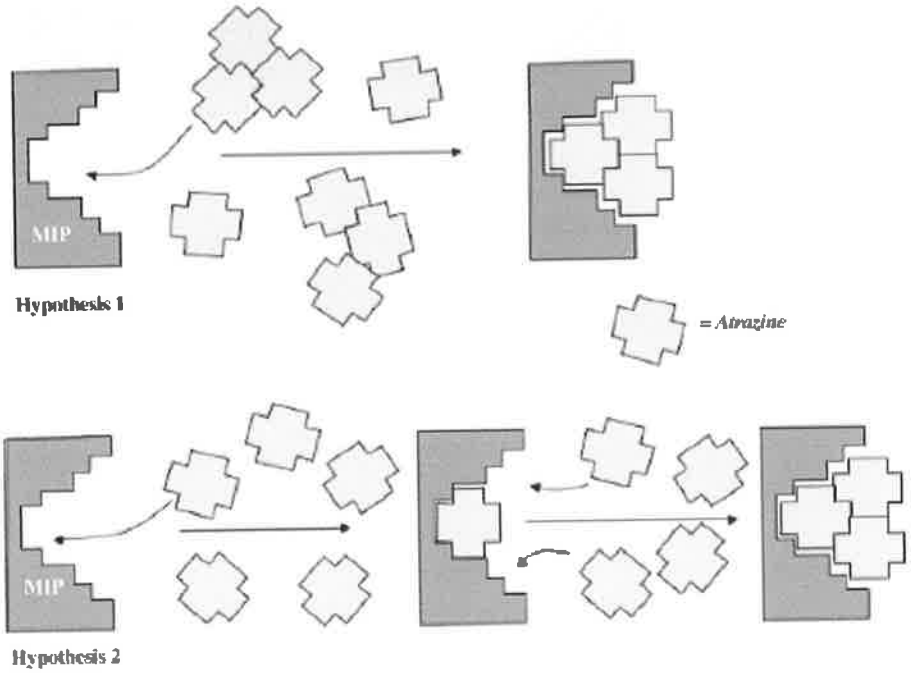

Figure 1.11 Atrazine complex formation and polymer association. Hypothesis 1: solution phase atrazine complex binding within an atrazine complex templated binding site. Hypothesis 2: uncomplexed atrazine nucleating within an atrazine complex templated binding site. Reproduced from Lavignac *et al.*, [66]

This suggests that template remaining in the polymer after attempted template removal is capable of acting as a nucleating site for the template in the rebinding experiment. Generally, though, selectivity increases with increasing recovery of the template.

1.5 The rational design of MIPs

MIP systems have been designed *ab initio* [94]. Over the last number of years there has been an increase in the understanding of physical and molecular level events influencing and indeed controlling both pre-polymerisation template-monomer interactions and ligand recognition in the finished MIP. What is known has been obtained through exhaustive chromatographic, spectroscopic and rebinding studies, reviewed by Mayes and Whitcombe, 2005, [46]. There is a very definite opportunity via the knowledge of the physical chemistry of MIPs for real advances to be made in the further elucidation of molecular processes. For systems imprinted in aqueous conditions, rebinding can occur in polar environments due to the hydrophobic effect, conversely, imprinting in organic solvents can be used for rebinding in water due to the contribution of electrostatic interactions. The effects of pH [95] and temperature on the ppc and the resultant recognition properties of the MIP have been well studied [96]. A lower polymerisation temperature reduces the effect of ΔG_{vib} though the mass transfer kinetics are affected somewhat by this. One area that has received a great deal of attention is the molecular modelling of template monomer interactions as reviewed by Nicolls *et al.*, [97]. In the rational design of MIP's this will be vital to firstly ascertain whether particular functional monomers are suitable for complex forming with target templates and secondly to generate virtual optimisation of the interaction to narrow down the choice of monomers.

Taking into consideration the physical factors discussed regarding ligand receptor interaction, modelling systems will ideally be able to incorporate this knowledge to predict the outcome of rebinding studies and to design MIPs specifically for certain needs e.g. whether a MIP is to be used for solid phase extraction, or for binding assays or for sensors should be known before the synthesis is initiated. In this regard the binding adsorption isotherms are critical as knowing the amount of binding sites (and their type) will influence the applications for which a particular MIP is suitable.

1.5.1 Trial and error approaches

The techniques of IR and NMR have been used in the elucidation of the molecular level events and have huge potential in furthering the understanding and generation of optimal MIPs. In particular NMR has been and will be critical in this regard.

Analytical method development for MIPs and their applications has been reviewed [98]. In particular, many papers comparing MIPs with template – functional monomer – cross-linker ratios, porogens (diluents) and polymerisation formats have been published. This approach is the so-called "trial and error" approach and is commonplace among MIP developers. The approach however has numerous drawbacks such as the polyclonality – akin to the production of polyclonal antibodies i.e. binding sites of non-uniform specificity and differing affinities. In particular the low yield of high fidelity sites is problematic [97]. Two different but related (in their scope) approaches have been conceived in response to these drawbacks. These are firstly combinatorial methods, which can select an optimal MIP formulation for a targeted analyte i.e. screening libraries of MIPs and secondly the rational design of MIPs which is based on the characterisation and understanding of the physical mechanisms underlying formation and MIP ligand recognition.

1.5.2 Optimisation of MIPs using combinatorial imprinting

As a result of these variables affecting the outcome of MIPs (or a successful imprint), there has been an overuse of certain standard formulations of template: monomer; cross linker ratio (e.g. 1:4:20). The determination of optimal MIP formulae is a process that is well suited for combinatorial screening. Batra *et al.*, [99] were the first to apply combinatorial methods in molecular imprinting. Here, a library of MIPs was constructed using a semi-automated approach. The concentrations of the functional monomer(s) were varied in this study. MIP synthesis and analysis occurred on the bottom surface of glass vials and were analysed by binding assays. Triazine herbicides (ametryn and atrazine) were used as templates for the synthesis of MIP libraries. The only variables in the study were the monomers (either MAA or TFMAA). Two screening steps were performed on the MIPs. The first one analysed

the amount of free template in solution following acetonitrile washing – giving an estimation of the affinity of the MIP. The second screening of the MIP was a batch rebinding study to determine the capacity factor for each MIP in addition to determining the selectivity over the non-imprinted polymer.

The results showed that the optimal imprinting formulations for the two triazines were significantly different. For ametryn, TFMAA (α=2.5) gave greater selectivity over atrazine than MAA rich polymers (α=1.5). However, for atrazine, selectivity over ametryn for MAA rich polymers proved better than for TFMAA (α 1.2 and 0.8 respectively). Figure 1.12 shows a flow diagram of the method of combinatorial imprinting applied by Batra *et al.*, [99].

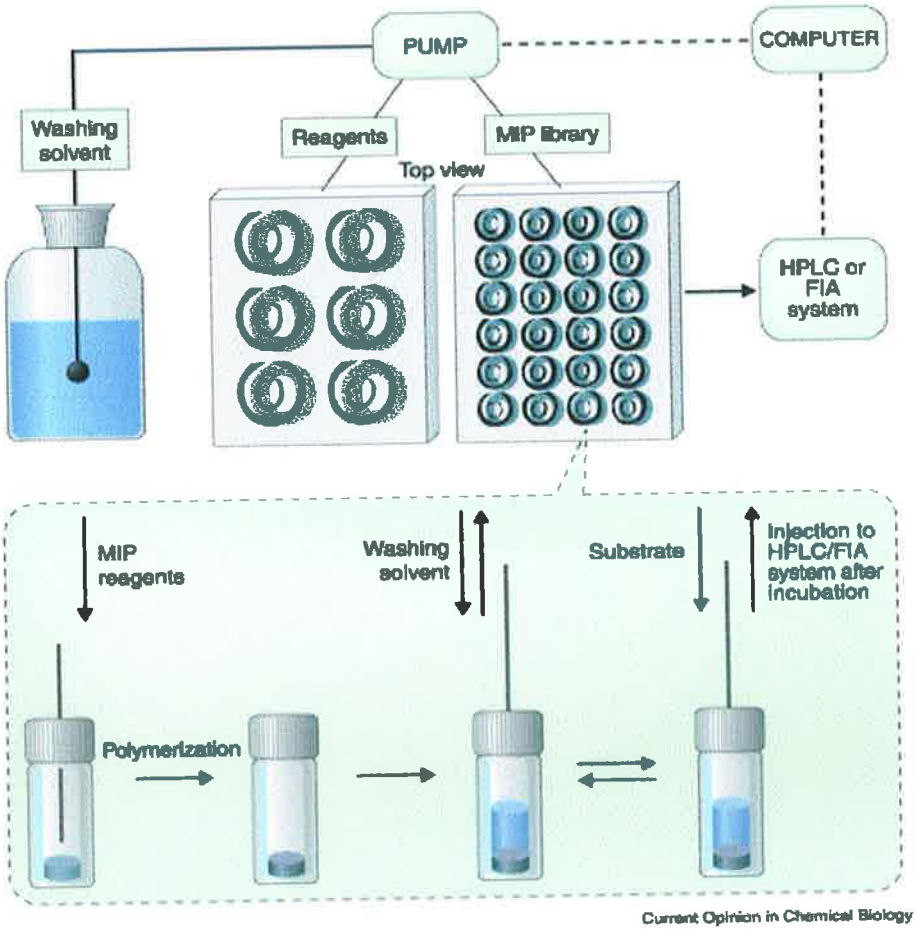

Figure 1.12: Illustration of an automated programmable liquid handling system used to prepare and analyse small-scale MIP's. Reproduced from Batra *et al.*, [99].

1.5.3 Parallel synthesis of MIPs

A small-scale polymerisation protocol was used with success in the search for functional monomers to imprint the poorly soluble templates such as phenytoin [100]. AAM and MAM were found to be the most suitable functional monomers, according to the small scale binding evaluation test, and good selectivity was found in the scaled up polymers when evaluated by HPLC. A remarkable difference was observed when the capacity factors of phenytoin on the AAM and MAAM polymers were compared, suggesting that a slight difference in the structure of the functional monomer can strongly influence the selectivity of the resulting polymers. The batch rebinding results given by the mini-MIPs, correlated well with binding observed from the HPLC studies. Despite these good results, the authors showed that this method does have limitations concluding that small scale rebinding results obtained at equilibrium cannot always be used to predict selectivity of MIPs in the dynamic HPLC mode.

Likewise, small variations in the solvent system can lead to changes in the recognition properties. Figure 1.13 shows the miniaturised searching procedure for the most suitable functional monomer for the template.

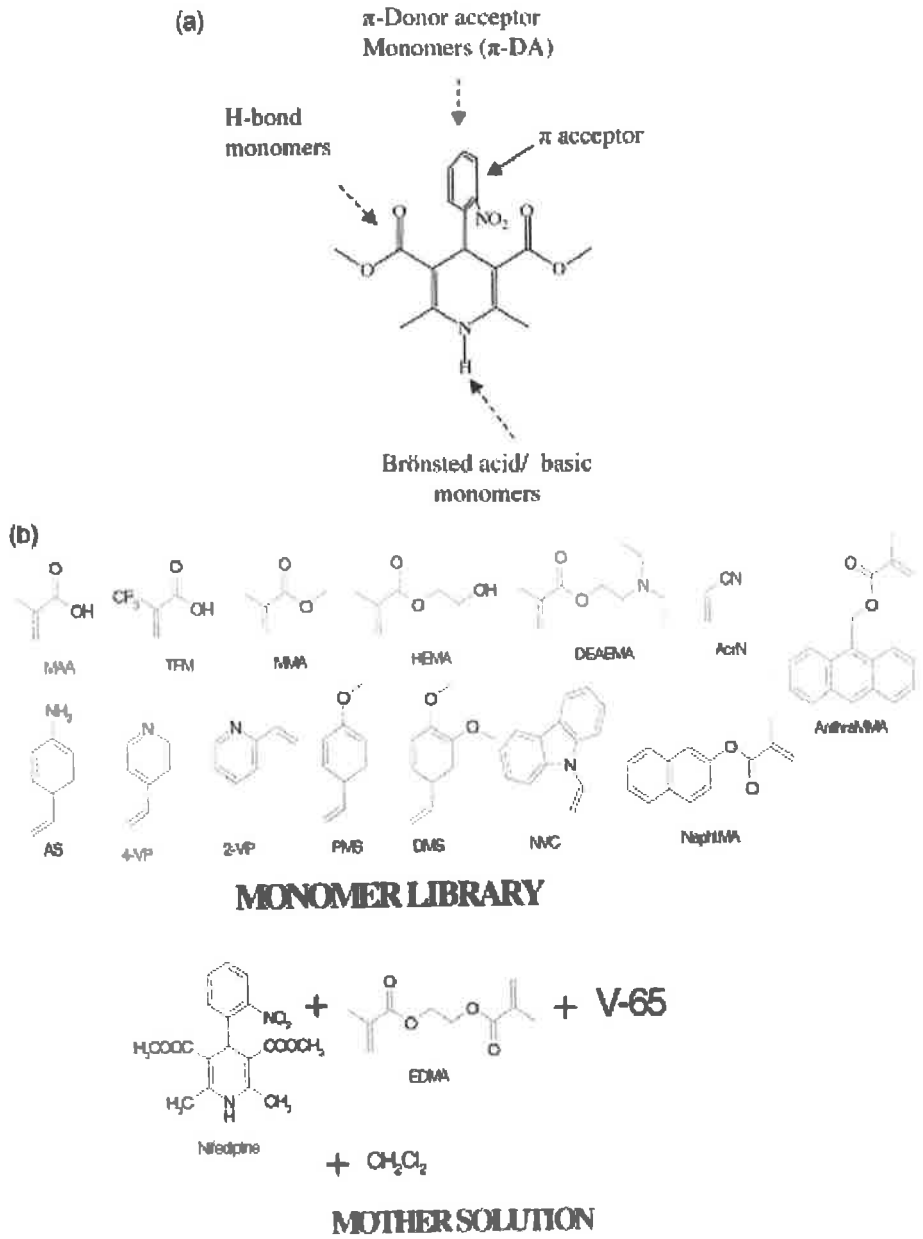

Figure 1.13 Search for functional monomers for nifedipine: (a) possible ways of targeting the template; (b) different monomers used and composition of the polymerisation mixture used in the small-scale polymerisation. Reproduced from Lanza *et al.*, [100]

1.5.4 Synthesis and Screening of MIP Libraries

A good example of the advantages of synthesising MIP libraries over more traditional trial and error methods and indeed the ultimate limitation of the combinatorial approach is the synthesis and screening of a MIP library for Penicillin G by Cederfur *et al.*, [101]. Penicillin G was not soluble in 100% acetonitrile but could be dissolved in the presence of methacrylic acid (MAA). Other functional monomers were examined but couldn't increase the solubility of Penicillin G. Hence; MAA was included in all of the MIPs in the library. MAA was used as the only functional monomer or else in combination with MAM or HEMA. The cross-linker was either TRIM or EDMA. The rebinding was assayed by radioligand ^{3}H labelled Penicillin G. The partition coefficients K_{MIP} and K_{CP} were calculated and K_{MIP}/ K_{CP} was used to identify the most suitable MIP. Within the sublibrary of MIPs prepared with MAA as the only monomer, the greatest relative partition coefficient was achieved with TRIM as the cross-linker and molar ratios of template – MAA-TRIM 1:10:40. Whereas, of the MIPs produced with both MAA and MAM, the highest partition coefficient was achieved also with TRIM as cross-linker with a molar ratio of template-MAA-MAM-TRIM of 1:10:10:60.

The best Penicillin G selective MIP candidate in the screening was then selected for competition studies with a number of compounds representing different classes of antibiotics and the cross reactivity of each antibiotic was determined. The greatest level of competition was seen with amoxicillin (19%), ampicillin (15%) and penicillin V (1%), with others tested being <0.1% save 6-aminopenecillanic acid. The antibiotics that showed cross reactivity are all β-lactam antibiotics and are derivatives of 6-aminopenecillanic acid.

1.5.5 Applicability and Limitations of the Combinatorial Approach

There is a trend towards the use of screening to identify suitable MIPs for specific target analytes and no doubt they are a significant improvement on the intuition and trial and error approaches. Because a large number of parameters can be varied and optimised a combinatorial library approach is in theory a viable strategy. It has been

shown that this approach is useful for phenytoin [100] and has yielded MIPs with high selectivities for their ligands. The limitations of the method whilst have been demonstrated looking for optimal functional monomers for phenytoin and nifedipine and while synthesising a useful MIP for Penicillin G [101] it was found that the *in situ* synthesis of monolithic MIP libraries in HPLC vials – the so called "mini-MIP" approach proved to be unsuitable for automation due to stability difficulties and the instability of the template. Hence, monolithic polymers of a scale large enough to allow visual inspection during preparation and polymerisation were required thus reducing the potential high throughput of the system. One of the great potential advantages of the combinatorial approach is high throughput in the screening of optimal MIPs especially if faster screening methods than the currently employed HPLC or FIA could be found.

At this point in the evolution of combinatorial methods for MIPs, they have only been used in determining optimal functional monomers – just one variable. There have been few reports of screening porogen or initiator. It is clear that combinatorial methods can only bring predicting the optimisation of MIPs so far.

1.5.6 Rationale for designer MIPs

For the molecular imprinting field to fulfil its considerable potential, a greater knowledge of imprinting at the physico-chemical level is required. At this point in time, what is known has been comprehensively reviewed about the reactions on a molecular level that underlies the imprinting process [97]. The authors have split the molecular level events into two sections. Firstly, the physical factors governing template-monomer interactions with an emphasis on non-covalent interactions is described and secondly, the physical mechanisms regulating MIP-ligand binding events are considered. Complementary approaches to the rational design of MIPs – molecular modelling and NMR/IR spectroscopy - have both yielded important structural, thermodynamic and chemical information regarding the nature and organisation of the pre-polymerisation complex. Such studies have demonstrated the importance of hydrogen bonding [102], π-π stacking interactions [23] and electrostatic interactions [103] in the self-assembly of the PPC.

1.5.7 Spectroscopic analysis of monomer-template interactions

The formation of template-monomer solution complexes in the pre-polymerisation mixture is the basis for molecular memory. The greater or lesser strength of these interactions – hydrogen bonding, ionic bonding, hydrophobic interactions, van der Waals forces or reversible covalent bonds is vital to the rebinding selectivity of the polymer. Importantly, the equilibrium position for complexes self-assembled in solution between templates and functional monomers (ΔG) will determine the number of ligand binding sites and the degree of non-specific sites (receptor heterogeneity). Consequently, the more stable the template-monomer complex, the higher the number and fidelity of ligand receptors that will be produced during polymerisation. The strength of the non-specific interactions i.e. monomer-monomer, template-template, template-solvent (porogens) and monomer-solvent will influence the position of equilibrium (ΔG_{bind}) and subsequently, the quality of ligand receptor interactions in the resultant MIP.

In addition to the spectroscopic methods, other systems used to study complexation in solution include electrochemical and calorimetric. This discussion will concentrate primarily on NMR studies, as it is the most widely used method to study complexation events in the pre-polymerisation solution. NMR spectroscopy measures parameters directly related to structure and structural changes in a variety of solvents.

Nuclear Magnetic spectroscopy involves transition of a nucleus from one spin state to another with the resultant absorption of electromagnetic radiation by spin active nuclei (having spin not equal to zero) when they are placed in a magnetic field. The energy associated with NMR experiments is incapable of disrupting even the weakest of chemical bonds [104]. When the sample is placed in the magnetic field, the nuclei of the atoms align with the magnetic field. A second transverse oscillating magnetic field is superimposed. The NMR experiment consists of applying short pulses of energy in the radio frequency (RF) range, typically 40-800 MHz, to the sample. These pulses of RF cause the nuclei to rotate away from their equilibrium position and they start to rotate around the axis of the magnetic field. The exact frequency at which the nuclei resonate is related to both the chemical and physical environment of the atom

in the molecule. By using different combinations of RF pulses and delays it is possible to determine how each atom in the molecule interacts with other atoms in the molecule.

This induces transitions between energy levels at the respective resonance frequencies. The magnetic field experienced by a nucleus in a molecule is different from the external field with the exact resonance frequency being characteristic for the chemical environment of the nucleus (chemical shift δ). Chemically non-equivalent nuclei in a molecule are therefore differently shielded leading to separate signals in the NMR spectrum (only for nuclei with a spin quantum number $I \neq 0$). The applied magnetic fields are in the range of 1.4-14.4 T leading to proton resonance frequencies of 60-600 MHz. Intermolecular interactions will change the chemical environment of a nucleus, inducing changes in the chemical shift which can be monitored [105]. NMR spectroscopy has become the main method used for structure elucidation, kinetics and dynamics of supramolecular complexes in solution.

NMR has been utilised by Idziak *et al.*, [106] to predict the extent of complex formation between the target analyte 17 α-ethynylestradiol (17α-EE) and the functional monomers MAA and VP in the solvents toluene and methylene chloride. The results of their binding studies indicated that the MIP that was prepared in toluene with VP as functional monomer had a high affinity for the template in toluene. As the 17 α-ethynylestradiol was only sparingly soluble in toluene but could be brought into solution by the addition of either of the monomers, it was likely that a hydrogen bonded complex existed between the template and monomers in toluene. This was verified by the use of ^{1}H-NMR. The addition of monomer substitutes to the 17α EE solutions resulted in a downfield shift of the 3-OH and the 17-OH protons. For the sake of simplicity and clarity of the spectrum, acetic acid and deuterated pyridine were substituted for MAA and VP respectively. Pyridine (VP) showed a 3-OH downfield shift of 4.55 in toluene and 3.58 inCD_2Cl_2, with 17-OH downfield shifts of 1.48 and 1.20 respectively. As regards acetic acid, in toluene, a 3-OH downfield shift of 3.23 was observed. The 17-OH proton signal in the acetic acid spectrum in toluene was not detectable. The above results are shown in table 1.2:

Table 1.2 Binding capacity of EE MIPs, measured by radioassay as the percentage of EE bound to the polymer, correlated to the change in NMR shift of the EE hydroxyl protons in response to the addition of pyridine d_5 or acetic acid in non-polar solvents. Reproduction of Table 1 from Idziak *et al.*, [106]

MIP (f.m.[b], polymerization solvent)	MIP-blank binding capacity			Corresponding NMR model	Downfield NMR shift (Δ, ppm)	
	Toluene	Toluene + CH_2Cl_2			3-OH	17-OH
		2.7/1	1/1			
P1 (VP, toluene)	80–0	61–0	31–0	EE-pyr d_6 (toluene)	4.55	1.48
P2 (VP, CH_2Cl_2)	38–26	38–6	16–2	EE-pyr d_6 (CH_2Cl_2)	3.58	1.20
P3 (MAA, toluene)	21–8	6–0.7	0–0	EE-HOAc (toluene)	3.23	ND[c]
P4 (MAA, CH_2Cl_2)	31–28	19–7	2–0	EE-HOAc (CH_2Cl_2)	ND[c]	ND[c]

[a] The polymer concentration was 0.80 mg ml^{-1}.
[b] Functional monomer.
[c] Not detectable.

Neither the 3-OH nor the 17-OH was found in the spectrum run with acetic acid in CD_2Cl_2. The data obtained from the NMR spectra clearly show that pyridine forms stronger hydrogen bonds with 17α-EE than acetic acid and that toluene is the better solvent to promote this kind of complexation. Thus, the NMR model study results are consistent with the demonstrated superior affinity and specificity of the VP containing MIP in toluene.

Chemical shifts and line broadening interpretations [64] have also shown the establishment of MAA-phenylalanine anhydride complexes. Furthermore, the presence of template-template complexes was also suggested. NMR studies have also been used by to calculate association constants and as such predict binding capacities of MIP's. Ansell and Huah [107] have employed NMR titrations to demonstrate that there is a very strong 'stoichiometric' (K~ 10000 M^{-1}) interaction between ephedrine and a single MAA molecule. Polymers prepared with this 1:1 ratio were capable of enantioseparation. Furthermore, it was noticed that higher monomer: template ratios caused changes in the NMR signals. This was seen as being indicative of at least one more MAA molecule interacting with the amine group of ephedrine. Dong *et al.*, [108] have used ^{1}H-NMR spectroscopy to show that the H-bond between theophylline and MAA is the major force in molecular recognition, and this can be significantly affected by the solvent used in the polymerisation process. Figure 1.14 shows H-NMR

spectra from Dong *et al.*, [108] demonstrating the chemical shifts associated with the theophylline/MAA complex in $CDCl_3$ solution.

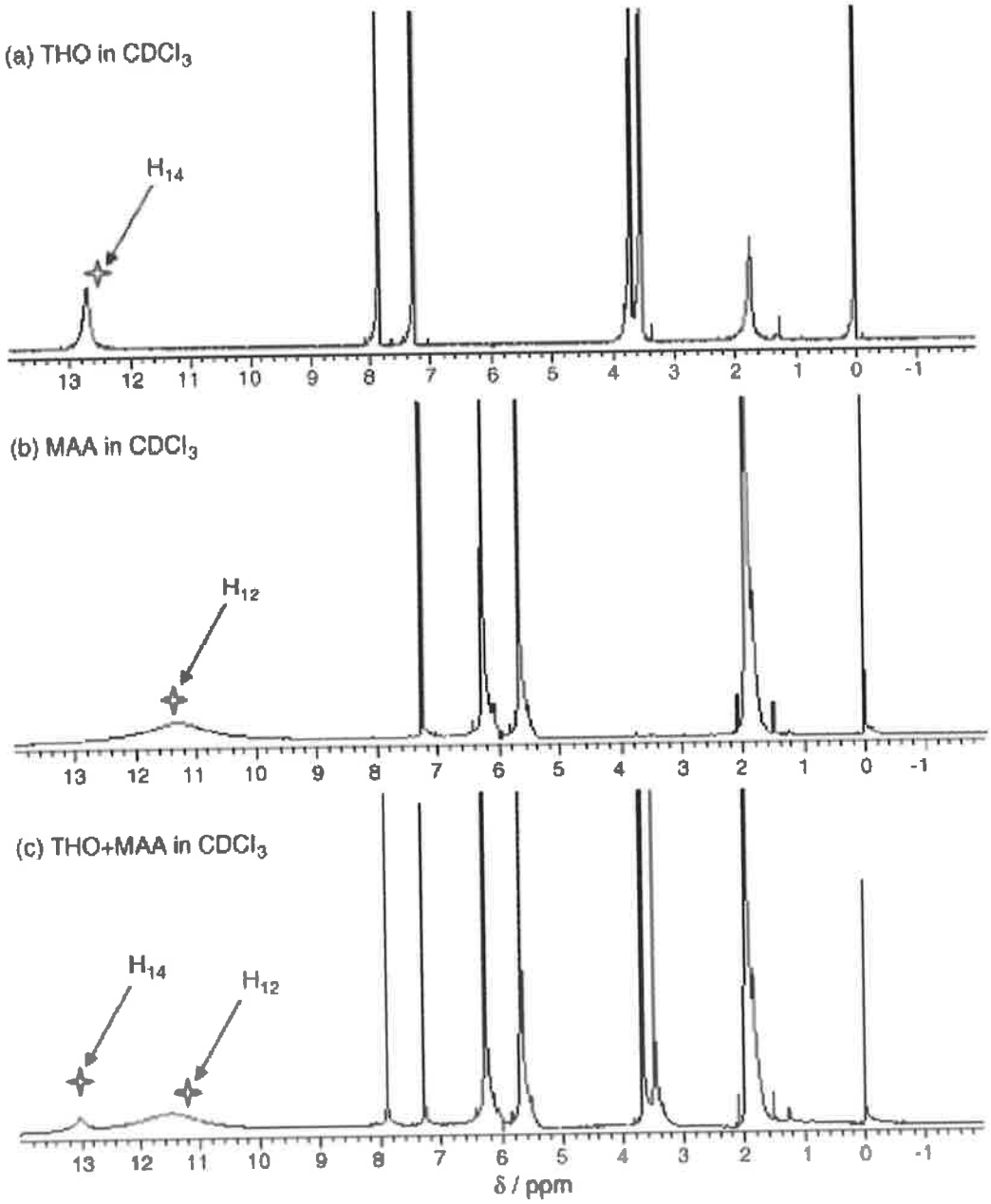

Figure 1.13 shows chemical shifts associated with the theophylline/MAA complex in $CDCl_3$ solution. Reproduced from Dong *et al.*, [108]

Nomachi *et al.*, [109] performed an NMR study investigating the solvent effects on the interaction of MAA with melatonin. They stated that hydrogen bonding between the template, the functional monomer and the solvent can be estimated from the chemical shifts in the ^{1}H NMR spectra. The data suggested that melatonin forms strong hydrogen bonds with THF and MeCN relative to when $CHCl_3$ was used as solvent. They concluded that the ratio of hydrogen bonding between melatonin and the solvent relative to that between melatonin and MAA is the most important factor for the formation of effective imprinting sites. A series of metoclopramide (MCP) MIPs were prepared by Xu *et al.*, [110]. Utilizing MAA or 2VP as functional monomer and chloroform, acetonitrile or methanol as porogen, the affinity and selectivity of these polymers were evaluated by equilibrium binding experiments. ^{1}H NMR studies on interactions between the template and functional monomer analogues, acetic acid and d_5-pyridine, were performed in the same solvents that were used as porogens. A correlation was found to exist between the binding strength and specificity of a particular polymer and the extent of monomer–template interactions shown by the corresponding NMR spectra. The addition of acetic acid to solutions of MCP in $CDCl_3$ or CD_3CN resulted in 0.24–0.65 ppm shifts of a number of resonances arising from protons in the vicinity of the basic tertiary nitrogen. The relative large shift of the protons indicates that protonation of the tertiary amine and subsequent interaction, by ion pairing with the carboxylate anion, results in a significant change in the magnetic environment of adjacent protons. When chloroform or acetonitrile was used as solvent, the chemical shifts of the protons of the amino group (NH_2) and amido group (CONH) were downfield in response to the addition of acetic acid. This provides clear evidence of hydrogen bonding between these two groups of MCP and carboxyl group of acetic acid. The authors [110] went on to describe that when methanol was used as solvent, no observable chemical shifts of the protons of NH_2 and CONH were seen. They concluded that methanol has strong hydrogen bonding ability and can efficiently compete with the functional monomer for the functional groups of the template. Thus, it can weaken or block the formation of hydrogen bonding between the functional monomer and the template. Figure 1.15 demonstrates the formation of the pre-polymerisation complexes for MCP with MAA in the different solvents.

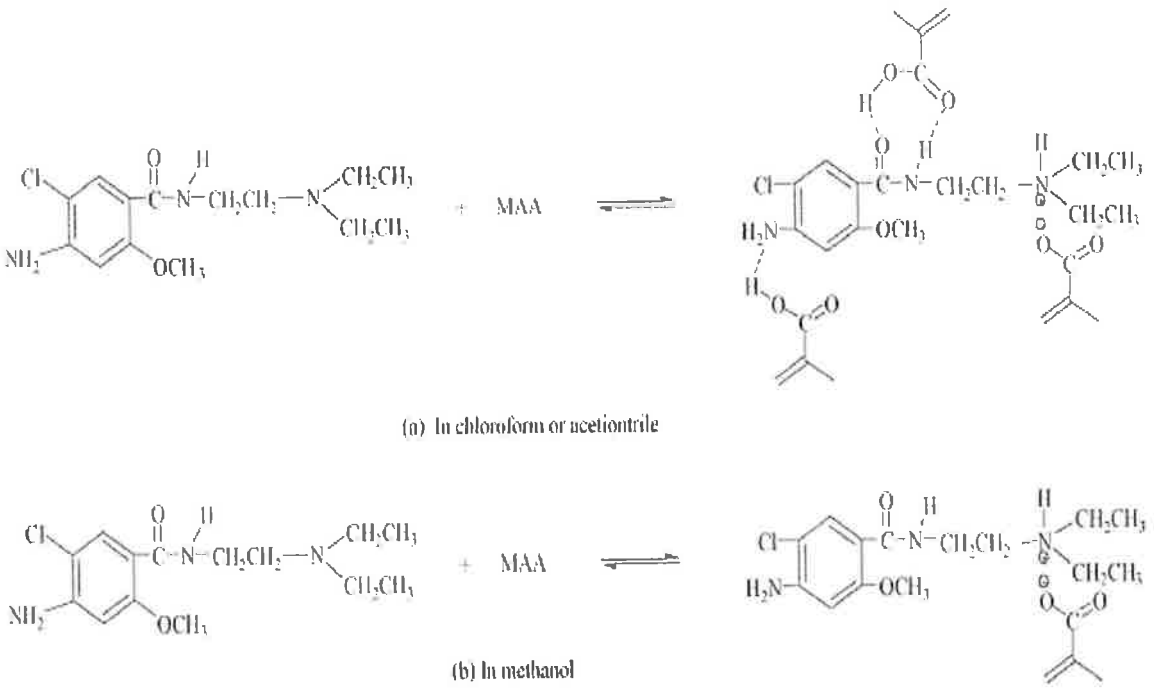

Figure 1.15 Schematic illustration of the formation of the template–monomer complexes in different porogens. Reproduced from Xu *et al.*, [110]

NMR then is a vital tool for estimating both qualitatively and quantitatively complex formation. Two of the most important techniques in NMR for the study of complex formation are the mole ratio method and Job plot method [104,105] and both are considered in 1.5.7.1 and 1.5.7.2 respectively.

1.5.7.1 NMR titration studies: mole ratio method

Complexation events in the pre-polymerisation solution such as hydrogen bonding and π-π stacking may be observed by ^{1}H NMR titration experiments. In NMR titration studies, measurements are performed at variable concentration of one component and at a fixed concentration of the other component. The experimental conditions are selected such that the degree of complexation is high. The changes of NMR shifts of independent signals upon complex formation are used to monitor complex formation and calculate association constants. Given a rapid exchange between ligand L and substrate S, a sharp signal is observed at a mean weighted shift between the signals for free and complexed compound:

$$\delta_{OBS} = \delta_0 N_S + \delta_{SL} N_{SL} \qquad \text{Eqn 1.1}$$

with δ_0 and δ_{SL} chemical shifts of a monitored nucleus in the free (S) and complexed (SL) state

N_S and N_{SL} molar fractions of the free and complexed state.

$$\delta_{OBS} = (\delta_0 + \delta_{SL} \cdot K[L]/\ 1+K[L]) \qquad \text{Eqn 1.2}$$

With K equilibrium constant

[L] ligand concentration

1.5.7.2 Method of continuous variation – Jobs method

In the method of continuous variation [111], a series of mixed solutions of S and L are prepared such that the total concentration [S]+[L] is kept constant while the ratio [S]/[L] varies. A property of the mixture such as the absorption (optical spectroscopy) or the complex concentration (NMR spectroscopy) is plotted as a function of the molar fraction of one of the two components. If both S and L have a non-zero absorbance at the measured wavelength, the absorbance of the free species at each molar fraction is subtracted from the observed value of the mixture. An extreme value in the graph – maximum or minimum – indicates the presence of a complex with a composition of S_mL_n where the molar ratio, *x*, at the extreme represents the complexation stoichiometry according to:

$$x = \frac{n}{n+m} = \frac{1}{\frac{m}{n}+1} \qquad \text{Eqn 1.3}$$

A maximum appearing at e.g. x=0.5 indicates that a 1:1 (or 2:2) complex is the predominant structure at equilibrium conditions. Job plot analysis is a valuable tool in determining complex stoichiometries since it also allows determination of stoichiometries other than 1:1 [112].

A method based on UV titration has been used to calculate dissociation constants. The possibility of template-template self-association should be included in models describing the influence of the monomer-template ratio and sample load on the retention and selectivity [113]. The authors examined the influence of the monomer-template ratio in the pre-polymerisation mixture on the recognition characteristics of the resultant polymer. (-)Nicotinamide MIPs were synthesised and evaluated in the HPLC mode. Different template-monomer interactions exist in the pre-polymerisation mixture, which can to a greater or lesser extent, affect the selectivity of the resultant MIP. The above is described by the term $\Sigma\Delta G_p$ – the sum of the interacting polar group molecules. The use of 2-(trifluoromethyl) acrylic acid as a functional monomer has been described [114] and it was shown that it can be used to increase or improve ligand recognition.

At monomer concentrations, where the respective concentration curves level off, complexation is assumed complete and higher monomer concentrations will contribute only to non-specific binding and counteract the separation. Knowledge of the association constants between the template and the monomer in solution may thus be used to predict suitable starting concentrations of monomer and template, leading to a larger fraction of high affinity sites. The latter parameter is of particular importance when the template is available only in small amounts, when it is poorly soluble in common diluents or when only a limited saturation capacity is required.

Detailed studies on the PPC provides essential information on the preferred ratios between template and functional monomer within the formed complexes, solvent effects, the influence of the cross linker on the complexation events and the types of occurring molecular interactions. As a result of this, spectroscopic studies of PPC mixtures provide relevant data on the imprinting process. The majority of studies have used either ^{1}H NMR or UV-visible studies to investigate template and functional monomer in porogenic solvents. Complementing NMR and UV methods by ITC and FTIR should augment the obtained results for a rational assessment of optimised polymerisation conditions based on additional validation/confirmation of the derived molecular interactions.

The formation of multiple non-covalent bonds between the template molecule and the functional monomer is vital for the success of a non-covalent imprinting strategy [115]. The observation of bond formation during self-assembly in solution aids in predicting the suitability of a functional monomer to associate with a particular target species. NMR titration experiments facilitate the observation of H bond formation. This is confirmed by studies on the bonding between nucleic acid bases and carboxylic acid bases [116] and H bonding properties of monosaccharides [117].

Evaluating the shift of a proton signal due to participation in a hydrogen bond was used as a selection criterion for suitable monomers and deriving data on complex formation ratios and interacting forces [118]. Furthermore, the investigation of chemical shifts by NMR enables the calculation of association constants [119]. In addition, complexation studies have been performed between 4-L-phenylalanylaminopyridine was determined using ^{1}H NMR and UV-VIS spectroscopy [120], investigating the mechanisms of chiral recognition. While these and similar NMR experiments reveal the potential for NMR experiments in elucidating the nature of molecular level interactions in pre-polymerisation mixtures, the results also indicate limitations when dealing with more complex systems.

UV spectroscopy has been used in titration experiments following the saturation of template molecules with functional monomer building blocks by recording changes of absorbance spectra. Based on these studies rapid estimation of the extent of complex formation with templates such as the dipeptide N-acetyl-L-phenylananinyl-L-tryptophanyl methyl ester [121] and nicotine [122] have been reported. Binding plots from UV studies allowed the calculation apparent dissociation constants and ΔG values.

1.5.8 Solvent considerations

A series of D-phenylalanine MIPs was prepared in the presence of differing diluents with differing hydrogen bonding properties and polarities and the structure, pore volume and surface area of the MIPS were then examined and recognition (rebinding) by HPLC [123,124]. It was found that the hydrogen bonding capacity of the diluent

was the only variable that corresponded with the recognition properties hence, MIPs prepared using the poorly hydrogen bonded diluents showed better (enantio) selectivity than those with greater hydrogen properties, thus, it could be concluded that there is no correlation between morphology and selectivity in this system. This work agrees with other studies showing MIP targeting towards less polar ligands interacting electrostatically with the monomer [126]. In the case of strong electrostatic interactions such as in hydrogen bonded ion pairs, polymerisation can be performed in relatively competitive solvents such as mixtures of alcohol and water with good rebinding selectivities [127]. Increasing the aqueous content is used for imprinting of templates of lower polarities that interact by hydrophobic interactions with the monomer [128]. It is apparent then that the solvent can facilitate or preclude the formation of strong complex interactions as well as affect morphology. In both of these respects the solvent then has comprehensive influence on the shape of the resultant binding cavity produced in the resultant MIP.

1.6 Molecular modelling and computational approaches

Besides the approaches described so far the optimisation of MIP synthesis increasingly utilises molecular modelling based on computational analysis [129]. In principle this approach may be performed without empirical knowledge of the complex in question. However the presence of analytical data can establish a platform for extensive modelling of complex systems including production of data related to the nature of the pre-polymerisation complex in solution or the binding events.

Molecular dynamics methods allow studying complex macroscopic systems or processes by considering small replications of the investigated systems. The relatively small amount of molecules allows generating optimised configurations on an energy surface providing structural and thermodynamic properties. However, comprehensive molecular modelling is challenging mostly due to limitations computational difficulties and the limited accuracy of the force fields characterising the interatomic distances. While predictive modelling is a future aspect computational approaches certainly have the short term potential for a more rapid evaluation of parameters intrinsic to molecular imprinting and for facilitating rational design and optimisation of MIP synthesis.

To elucidate the true nature of the PPC in terms of understanding the factors that drive rebinding of the MIP to a particular template and selective discrimination between the template and similar compounds, a more fundamental knowledge of the development of the PPC and its interaction with its immediate environment i.e. solvent (or porogen) is required. This can be achieved in a number of ways, namely molecular and NMR spectroscopy or by the employment of computational analysis based on molecular modelling. Molecular modelling itself has attracted significant attention throughout the history of the rational design approach to MIPs. The Sybyl software [130], (www.tripos.com) incorporating the LEAP algorithm was employed [131] to generate a library of functional monomers and screen them against templates. Each template-monomer complex was then given a binding energy score and the monomer showing the highest score was deemed to be the most suitable for use in the generation of a subsequent MIP. This approach has proven successful for application to the custom synthesis of numerous polymers by the group of Piletsky. Docking

studies [132] have proven successful in understanding the molecular conformation of template-monomer interactions. Furthermore, site mapping techniques have been shown to be effective in identifying chemical groups for selective interactions and spatial information. Many molecular modelling software packages are capable of this approach, however often the effect of the solvent is neglected and the energy calculation performed *in vacuo*. This can manifest itself in the monomer of choice failing to give the best imprint (in terms of rebinding analysis). Chianella *et al.*, [94] employed sybyl and the structure of abacavir was drawn and its energy minimised both in vacuum (dielectric constant = 1) and in water (dielectric constant = 80) to get stable conformations in such extremely different environments. However the actual polymerisation was conducted in DMF. DMF has previously shown to be compatible with the future use of a MIP in rebinding under aqueous conditions [133].

Given the differences in solvent properties between water and DMF however, the model (in water) may not accurately predict the type (or at least give inaccurate representation of the strength) of the molecular level interactions. For instance water will form hydrogen bonds with template functionalities potentially precluding hydrogen bond formation with the functional monomer. DMF has a lower propensity to form hydrogen bonds however. Table 1.3 and Figure 1.16 are the energy levels and molecular interactions between the template (abacavir) and a selection of functional monomers respectively. Both of these figures are part of Chianella *et al.* [94] and are reproduced here without modification.

Table 1.3 Result of LEAPFROG™ algorithm: tabulated binding energies of complexes between the monomers and abacavir minimised both in vacuum and in water. Reproduced from Chianella *et al.*, [94].

Monomers	Binding energy (kcal mol^{-1}) in vacuum	Binding energy (kcal mol^{-1}) in water
Acrylamide	−33.40	−35.38
Bisacrylamide	−29.25	−31.38
Itaconic acid	−23.99	−27.81
Urocanic acid	−23.50	−23.57
Methacrylic acid	−17.00	−18.39

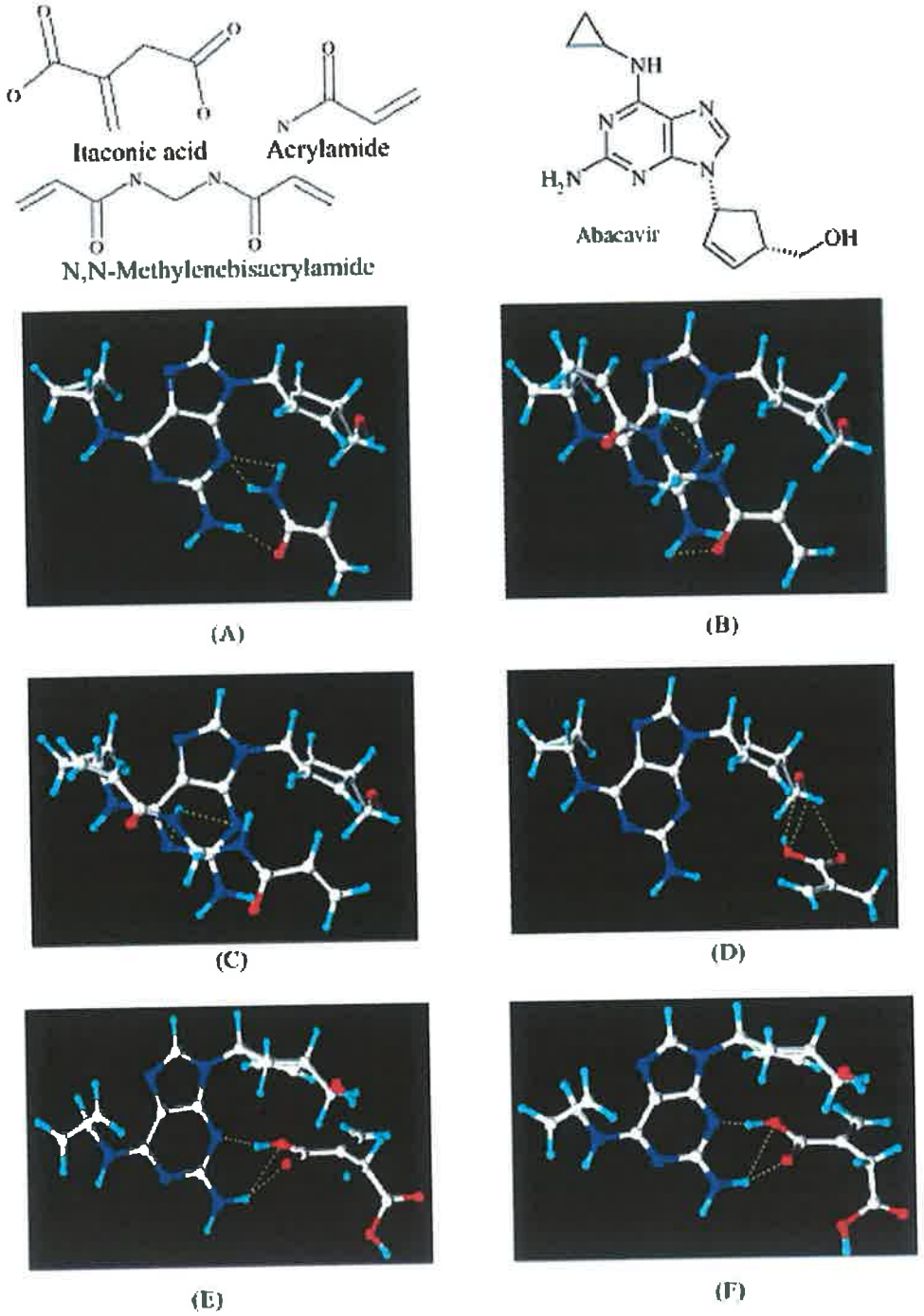

Figure 1.16 LEAPFROG™ results: the interactions between abacavir and the three best monomers (minimised both in vacuum and in water). (A) Abacavir–acrylamide in vacuum; (B) abacavir–acrylamide in water; (C) abacavir–bisacrylamide in vacuum; (D) abacavir–bisacrylamide in water; (E) abacavir–itaconic acid in vacuum; (F) abacavir–itaconic acid in water. Reproduced from Chianella *et al.*, [94].

Molecular simulation software for materials science cerius^2 has also been used to study non-covalent interactions [134]. It was found that electrostatic interactions play a highly significant role in the formation of molecularly imprinted materials. In addition to the above, it was also demonstrated [134] that a molecular substrate without functional groups can still be effective in the generation of imprinted polymers (in terms of the formation of the PPC). The explanation of this phenomenon is that in regards to solvated monomer (or polymer) systems, the presence of the solvent favours the formation of more stable clusters with theophylline than with its analogues or derivatives. This point further emphasises the importance of solvent in molecular modelling and MD simulations. Indeed the importance of solvent in subsequent recognition ability of MIPs has been the subject of several studies [135,136]. Both functional and morphological effects of different porogens on MIPs have been investigated. A comparative study on the influence of porogens on the rebinding ability and selectivity of a MIP towards Nicotinamide was performed [136]. The results of the study found that the properties of the porogen namely hydrogen bond capacity and dielectric constant had significant effects on the interaction energies (ΔE) of the template monomer interactions. Aprotic solvents were predicted to lead to MIPs with better affinity and selectivity. There are other examples of this phenomenon also. A morphological study using SEM on imprinted polymers (made with different porogens) was performed [135]. It was demonstrated that MIPs generated in acetonitrile demonstrated better defined spherical polymer microparticles. Importantly, it was observed that the MIPs prepared with acetonitrile showed greater specific % rebinding that MIPs prepared with the more non-polar dichloromethane. This is further testament to the theory that of polar aprotic solvents (e.g. acetonitrile, DMF) enhancing subsequent rebinding in resultant MIPs.

Molecular dynamics simulations using Amber have also been explored [137]. Amber comprises numerous programs for modelling and MD simulations. Furthermore, a hydrogen bonding interaction was confirmed between 2,4-dichlorophenoxyacetic acid and 4-vinylpyridine in chloroform. In water the dominant interaction in complex formation was shown to be a π-π stacking arrangement. From this study it is again evident that the solvent used has a significant effect on the nature of the interaction of template and monomer in the formation of the pre-polymerisation complex.

Given the diversity of the reported results, it is evident molecular modelling and rational design for next generation non-covalent MIPs require thorough investigation. In particular, information on the interactions of template and functional monomer in the porogen along with their ratios and the properties of the porogen at a molecular level are demanded as they govern the achievable MIP selectivity.

1.7 The study of spatial complementarity

It is of considerable interest to analytically determine whether the functional groups within a binding cavity maintain the spatial arrangement of the complexes formed in the pre-polymerisation solution. Reflectometric interference spectroscopy (RifS) has been employed to study the interaction of molecularly imprinted polymers (imprinted with either (R, R)- or (S, S)-2,3-di-O-benzoyltartraric acid [138]. The interaction between the template(s) and thin polymeric layers was detected. For the imprinted polymers, chiral separation with a separation factor of 1.2 was achieved whereas the reference polymer resulted in no separation (α=0.98). FTIR has been used together with ^{13}C-CP/MAC NMR (cross polarisation magic angle spinning) to quantitatively assess the binding modes of 1,3-diacetylbenzene to templated polymers showing that binding of difunctional molecules to a difunctional site occurs in a stepwise process [139].

Recently, Skogsberg *et al.*, [140] used solid-state NMR measurements to acquire information on the different types of binding sites in imprinted polymers. Template-related structural differences between the materials were revealed by contact time measurements and solid-state NMR. Binding site reoccupation resulted in shorter contact times for nuclei believed to be involved in the binding site interactions. This indicates a lowering of their mobility upon template binding; the template thus acts analogously to a physical cross-linking agent. More detailed information was obtained from suspended-state saturation transfer difference high resolution/magic angle spinning (STD HR/MAS) NMR experiments. These revealed the molecular level details concerning the interactions of the adenine guests with the polymer binding sites. Thus, a relatively larger transfer of magnetization was observed in the solute when bound to the MIP at a position where multiple hydrogen bonds between the analyte and the template can be expected to take place in the MIP only. Together with induced shifts observed in the ^{15}N solid-state NMR experiment, these results proposed a binding site structure involving up to three converging carboxylic acid groups capable of forming complementary hydrogen bonds with adenine containing guests.

Current studies concentrate on characterisation of the PPC and the resulting MIP. In a recent study by Simon *et al.*, [141], a systematic survey of related molecular probes differing in shape or functional group orientation was used to compare the effects of shape selectivity versus pre-organization of functional monomers on imprinting and rebinding performance. These studies revealed that templates with two functional group interactions with the MIPs are influenced to a larger degree by shape selective interactions than templates with three functional group interactions. It was pointed out that the effects of shape selectivity and pre-organization of functional groups do not appear to work in concert with each other during the imprinting process or in the rebinding behaviour. Furthermore, greater selectivity was generally found for templates with two functional groups, where the dominant mode of molecular recognition is shape selectivity. However, pre-organization of functional groups dominated the performance of MIPs elicited toward templates with three template–functional group interactions.

Shape complementarity is also the single biggest factor with regard to the use of molecularly imprinted materials in catalysis [142]. In this study, the shape and stereo-selective esterase activities of cross-linked polymers imprinted with a transition-state analogue for the hydrolysis of amino acid esters was demonstrated. In the study by Lu *et al.*, [61], the contribution of the placement of functional groups in non-covalent MIPs towards selectivity was investigated. 2-L-phenylalanylamino-pyridine, 3-L-phenylalanylamino-pyridine, or 4-L-phenylalanylamino-pyridine were used as template molecules. The polymers exhibited efficient enantiomeric resolution of the racemic mixture of their printing molecules and could hardly resolve the enantiomers of other substrates that were structurally analogous to the imprinting molecules, but different from spatial interaction sites on the polymer with the methacrylic acid residues. These results demonstrate that the shape and spatial orientation of functionality of imprinted binding sites were critical for recognition and the recognition properties of MIPs were greatly influenced by the minor difference of N position on the pyridine ring and caused by the distance accuracy of functional groups in the binding sites. In another study [63] investigating the selectivity features of MIPs recognising the carbamate group, it was pointed out that in terms of structural motifs, which can accentuate selectivity, the carbamate functionality strictly controls the presence/absence of molecular recognition, while shape and dimension of the

substituents modulate the recognition itself. This study also found that the MIPs displayed a marked recognition for analogues that were slightly bigger than the template. This phenomenon may indicate that a particular portion (substructure) of the template molecule is responsible for the generation of imprints. Hence, larger molecules containing the same functionality would still demonstrate a good "fit" to the imprinted cavity.

Molecular level appreciation of the complexation events in the PPC solution, during the rebinding events, and, on the binding site properties is the fundamental basis for a more rational approach to molecular imprinting. This enables the development of thoroughly optimised MIPs with enhanced selectivity. Many studies however only briefly discuss the events occurring during the radical polymerisation process cross linking the present components without delivering due regard to the extent to which the complexes formed in the pre-polymerisation solution survive such polymerisation conditions. MIPs synthesised by thermal or UV initiation do not necessarily demonstrate identical recognition properties. In order to understand this diverse behaviour, on-line monitoring of the polymerisation process, using methods such as *in situ* NMR spectroscopy may provide new insights on the governing mechanisms of molecular imprinting. Furthermore, single molecule microscopy along with orientational studies [138] may be the most suitable technique capable of characterising single binding events in real time within the polymer matrix. It is important to appreciate that the shape selective recognition ability of MIPs will significantly contribute to their ability to recognise biomolecules. In terms of biomedical analysis of peptides and nucleic acids, it is vital that they are recognised in their natural form i.e. not denatured. If a biomolecule were denatured then the ability of a MIP to selectively extract it from an aqueous solution would be lost.

1.8 The characterisation of complex formation in the pre-polymerisation solution by Molecular Dynamics Simulations

1.8.1 Introduction

Molecular dynamics (MD) and Monte Carlo (MC) methods are the two most common simulation techniques used in molecular modelling. These simulation methods generate minimum energy configurations on energy surfaces providing structural and thermodynamic properties within reasonable computational expenses [143,144].
In molecular dynamic simulations [145], successive configurations of a selected system are generated by integration of Newtons laws of motion. Using, the Newtonian equations of motion, potential energy functions are associated with force fields that enable following the displacement of atoms in a molecule over a certain period of time, at a certain temperature and for given pressure. Force field methods allow calculating the energy of a system as a function of the nuclear positions ignoring the electronic motions. MD simulations result in a trajectory, defining the positions and velocities of each particle in the system with time. The system is under the influence of a continuous potential and the motions of all particles in the system are coupled creating a many body problem that cannot be analytically solved [143,144,145]. The equations of motion have to be integrated using finite difference methods based on algorithms such as the Verlet [146,147] or the leap frog [148,149]. A wide variety of algorithms are available for this purpose, depending on the accuracy and efficiency requirements for the application of choice.

The results from the MD simulations demonstrated in this thesis were generated using the AMBER7 (assisted Model Building with Energy refinement) MD computational package [150]. The AMBER package is composed of numerous subprograms. The AMBER programs relevant to this work along with example AMBER parameter and topology file formats are described in appendix A. Further information regarding AMBER 7 software, as well as a more detailed account of the commands is in the AMBER 7 manual at http://amber.scripps.edu.

In general a MD simulation is composed of four stages [144]. Initially a stable configuration of the system is found. Atoms of the molecules and of the surrounding solvent are subjected to a relaxation phase usually lasting for tens or hundreds of picoseconds before the system reaches a stationary state. Thermodynamic properties such as temperature, energy and density are monitored until these values appear stable. The initial non-stationary segment of the simulated trajectory is discarded in the calculation of equilibrium properties. Before performing long (i.e. period of a nanosecond) MD simulations, the system must be equilibrated using volume, pressure and temperature control to adjust e.g. the density of the solvent to experimental values and the temperature of the system to the selected temperature. After equilibration, the production phase is started which will produce the actual simulation results with an MD simulation of approximately 1 ns duration [143].

Basically, the same protocol used in the final stage of equilibration can be used. The MD simulation is simply continued until a satisfactory molecular configuration is obtained. The production MD run is performed at conditions of a constant number of particles (N), volume (V) and energy (E) representing a microcanonical NVE ensemble and allows observation of the molecule(s) of interest interacting with their environment during a pre-determined time interval – usually on the order of nanoseconds [143]. Finally the simulation is analysed. This is represented diagrammatically in figure 1.17 showing the main points of the simulation for the Naproxen/4VP system.

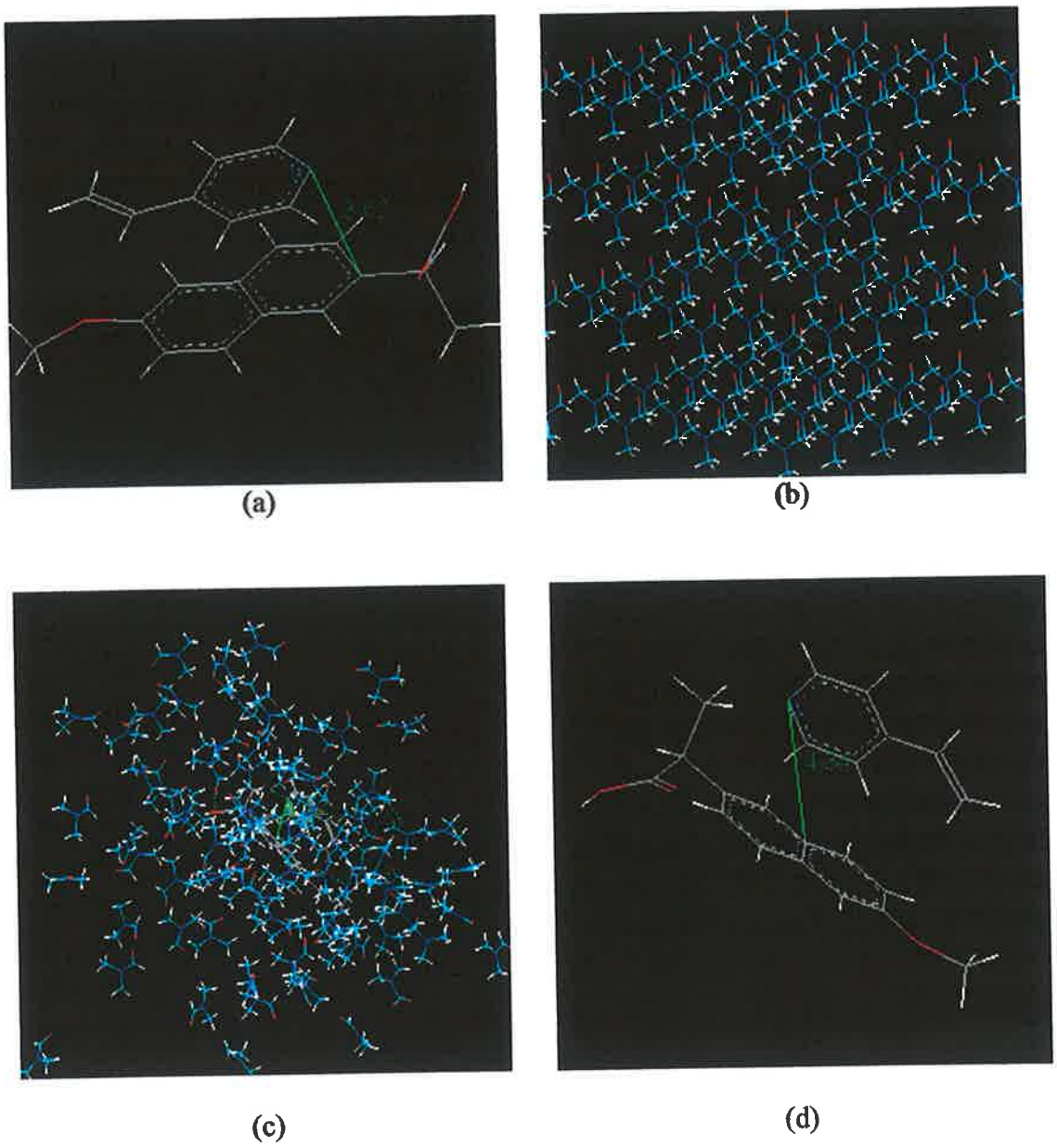

Figure 1.17 shows the highlights of the processing steps for the solvation and MD simulation of the Naproxen/4VP complex in DMF. In (a) can be seen the initial system configuration (π-π stacking). Part (b) shows the unequilibrated DMFBOX for solvation. (c) shows the DMFBOX and complex post simulation and (d) demonstrates the final energy minimised configuration of the complex post MD simulation with the solvent molecules removed for clarity

1.8.2 Solvent models in AMBER

Energy models are used to describe the molecular interactions within the system. The inter-and intra-molecular interactions are illustrated using what are termed empirical energy models. The main components of the force field are stretching, angular bending, torsional and non-bonded interactions. The force field is then defined by a potential energy function. At each stage of the MD simulation, the force applied on each atom is calculated by differentiating the potential function. The force fields 'leaprc.ff99' [151] and 'leaprc.gaff' [152] (GAFF General Amber Force Field) were used within the AMBER package. The ff99 and gaff are 'general purpose' force fields. Both of the forcefields were sourced from LEaP. LEaP is the X-windows based program in the AMBER 7 suite. It allows for basic model building and the creation of topology input files.

Sander – the main program used for molecular dynamics simulations within the AMBER package – implements the forcefields. The intra- and inter-molecular forces within the system can be described by Eqn 1.4 below: [144,150]

$$U(R)=\sum_{bonds}K_r(r-r_{eq})^2+\sum_{angles}K_\theta(\theta-\theta_{eq})^2+\sum_{dihedrals}\frac{V_n}{2}(1+\cos[n\phi-\gamma])+\sum_{i,j}^{atoms}\left(\frac{A_{i,j}}{R_{i,j}^{12}}-\frac{B_{i,j}}{R_{i,j}^{6}}\right)+\sum_{i,j}^{atoms}\frac{q_iq_j}{\varepsilon R_{i,j}} \quad \text{Eqn 1.4}$$

Where U(R) is the potential energy as a function of the position R of N particles.

- The first two energy contributions are energetic penalties associated with the deviation of bonds (bond stretching) and angles (angular bending) from reference values r_{eq} and θ_{eq}.
- The interactions between pairs of bonded atoms (bond contribution) and the summation over valence angles (angle contribution) are modelled by a harmonic potential. K_r and K_θ are force constants.
- The third energy term is a torsional potential modelling changes in energy due to bond rotation (torsion angle φ, phase factor γ, barrier height to rotation V_n).
- The fourth and fifth energy terms are non-bonded terms for non-bonded Van der Waals forces (modelled using a Lennard-Jones potential) and non-bonded

electrostatic interactions (modelled using a Coulomb potential term; distance R_{ij}, and charge q). These terms are calculated between all pairs of atoms (i,j) in any molecule, or in the same molecule but separated by at least three bonds. The Lennard-Jones 6-12 potential is a pair potential describing the energy of interaction between two atoms (i,j) as a function of the distance between their centres. It is characterised by an attractive part varying at R^{-6} and a repulsive part varying at R^{-12}. The term R^{-6} dominates at large distance and the attraction is originated by Van der Waals dispersion forces while the term R^{-12} dominates at short distance and models the repulsion between atoms (i,j) at close proximity.

AMBER uses a leap-frog version of the Verlet algorithm, in which the coordinates are determined at times t, $t + \Delta t$, $t + 2\Delta t$,……, and the velocities at times $t - \Delta t/2$, $t + \Delta t/2$, $t + 3\Delta t/2$, etc. AMBER provides direct support for several solvent models. The default water model is 'TIP3P' [153]. The TIP3P model defines a charge of -0.834e at the oxygen atom and 0.417e at each hydrogen atom. WATERBOX216 is a pre-equilibrated box of TIP3P water. CHCL3BOX is a pre-equilibrated box of chloroform atoms. This is shown in figure 1.18

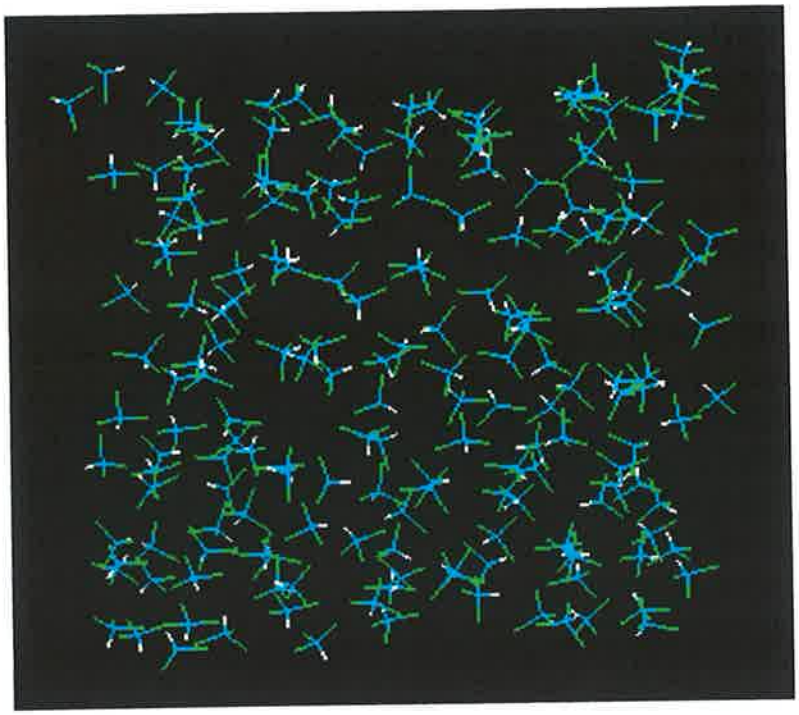

Figure 1.18 The CHCl3 solvation box from AMBER 7

After building up the structure, minimisation and molecular dynamics simulations can be executed.

1.8.3 Boundary conditions

Periodic boundary conditions allow performing MD simulations using only a minimum amount of molecules thus ensuring minimised boundary effects. At these conditions, the molecules are influenced by forces as if they were surrounded by bulk fluid. The molecule(s) are placed in a solvent box of specific size. The box is surrounded with an image of itself in all directions. The solute in the box of interest only interacts with its nearest neighbour images. Since each box is an image of the other, a molecular trajectory resulting in the particle leaving a box would re-enter from the opposite side ensuring the conservation of the total number of molecules and the atoms in the box in agreement with the represented microcanonical NVE ensemble [150]. The box size should be large compared to the range of the interactions present in the system. Long range forces can be a problem in molecular simulations and require specific attention during modelling. In AMBER 7, the particle-mesh Ewald (PME) procedure is used to handle long-range electrostatic

interactions [154], while long range Van der Waals interactions are estimated by a continuum model.

1.8.4 Introduction of restraints during equilibration

In restrained molecular dynamic simulations, additional terms called penalty functions are added to the potential energy function. Internal restraints can be applied to bonds, valence angles, and torsions. The force constants and target values for the restraints can vary during the simulation. The penalty function or violation energy can consist of as many as three types of regions comprising a well with a flat bottom with an "inner" set of upper and lower boundaries r2 and r3 (figure 1.19) [143,144,145].

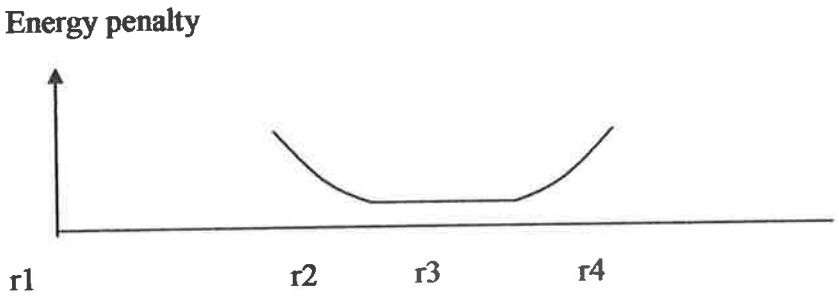

Figure 1.19: Plot of the penalty function. Reproduced from [144]

To the left and right of r2 and r3 the penalty function parabolically rises if the internal coordinate violates these boundaries. Finally, since large violations may lead to excessively large parabolic penalties, these parabolas can turn into linear penalties outside wider upper and lower boundaries (r1 and r4).Default values defined in AMBER 7 along with the penalty functions applied during the studies of this thesis are listed in Appendix B.

MD simulations are a widely accepted technique for simulating solvated molecule(s) in atomic detail. However, for specific applications, such as the study of complex formation in solution new algorithms better suited for the investigated problems may need to be developed. Furthermore, a statistical problem arises when extending simulation results from a single substrate/ligand complex to the ensemble-averaged

data measured in experiments such as NMR. Nevertheless, MD simulations have demonstrated the potential to provide accurate models for experimental observations in complex systems.

1.9 Alternatives to MIPs – molecularly imprinted sol gels

1.9.1 Background – sol gel chemistry

A sol gel is a colloidal suspension that can be gelled to form a solid. The resulting porous gel then is chemically purified and fired at high temperatures into high purity oxide materials. The gel can be modified with a number of dopants to produce unique properties in the resultant glass unattainable by other means. It can be used in ceramics manufacturing processes, as an investment casting material, or as a means of producing very thin films of metal oxides for various purposes, including a form superior to teflon. Sol-gel derived materials have diverse applications in optics, electronics, energy, space, sensors and separation technology.

The sol-gel process is a process for making glass/ceramic materials. The sol-gel process involves the transition of a system from a liquid (the colloidal "sol") into a solid (the "gel") phase. The sol-gel process allows the fabrication of materials with a large variety of properties: ultra-fine powders [155], monolithic ceramics [156] and glasses [157], ceramic fibers [158], inorganic membranes [159], thin film coatings [160] and aerogels [161]. The precursors for synthesizing these colloids consist of a metal or metalloid element surrounded by various reactive ligands. Metal alkoxides are most popular because they react readily with water. The most widely used metal alkoxides are the alkoxysilanes, such as tetramethoxysilane (TMOS) and tetraethoxysilane (TEOS). However, other alkoxides such as aluminates, titanates, and borates are also commonly used in the sol-gel process, often mixed with TEOS. At the functional group level, three reactions are generally used to describe the sol-gel process: hydrolysis, alcohol condensation, and water condensation. The characteristics and properties of a particular sol-gel inorganic network are related to a number of factors that affect the rate of hydrolysis and condensation reactions, such as, pH, temperature and time of reaction, reagent concentrations, catalyst nature and concentration, H_2O/Si molar ratio, aging temperature and time, and drying [155]. Figure 1.20 shows the general reaction scheme for sol gels.

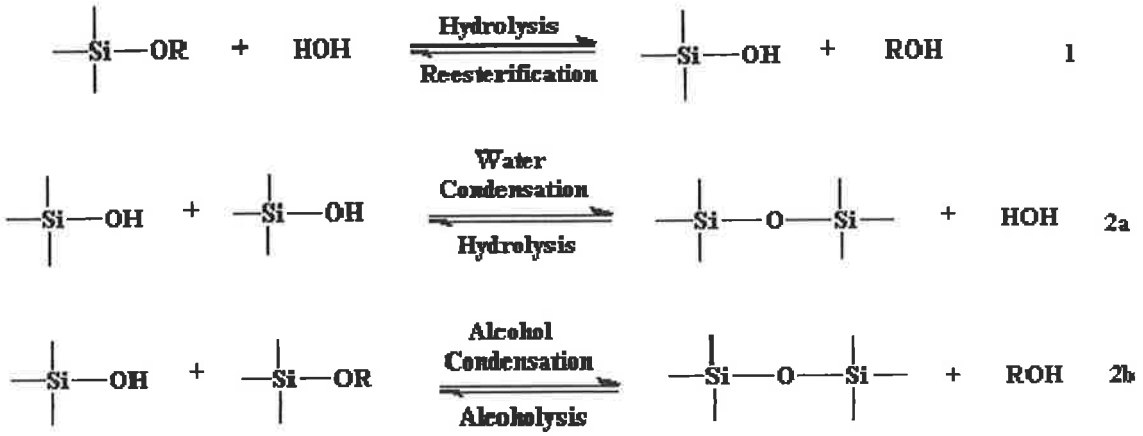

Figure 1.20: the sol-gel process: hydrolysis, water condensation, and alcohol condensation. Reproduced from [163]

1.9.2 Molecularly imprinted sol gels

Pauling [164] first proposed the concept of prearrangement of monomer units around a chemical species (in this case an antigen) in terms of explaining the production of antibodies in mammalian systems. The arrangement of these monomer units around the antigen was achieved by weak intermolecular interactions such as electrostatic interactions , van der Waals forces and by hydrogen bonding. Although abandoned as an immunological concept, the work of Pauling resurfaced in the studies of Dickey *et al.*, [165]. Dickey noted that a silica gel synthesised in the presence of methyl orange exhibited selective memory for this compound when rebinding experiments were performed in the presence of related compound structures (n-butyl, n-propyl and ethyl orange). This (early) process whereby nanostructured silica based solids exhibit selective molecular recognition is now referred to as the imprinted sol gel process. Imprinted sol gels are a rapidly developing area of synthetic receptor science. They have had application in sensor development [166], solid phase extraction or selective clean up [167] for analysis of the specific compounds propanolol [168], 2,4-dichlorophenoxyacetic acid [169], nafcillin [170], for selective discrimination of methylxanthines [171] and in protein/peptide recognition [172,173].

Sol gels based on a silica backbone and inorganic-organic hybrid materials based on organically modified silicas (ormosils) offer an attractive alternative to molecularly

imprinted polymers. Indeed imprinted sol gels possess significant advantages over MIPs, including, ease of preparation, gelation at ambient temperatures (particularly important when preserving weak interactions). In addition to this sol gels exhibit significantly higher porosity and surface area than MIPs along with negligible swelling in organic solvents and good optical (transparent) properties [174].

1.9.2 Comparison with MIPs

Sol gel chemistry utilises mild acid or base catalysed conditions to achieve hydrolysis and condensation of numerous silane monomers. Gelation of the silane(s) such as tetraethyl orthosilicate (TEOS), 3-Aminopropyl triethoxysilane (APTES) and phenyltrimethoxy silane (PTMOS) under aqueous conditions with alcohol cosolvent (usually ethanol or ethoxyethanol) in the presence of a template molecule leads to the imprinted ormosil [175]. The pH of the mixture will determine whether the dominant process is hydrolysis or condensation. At low pH, i.e. acid catalysed sol gels, condensation occurs at an enhanced pace in comparison to hydrolysis. The result of this being that polymer growth is favoured over cross linking. The resultant acid catalysed gel is optically transparent with very small pores and high surface area. Sol gels have significant potential in the development of thin films and layers. A sol gel film has been developed for the analysis of propanolol [168]. A direct comparison between the sol gel and the acrylic based molecularly imprinted polymer was performed. The findings were that the sol gels exhibited a lower total uptake of propanolol but significantly lower non-specific binding. Furthermore, the binding was found to be abrogated when aqueous solutions were replaced with organic solvents. Since it is known that sol gels do not exhibit the same degree of swelling as MIPs do, the loss of affinity may be due to shrinkage of sol gels.

Sol gels in bulk form however have strong potential for use in solid phase extraction and recently these applications have been highlighted [176,177]. Given that swelling and changes in pH should not be as significant an issue as with MIPs, this means that the internal structure of the nanocavities within the sol gel should be maintained when loading in organic solvents or at lower pH's. Furthermore given that the nature of the functional interactions are weak (hydrogen bonding, electrostatic, van der Waals)

spatial complementarity is a considerable determinant of the potential of sol gel selectivity.

1.9.3 Spatial complementarity in imprinted sol gels

Sol gels have been employed for the preparation of catalytic materials [178]. Here it was shown that the amorphous microporous oxide retained structural memory for the kinetic diameter of the alcohol used. This is indicative of the shape of the molecule being a determinant or at least a major component of selectivity. This phenomenon has been further characterised. In this study the imprinting of amorphous bulk silicas with single aromatic rings containing up to three 3-aminopropyltriethoxysilane side groups was performed. The triethoxysilane portions of the molecules side groups were incorporated into the silica framework during synthesis. The aromatic portion is cleaved thus creating a cavity in which the aminopropyl groups are spatially orientated and covalently attached to the pore surface. Leung et al. [169] have employed a tailor made organo-silane3-[*N,N*-bis(9anthrylmethyl)aminopropyltriethoxysilane as a functional monomer forming an acid base ion pair with the template 2,4-dichlorophenoxyacetic acid. The resultant sol gel material displayed good selectivity for 2,4-D over acetic acid and benzoic acid. The authors here have concentrated on selectivity achieved by the functionalities within the pores of the sol gel rather than the shape of the cavity or hydrophobic interaction. A three monomer approach to the sol gel imprinting of lisinopril dehydrate [32] and a similar approach for 2-aminopyridine were used [177]. It is likely that both chemical functionality and spatial complementarity of the binding cavities play significant roles in the potential selectivity of an imprinted sol gel.

The sol gel technique offers a wide range of processing approaches that can produce 3-dimensional matrices in different configurations (thin films, porous materials bulk structures) for use as sorbent and separation materials and sensors. The main approach for the production of molecularly imprinted sol gels is the self-assembly or non-covalent approach. Complex formation results from non-covalent co-ordination interactions. The template is directly added to a sol gel solution prior to acid catalysed hydrolysis and condensation. By using a polar solvent such as ethanol and a non-polar

sol gel precursor imprinted sites are generated by van der Waals, π-π stacking (for aromatic molecules), hydrogen bonding, and electrostatic interactions between the template and the sol gel network. The solvent is then evaporated at elevated temperatures (c.80°C) yielding a solid porous material. The precursor must be chosen so as to enhance the porosity hence facilitating diffusion of the template through the gel. Post drying, the template needs to be extracted using a suitable solvent.

1.10 Investigated template analytes

1.10.1 Caffeine

Caffeine is a central nervous system and metabolic stimulant and is used both recreationally and medically to reduce physical fatigue and restore mental alertness when unusual weakness or drowsiness occurs. Caffeine stimulates the central nervous system first at the higher levels, resulting in increased alertness and wakefulness, faster and clearer flow of thought, increased focus, and better general body coordination, and later at the spinal cord level at higher doses. Caffeine is metabolized in the liver by the cytochrome P450 oxidase enzyme system (specifically, the 1A2 isozyme) into three metabolic dimethylxanthines

- Paraxanthine (84%) – Has the effect of increasing lipolysis, leading to elevated glycerol and free fatty acid levels in the blood plasma.
- Theobromine (12%) – Dilates blood vessels and increases urine volume. Theobromine is also the principal alkaloid in cocoa, and therefore chocolate.
- Theophylline (4%) – Relaxes smooth muscles of the bronchi, and is used to treat asthma. The therapeutic dose of theophylline, however, is many times greater than the levels attained from caffeine metabolism.

The structure of caffeine and its main metabolites is shown below in figure 1.21

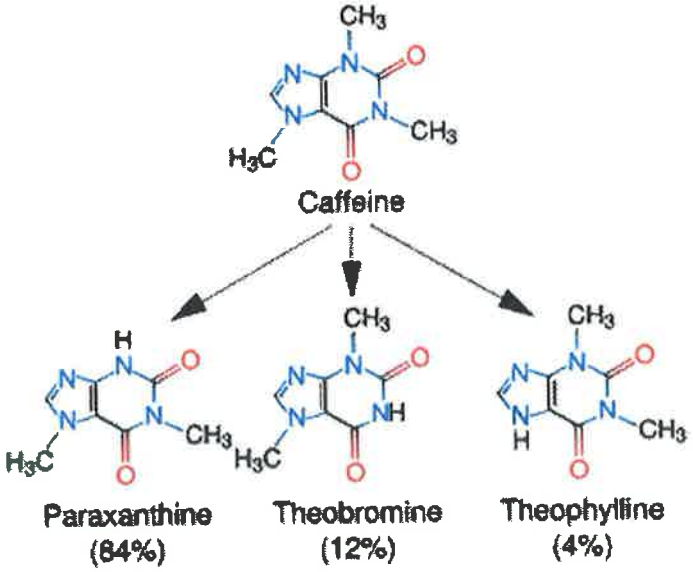

Figure 1.21: Caffeine is metabolized in the liver into three primary metabolites: paraxanthine (84%), theobromine (12%), and theophylline (4%)

Numerous extraction techniques have been developed for caffeine and its analytical determination is well documented. It is easily extracted by conventional SPE means. The rationale for the selection of caffeine as a template for the development of a MIP was as proof of principle and to develop the methods (NMR, basic molecular modelling and MISPE) which would form the basis of the remainder of the studies. Given that caffeine MIPs have been produced, the results obtained would be comparable to the work of other researchers in the area.

1.10.2 Methotrexate

Methotrexate (MTX) is a folic acid antagonist and blocks the intracellular enzyme dihydrofolate reductase, thereby disrupting the synthesis of nucleic acids. The effect is almost always independent of species i.e. the metabolism of all rapidly proliferating cells is affected in the same way. A serum level of 10^{-8}mol has a strong inhibiting effect on dihydrofolatereductase [179]. For this reason, the substance is highly toxic and is classified as "toxic" in the EU and "very toxic" in the U.S.A. In addition to acute effects, chronic toxicity (teratogenicity, mutagenicity) may be assumed. MTX is a promising marker (tracer) of the contamination levels of workspaces due to both surface-to-surface carry over e.g. from spillage or gloves and to aerosol transport e.g. from syringe manipulation procedures. In fact, MTX is a polyelectrolyte, with a high water but low organic solvent solubility, a negligible vapour pressure and a high chemical robustness to environmental stress. It is widely employed not only in oncologic chemotherapy but also as a general immunosuppressant in the therapy of autoimmune diseases.

The molecule of MTX is composed of a heterocyclic portion (a 2,4-diamino-substituted ring) linked to a ρ-aminobenzoyl portion, which is in turn amide bonded to a glutamic acid unit. The molecule is thus a polyelectrolyte carrying two carboxyl groups with dissociation constants (pK_a) of 3.36 (α-carbon) and 4.70 (β-carbon) – and a number of potentially protonated nitrogen functions, the most basic of which is the guanidinic *N*-1 on the pterine ring (pK_a 5.71). Its water solubility is pH dependent ranging from 0.9mM at pH 5 to 20nM at pH 7.The structures of MTX and its main metabolites are shown below in figure 1.22:

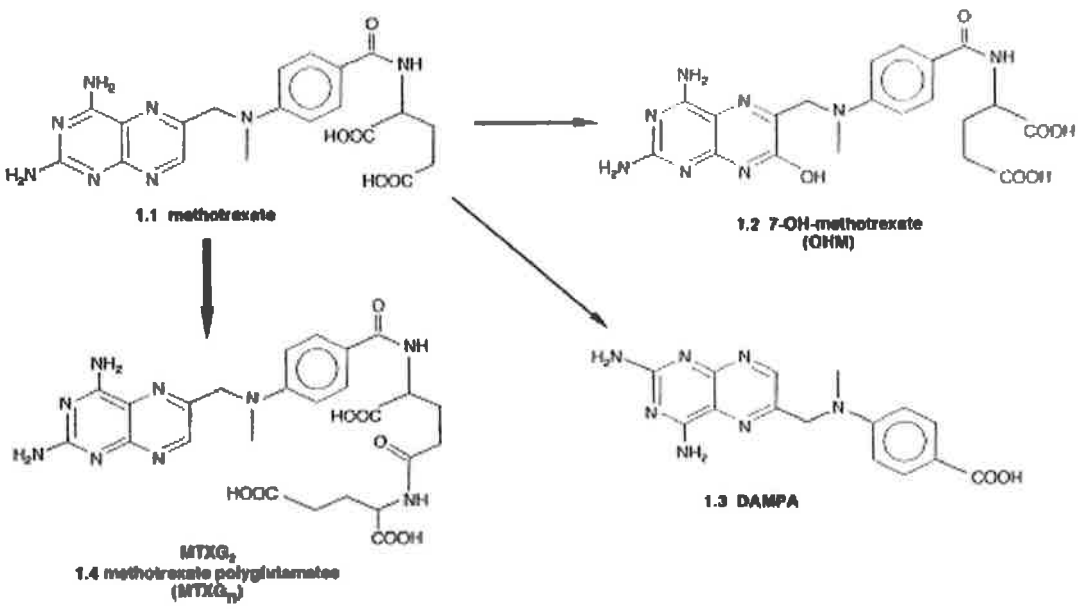

Figure 1.22: Structures of MTX and its major metabolites. Reproduced from Maria Rubino [180]

MTX is one of the few anticancer agents for which therapeutic drug monitoring is currently employed in clinical practice. MTX can be measured in biological samples by a number of different analytical techniques: bioassays, immunoassays, chromatography, (each method having its own advantage in terms of sensitivity, specificity, speed, cost). The search for monitoring of therapeutic drug levels in easy to collect biological fluids such as saliva, which are an alternative to the invasive venipuncture, has triggered interest. A simple, specific assay with a low limit of detection to determine qualitatively methotrexate in hospital environments and work areas would be of great use.

1.10.3 Ibuprofen, ketoprofen and naproxen

Ibuprofen is a non-steroidal anti-inflammatory drug (NSAID) originally marketed as Nurofen. It is used for relief of symptoms of arthritis, primary dysmenorrhoea, fever, and as an analgesic, especially where there is an inflammatory component. Ibuprofen is an NSAID which is believed to work through inhibition of cyclooxygenase (COX), thus inhibiting prostaglandin synthesis. There are at least 2 variants of cyclooxygenase (COX-1 and COX-2). Ibuprofen inhibits both COX-1 and COX-2. It appears that its analgesic, antipyretic, and anti-inflammatory activity are achieved principally through COX-2 inhibition; whereas COX-1 inhibition is responsible for its unwanted effects on platelet aggregation and the GI mucosa.

Ibuprofen, like other 2-arylpropionate derivatives (including ketoprofen, flurbiprofen, naproxen) contains a chiral carbon in the α-position of the propionate moiety. As such there are two possible enantiomers of ibuprofen with the potential for different biological effects and metabolism for each enantiomer. (*S*)-(+)-ibuprofen (dexibuprofen) is the active form both *in vitro* and *in vivo*. Further *in vivo* testing, however, revealed the existence of an isomerase which converted (*R*)-ibuprofen to the active (*S*)-enantiomer. Thus, due to the expense and futility that might be involved in marketing the single-enantiomer, most ibuprofen formulations currently marketed are racemic mixtures. Ibuprofen along with its structural and functional analogues ketoprofen and naproxen is shown in figure 1.23 (sigma)

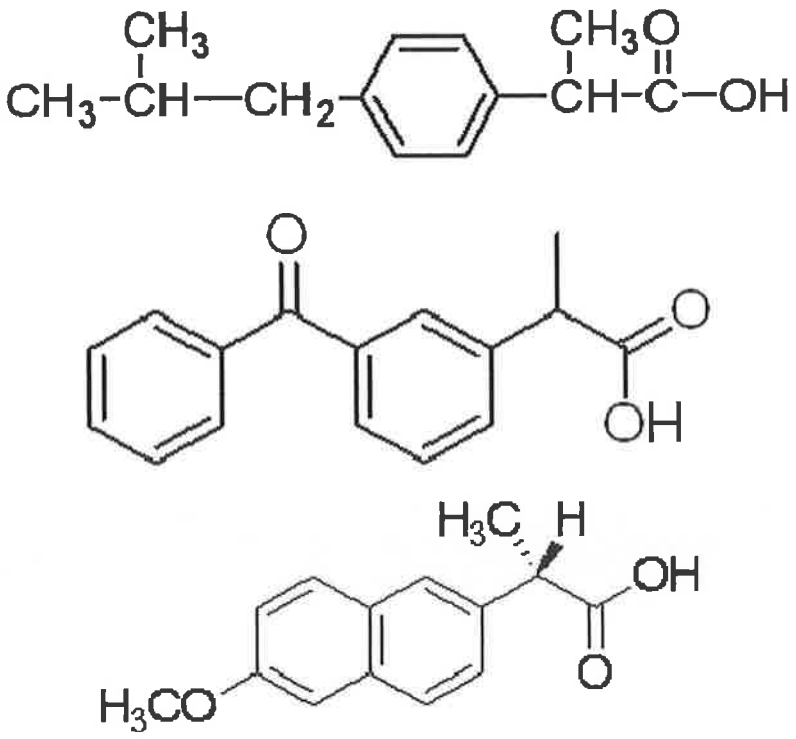

Figure 1.23: Ibuprofen (top) long with the analogues ketoprofen (middle) and naproxen (bottom).

Since the analogues of ibuprofen have a similar in vivo effect, (in essence they act upon the same receptors), they are interesting candidates to study the selectivity of an artificial receptor. The three molecules possess similar functionalities however the shape and spatial arrangement of the functionalities within each of the molecules differ considerably. As such they are good candidates to assess the contribution of shape complementarity towards rebinding.

Chapter 2

Predicting the performance of molecularly imprinted polymers: Selective extraction of caffeine by molecularly imprinted solid phase extraction

2.1 Introduction

The general theory of molecular imprinting suggests that it affords a relatively straight-forward method of establishing molecular recognition via functional groups incorporated within a highly cross linked polymeric monolithic phase or matrix [181]. What has accounted for the greatest number of applications of imprinted polymers, in terms of the volume of published reports, is use of the imprinted polymers as selective solid phase extraction sorbents or HPLC stationary phases [182]. The aim of this work was to develop a molecularly imprinted polymer to selectively extract caffeine, a methylxanthine, by means of the aforementioned solid phase extraction. Furthermore, it was anticipated that this would yield a somewhat greater level of appreciation of template rebinding, thus leading to a higher degree of exploitation and development of MIPs for use in SPE.

The method applied for the manufacture of the MIP in this instance was bulk polymerisation. A conventional highly cross linked methacrylate (EGDMA) based polymer with a variation in functional monomer type and ratio and hence functional group was used. It was anticipated that this would introduce disparity in the recognition element and thus differences in selectivity would correspond to variations in functional monomer. The process involved polymerisation of the functional monomer with the cross linking agent in the presence of the template to form the monolith. The bulk polymer produced is then ground to a fine and uniform consistency and packed dry into solid phase extraction cartridges. This then means that the polymer is acting as a solid stationary phase. Evaluation occurs by subjecting the sorbent to a standard solid phase extraction procedure and testing its ability to selectively isolate and concentrate the required template from a mixture.

The analyte chosen for this initial study was caffeine, a methylxanthine. Xanthines are well studied compounds. MIPs against theophylline have been used in bulk form for separations [181-184] and binding assays [185] and a caffeine MIP for use in SPE of blood plasma has been constructed by Theododoris *et al.*, [186]. Caffeine represents a model compound for the development of MIPs having been the subject of several studies ranging from separations [187] to caffeine MIPs as sensing elements [188]. Also, several studies have used caffeine as a model compound to investigate

alternative MIP formats [189,190]. The structures of caffeine and theophylline are shown below in figure 2.1

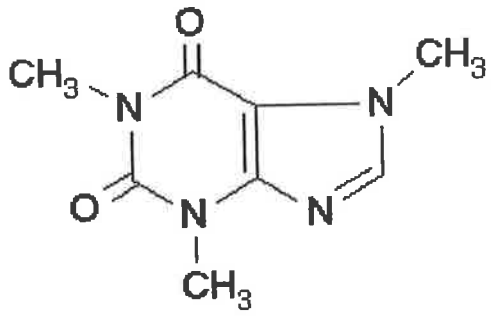

Figure 2.1 (a): Caffeine

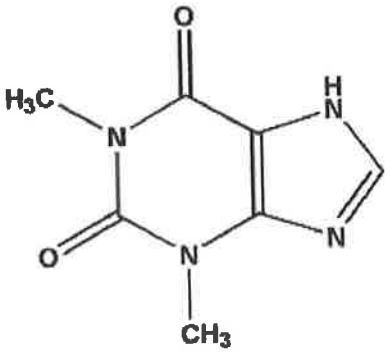

Figure 2.1 (b): Theophylline

As can be seen both structures are very closely similar. The molecules were chosen for their structural simplicity and the fact that they are well characterised and easy to work with. Caffeine is one of the most common analytes studied in modern instrumental analysis. It is expected that the presence of the lone pair of electrons on the aromatic nitrogen of the caffeine molecule would facilitate interaction with the –OH group on the methacrylic acid monomer yet not with the 2-vinylpyridine monomer (both shown below in figure 2.2)

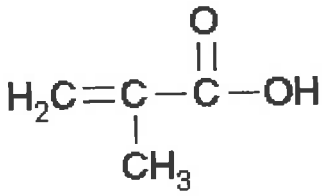

Fig 2.2 (a) methacrylic acid

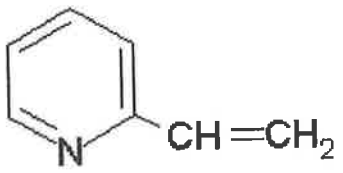

Fig 2.2 (b) 2-vinylpyridine

The main advantage that MIPs possess over conventional solid phase extraction packing materials is their selectivity. Retention mechanisms of many of the commonly employed SPE materials are based on hydrophobic interactions and a major drawback of SPE can be the co-elution of interfering species. The nature of the MIP – template rebinding is such that non-specific interactions such as hydrophobic should be minimised due to the fact that other compounds will not form the same interactions with the functional monomer. This is also in part owing to the nature of the shape arrangement of the complex. This is related to the character of the actual cavities (pores) themselves or "binding pockets". In this regard, the relative size distribution of the pores is critical to the arrangement of the binding site locations which are located within the pores. A crucial aspect of engineering MIPs with pores of defined size distribution is the choice of porogen. Typical pore forming solvents include acetonitrile, ethyl acetate whereas non-polar solvents such as chloroform and tend to not form a porous matrix with high surface areas. As a general rule by increasing the volume of porogen used in the polymerisation process or decreasing the amount of cross linker will lead to a greater pore size distribution (meso–macropores). Decreasing the volume of porogen or increasing the amount of cross linker will lead to polymers of smaller average pore sizes.

In this respect it would be advantageous to engineer the polymerisation conditions and process to optimise the efficiency of the resultant MIP in terms of rebinding. Traditionally, the production of imprinted polymers has been based on the trial and error approach. This method involved the generation of numerous MIPs for a particular template. Typically, relative ratios of template to functional monomer were varied. In addition, the volume of cross linker is varied together with the porogen itself. All of the polymers constructed are washed, sieved to appropriate size and tested for effectiveness in rebinding studies. This process is labour intensive, laborious and wasteful of laboratory resources. Hence, to improve the efficiency of selection of suitable MIPs attention is now turning towards a more calculated approach to the design of imprinted polymers. This method has been termed the rational design approach and is discussed in chapter 1. In order for this to be effective, a greater level of understanding of the molecular level events surrounding the formation of the pre-polymerisation complex is required. Furthermore, knowledge of the stability of the complex during the early stages of the polymerisation is desirable.

Within the field of molecular imprinting NMR spectroscopy is now being widely used to predict the influence of ratios of template to functional monomer Molecular modelling software is a relatively newer tool in this regard. Its potential has been recognised in various recent reports. In this chapter the Hyperchem 7.5 molecular modelling software has been employed.

The application of NMR spectroscopy and molecular modelling software in elucidation of the nature of non-covalent interactions present during the formation of the pre-polymerisation complex is demonstrated. Firstly, a number of MIPs for caffeine were synthesised based on the data acquired from the NMR and modelling studies and assessed (in terms of rebinding) by solid phase extraction. Secondly, and based on the SPE results, two MIPs were selected for analysis by nitrogen porosimetry, a MIP which had performed well and one which had been unsuccessful. Both the surface areas and the pore size distributions were analysed by nitrogen porosimetry.

2.1.1 Aims and objectives

This chapter aims to show that the data obtained from the modelling and NMR studies allied to the post polymerisation pore size data allow the engineering of functional MIPs. The basis of this engineering is an enhanced understanding of the nature of complex formation and behaviour of the complex during polymerisation. A rational design approach was taken to the planning and synthesis of a molecularly imprinted polymer capable of extracting caffeine (the template molecule) from samples containing caffeine. Data from NMR titration experiments in conjunction with a molecular modelling approach were used in predicting the relative ratios of template to functional monomer and furthermore determined both the choice of solvent (porogen) and the amount used for the study. It was further intended that post polymerisation analysis of the polymer itself by analysis of the pore size distribution and surface area would yield significant information regarding the size and distribution of the pores within the polymer matrix. Here is proposed a stepwise procedure for the development and testing of a molecularly imprinted polymer using a well studied compound – caffeine - as a model system. It is shown that both the

physical characteristics of a molecularly imprinted polymer (MIP) and the analysis of the pre-polymerisation complex can yield vital information that can predict how well a given MIP will perform.

2.2 Experimental

2.2.1 Materials

Acetonitrile, methanol, water (HPLC grade), caffeine, theophylline, theobromine, methacrylic acid, (MAA), ethylene glycol dimethacrylate, 2-vinylpyridine, sodium phosphate were purchased from Sigma-Aldrich (Dublin, Ireland). Azoisobutyronitrile was purchased from Fisher Scientific (UK). Deuteratated acetonitrile, methanol and chloroform were purchased from Apollo Scientific (Bredbury, UK) and used as supplied. 2-Vinylpyridine, methacrylic acid and Ethylene glycol dimethacrylate (EGDMA) were purified by vacuum distillation prior to use in order to remove inhibitors. The 25 μm mesh size sieve used was purchased from Retsch.

2.2.2 Preparation of imprinted polymers

One mmol of template (caffeine 194.19 mg) was dissolved in 4 or 8 ml acetonitrile or chloroform in a borosilicate test tube. To this was added 4 mmol of MAA (344 mg). The mixture was stirred at room temperature for 5 min. EGDMA, 20 mmol (4167 μl) was then added followed by AIBN, 50 mg per polymerisation. The ratio of EGDMA to functional monomer was kept below 10:1. The mixture was stirred for a further 10 min to ensure complete dissolution of all the components. The mixture was then sonicated for 10 min. In order to completely degas the solution it was sparged with N_2 for 5 min. The tubes were then plugged under vacuum and gradually heated to 60^0C in a water bath. A 16 hour polymerisation time was used. Following polymerisation, the tubes were smashed and the polymer was removed. The polymer was broken up before being ground with a mortar and pestle and finally ground by hand. The particles were then sieved to <25 μm using acetone. Repeated cycles of grinding and sieving were necessary in order to acquire enough of the polymer (200-300 mg) at size <25 μm. Smaller particles (<5μm) were removed by standing in acetone. Typically, 100 ml of acetone was added to the polymer in a graduated cylinder. The polymer was allowed to settle for ~1 hour and then the acetone was removed. This was repeated 4-6 times per polymer. Control polymers were prepared in the same way with the omission of template. As regards washing, following sieving to the correct

particle sizes, the MIPs were washed in a solution of hot methanol with 10% acetic acid. The solution was also stirred vigorously. This procedure was repeated numerous times until no trace of caffeine could be detected in the washings. HPLC was used to analyse the washing solutions. During the solid phase extraction procedure the packed cartridge was pre-washed (before) conditioning with both methanol and acetonitrile. These pre-load washings were analysed and no caffeine was found.

2.2.3 NMR Analysis

All NMR spectra were recorded on a Brucker 400 MHz instrument at 25^0C. The volume for analysis was 750 µl and the concentrations of both caffeine (template) and functional monomer substitute were 0.04 *M*. The deuterated solvents used were acetonitrile and chloroform. Processing of spectra was performed on a silicon graphics workstation operating off a UNIX platform.

2.2.4 Molecular modelling

The molecular modelling software program used for this study was Hyperchem 7.5 (Hypercube inc., Gainsville, Florida). The structure of caffeine, theophylline and the functional monomers (methacrylic acid and 2-vinylpyridine) were drawn in the Hyperchem program and minimised to the lowest energy conformation allowed by the molecular mechanics (MM+) method and then refined using the semi-empirical mechanic (PM3) method. The conformation of lowest energy was refined with an *ab initio* (3-21 G) quantum mechanic basis set. To analyse possible interactions between template and functional monomer and for calculation of binding energies, the Amber MM method was used. The force–field was set up with constant dielectric and van der Waals and electrostatic scale factors as 0.5. The calculation of the binding energies (between template and monomer) was performed using Equation 2.1 shown below:

$$\Delta E = [E_{complex} - E_{caffeine} - E_{monomer}] \qquad \text{Eqn 2.1}$$

2.2.5 UV-VISIBLE mole ratio analysis

A molar ratio plot was constructed by the systematic variation of the relative molar ratio of caffeine and methacrylic acid. The initial concentration of both compounds was 0.4 *M*. The concentration of the caffeine was kept constant and the ratio of methacrylic acid was increased from 1:0 to 1:5. The total volume for each analysis was 3 ml and all UV –Visible spectra were recorded at 272 nm. For control studies MAA was added to the same volume of water at increasing concentrations but without the presence of template.

2.2.6 Molecularly Imprinted Solid Phase Extraction (MIPSE)

Empty plastic solid phase extraction cartridges were used for this study. A 200 mg weight of the dry polymer was placed into the cartridges with frits at either end. The system was washed through thoroughly with acetonitrile to remove any air bubbles that may affect solvent flow. The packed polymer was further washed with methanol to ensure the absence of caffeine and to study the effectiveness of the washing procedure. The extraction experiments involved loading the MIP-SPE column with a 1 ml aliquot of a solution of 50 μg ml^{-1} of caffeine. All SPE experiments were performed using VacMaster 20 SPE processing system. Samples were loaded in 50 mM Sodium phosphate. A first wash in the same buffer (1 ml) was followed by a second in 1% TEA in acetonitrile also 1 ml. Elution was performed using 1ml of 1% acetic acid in acetonitrile. All solutions were evaporated to dryness under N_2 and reconstituted in 800 μl methanol

2.2.7 Sample preparation

Samples of Red Bull™ a high caffeine soft drink containing 32 mg of caffeine per 100 ml (amongst other ingredients) were diluted 1/100 with water and applied directly (1ml) to the MIP SPE column. Also the undiluted Red Bull was applied to the column (also 1 ml).

2.2.8 HPLC determinations

HPLC analyses were conducted on a Hewlett Packard series 1050 system with a Rheodyne injection valve using an Alltech BRAVA ODS column (25 cm x 4.6 mm, particle size 5μm). The mobile phase was a 80:20 v/v mixture of 0.05M aqueous sodium phosphate: Methanol and the flow was maintained at 1.0 ml/min. A 10 μl injection volume was used for all analyses. Separations were performed at 25^0C (isocratic elution). The wavelength used for detection was 272 nm.

To facilitate quantitative determinations in extracts a calibration curve was constructed. Reference standard solutions of caffeine and theophylline at concentrations 0.1, 0.5, 1, 5, 20, 50, 100 and 200 μg ml^{-1} were determined in triplicate and the peak areas were plotted against the concentrations.

2.2.9 Pore size and surface area analysis

Pore size distribution and surface areas of the washed polymers were analysed by Nitrogen porosimetry (using the Brunauer-Emmett-Teller (BET) method). The analysis was performed on an ASAP 2010 from RMIT Applied Chemistry (Micromeritic). A 300 mg quantity of the dry polymer was used for analysis. Relevant information was obtained as follows: A plot of pore size vs. incremental pore volume gave pore size distribution. A plot of pore size vs. pore volume gave total pore volume. The surface areas and total pore volumes of the polymers were also obtained.

2.3 Results and discussion

2.3.1 Molecular modelling of template – monomer interactions

In order to study the interactions between monomers and caffeine, a series of molecular modelling interaction studies was performed using the Hyperchem 7.5 software package (Gainsville, Florida). Molecular modelling is useful in this regard as it allows the calculation of the partial charges on each of the atoms of the molecule [192-194].

Figure 2.3 presents the partial charges calculated for the caffeine molecule:

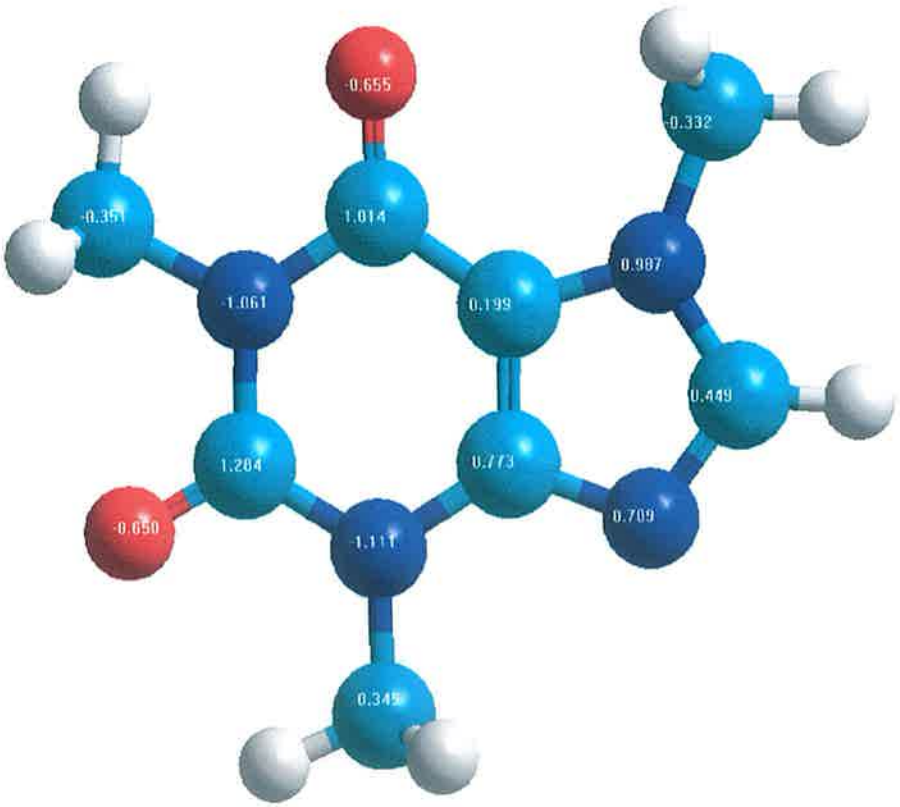

Figure 2.3: The partial charges obtained by molecular modelling of atoms on the caffeine molecule. Nitrogens are represented in blue, carbons in green and oxygens in red. Hydrogens are shown in white and always have partial charges between 0.2 and 0.29.

From this it can be seen that there are several sites on the molecule capable of undergoing electrostatic or hydrogen bonding interactions. In particular the two nitrogens of the 5 membered ring and both of the oxygens are likely to become hydrogen bond acceptors with a proton present in a functional monomer.

Dong *et al.*, [108], have used the calculation of partial charges on the theophylline molecule as an indication of the hydrogen bonding capacity of each of the oxygen, nitrogen and hydrogen atoms (in terms of being a donor or acceptor). The molecular modelling method employed here shows that there is some degree of delocalisation of electrons of the nitrogen atoms on the 5-membered ring. Looking at the model of methacrylic acid shown in figure 2.4a, it can be seen that the nitrogens (of caffeine) may participate in hydrogen bonding with the proton on the hydroxyl group. Figure 2.4b shows the model of 2-vinylpyridine. Here it can be seen that caffeine could form a hydrogen bonding interaction or ion pair with the nitrogen of 2-vinylpyridine although the caffeine protons may not be sufficiently acidic.

(a)

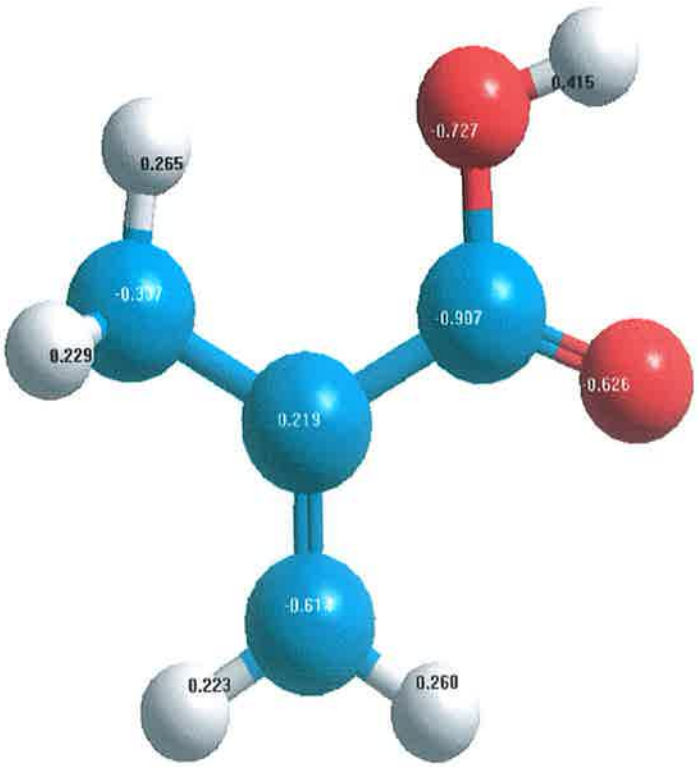

(b)

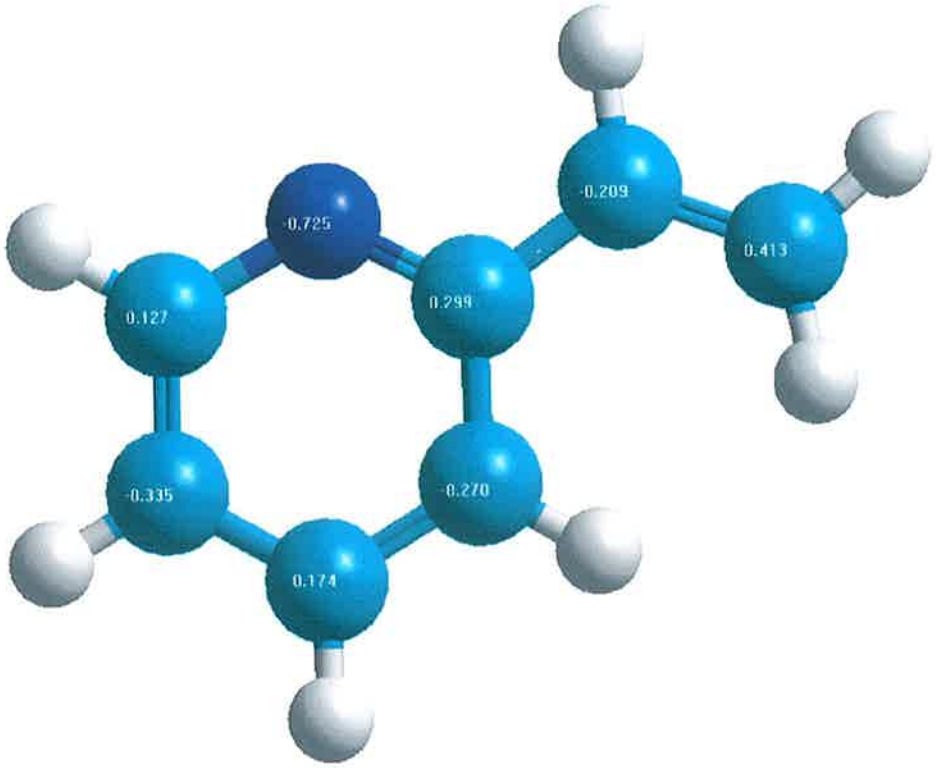

Figure 2.4a shows the hyperchem calculated partial charges for methacrylic acid (MAA) and figure 2.4b illustrates the partial charges for 2-vinylpyridine (2Vpy). Nitrogen = blue. Carbon = green. Oxygen = red. Hydrogen = white.

In order to evaluate the possibility of template monomer interactions, the binding energies (ΔE) of caffeine with methacrylic acid and 2 vinylpyridine were calculated and are shown in table 2.1. It is documented [44], that when a library of functional monomers is screened against a template using molecular modelling software, the monomers giving the highest binding energy are more likely to form strong complexes. Table 2.1 shows that ΔE (MAA) > ΔE (2Vpy).

Table2.1: Calculated binding energies (ΔE) of caffeine with methacrylic acid, 2-vinylpyridine and 4-vinylpyridine in vacuum

Molecules	Energy ($kJ\ mol^{-1}$)	ΔE (Binding energy) ($kJ\ mol^{-1}$)
Caffeine	-24.74	-
Methacrylic acid	-36.63	-
2-Vinylpyridine	-12.52	-
Complex (Methacrylic acid)	-77.27	-38.41
Complex (2-Vinylpyridine)	-56.04	-17.95

This is indicative of complex formation between caffeine and methacrylic acid being stronger than with 2 -vinylpyridine. Hence, the Hyperchem study predicts that a MIP for caffeine generated with methacrylic acid is more likely to have greater rebinding and selectivity than a MIP manufactured with 2- vinylpyridine. The mechanism of interaction is likely to be hydrogen bonding. For refinement of the conformation of the complex post minimisation the PM3 semi-empirical method was used. According to reports [194], the PM3 method is computationally very efficient. Furthermore PM3 has been shown to be superior to AM1 in modelling of biochemical interactions [195]. This is due to an improvement in the treatment of non-covalent interactions and in particular hydrogen bonding, van der Waals forces and interestingly, steric effects. This is a good rationale for the selection of the PM3 method for the modelling of imprinted polymer pre-polymerisation complexes. The flexibility of the PM3 method is demonstrated in a study on the CE separation and theoretical study of inclusion complexes of cyclodextrins with estrogen hormones [196]. Both PM3 and AM1 are derivatives of the MNDO (modified neglect of differential overlap) force field. Essentially they are both approximate molecular orbital theories and are composed of a group of force fieldsdesigned to approximate the lengthy calculations necessary for *ab initio* modelling studies. They require significantly less computational resources while giving a high level of accuracy by considering only valance electrons rather than considering a full treatment of the molecules electrons e.g. by incorporating Slaters rules.

Furthermore, molecular modelling, in this case, can also be used to analyse the likely molar ratio of the interactions. Table 2.2 presents the binding energies (ΔE) for the further addition of molecules of methacrylic acid to the system:

Table 2.2: Calculated binding energies on addition of further molecules of methacrylic acid to the system (in vacuum)

Amount of methacrylic acid molecules	ΔE (Binding energy) (kJ mol^{-1})
1	-38.41
2	-60.28
3	-65.84
4	-52.12

Interestingly, the binding energy increases significantly upon the addition of a second molecule of methacrylic acid however the addition of a 3rd or a 4th molecule to the system produces little change in ΔE. This would indicate that the energy of the system is optimal and further additions of functional monomer will not lead to a greater level of complexation. This is in contrast to conventional thinking in non covalent imprinting in which an excess of functional monomer is used in order to ensure that the template molecule is fully complexed. In short, the Hyperchem molecular modelling studies point towards methacrylic acid forming a strong complex with caffeine at a 1:2 ratio of template: functional monomer. Figure 2.5 shows the Hyperchem predicted complex structure between caffeine and the two molecules of methacrylic acid. Two limitations of the method described are firstly that solvent is not considered in the energy calculations and secondly that monomer – monomer or template – template interactions are not considered in the calculation. Given these considerable drawbacks, it must be considered that the semi-empirical methods can act as a guide only for selection of suitable monomers and monomer template ratios.

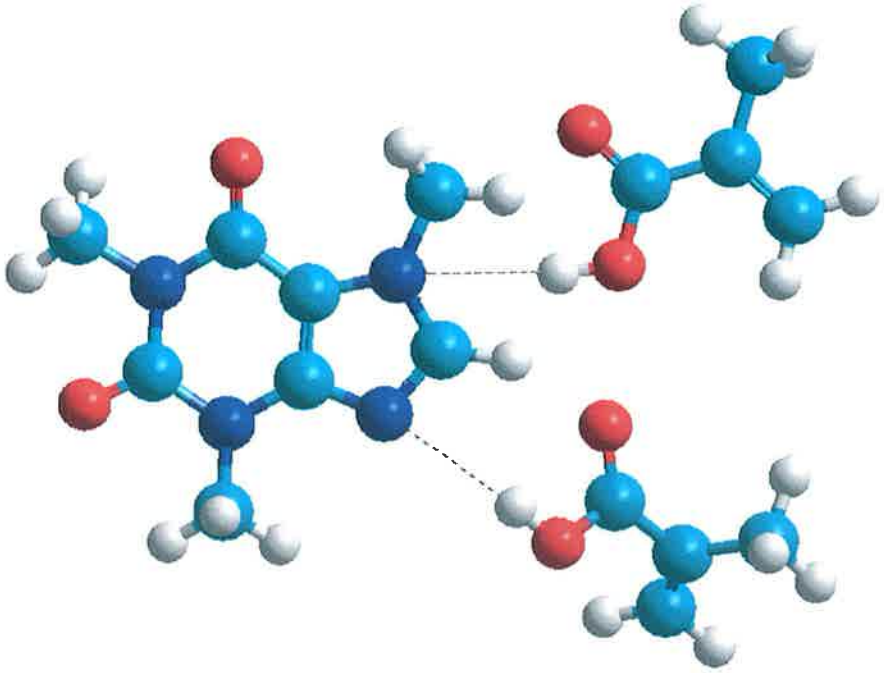

(a)

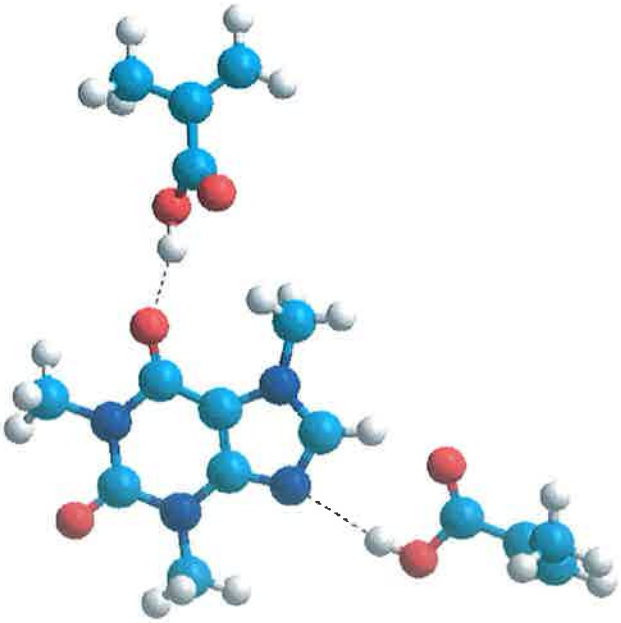

(b)

Figure 2.5a: The Hyperchem derived structure of the complex formed between the caffeine molecule and two molecules of methacrylic acid. The presence of hydrogen bonds is indicated by the dashed white lines. Figure 2.5b shows an alternative possible configuration

2.3.2 Spectral analysis of template – monomer interaction

2.3.2.1 NMR

The molecular modelling studies using Hyperchem have suggested the possibility of hydrogen bond formation between the caffeine proton and the –OH of methacrylic acid. Also possible is the interaction of the –OH of methacrylic acid and the nitrogen atoms of the 5 membered ring on the caffeine molecule. This has been shown by the increased stabilisation of the complex relative to the use of 2Vpy. However given the drawbacks of the modelling method as outlined, NMR stidies were performed to gauge potential interaction between the two components in solvent. The interaction of the template and methacrylic acid and 2-vinylpyridine were further characterised by proton NMR. NMR techniques have been widely employed for the study of pre-polymerisation complexes in MIP rational design approaches. To a solution of caffeine in deuterated acetonitrile (CD_3CN) or deuterated chloroform ($CDCl_3$) was added an equimolar concentration of deuterated acetic acid (substituted for methacrylic acid for clarity of the spectrum). The effect of the addition of deuterated acetic acid on the chemical shifts of the caffeine protons is shown in figure 2.6.

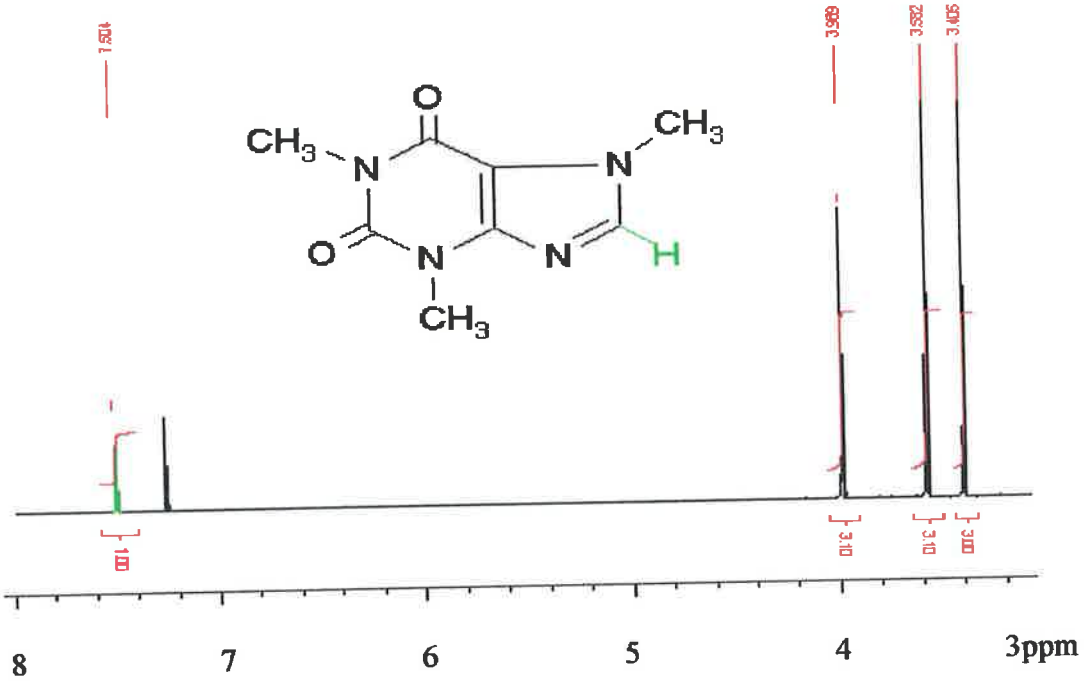

(A)

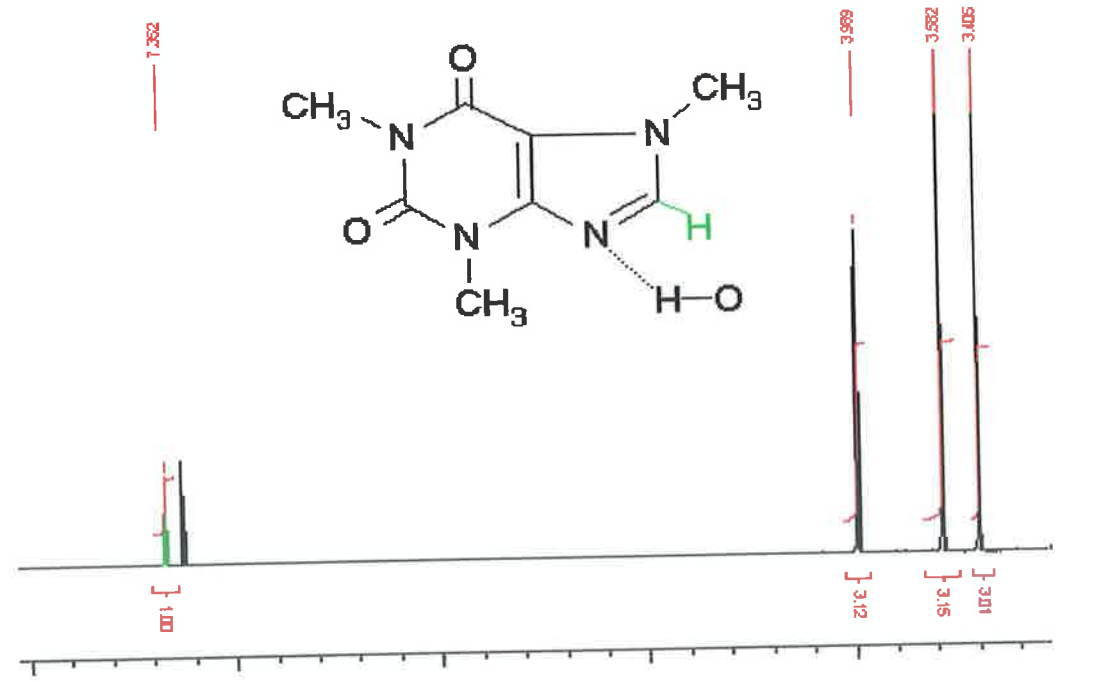

(B)

Figure 2.6a shows the ^{1}H NMR spectrum of caffeine and figure 2.6b shows that of caffeine as part of the pre-polymerisation complex. To simplify the spectrum, methacrylic acid was replaced with deuterated acetic acid.

The highlighted proton at 7.504 ppm is seen to shift upfield to 7.362 ppm (Δδ 0.142 ppm in $CDCl_3$) on complexation with the deuterated acetic acid. The NMR study confirmed the existence of a hydrogen bond or electrostatic interaction between caffeine and deuterated acetic acid and by proxy methacrylic acid in $CDCl_3$. When the experiment was repeated in deuterated acetonitrile the same proton showed a change in chemical shift of $\Delta\delta = 0.137$. Chemical shifts in NMR can be affected by the local electric fields arising from charged or polar groups e.g. –OH. Positive charges usually deshield nearby protons while negative charges generally perturbate shielding [103]. If the proton which is shown to shift upfield is not directly involved in the template – monomer interaction, it is likely that the interaction causes an electron delocalisation effect forcing the proton upfield. Figure 4b also displays shows the proposed mechanism of interaction between the template (caffeine) and the functional monomer (methacrylic acid). Importantly though, the prediction of interaction between caffeine and methacrylic acid postulated by Hyperchem has now been confirmed by NMR. Regarding the use of 2Vpy no changes in shift of any of the caffeine or 2Vpy protons were observed by ^1H NMR titration. This means that NMR did not observe any interactions. Given the decreased likelihood of caffeine protonation of the pyridine nitrogen it is likely that there exists a much stronger interaction between caffeine and MAA in the solutions tested.

2.3.2.2 UV-Visible analysis of template monomer interaction

UV-visible spectroscopic studies on pre-polymerisation complex formation have been conducted previously with notable success [60]. In terms of further investigating the stoichiometry of the complex formation, a UV-Visible mole ratio plot was used. The procedure was conducted in both chloroform and acetonitrile. The concentration of caffeine was kept constant while the ratio of caffeine: methacrylic acid was increased from 1:0 to 1:5. Figure 2.7 shows the plot of absorbance at 272 nm against the mole ratio:

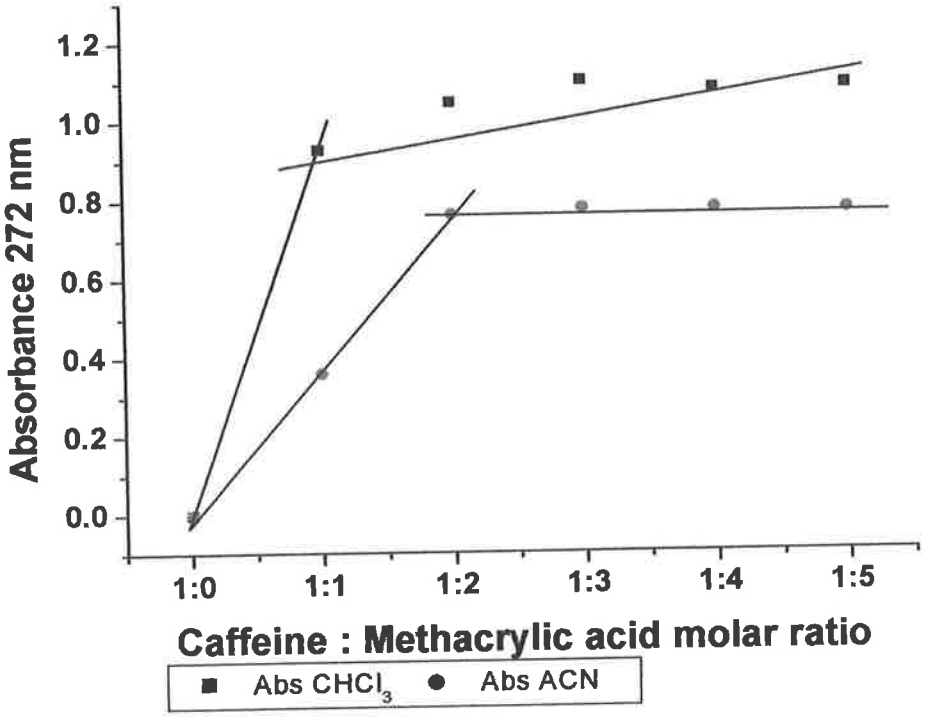

Figure 2.7: UV-Visible mole ratio plot of caffeine against methacrylic acid at 272 nm in both chloroform and acetonitrile.

With the mole ratio plot, two straight lines of different slopes are obtained. The two lines intersect at the mole ratio corresponding to that of the complex. As can be seen from figure 2.7 when the mole ratio plot is performed in chloroform (above) an optimal ratio of caffeine: methacrylic acid of 1:1 is observed whereas in acetonitrile (below) the optimum ratio is 1:2. Hence the UV-Visible study has shown the presence of a second point of interaction. Table 2 shows that Hyperchem had suggested that a 1:2 caffeine: MAA complex maybe stable. This experiment underlies the importance of the porogen itself in the polymerisation process [113]. Given that the second point of interaction is observed in acetonitrile and not in chloroform, it is indicative of that being electrostatic in nature. However the 1:2 complex has more curvature at the stoichiometric ratio than is seen that the stoichiometric ratio of the 1:1 complex. This is indicative of a less stable complex. It is therefore possible that a second labile non-covalent interaction exists when acetonitrile is used as porogen. This interaction is not evident when chloroform is employed.

As reported by Andersson and Nicholls, [60], the self assembly of template with the functional monomer in the pre-polymerisation complex is in a constant state of molecular flux where the extent of template complexation at equilibrium is subject to changes in ΔG. Complexation then, requiring the conformational configuration of two or more species will incur energetic penalties caused by barriers to rotation and translation. This is responsible for the instability of the second interaction observed in the mole ratio plot. Despite this however, table 2 shows a significant increase in binding energy at the 1:2 ratio. It is important to note however, that all Hyperchem studies were performed in vacuum. It is likely that the inclusion of solvent effects would reduce the binding energy somewhat. Overall, the UV studies show that the complexation is weak with no strong evidence of a particular stoichiometry

2.3.3 Synthesis of molecularly imprinted polymers

The molecularly imprinted polymers synthesised for the study are shown in table 2.3

Table 2.3: Polymers synthesised for this study

MIP Number	Monomer & Ratio	Template	Solvent used
CAF 1	MAA (1:3)	Caffeine	4 ml ACN
CAF 2	MAA (1:4)	Caffeine	8 ml $CHCl_3$
CAF 3	MAA (1:4)	Caffeine	8 ml ACN
CAF 4	MAA (1:4)	Caffeine	4 ml ACN
CAF 5	MAA (1:4)	Caffeine	4 ml $CHCl_3$

CAF 1-5 were synthesised for Solid Phase Extraction studies. Although, the modelling studies predicted a 1:2 ratio typically in molecular imprinting an excess of functional monomer is required [113]. Therefore, a 1: 4 ratio was used in all but one of the MIPs. It was expected that CAF 3 would perform best in rebinding studies given that it was generated in a higher volume of acetonitrile. This is due to the ability of a greater amount of solvent to lead to a higher surface area and more well formed pores, thus increasing the template accessability. CAF 2 was expected to perform less well. Given the fact that there are specific interactions between monomer and template in chloroform and due to the amount of chloroform used, CAF 4 was expected to perform at least as well as CAF 5 based on the Hyperchem energy calculations and the NMR study.

2.3.4 Molecularly imprinted solid phase extraction

Given that MIPs perform well in terms of rebinding when used in the solvent they were prepared in it was decided to use acetonitrile as the loading solvent for SPE. This is based on the likelihood of a reduced swelling of the polymer when exposed to the polymerisation conditions and hence the provision of an optimal environment for the template – functional site interaction [197]. However, it was noted that the caffeine was not retained on any of the MIPs (or non-imprinted polymers), most likely due to strength of acetonitrile as an eluting solvent. Methanol showed similar problems to acetonitrile as it is also a highly polar solvent. When chloroform was used as loading solvent a high degree of non-specific binding to the control polymer was observed. This is possibly due to the electrostatic nature of the template – functional monomer interactions. In non-polar solvent non-specific interactions will be more pronounced leading to the non-specific retention observed. This non-specific interaction is likely due to interaction with randomly dispersed functional groups in the polymer.

In a subsequent experiment, aqueous loading conditions were investigated i.e. loading the caffeine standard in water. This resulted in strong retention of caffeine on the polymer however the majority (91% on the MIP) was eluted during the washing phase and hence the majority of the binding was credited to non-specific hydrophobic binding. Theodoridis *et al.*, [186] have described the development of a MIP with sorbent properties for caffeine. Their work was based on a similar study by other groups [198,199]. They decided upon the use of aqueous based loading conditions using 0.05 M CH_3COONH^4-NH_3(aq.) at pH 9 and obtained high recoveries. The role of their buffer was to suppress non-specific interactions by masking the reactive acidic moieties on the surface of the polymer. For this study a sodium phosphate buffer at pH 10.5 was used. Figure 2.8 shows a graph of percentage recoveries of caffeine using the 5 caffeine MIPs from a standard solution of 1 ml of 50 µg/ml caffeine.

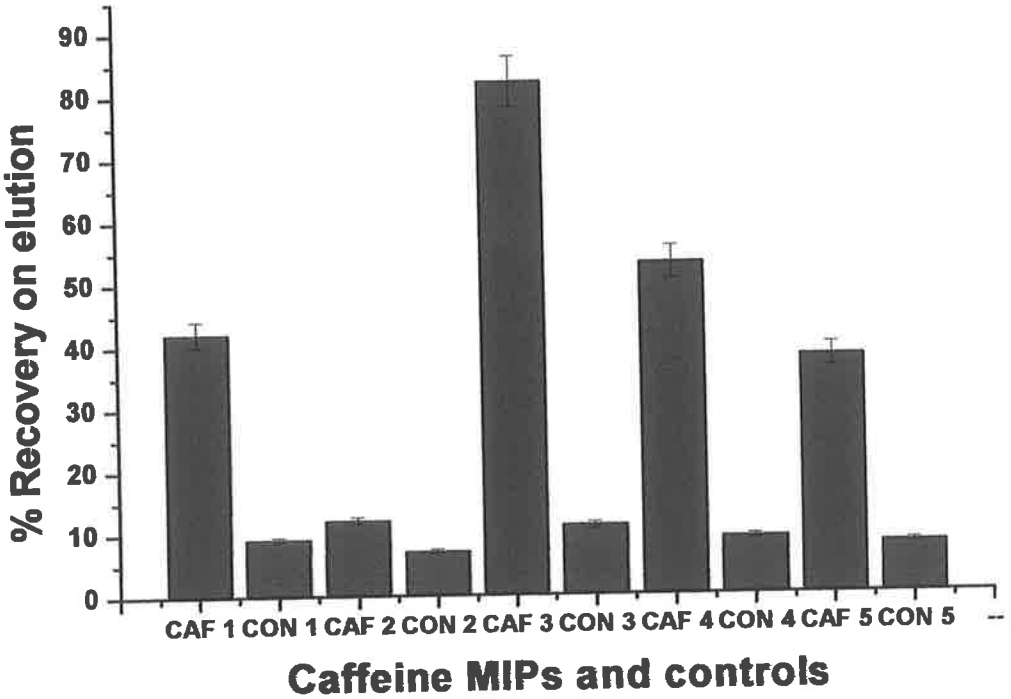

Figure 2.8: The % recovery on elution for all 5 of the caffeine MIPs (CAF 1-CAF 5) in addition to the five control polymers (CON 1- CON 5).

The maximum recovery of caffeine on elution was found to be 81.6 ±5.0% (CAF 3). This compares well with conventional solid phase packing materials. Other authors have observed similar values for the recovery of caffeine by MISPE. Recoveries of up to 80% have been observed for MISPE determination of Sudan I in food matrices [200]. Their highest recovery was determined using an elution solution of 1% acetic acid in methanol. In this study reproducibility was found to be good (±5%).

2.3.5 Real sample analysis

The usefulness of the MIPSE procedure was tested using real samples. The sample chosen was Red Bull™ a "high caffeine" soft drink. This soft drink contains 32 mg of caffeine per 100 ml. The sample was adjusted to pH 10.5 to facilitate specific binding (as standard caffeine had been dissolved in the loading buffer at pH 10.5), apart from this the procedure was performed as in the materials and methods section. A 1 ml volume of Red Bull was loaded per SPE column undiluted. The washing and eluting steps were as already stated. Figure 2.9 shows the clean up obtained for Red Bull.

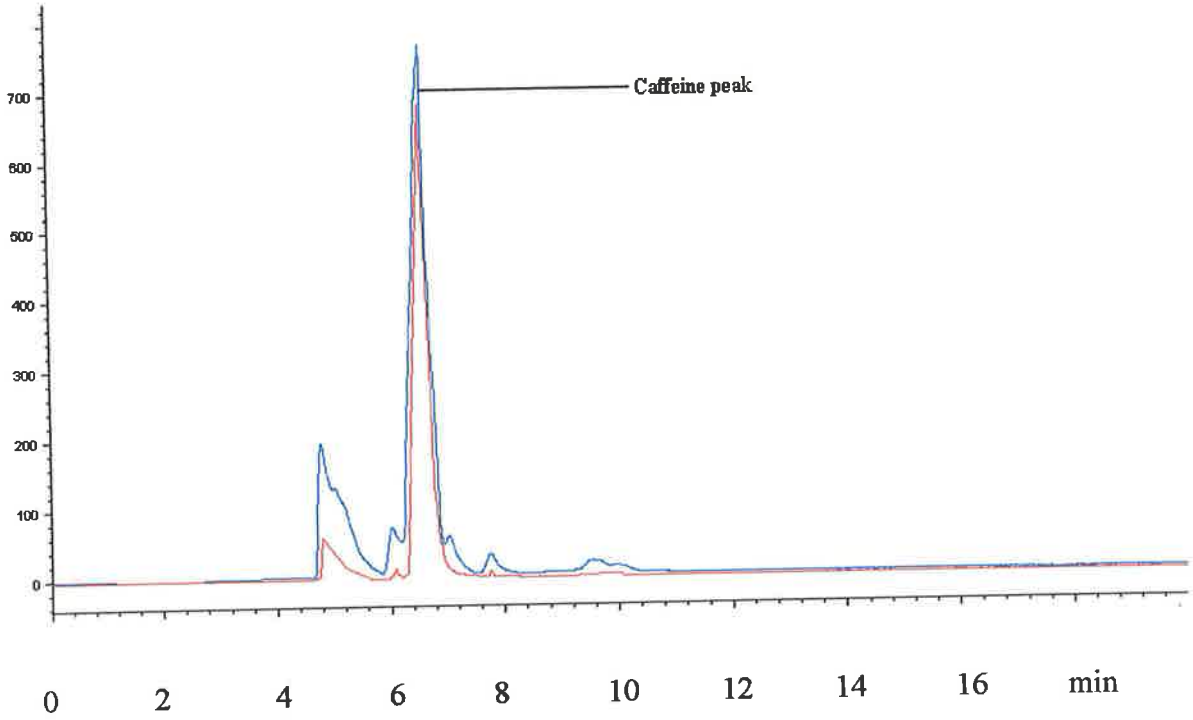

Figure 2.9: Solid phase extraction clean up of caffeine from a Red Bull™ sample on an SPE cartridge packed with MIP CAF 3. Chronmatograms obtained as described in section 2.2.8

Pre-MISPE **Post-MISPE**

It is evident from the HPLC chromatogram that a front appears on the caffeine peak. It is possible that there is a very small amount of a second species co-eluting with the caffeine. None of the other ingredients of the Red Bull™ soft drink approximate the high concentration found in the beverage. The ingredients of Red Bull™ are

carbonated water, sucrose, glucose, sodium citrate, taurine, glucuronolactone, caffeine, inositol, niacin, D-pantothenol, pyridoxine HCL, vitamin B12, artificial flavours, colours. It is possible that trace levels of one of these compounds co-elutes with caffeine. Given that the specific aim of the development of the MIP was to demonstrate an efficient "first phase" clean up and extraction of caffeine from Red Bull™, an attempt was not made to identify the nature of the co-eluting species. Based on the modelling data, the given MIP, CAF 3, was expected to outperform the other MIPs -which it did. Taken together, the aim was not to develop a definitive online SPE-HPLC assay for caffeine (many are available already) but to show the potential of a MIP in off line selective clean up of a food sample -this aim has been achieved. Figure 2.9 does show a highly cleaned up sample and selectivity towards caffeine. Furthermore, given the relative complexity of the sample (see ingredients, above), it is likely that many solid phase extraction resins would struggle to extract caffeine and only caffeine from such a matrix. A % Recovery of 65.8 ±2.4% was obtained upon elution. For the control polymer a recovery of 3.2 ±0.7% was determined (a result of 3 assays).

2.3.6 Cross reactivity towards caffeine analogues

In order to determine the selectivity of the optimal caffeine MIP (CAF 3) towards caffeine over the closely related structures theophylline and theobromine, a mixed solution containing all three of the compounds at a concentration of 50 μg/mL was prepared. SPE was conducted as before. The level of cross reactivity is shown below in figure 2.10

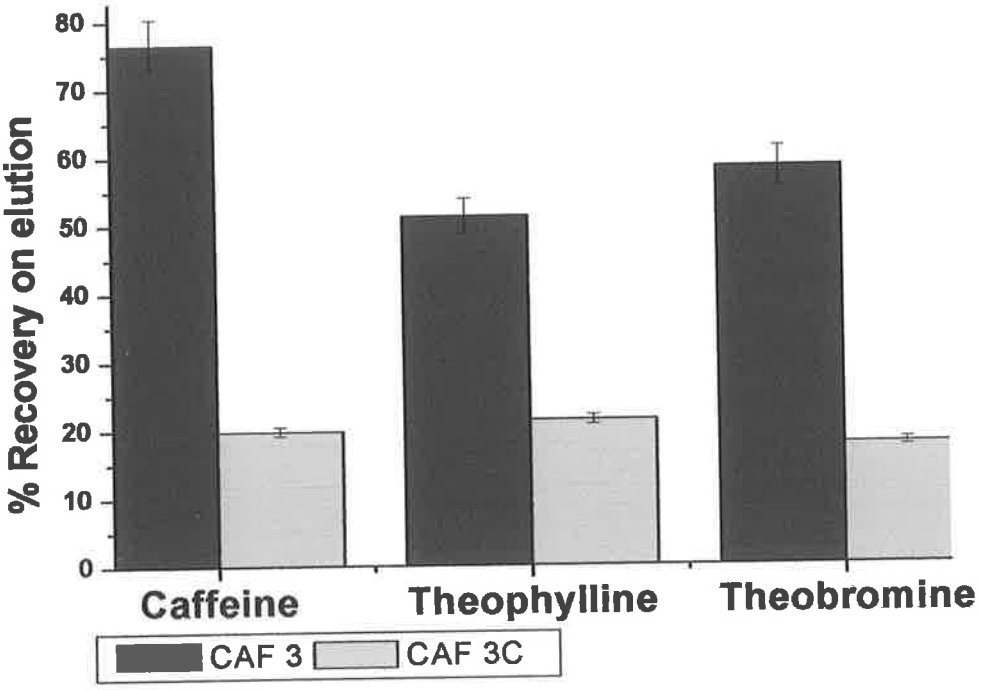

Figure 2.10: The % recovery on elution of an equal concentration of caffeine, theophylline and theobromine loaded onto MIP CAF 3 (and corresponding control)

As is evident from this study there is a substantial degree of cross reactivity of the MIP towards both theophylline and theobromine. This effect is not observed in the non-imprinted control indicating that the binding is specific and not due to hydrophobic binding. Nonetheless, CAF 3 does extract more caffeine than theobromine or theophylline indicating the selectivity of the MIP. All three of the

molecules are similar is shape and molecular volume and possess similar functionalities. The structure of theobromine is shown in figure 2.11

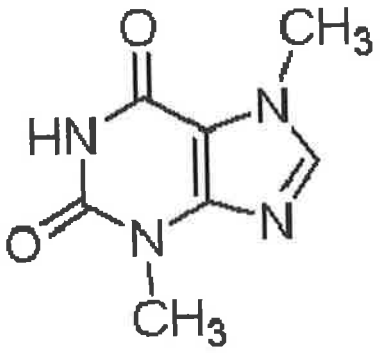

Figure 2.11: Structure of theobromine

Looking at figure 2.11 and comparing it to figure 2.1a (caffeine) and 2.1b (theophylline) it can be seen that both of the molecules will be capable of undergoing similar functional interactions with methacrylic acid as caffeine. Furthermore, since all three are rigid planar molecules they will have a similar shape induced fit to the binding cavity. The result of this being that the energy barrier to binding will be similar for all three molecules. Since the molecules are different though it is likely that spatial complementary plays a role in the selectivity observed. There are other important differences however such as pKa with caffeine having a pK_a of 14.0, theophylline 8.8 and theobromine 10.0. It is likely that these differences (along with small difference in spatial arrangement of molecules and functionalities) are responsible for the differences in selectivity between caffeine (the template) and the analogues.

2.3.7 The pore size distribution studies by BET

The study of certain traits of the polymers can yield important information on the physical characteristics of rebinding. Given that the importance of porogen has been demonstrated firstly by the NMR and UV studies and secondly by the MISPE, it can be concluded that the type and amount of porogen used can have an impact on the rebinding ability of the resultant MIP. To investigate this, two of the caffeine MIPs were selected (CAF3 and CAF5). These represented firstly a MIP which had performed well in the solid phase extraction studies (CAF3) and secondly a MIP which had shown poor rebinding data (CAF5). CAF 3 was prepared using 8 ml of acetonitrile as porogen and CAF 5 was prepared using 4 ml acetonitrile. Studies by

Brüggemann [201] have shown that a MIP may have over five times the surface area of the control MIP. Further to this, at least as an important forecast of how well a given MIP will perform, is the pore volume and pore diameter. Typically pore sizes have been separated into 3 size categories; micropores (<2 nm), mesopores (2-50 nm) and macropores (over 50 nm). Table 2.3 shows the surface areas, total pore volumes and average pore sizes (diameter) for the MIPs CAF 3 and CAF 5 along with their corresponding controls.

Table 2.3: The surface area, total pore volume and average pore diameter data obtained from the BET studies.

Polymer	Surface Area (m^2/g)	Total pore volume (cm^3/g)	Average pore diameter (nm)
CAF 3	345.59	0.8487	12.02
CAF 3 Control	301.42	0.4750	5.01
CAF 5	289.62	0.5155	8.08
CAF 5 Control	290.99	0.3472	3.42

It was found that by increasing the volume of porogen a major impact on the pore size distribution and pore volume was observed in otherwise identical polymers. As the average pore size diameter increases, the caffeine molecule (template) has more steric manoeuvrability within the pore and it more likely that there will be a higher rate of rebinding as attested by the solid phase extraction data. Furthermore the higher pore volume and surface area are indicative of a higher capacity and better formed pores. One potential misinterpretation of this result is that there is an apparent increase in rebinding which may not be caused by specific complexation but by template self-association via aggregation of numerous caffeine molecules together within the same pore. An increase in the amount of diluent (porogen) causing an increase in the average pore size in the MIP should have the same effect in the control polymer though. If template molecules aggregate inside the pores of the MIP then they should do likewise inside the pores of the control and this should be reflected in an increase in rebinding. This is not seen however, so it is likely that the correlation between increased average pore size and rebinding means that there is a greater level of access to the functional groups for the template.

In terms of the surface area of the MIPs, CAF 3 produced a surface area of 345.59 m^2/g whereas CAF 5 produced a surface area of 301.42 m^2/g. From this it can be seen that doubling the amount of porogen increased the surface area by over 12%. Typically, a higher surface area and pore volume is indicative of more well formed and uniform pore distribution It would be expected that increasing the size of the pores would have led to a larger decrease in surface area. However there is still a relatively large population of pores in the micro- and lower mesoporous range. This may also help to explain the recoveries in the SPE studies. Given that the highest % recovery on elution was with CAF 3 and that amounted to approximately-80% (conventional SPE cartridges would be in the region 80-85%) it is likely that a further increase in average pore size would lead to better recoveries in the SPE procedure.

2.4 Conclusion

The objective of this study was to offer an insight into the possibility of engineering molecularly imprinted polymers for a specific analysis. The rationale was based on an gaining an intrinsic understanding of the nature of complex formation between template and functional monomer with a view to exploiting this knowledge in terms of rationally designing a procedure for MIP production. Furthermore, the physical characterisation of the polymer in terms of the pore sizes could predict the performance of the MIPs regarding rebinding. The caffeine molecule is a well characterised compound and was selected for study so that the method could be compared and contrasted with other available analytical techniques. Given the success of the rational design approach for caffeine it is expected that the same approach could be easily adapted for the development of a MIP against a more complicated molecule / biomolecule and herein lies the usefulness of the rational design approach. To develop a fully operational chemical sensor or analytical method will inevitably involve an element of trial and error however this work suggests that it is possible to significantly reduce the time and materials involved in such a process.

Chapter 3

A molecularly imprinted polymer for methotrexate using the substructure / epitope approach

3.1 Introduction

The moleculeular structure of methotrexate (MTX) is composed of a heterocyclic portion (a 2,4-diamino-substituted ring) linked to a ρ-aminobenzoyl portion, which is in turn amide bonded to a glutamic acid unit. The molecule is thus a polyelectrolyte carrying two carboxyl groups with dissociation constants (pK_a) of 3.36 (α-carbon) and 4.70 (β-carbon) – and a number of potentially protonated nitrogen functions, the most basic of which is the guanidinic *N*-1 on the pterine ring (pK_a 5.71). Its water solubility is pH dependent ranging from 0.9 mM at pH 5 to 20 nM at pH 7. The structure of methotrexate is shown below in figure 3.1

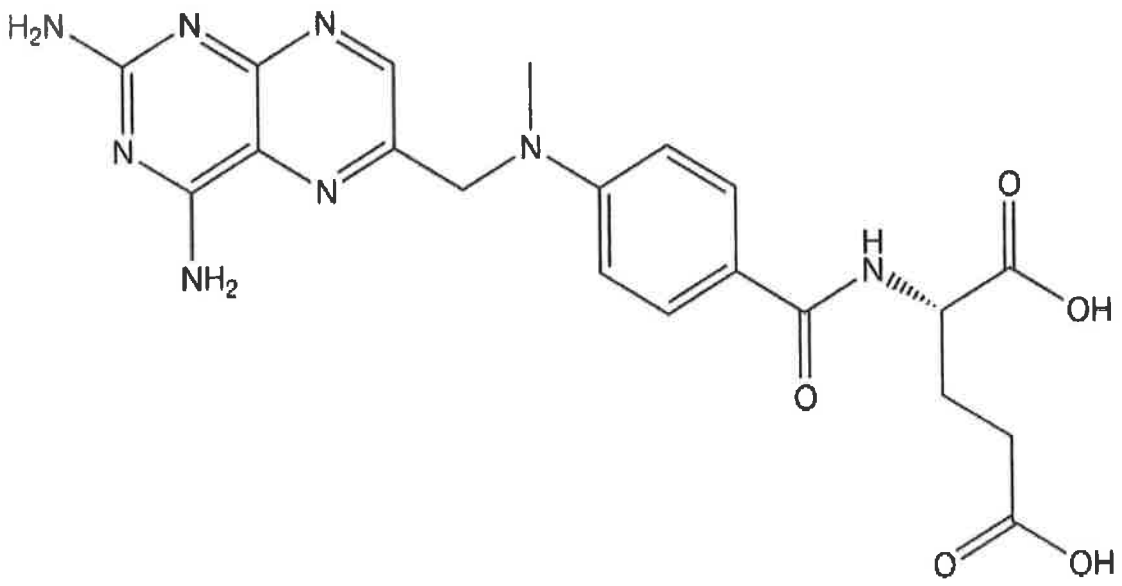

Figure 3.1: The chemical structure of the template methotrexate.

As can be seen there are several functionalities on this molecule capable of undergoing complex formation with numerous functional monomers. A cursory examination of the molecule shows that the glutamic acid portion of the molecule can potentially form hydrogen bonds with methacrylic acid or with an amine containing functional monomer. The pteridine part of methotrexate may be capable of forming both hydrogen bonds and undergoing π-π stacking with an aromatic functionality. Quaglia *et al.*, [202] used methotrexate as a "dummy" template for the development of a MIP for the closely related structural analogue folic acid using 2-vinylpyridine as

functional monomer. The porogen employed was a 2:1 ratio of ACN:NMP However, the retentivity and selectivity of this phase were insufficient for anticipated applications. In a second approach, using methacrylic acid as the functional monomer, organic soluble inhibitors for the enzyme dihydrofolate reductase were used to develop sites complementary toward the pteridine substructure. This resulted in materials showing enhanced selectivity for substituted pteridines when evaluated by HPLC. Thus, methotrexate and leucovorine (MTX analogue) were selectively retained in mobile phases.

Research studies in chapter 2 demonstrated the importance of the porogen in optimising the performance of MIPs. The major functions of the porogen are to firstly dissolve the components of the polymerisation mixture and secondly to provide an environment which assists in, or at least is neutral towards the development of the self-assembly of the pre-polymerisation complex. Methotrexate is a molecule that is sparsely soluble in the majority of organic solvents. Given that high concentrations of template are necessary for inclusion in the imprinting mixture finding a suitable solvent for imprinting this molecule is challenging. Therefore alternative strategies are investigated in addition to direct imprinting of the methotrexate molecule. In addition, a clear mechanism of complex formation was more difficult to deduce for the imprinting of methotrexate. This is in part due to the failure of ^{1}H-NMR to offer evidence for hydrogen bonding or electrostatic stacking interactions. However as specific uptake was observed in the MIP, the mechanism of pre-polymerisation complex formation is likely to be electrostatic in nature with a significant contribution from shape complementarity.

An interesting approach to the development of MIPs is the epitope approach. Rachkov and Minoura [40] have employed this method to the production of a MIP for the peptide hormone oxytocin. The tetrapeptide, Tyr–Pro–Leu–Gly–NH_2 (YPLG), was used as a template for the preparation of the MIPs by the epitope approach. It was shown that in organic (acetonitrile-based) chromatographic mobile phases the MIP can recognize not only the template but some other peptides possessing Pro–Leu–Gly–NH_2 sequence at the C-terminus (including the neurohypophyseal hormone oxytocin) as well. The same authors [203] have shown the applicability of this method to larger peptides and proteins.

3.1.1 Aims and objectives

The aim of this chapter is to develop a MIP for methotrexate by investigating which functional monomer was most likely to form the strongest complex with methotrexate (or part of the molecule thereof) and use this to develop a specific MIP. Given the relative insolubility of the molecule, DMSO is used as porogen for imprinting the whole molecule. Direct imprinting of MTX is performed in DMSO along with direct imprinting of the substructure *N*-Z-L-Glu-OH.

3.2 Experimental

3.2.1 Materials

All deuterated solvents (DMSO, Chloroform, Methanol) were obtained from Apollo Scientific (UK). Methanol, dimethylsulfoxide, acetonitrile, acetone, methotrexate, *N*-Z-L-Glu-OH were acquired from Sigma-Aldrich (Ireland). Methacrylic acid, ethylene glycol dimethacrylate, 2-vinylpyridine were also purchased from sigma Aldrich (Dublin)

3.2.2 NMR studies

Studies were performed on a Brucker Avance 400 MHz Ultrashield instrument. Concentrations of 0.04M of both methotrexate in d_6-DMSO and monomer substitute (deuterated pyridine or deuterated acetic acid) were used. The total volume used for NMR analysis was 0.75 ml.

3.2.3 UV Job method studies

Studies were performed on a Varian 50 Scan UV visible spectrophotometer equipped with Cary UV50 software. Concentrations used were 0.04M of methotrexate and functional monomer.

3.2.4 HPLC studies

HPLC analyses were conducted on a Hewlett Packard series 1050 system with a Rheodyne injection valve using Alltech BRAVA ODS column (25 cm x 4.6 mm, particle size 5μm). The mobile phase consisted of ACN/water/HOAc (92:6:2). A 10 μl injection volume was used for all analyses. Separations were performed at 25^0C (isocratic elution). The wavelength used for detection was 288 nm.

3.2.5 Batch rebinding analysis

Given that methotrexate was not soluble even at low concentrations (7.5 µg/ml) in commonly used organic solvents (ACN, MeOH, $CHCl_3$, water) DMSO was used as the solvent for the study. A range of methotrexate concentrations were prepared in DMSO and a standard curve was constructed. The concentrations used were in the range 7.5 µg/ml to 300 µg/ml. The level of % uptake of analyte at the different concentrations was assessed by HPLC. A 20 mg quantity of polymer was used for this experiment and the incubation time was varied from 30 min to 16 h. Note: Incubation time is defined as the time period that the analyte was in contact in solution with the MIP.

3.2.6 Solid phase extraction

SPE studies were performed by packing 200 mg of dry polymer (or corresponding non-imprinted control) into empty SPE cartridges of 3 ml volume. The system was washed through thoroughly with acetonitrile to remove any air bubbles that may affect solvent flow. The packing was further washed with methanol to ensure the absence of template and the effectiveness of the washing procedure. Suitable solvents were then tested for the loading, washing and elution stages as explained in the results and discussion section.

3.2.7 Generation of molecularly imprinted polymers

MIPs were produced using the following procedures:

For methotrexate MIPs, 0.4 mmol of the compound was weighed out and dissolved in 8 ml DMSO. To this was added the appropriate quantity of either methacrylic acid or 2-vinylpyridine as functional monomer. Both 1:2 and 1:4 ratios of template: functional monomer were used for this study. The mixture was stirred at room temperature for 5 min. The cross linker (EGDMA), 20 mmol (4167 µl) was then added followed by initiator (AIBN) at 50 mg per polymerisation tube. The ratio of EGDMA to functional monomer was kept below 10:1. The mixture was stirred for a

further 10 min to ensure complete dissolution of all the components. The mixture was then sonicated for 10 min. In order to completely degas the solution it was sparged with N_2 for 5 min. The tubes were then plugged under vacuum and gradually heated to 60^0C in a waterbath. A 16 hour polymerisation time was used. Following polymerisation, the tubes were smashed and the polymer was removed. The polymer was broken up before being ground with a mortar and pestle. The particles were then sieved to <25 μm in acetone. Repeated cycles of grinding and sieving were necessary in order to acquire enough of the polymer at size <25 μm. Smaller particles (<5μm) were removed by standing in acetone. Typically, 100 ml of acetone was added to the polymer in a graduated cylinder. The polymer was allowed to settle for ~1 hour and then the acetone was removed. This was repeated 4-6 times per polymer. Control polymers were prepared in the same way with the omission of template. As regards washing, following sieving to the correct particle sizes, the MIPs were washed in a solution of hot methanol with 10% acetic acid. The solution was also stirred vigorously. This procedure was repeated numerous times until no trace of methotrexate could be detected in the washings by HPLC.

For the *N*-Z-L glutamic acid imprinted polymers the procedure was as described above except methotrexate was substituted with the *N*-Z-L-glutamatic acid (0.4 mmol).

3.3 Results and discussion

The approach of Quaglia *et al.*, [202] used for the generation of an imprinted polymer using methotrexate as template employed a lower amount of methotrexate and a porogen consisting of acetonitrile: NMP 2:1. Initially, a solubility profile was performed on methotrexate. Of the solvents commonly used in molecular imprinting, methotrexate was found not to be soluble to any extent in any of the following: acetonitrile, methanol, ethanol, chloroform, hexane, toluene, dichloromethane or water.

Methotrexate was soluble to the extent of approximately 14.125 mg per ml in DMSO. It was also soluble to a lower degree in DMF. Hence, the most viable solvent to use for the polymerisation process was found to be DMSO.

3.3.1 NMR Analysis

The ^{1}H-NMR spectrum of methotrexate is shown below in figure 3.2

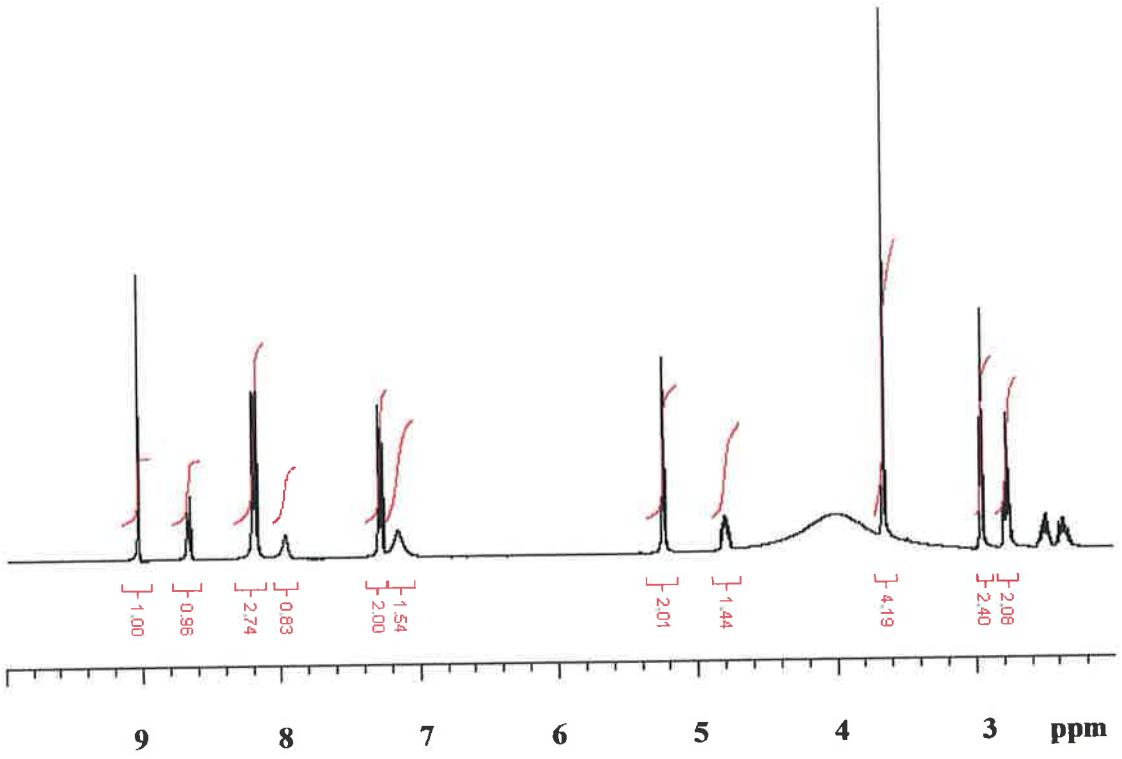

Figure 3.2: NMR of methotrexate in d_6-DMSO

It was found in the NMR study t substitutes) no changes in chemical shift of any of the proton signals of methotrexate were observed. Deuterated DMSO was used for dissolution of methotrexate. DMSO is a strong hydrogen bond acceptor and it is probable that it blocks potential hydrogen bond interactions between the functional monomer(s) and the methotrexate molecule. Since there are a number of hydrogen bond acceptors on the methotrexate molecule, it would be expected that hydrogen bonds would form readily in (a) a less polar solvent or (b) a solvent with poor hydrogen bond forming ability. The deuterated solvent was switched to MeOD and also no shift changes were seen. MTX was not soluble at 0.04 M - the concentration used fort the NMR studies - in $CDCl_3$. As the NMR experiments did not reveal complex formation, a UV Job plot was employed to gain a greater insight to the effect of monomer: template ratio.

3.3.2 UV-visible mole ratio plot analysis

Firstly a mole ratio plot of methotrexate against the functional monomer 2-vinylpyridine was constructed in DMSO at 288 nm and is shown below in figure 3.3 (a). The mole ratio plot with methacrylic acid is shown in figure 3.3 (b)

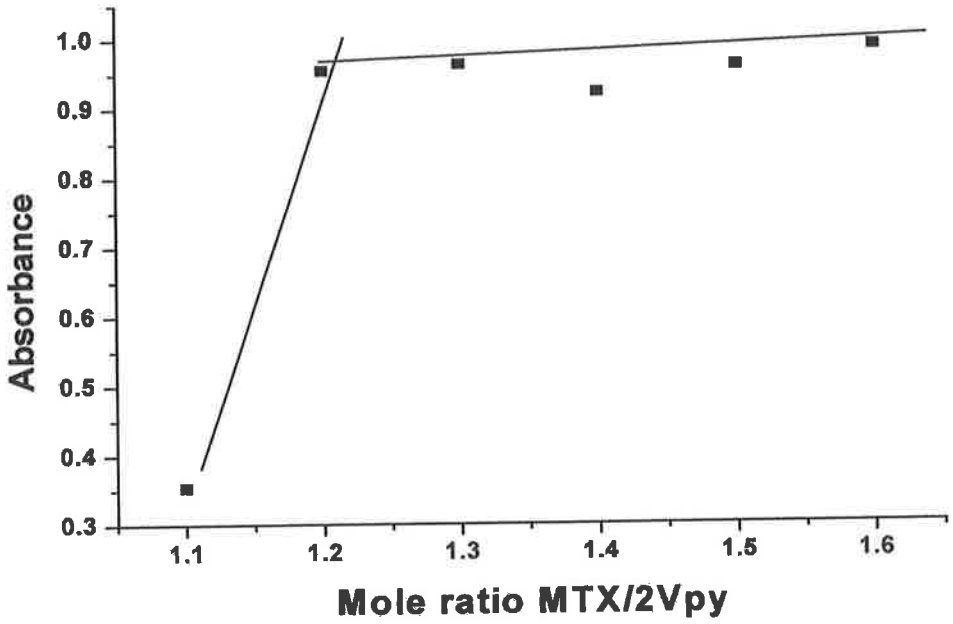

Figure 3.3 (a) UV mole ratio plot of MTX in DMSO with increasing ratios of 2Vpy at 288 nm

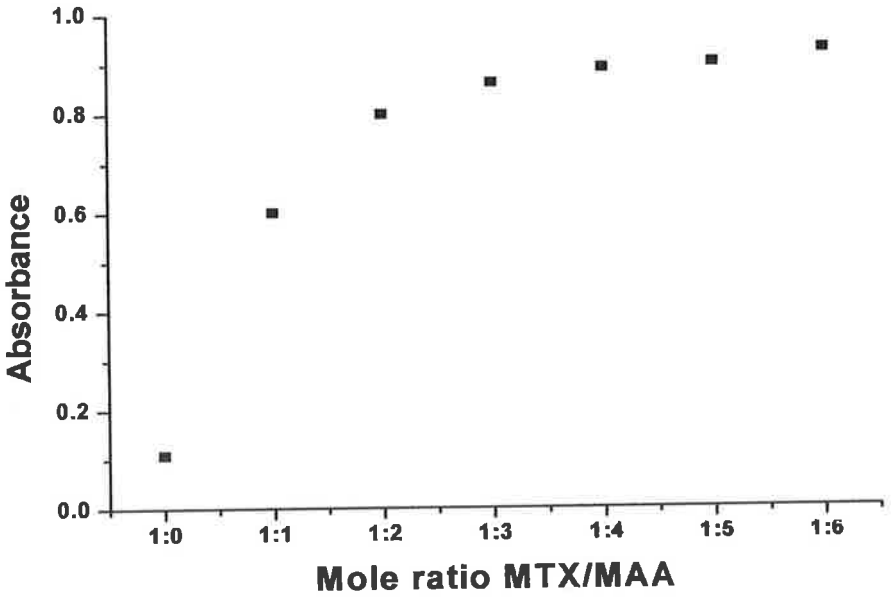

Figure 3.3 (b) UV mole ratio plot in DMSO increasing the ratios of MAA to MTX at 288 nm

Figure 3.3 (a) shows the mole ratio plot suggesting an optimal molar ratio of 1:2 for complexation between 2-vinylpyridine and methotrexate in DMSO. It is not likely that a vinylpyridine molecule forms a complex with the pteridine portion of the molecule, as there will be a degree of charge repulsion. However, the nitrogen of the vinylpyridine ring may form electrostatic interactions or undergo hydrogen bonding with the –OH molecules of the glutamic acid portion in a 1:2 ratio. Also, there is a possibility of forming π-π stacking interactions with the glutamic acid aromatic ring, depending on steric factors.

Regarding, methacrylic acid, there are more sites on the methotrexate molecule capable of undergoing complex formation. The mole ratio plot indicated conclusions cannot be drawn about the stoichiometry from these studies as the observed interactions are too weak. To investigate this further a Jobs plot of MTX/MAA was performed and is shown below in figure 3.4

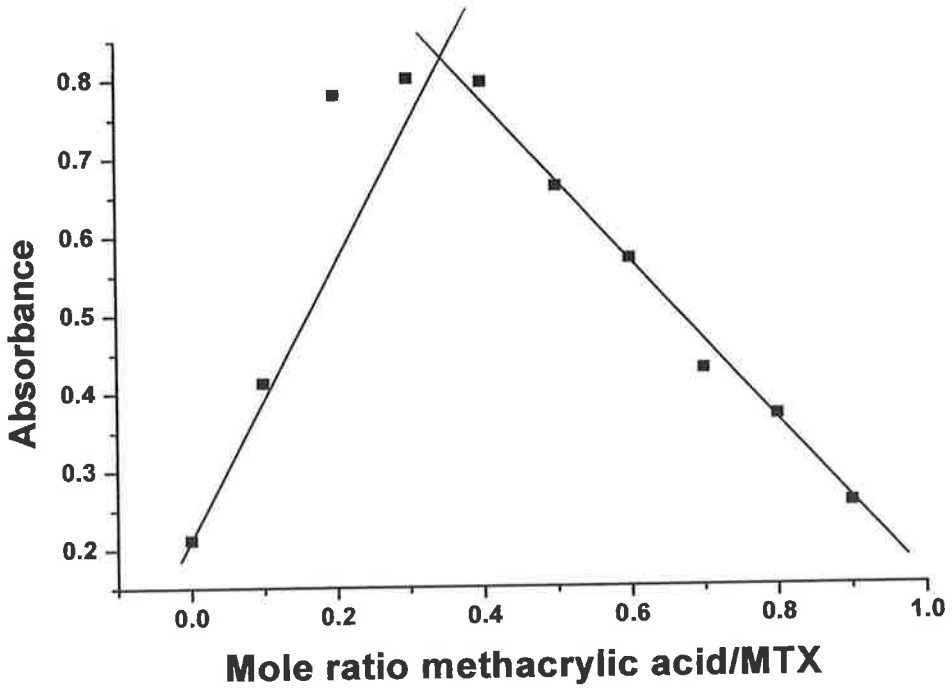

Figure 3.4: Jobs plot of MTX/MAA

From the study it is shown that the dominant complex may correspond to ratios of 2:3, 1:4, 3:7. It is important to note that the optimum molar ratio may contain more than one methotrexate molecule. In this respect, it is prudent to include an excess of functional monomer in the polymerisation mixture to ensure that all of the methotrexate was complexed.

3.3.3 Generation of molecularly imprinted polymers and batch rebinding studies.

Two MIPs were generated, using different functional monomers in the polymerisation mixture. MTXVP 1 contained 2-vinylpyridine, and MTXMA 1 contained methacrylic acid. Non-imprinted controls were also prepared identical to the MIPs but without the inclusion of methotrexate. Following crushing, grinding, sieving and washing batch type adsorption analysis was performed on each of the MIPs (and controls generated). A 20 mg quantity of Polymer was used for this experiment and the incubation time was 30 min at room temperature. Varying concentrations of methotrexate were

dissolved in DMSO and added to the polymer, shaken and centrifuged at 12,000 rpm x 10 min. The % uptake i.e. total concentration minus that calculated in the supernatant for both polymers and controls is shown in table 3.1:

Table 3.1 % Uptake of methotrexate on the polymers at different concentrations in DMSO at 30 min incubation

MTX conc^{n} (µg/ml)	MTXVP 1	CONVP 1	MTXMA 1	CONMA 1
7.5	<1	<1	<1	<1
15	<1	<1	<1	<1
30	2.62	<1	2.97	<1
60	2.71	<1	1.31	<1
120	0.88	<1	1.89	<1
300	3.74	<1	1.51	<1

As can be seen from the results obtained only minimal % rebinding was observed in both of the MIPs over the concentration range and negligible uptake was observed in the control polymers. There are numerous theories that may be presented to explain the low uptake. Firstly, the incubation time was short – 30 min. It is likely that times exceeding 1 hour are required. The above procedure was repeated and the incubation time was increased to 16 h at RT. The % rebinding of MTX is shown in table 3.2:

Table 3.2 Uptake of methotrexate on the polymers at different concentrations in DMSO at 16 h incubation

MTX conc^{n} (µg/ml)	MTXVP 1	CONVP 1	MTXMAA 1	CONMAA 1
7.5	37.31	9.05	33.78	19.49
15	37.59	11.17	31.24	18.74
30	36.76	12.67	36.85	21.67
60	33.81	12.95	34.98	23.54
120	30.94	11.77	31.42	21.60
300	39.43	12.84	33.86	23.97

It was found that the polymers containing methacrylic acid show a higher level of non-specific uptake (CONMAA). The overall specific rebinding for both MIPs is low at all concentrations tested (MTXVP 1 and MTXMAA 1) with significant non-specific adsorption as shown by the high control uptake. However, the level of non-specific adsorption on CONMAA 1 (18-24%) is approximately double that of CONVP 1 (9-13%). This result suggests that using an excess of methacrylic acid, as functional monomer is detrimental to overall MIP performance in comparison to using an excess of 2-vinylpyridine. The finding is somewhat in contrast to the UV mole ratio plots, which indicated that an excess of methacrylic acid would be necessary to fully complex all of the methotrexate. However considering that weak nature of the complexes formed it is possible that during polymerisation there is more free MAA leading to random distribution around the polymer.

To investigate this further, two additional polymers were prepared MTXVP 2 and MTXMAA 2 Both of these MIPs were generated with a 1:2 ratio of template: functional monomer. They were subject to the same rebinding procedure. The % uptake was measured after 16 h incubation and shown below in table 3.3:

Table 3.3: % Rebinding of MTX to MIPs MTXVP 2 and MTXMA 2 in DMSO at different concentrations at 16 h incubation

MTX conc^{n} (µg/ml)	MTXVP 2	CONVP 2	MTXMAA 2	CONMAA 2
7.5	34.87	1.32	21.46	1.89
15	33.21	1.09	20.38	2.14
30	36.57	2.84	21.97	3.62
60	36.96	2.96	22.19	3.19
120	35.84	1.90	21.45	3.84
300	38.68	2.11	21.80	3.46

Interestingly, it was found that when the ratio of template: methacrylic acid (functional monomer) is reduced from 1:4 to 1:2; there is a large decrease in non-specific rebinding. This may be attributed to most of the available functional monomer being complexed with methotrexate. This in turn suggests that there may be non-complexed methotrexate in the polymerisation mixture. This has manifested itself in the significant reduction observed in specific uptake by MIP MTXMAA 2 in contrast to MIP MTXMAA 1. A similar (though not as pronounced) trend occurs with MTXVP 2. Here there is a considerable decrease in non-specific binding however there is no decrease in the amount of specific methotrexate uptake on changing from MTXVP1 to MTXVP 2.

Chianella *et al.*, [204] have employed DMSO as porogen to generate MIPs for MISPE detection of microcystin-LR. Here it was stated that DMSO was chosen as porogen for the polymerisation reaction due to its power to dissolve microcystin-LR. Moreover the polymer produced by using this solvent is expected to be compatible with aqueous environment (the swelling of the polymer in DMSO and aqueous solutions should be

very similar). In subsequent experiments, they found a high level of non-specific binding (i.e. binding to the control polymer) along with high levels of cross reactivity of the YR and RR analogues of microcystin-LR

Given this drawback the very low non-specific binding observed and shown in table 3.3 compares favourably. Furthermore, it should be noted that the non-specific binding remains low at concentrations of less than 15 μg/ml. Dong *et al.*, [205] have performed a molecular simulation and experimental validation of the influence of the solvent on the molecular recognition capability in MIPs towards theophylline. The ΔE of theophylline in three solvents, chloroform, THF and (DMSO), was calculated, in which chloroform gave the smallest ΔE and DMSO gave the largest. The same order for ΔE was obtained for the monomer, MAA, in the three solvents. The calculated results indicate that chloroform is the most suitable solvent for the preparation of MIP for THO. DMSO, however, is not since it has high affinities to THO and MAA, and these inhibit the interaction between the THO and MAA. To examine the validity of the simulated results, MIPs for THO were synthesized in the three solvents and used for the adsorption of THO, respectively. The MIP synthesized in chloroform showed the maximum selectivity while that synthesized in DMSO showed the worst, in agreement with the molecular modelling study.

3.3.4 The glutamic acid substructure approach

Referring to figure 3.1, it is likely that 2-vinylpyridine interacts more so with the glutamic acid portion of the molecule of methotrexate than with the pteridine portion. Hall *et al.*, [206] have employed a method based on an epitope approach described in section 3.1. This paper described the preparation of a molecularly imprinted polymer against *N*-Z-L-glutamic acid using a novel bis-urea functional monomer. The polymer exhibited affinity for the template over *N*-Z-protected aspartic acid and glycine and, further, was capable of binding larger molecules, e.g. methotrexate containing the glutamate substructure. The structure of the *N*-Z-L-glutamic acid is shown in figure 3.5:

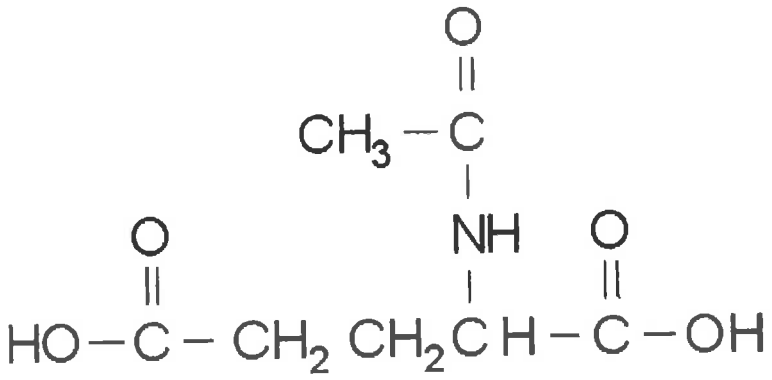

Figure 3.5: The structure of *N*-Acetyl-glutamic acid (sigma)

The –OH groups can be targeted with both of the functional monomers used in the previous sections of chapter 4. Hall *et al.*, [206] employed the synthetic functional monomer shown below in figure 3.6:

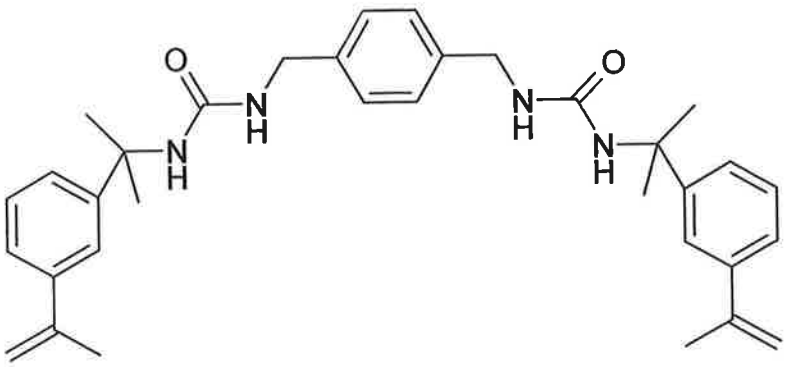

Figure 3.6: The novel functional monomer used by Hall *et al.*, Reproduced from Hall *et al.*, [206]

The group however, did not use *N*-Z-L-Glu-OH directly as a template rather they used a derivatised form.

In this study, two MIPs were prepared directly against the Glutamate substructure as the template. GLUVP 1 and GLUMA 1. The % rebinding of both *N*-Z-L-Glutamic acid and methotrexate was assessed by batch rebinding. Importantly, the molecule was found to be soluble in other solvents apart from DMSO, however to ensure consistency with the earlier work, the MIP was prepared in DMSO and the rebinding performed in the same solvent. Furthermore, the molar ratio of 1:2 was kept for both functional monomers. The rebinding data (methotrexate)are presented in table 3.4.

Table 3.4: The % rebinding of methotrexate from a DMSO solution at differing concentrations at 16 h incubation on MIPS GLUVP 1 and GLUMA 1

MTX conc^n (µg/ml)	GLUVP 1	GCONVP 1	GLUMA 1	GCONMA 1
7.5	48.70	6.73	14.82	2.93
15	44.63	6.99	15.10	3.05
30	44.18	7.21	14.71	3.62
60	42.22	9.40	13.62	3.51
120	41.92	10.37	13.57	4.08
300	41.27	12.51	13.91	3.92

It was found that GLUVP 1 has significantly outperformed GLUMAA 1 in specific rebinding of methotrexate showing % rebinding of 41-49% and 4-15% respectively). Also of interest is that the glutamate substructure approach is more successful than the direct imprinting of the MTX molecule. Notable is the low non-specific rebinding in GLUMAA 1. As the concentration of methotrexate increases there is also a considerable increase in the level of non-specific binding in CCONVP 1 (increasing from 6.73% to 12.51%). This is not observed in CGCONMAA 1 and is attributed to the saturation of the binding sites of the polymers. This is suggestive of a MIP with low capacity that would be better suited to applications requiring qualitative or semi-quantitative analysis. In order to determine the effect of a change of solvent on the rebinding in GLUVP 1 the following solvents were employed, methanol, acetonitrile, chloroform. Due to solubility issues, only lower concentrations were analysed for rebinding. The results are shown in table 3.5.

Table 3.5: % Rebinding of methotrexate to MIP GLUVP 2 upon changing of rebinding solvent

MTX concn (µg/ml)	MIP MeOH	CON MeOH	MIP ACN	CON ACN	MIP Water	CON Water
7.5	9.61	5.29	39.76	10.69	51.28	39.28
15	8.48	5.87	38.43	15.43	53.67	42.64

Table 3.5 shows that changing DMSO for methanol has a detrimental effect on specific rebinding with an almost complete abrogation of rebinding observed. This is most likely due to the strong hydrogen bond forming ability of methanol. It will preferentially form interactions with the template and the functional monomer and thus precludes the interactions between the template and functional monomer. Consequently, the same environment of the pre-polymerisation complex solution is not replicated and hence reduction in rebinding is observed. Acetonitrile is a polar aprotic solvent like DMSO, it was therefore anticipated that it would be less likely to interfere with the rebinding to the same extent as methanol. Table 3.5 confirms this hypothesis and although the non specific bending is higher (15.43% at 15µg/mL MTX) than with either DMSO or methanol (5.87 µg/mL) the specific binding is

comparable to that observed using DMSO (~39% and 41-48% respectively). The use of water led to high non-specific binding (42.64% at 15µg/mL). This is attributed to the formation of hydrophobic interactions. Given the high level of rebinding with water it is likely that it can be used as a loading solvent in SPE studies as the non-specific hydrophobically interacting molecules can be washed from the column using a suitable solvent leaving specific interactions in place.

3.3.5 Molecularly imprinted solid phase extraction

A direct comparison was performed between the MIP produced directly for methotrexate (MTXVP 2) and that produced by the substructure approach (GLUVP 1) using 1:2 ratios of template: functional monomer. Initially, water was used as the loading solvent. Methotrexate was loaded at a concentration of 10 µg/ml. The principal challenge in MISPE is finding a suitable washing solvent to break up non-specific adsorption to the MIP (e.g. hydrophobic interactions) while at the same time enhancing (or leaving undisturbed) the specific interactions in the binding pockets.

In this study, the following solutions were tested. DMSO, DMF, ACN, MeOH, water, toluene, water 1% HOAc, ACN 1% HOAc. The solution found to remove most of the methotrexate from the control non-imprinted column while at the same time leaving the majority of the methotrexate remaining bound to the imprinted column was deemed to be the most suitable solvent in this regard. The % methotrexate removed from the column with a single 2 ml aliquot of appropriate solvent is shown in table 3.6:

Table 3.6 MISPE washing optimisation. Shows the % of the original MTX in the applied water.

MTXVP 2	CON	GLUVP 1	CON	Washing solvent
83.45	91.55	75.98	86.30	DMSO
76.78	94.29	71.46	69.97	DMF
99.68	99.42	89.71	96.45	MeOH
58.77	93.76	47.26	91.86	ACN
56.65	98.36	39.27	92.39	ACN (1% HOAC)
2.49	2.73	3.99	6.87	WATER
3.61	5.39	3.22	10.01	WATER (1% HOAc)

From the results obtained, as acetonitrile acidified with 1% acetic acid removed the lowest portion of the loaded methotrexate from the MIP with reference to the control it was chosen as the washing solvent. Furthermore, since methanol could quantitatively extract all of the methotrexate from both columns it was employed at the eluent.

3.3.5.1 Elution and quantification of methotrexate; A comparative performance

Methotrexate in a standard solution of 10 µg/ml in water was applied to an SPE column packed with either MTXVP 2 or GLUVP 1.The columns were washed with 1% HOAc in ACN and eluted with MeOH The result is shown in figure 3.7

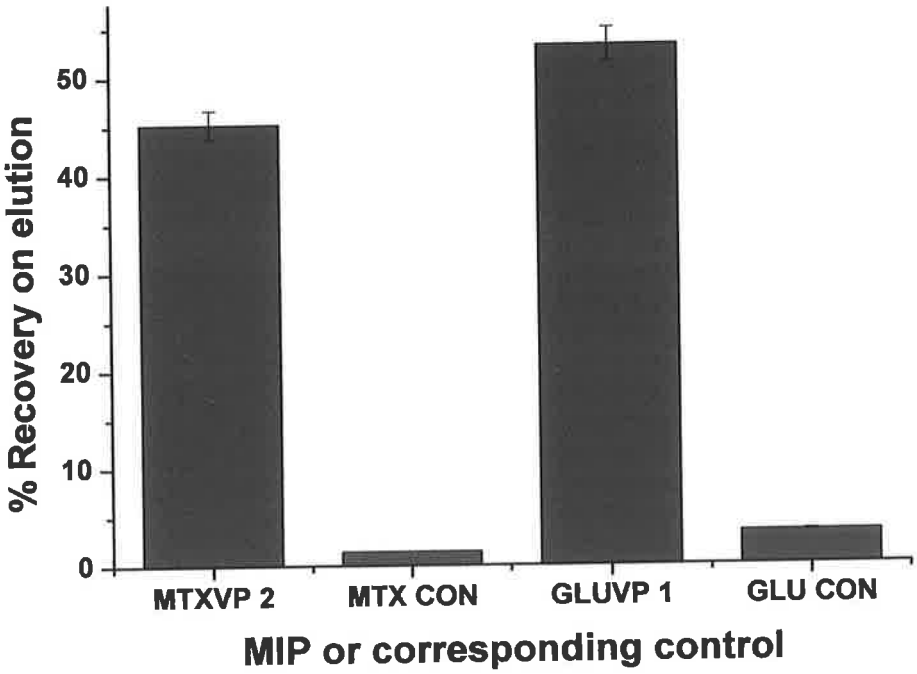

Figure 3.7: The recovery on elution of methotrexate for the 2 MIPs

From figure 3.7 it can be seen that the substructure approach was slightly more successful in terms of extraction of methotrexate from solution than imprinting of the whole molecule. This result is a validation of this approach. The advantages of the epitope approach are its simplicity, cost and removal of problems associated with template bleeding and toxicity of methotrexate.

3.4 Conclusion

Chapter 3 shows the obstacles that can prevent the generation of successful imprints. One of the most critical features in the development of the MIP is as reviewed in chapter 1, the porogen (or solvent). A good solvent should be able to dissolve fully the template and allow template: monomer complex formation without having an adverse effect. Typically in non-covalent molecular imprinting non-polar solvents such as chloroform, toluene and dichloromethane or polar aprotic solvents such as acetonitrile have been employed. Acetonitrile has also been widely used due to its poor hydrogen bond forming ability. Other highly polar solvents such as DMSO or methanol have been less frequently employed. Yet imprints have been reported with DMSO [204] and methanol [207] as porogen. It is evident then that four factors affect the use of a particular solvent

(i) Solubility of template
(ii) Polarity of the solvent
(iii) Pore forming abilities of the solvent
(iv) Effect of the solvent on PPC template – monomer interactions

Furthermore, given these features, an element of trial and error will be present in all MIP development procedures unless the explicit effects of solvent are taken into account (see chapter 5). Future work with the generation of methotrexate imprints will centre on solubility. DMF and THF may offer greater possibilities than DMSO in terms of both dissolution and augmentation of PPC interactions. Moreover, neither of these solvents participates to a large extent in hydrogen bonding as donors or acceptors. In both these respects they should be more amenable to allowing complex formation between the methotrexate molecule and the functional monomer(s). This chapter does demonstrate low non-specific rebinding when using DMSO as solvent. Furthermore direct imprinting of methotrexate was shown to be possible along with the substructure approach with "off the shelf" functional monomers.

Chapter 4

Selectivity in aqueous media: The rational design of a molecularly imprinted polymer for ibuprofen

4.1 Introduction

Recently, molecularly imprinted synthetic receptors, capable of recognising analytes under aqueous conditions have achieved significant attention [208-210]. This aspect of molecular imprinting is particularly relevant to molecularly imprinted solid phase extraction (MISPE) techniques as applied to environmental samples [211,212], samples containing biomolecules [213] and pharmaceutical preparations [214]. A molecularly imprinted solid phase extraction method was developed for determination of non-steroidal anti-inflammatory drugs in river water for which ibuprofen and naproxen were used as the template molecules [215]. The mechanism of template recognition by the MIP under aqueous conditions has been shown to be essentially dependent on factors that affect the polymer formation and arrangement [216].

As discussed in Chapter 1, three important factors that affect the formation of the pre-polymerisation complex are: the type of functional monomer employed for complexation with the template; the relative ratio of functional monomer to template that will determine the degree of complexation of the template and the solvent (or porogen). The latter will regulate important features in the pre-polymerisation complex such as hydrogen bond formation and the formation of pores of differing sizes and volumes. The functions of the porogen are to dissolve all of the components of the polymer and to allow the arrangement of the template-functional monomer pre-polymerisation complex. Moreover, the nature of the solvent employed for the rebinding step will influence events such as the relative swelling of the polymer(s).

An important aspect related to the polymer swelling which has achieved relatively little attention to date, is the particle size distribution of the MIP. The actual particle sizes of the polymer itself are not uniform. This is related to the fact that in traditional bulk polymerisation, following crushing and grinding the polymer is sieved to particle sizes within the range 25 and 75 μm. Numerous reports have dealt with alternative MIP formats such as sol–gel MIPs [217], or suspension polymerisation [218]. However, when bulk polymerisation is the method used the MIP particles will be subject to increases in size (diameter) depending on the type of solvent used in rebinding. Studies investigating swelling [219,220] have recognised

the fact that swelling of the polymer particles will cause changes in the binding site cavities. The latter leads to a loss of recognition not by weakening the interactions between the individual functionalities but rather, by changing the arrangement of the functional groups, i.e. swelling will alter the proximity of the interacting groups. It is probable that shape complementarity is at least as important a factor in affecting analyte rebinding as the functional sites themselves.

In order to successfully use MIPs as viable tools in analytical assays, it is imperative that MIPs are capable of functioning under aqueous conditions. Typically, MIPs have performed well when used in the same solvent in which polymerisation was performed i.e. a higher level of rebinding has been observed in contrast to when a different rebinding solvent is used. Of vital importance in generating a MIP competent in an aqueous environment such as water or urine is the choice of porogen [221,222]. MIPs manufactured using porogens typically employed in molecular imprinting such as chloroform [223], dichloromethane [224] or toluene [225] are expected to be incompatible with template-MIP rebinding under aqueous conditions. To produce a MIP capable of recognising a given template in an aqueous environment a relatively polar aprotic solvent may be preferred [226]. Furthermore, in order to strengthen the pre-polymerisation complex certain solvents with a high capacity to form hydrogen bonds with either the template or the functional monomer should not be employed [227]. Typical polar aprotic solvents include acetonitrile, DMSO,dimethylformamide (DMF), ACN and THF. DMSO may not be particularly suitable as a porogen (chapter 3) as it has a high propensity to form hydrogen bonds with both template and functional monomer. DMF was employed in the manufacture of a MIP capable of recognising ochratoxin A under aqueous conditions [228]. In the study, the solvent was chosen due to its ability to dissolve all of the components of the polymerisation mixture and its expected compatibility with aqueous conditions. Furthermore, DMSO and THF have been used as porogen in the development of a MIP for ampicillin [229]. The MIP prepared in DMSO was shown to be capable of efficient binding of ampicillin from aqueous buffers.

4.1.1 Aims and objectives

This chapter describes the rational design, generation and testing of a molecularly imprinted polymer specific for ibuprofen. The aim is to produce a MIP that is capable of recognising ibuprofen in aqueous media such that the drug may be selectively extracted from aqueous conditions by molecularly imprinted solid phase extraction (MISPE). Recoveries were typically high (>80%) and good selectivity for ibuprofen over structurally related analogues was seen. Moreover, the nature of the recognition between the MIP and template was investigated by NMR and molecular modelling to analyse whether or not it is possible to predict how well a given MIP will perform under set conditions. In addition, the physical characteristics of the MIP have been investigated including the particle size distribution on exposure of the MIP to different solvents. This has been related to the ability of the MIP to rebind ibuprofen under the same conditions. The data from the characterisation of the MIP have been used to further enhance the understanding of the nature of MIP recognition.

4.2 Experimental

4.2.1 Materials

Acetonitrile, methanol, dimethylformamide (DMF), water (HPLC grade), ibuprofen, methacrylic acid, (MAA), ethylene glycol dimethacrylate, 2-vinylpyridine, sodium phosphate were purchased from Sigma–Aldrich (Dublin, Ireland). Azoisobutyronitrile was purchased from Fisher Scientific (UK). Deuterated DMF was purchased from Sigma Aldrich. Deuterated DMSO and MeOH were purchased from Apollo Scientific, Bredbury, England.

4.2.2 Instrumentation

High performance liquid chromatography (HPLC) was performed on a Hewlett-Packard 1050 (HP 1050) LC system (pump, injector, detector) employing Chemstation software. The variable wavelength detector was operated at 220 nm for Ibuprofen determinations. A 10 µl injection volume was used. Separations were performed on a 25 cm × 4.6 mm, 5 µm Alltech Bravda ODS C18 column.

4.2.3 HPLC measurements

The mobile phase was a mixture of acetonitrile and 0.05 M sodium phosphate (80:20 (v/v) and the flow was maintained at 1.0 ml min^{-1}. For quantification of ibuprofen, a standard curve was constructed. Standard solutions of ibuprofen, at the following concentrations: 100, 50, 25, 12.5, 5, 1, 0.5 and 0.25 µg ml^{-1} were measured five consecutive times and the average peak areas were plotted against the concentration.

4.2.4 Synthesis of polymers

A mole ratio of 1:4 template: functional monomer was used during the polymerisation processes. A 206.28 mg weight of ibuprofen was dissolved in 4 ml of DMF in a borosilicate test tube. To this was added either 4 mmol of MAA (344.36 mg) or 2Vpy (420.56 mg) or allylamine (228.40 mg). The mixture was

stirred for 5 min. To this 20 mmol of EGDMA (4167 µl) was added and the mixture stirred for 5 min at room temperature. A 50 mg quantity of AIBN was added and the mixture was stirred for a further 10 min to ensure complete dissolution of all components. The mixture was sonicated for 10 min and sparged with N_2 for 5 min to degas it. The tubes were plugged under vacuum and gradually heated to 60 °C in a water bath for 16 h. A gel type matrix was observed after 2–3 h before solidification to form the polymer monolithic matrix. Following polymerisation, the tubes were smashed and the resultant hard polymer was removed. The polymer was broken up before being ground with a mortar and pestle and finally ground by hand. The ground particles were sieved to between 75 and 45 µm in size.

In order to verify that retention of template was due to molecular recognition and not to non-specific binding, a control (non-imprinted polymer) was prepared following the same procedure, including washing, but with the omission of the target molecule, i.e. ibuprofen.

To remove the template bound within the polymer matrix, the polymer was repeatedly washed with a mixture of hot methanol and acetic acid (10%) with vigorous mixing. The procedure was repeated until no trace of ibuprofen could be detected in the washing solution. The extracted particles were then washed with methanol alone numerous times to remove residual acetic acid and then oven dried at 70 °C for 6 h.

4.2.5 NMR studies

All NMR spectra were recorded on a Brucker 400 MHz instrument at 25 °C. The volume used for analysis was 750 µl and the concentrations of both ibuprofen (template) and functional monomer were 0.04 M. Typically, the ibuprofen was dissolved in the deuterated DMF and the monomer was added. For the purpose of spectral clarity, 2-vinylpyridine was replaced with deuterated pyridine. Data analysis was performed using the Mestrec software program. (http://www.mestrec.com).

4.2.6 Molecular modelling studies

The molecular modelling was performed using the Hyperchem software (Hypercube inc. Gainsville, Florida, US). The structures of ibuprofen and the functional monomers (methacrylic acid and 2-vinylpyridine) were drawn in the Hyperchem program and minimised to the lowest energy conformation allowed by the molecular mechanics (MM+) method and then refined using the semi-empirical mechanic (PM3) method. The conformation of lowest energy was refined with an *ab initio* (3-21 G) quantum mechanic basis set. To analyse possible interactions between template and functional monomer and for calculation of binding energies, the Amber MM method was used. The force–field was set up with constant dielectric, van der Waals and electrostatic scale factors at 0.5. The calculation of the binding energies (between template and monomer) was performed using Eq.2.1

The method employed for the modelling studies were based on that of Dong *et al.*, [205]. For calculation of the molecular volumes the Accerlys DS Viewer program was used. (http://www.accerlys.com)

4.2.7 Batch rebinding studies

For batch rebinding studies, a 30 mg aliquot of the dry polymer was placed in a 1.5 ml volume eppendorf tube. A 1 ml volume of a solution of ibuprofen at 10, 20 or 50 μg/ml was added. Uptake was assessed in water with increasing volumes of acetonitrile using a 4 h incubation period. Following this, the sample was centrifuged at high speed for 5 min and the ibuprofen present in the supernatant was quantified. The value obtained was subtracted from the initial concentration of ibuprofen added and this was taken as the amount of ibuprofen rebound. This was expressed as a percentage. All uptake studies were carried out at room temperature. For pH dependent studies, the uptake solution was adjusted to the appropriate p#H with dilutr HCl or dilute NaOH.

4.2.8 Molecularly imprinted solid phase extraction

The SPE conditions were as described in section 2.2.6. Before analyte loading, the polymer was conditioned with 1 ml methanol, 1 ml acetonitrile and 1 ml water. In the loading step, 20 μg/ml ibuprofen in 10 ml 10% acetonitrile in water was passed through. For the washing step, 1 ml of 1% triethylamine (TEA) in acetonitrile was used and ibuprofen was eluted with 1 ml of methanol. The experiments were repeated in triplicate. After each experiment the cartridge was regenerated by washing with 3 ml of water and 3 ml of methanol.

4.2.9 Sample preparation

Nurofen™ liquid capsules were used for the study. Each capsule contained 200 mg of ibuprofen. The contents of each capsule were dissolved in 10 ml acetonitrile and made up to 2 l with water to give a final concentration of 100 μg/ml. This was further diluted to a concentration of 20 μg/ml. This solution was passed through the SPE cartridge packed with appropriate polymer, washed and eluted as described above.

4.2.10 Pore size distribution and surface area studies

Pore size distribution and surface areas of the washed polymers were analysed by the Brunauer–Emmett–Teller (BET) method by nitrogen porosimtery. The analysis was performed on an ASAP 2010 from RMIT Applied Chemistry (Micromeritic). A 300 mg quantity of the dry polymer was used for analysis. The sample was degassed for 4 h at 150 °C before analysis. Relevant information obtained from this method included surface area, total pore volume and average pore diameter of the polymer.

4.2.11 Particle size studies

Particle size analysis was carried out on a Malvern Mastersizer 2000 instrument equipped with light scattering technology. The MIP (100 mg) was exposed to 20 ml of the solvent (methanol, acetonitrile or water) for 24 h before analysis. The particle size of the MIP was also acquired using the dry mode for comparison.

4.2.12 Swelling studies

Analysis of polymer swelling was conducted based on the method described by Liu *et al.,* [122]. Typically, 200 mg (the same mass used for SPE studies) was weighed into an empty SPE cartridge. A 1 ml aliquot of the appropriate solvent was added and left for 4 h at room temperature. Excess solvent was then removed and weights recorded. The swelling ratio was determined using the following equation:

$$\frac{M_w - M_d}{M_d} \qquad \text{Eqn 4.1}$$

where M_w is the mass of the wet polymer and M_d is the mass of the dry polymer.

4.3 Results and discussion

4.3.1 Analysis of the pre-polymerisation mixture

4.3.1.1 Molecular modelling and binding energy scores

The polymers were produced using the methodology described (section 4.2.4). The porogen chosen for analysis was dimethylformamide (DMF). This porogen was chosen due to its ability to dissolve ibuprofen (and all of the components of the polymerisation mixture). As a polar aprotic solvent, it was expected that DMF would be more compatible with aqueous environments than less polar solvents such as toluene or dichloromethane. DMF is classified as having a medium strength ability to form hydrogen bonds [174]. Based on the molecular modelling data obtained using Hyperchem (4.1), allylamine was deemed to be the most suitable monomer for complexation with ibuprofen due to its relatively high binding energy value as demonstrated in table 4.1

Binding scores calculated for various functional monomers with ibuprofen *in vacuo* by the Hyperchem molecular modelling program

Polymer*	Functional monomer	Binding energy ($kJ\ mol^{-1}$)
IBU 1	Allylamine	-87.94
IBU 2	2-Vinylpyridine	-55.12
-	4-Vinylpyridine	-54.62
-	Acrylamide	-43.50
-	1-Vinylimidazole	-12.01
IBU 3	Methacrylic acid	-11.80
-	HEMA	-3.74

*Only polymers using allylamine, 2Vpy and MAA were produced. 4Vpy, acrylamide, 1-Vinylimidazole and HEMA were used in the hyperchem study only.

Given the presence of a carboxylic acid functionality on the ibuprofen molecule (figure 1.24), it was expected that ibuprofen would undergo electrostatic interaction and potentially hydrogen bonding or ion pair formation with the nitrogen of allylamine and the Hyperchem derived optimised complex structure is shown in figure 4.1.

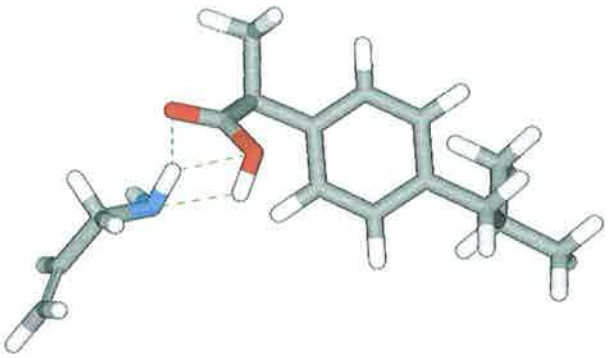

Figure 4.1: The hyperchem derived energy minimized structure of ibuprofen and allylamine. The presence of interactions is indicated by the dashed lines.

The dashed lines are representative of hydrogen bond formation. On washing the allylamine MIP (IBU 1), it was found that template bleeding was observed consistently. This continued despite vigorous washing in hot methanol with 10% acetic acid and also washing in acetonitrile and is shown in figure 4.2

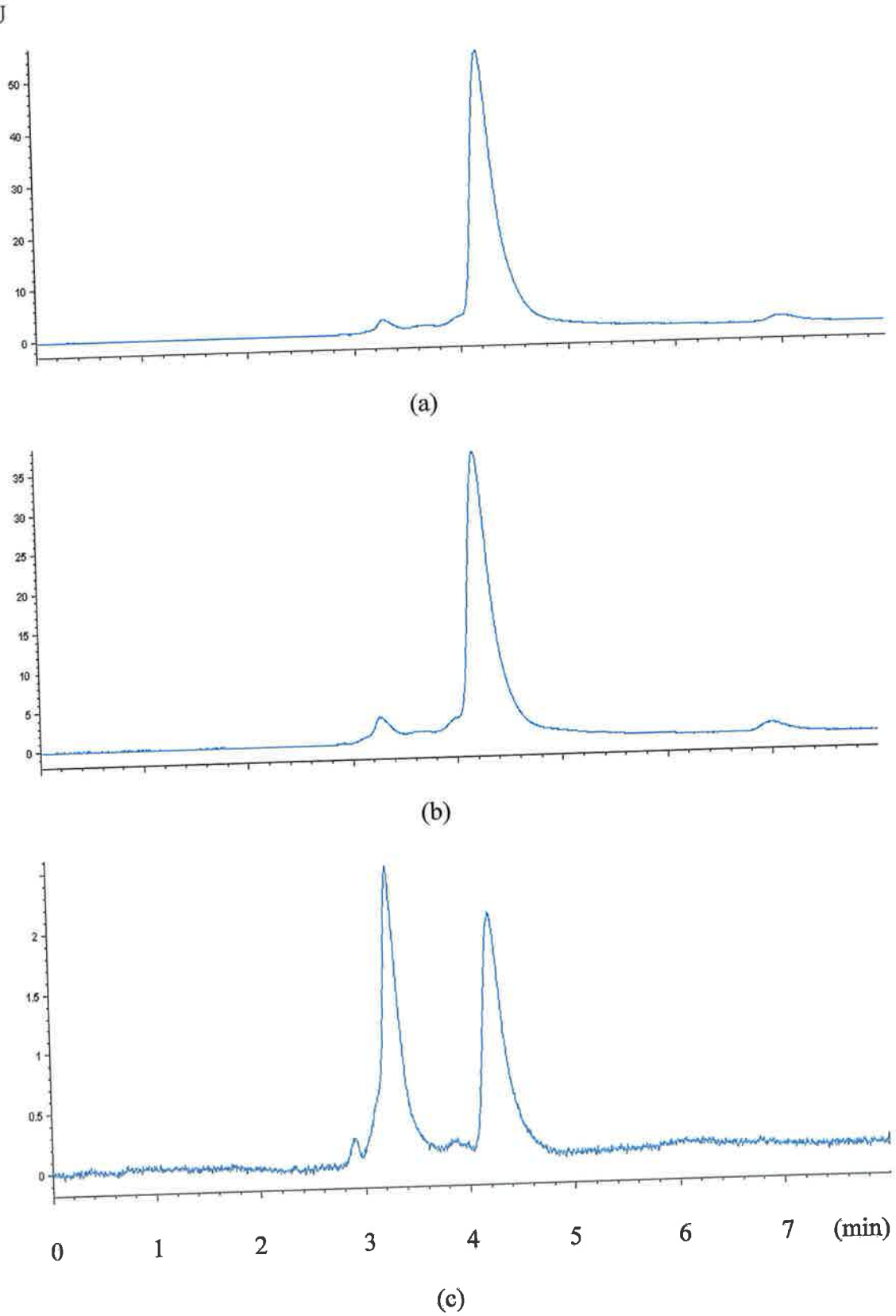

Figure 4.2 demonstrates the persistent bleeding of template (ibuprofen) observed from MIP IBU 1 showing (a) remaining ibuprofen after 10 washes in MeOH (10% HOAc) (b) after 15 washes and (c) following 20 washes.

The template bleeding may be explained by the very high value obtained for the binding energy of allylamine. This is indicative of a strong complex formation between allylamine and ibuprofen possibly an ion pair. Other authors have experienced this problem [230]. When DMF was switched for acetonitrile as the porogen, ibuprofen precipitated from solution during the nitrogen sparging process. Due to these physico-chemical factors, the development of a MIP using allylamine as functional monomer was not pursued.

The monomer(s) tested, that demonstrated the next highest binding score, were both 2- and 4-vinylpyridine. Both of these molecules were expected to demonstrate interaction with the –COOH group of ibuprofen. Furthermore, recent studies have attested to the shape complementarity of the pre-polymerisation complex being a vital aspect for the generation of high affinity binding sites in the resultant polymer. Moreover, given the presence of aromatic rings in both the template and functional monomer, it is possible that there is an electrostatic interaction between the two rings of the molecules. Hyperchem was employed to model potential interactions of the two functional monomers (2-vinylpyridine and methacrylic acid—another commonly used monomer in molecular imprinting). Methacrylic acid was shown to have a significantly lower binding score (-11.80 kJ/mol) than 2-vinylpyridine (-55.12 kJ/mol) and thus was not expected to form as strong a complex with ibuprofen. Table 4.1 shows that a stronger complex was attained when using 2-vinylpyridine. This result is in agreement with those of Haginaka *et al.,* [231] and Caro *et al.*, [215] who developed an imprinted polymer for ibuprofen and naproxen respectively using 4-vinylpyridine as functional monomer finding high selectivity. Haginaka et al., [231] suggested that hydrophobic and possibly hydrogen bonding interactions between ibuprofen and 4Vpy were responsible for selectivity. It was also found that the selectivity of the MIP decreased with increasing concentrations of ACN relative to water in the rebinding solution. Moreover, given the arrangement of the complex structure with the lowest energy minimum (Figure 4.3) the electrostatic interaction between the aromatic rings of monomer and template looked possible from modelling investigations.

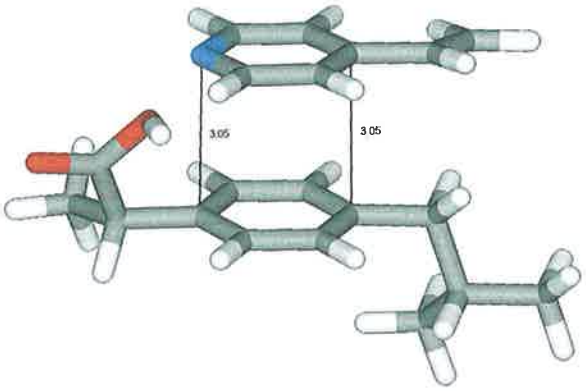

(a)

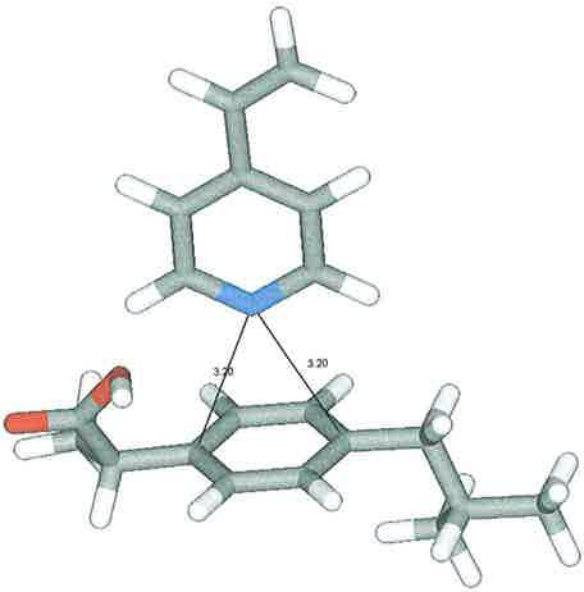

(b)

Figure 4.3: The hyperchem derived possible π-π stacking conformations for ibuprofen and vinylpyridine showing (a) the face to face stacking and (b) the edge on conformation.

4.3.1.2 NMR study

In order to investigate further the information provided by the molecular modelling studies, ^{1}H NMR experiments were carried out. Aromatic protons observed upfield due to the deshielding effect of the ring current on the aromatic ring. The latter contributes strongly to the strength of the magnetic field experienced by the protons located in the plane of the ring. At either side of the ring however, the extra magnetic field produced by the second ring opposes the applied magnetic field. Consequentially, protons that interact with this field will be deshielded and will resonate further upfield. As a result of this phenomenon, if the aromatic protons of ibuprofen undergo electrostatic interaction (or π–π delocalisation) with the aromatic protons of the 2-vinylpyridine monomer then an upfield shift will be expected. As discussed in chapter 1, aromatic π-π electron deocalisation interactions are comparatively weak and are likely to serve although important, as an additional interaction force, perhaps in terms of the stabilisation of a complex. This of course, is dependent on the relative strength of interaction between the π-electron rich donor and the relatively π electron deficient acceptor. Neither ibuprofen or 4Vpy are deficient in aromatic π electrons hence, it can be considered that any interaction between them based on electron delocalisation will be at best weak and at worst there may exist a net repulsive charge. The result of the ^{1}H NMR study is shown in figure 4.4.

An upfield shift was observed for all of the aromatic protons on addition of deuterated pyridine to a solution of ibuprofen in deuterated DMF. No changes in shift were seen at a ratio of 1:1 and only very slight changes at 1:2. Significant changes in chemical shifts of Δδ 0.32- 0.35 ppm were observed for all of the aromatic protons at the 1:10 ratio. This may indicate the formation of a weak 1:1 complex. There is also the possibility that at the lower ratios there exist the aforementioned net repulsive charge and this is overcome at higher ratios of ibuprofen: pyridine. Nevertheless, the NMR data does show an interaction between pyridine and ibuprofen in DMF.

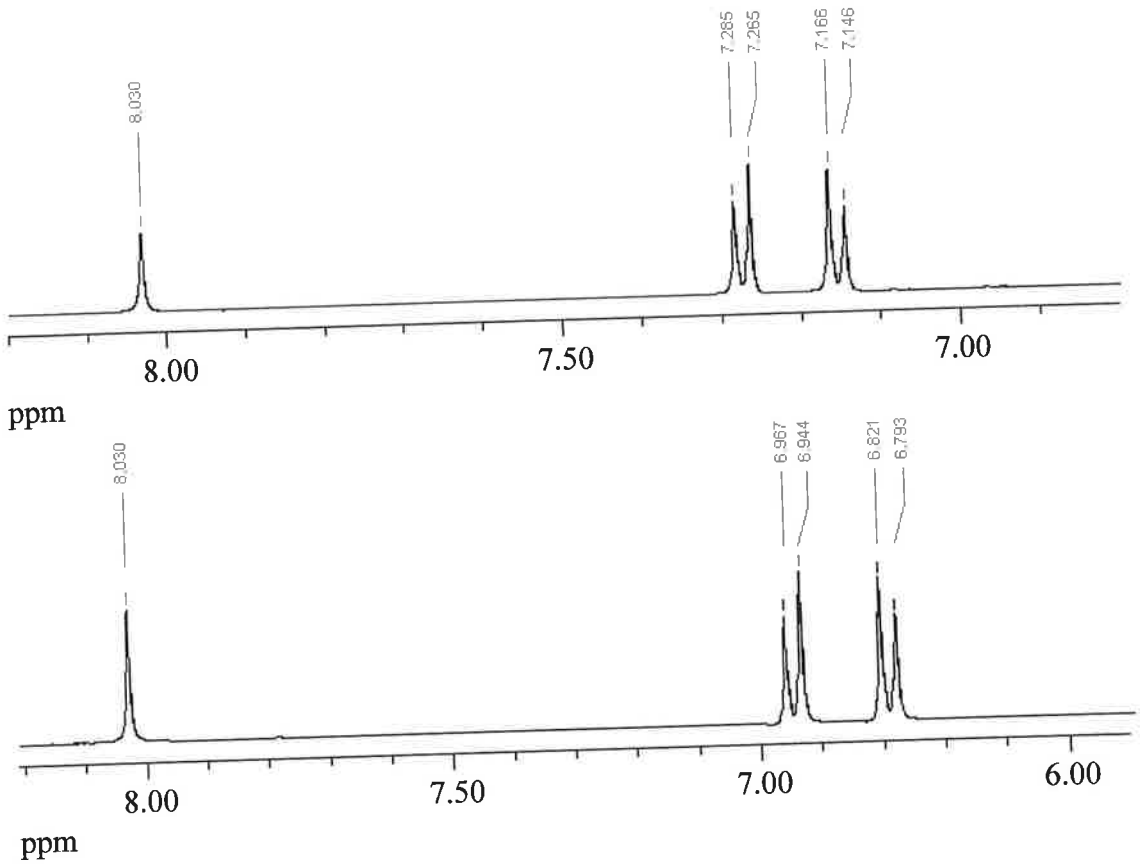

Figure 4.4: NMR (in deuterated DMF) showing the chemical shift of the aromatic protons of ibuprofen on formation of π-π stacking conformation of ibuprofen with vinylpyridine functional monomer. Above shows ibuprofen alone. Below shows ibuprofen with deuterated pyridine 1:10 ratio. The peak at 8.03 is deuterated DMF.

Interestingly, the change in chemical shift was not observed when deuterated DMF was replaced with either deuterated methanol or DMSO. This would suggest that ibuprofen undergoes a stronger interaction with the latter two solvents than with the vinylpyridine, i.e. the ibuprofen is completely solvated in these solvents, which precludes the access of vinylpyridine.

Erzöz *et al.*, [222], have described the generation of MIPs for the removal of phenolic compounds based on π-π and hydrogen bonding interactions from aqueous solutions. They synthesised a π-electron rich functional monomer, methacrylamidoantipyrine (MAAP). This monomer was then capable of becoming a π-electron donor as well as participating in H bonding interactions. It was shown to be superior to MAA as functional monomer for selective rebinding with the rationale that MAAP could undergo both H bonding and π-π interactions thus stabilising the complex at the PPC

stage. MAA was only capable of undergoing H bond interactions. The authors further state that the bound aromatic ring groups (presumably the functionality within the MIP binding cavity) had the additional ability to interact with hydrophobic compounds. The proposed mechanism of interaction of MAAP with 4-Nitrophenol is shown below in Figure 4.5

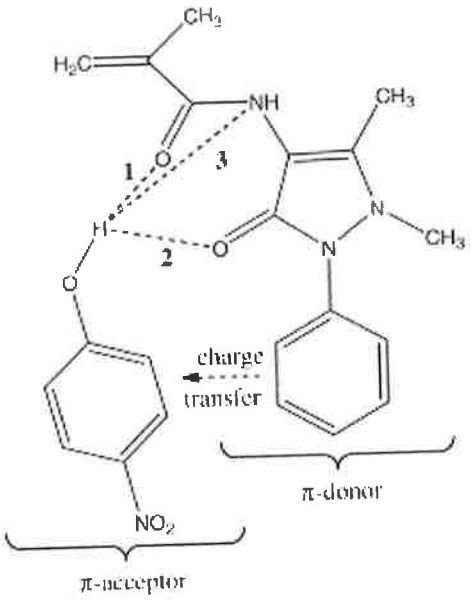

Figure 4.5 The proposed mechanism of complex formation between MAAP and 4-NP. Reproduced from Erzöz *et al.*, [222]

This is important in terms of the stability of the complex. As π-π stacking interactions are weak in nature they may not survive under polymerisation conditions – especially at elevated temperatures. However, as chapter 2 shows, a complex with multiple template-monomer interactions will be significantly more stable than with single point or 1:1 ratio interactions. Hence, it must be considered that in the correct environment the stacking interaction can be stabilised leading to the formation of an important secondary interaction. Chen *et al.*, [232] have studied the thermodynamic contribution of π-stacking towards entropy. They imprinted the pesticide 2,4-dichlorophenoxyacetic acid (2,4-D) using 4VP as functional monomer. The authors have interpreted equilibrium binding studies in aqueous media saying that among the interaction forces, electrostatic attraction provides the highest energy release in the order of tens of kJ/mol. π-stacking between the aromatic ring of 2,4-D and the pyridine group in the polymer can contribute up to 5–10 kJ/mol to the system free energy change. The stacking contributes more via the system entropy than the

enthalpy. The change of the system entropy is also due to the dehydration and rearrangement of water molecules, and to the steric fitting of 2,4-D molecules into the microcavities of the MIP. In terms of enthalpy, the measured enthalpy values are comparable with the calculated data for the dehydration of benzene, and for π-stacking [232,233]. Furthermore, the authors went on to describe that different electrostatic interactions between the molecules are responsible for rebinding at different pH's. They represented this in table form and it is reproduced in figure 4.6

Interaction forces	pH 3		pH 6		pH 9.5	
	MIP	CON	MIP	CON	MIP	CON
Structure specific interaction	+		+		+	
Electrostatic attraction (2,4-D–4-VP)			+	+		
Electrostatic repulsion (2,4-D–2,4-D)			–	–	+	+
π-stacking (2,4-D–4-VP)	+	+	–	–	+	+
π-stacking (2,4-D–2,4-D)	+	+	–	–	–	–

Note: +: favourable, –: unfavourable.

Figure 4.6 The contribution of different factors to the interaction of 2,4-D with the MIP and corresponding control. Reproduced from Chen *et al.*, [232]

Jorgensen and Severance [233] have performed monte carlo CS of pure liquid benzene in dilute aqueous solution and the benzene dimer in water and chloroform. This study found that in all cases a contact dimer with a ring centre-ring centre interatomic distance of approximately 5.5 Å was energetically preferred. The simulation also found that face-to-face structures were net repulsive, however, there were indications that shifted stacked structures become increasingly favourable with increasing arene size.

Given the nature of the pre-polymerisation complex, this provides two points of interaction. Firstly, there is the shape complementarity brought about by the proximity of the functional monomer and the incorporation of the complex into the cross-linked matrix of the resultant nano-cavities of the MIP. Secondly, there is the chemical functionality of the π–π stacking effect within the cavity. The shape of the binding cavity is as important in terms of rebinding as the distribution of the functional groups themselves. It has been demonstrated that the shape and size of the cavity in addition

to hydrogen bonding determines the selectivity of separation of phenols from anisole [234]. A detailed study has been performed by Kim and Spivak [235] on the structure-binding relationships between α-methylbenzylamine derivatives and has provided substantiation of shape selectivity in non-covalent MIPs. Shape complementarity qualifies the prediction of molecular recognition in terms of rebinding based on the data obtained from the study [235] of the pre-polymerisation complex. NMR has indicated the presence of π-π stacking interactions in this study, which may augment the dominant shape interaction.

4.3.2 Rebinding studies

For the purpose of this work, rebinding is defined as the percentage uptake of ibuprofen by the MIP when a defined concentration of ibuprofen is added to a known weight of MIP. The porogen used for the generation of the MIPs was DMF. Due to the polar aprotic nature of this solvent, it was expected that DMF would be more compatible with rebinding in an aqueous system. Initially, the rebinding was assessed in the solvent in which the MIP was prepared, i.e. DMF. Figure 4.7a shows that the % rebinding was high (>85%) for ibuprofen in DMF at the three concentrations tested, 10, 20 and 50 µg/ml.

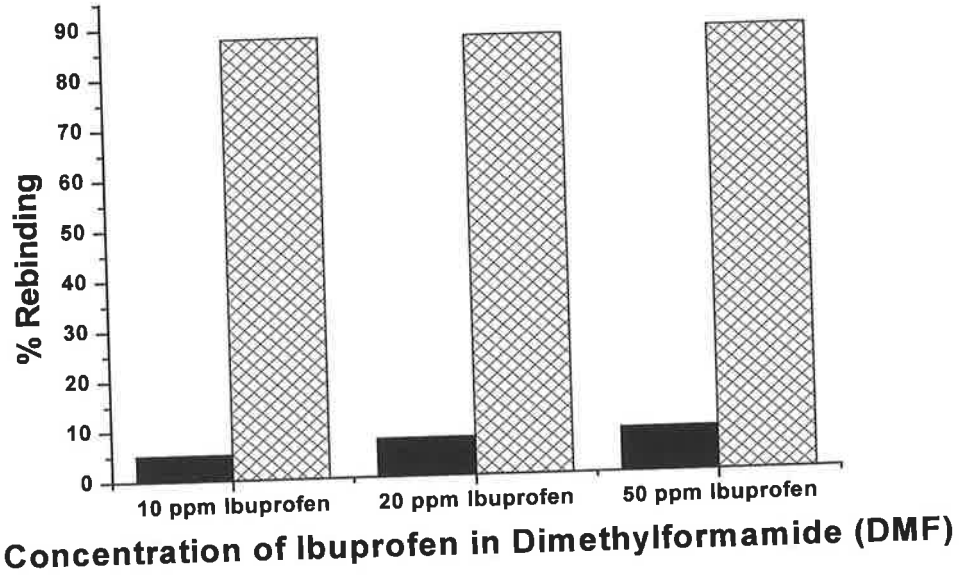

(a)

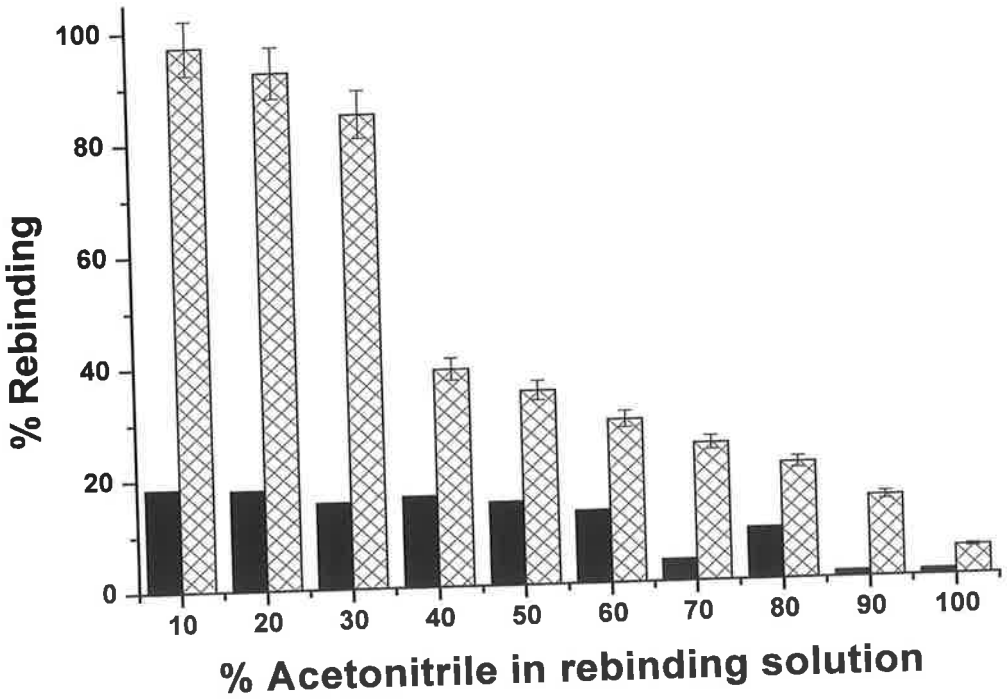

(b)

Figure 4.7: Bar graph showing the uptake of ibuprofen by 20 mg of polymer at different concentrations in 1 ml dimethylformamide (DMF) alone Control Polymer MIP **(a) and showing the effect of increasing ratios of acetonitrile in the rebinding solution on the % uptake of ibuprofen by the MIP IBU 2 and its corresponding control polymer (b)** MIP Control Polymer

The uptake of ibuprofen by the control polymer was found to be low and below 10% of that for the same concentrations of template on the imprinted polymer. The rebinding of ibuprofen to the MIPs was then assessed in an aqueous matrix with an increasing ratio of acetonitrile. Given the relative insolubility of ibuprofen in water, it was necessary to include acetonitrile in each rebinding solution. Hence, the ratio of the rebinding solution varied from 100% acetonitrile to 10:90 acetonitrile: water.

The percentage uptake, for these experiments is defined as the quantity of ibuprofen present in the supernatant subtracted from the original added concentration. The % uptake of ibuprofen on MIP IBU 2 as compared to the corresponding control polymer is shown in figure 4.7 b. As is evident from the results obtained rebinding was found to be highly efficient when lower ratios of acetonitrile were included in the rebinding solution. At a composition of greater than 30% acetonitrile, a drop in specific rebinding of approximately 40% was observed. At higher concentrations of acetonitrile, the percentage rebinding was only approximately 20%. This study indicates that the rebinding is solvent specific and that the conditions for selective rebinding are promoted by the aqueous rather than the organic solvent. Rebinding had already been shown to be efficient in DMF. Acetonitrile was chosen as it is a polar aprotic solvent and also due to its expected compatibility with the π–π interaction environment. As can be seen though, a significant decrease in rebinding was observed on addition of acetonitrile to the binding solution (see below morphological characterisation of the imprinted polymers).

4.3.2.1 pH dependent rebinding

As the % rebinding was higher when a greater volume of water was present the effect of pH on rebinding was investigated. pH values from 5 to 8 were tested with the same uptake solution ratios as discussed above. The pH dependent uptake is presented graphically in figure 4.8

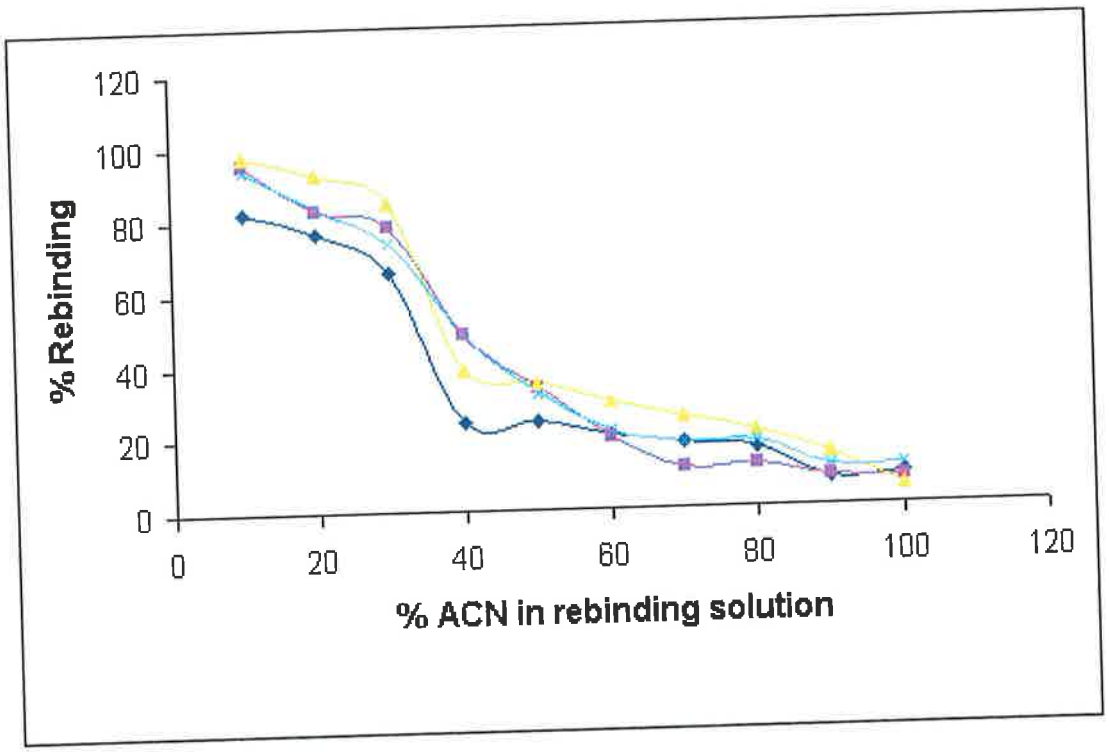

Figure 4.8: The effect of pH on the specific uptake of ibuprofen in 1 ml uptake solution by the MIP IBU 2 (20 mg)

From this study, it can be seen that the % rebinding is lower by approximately 20% at pH 5, whereas there is no significant variation between pH 6 and 8. This illustrates that the nature of the rebinding of ibuprofen to the MIP is pH independent above the pK_a value. At one pH unit above the pK_a value, >90% of the molecule will be deprotonated (negatively charged). As the pH nears the pK_a value the amount of molecules negatively charged increases (it will be 50% at the pK_a value).

This may indicate a contribution towards complex formation from hydrogen bonding or electrostatic interaction at a lower pH. As an acid–base equilibrium or hydrogen

bond interaction is subject to changes in pH however, it can be argued that contribution to the selectivity of the MIP from these interactions is minimal or at best augments the shape selectivity and π–π stacking effect. Furthermore no evidence for hydrogen bond formation in the pre-polymerisation complex was observed by NMR studies in DMF.

4.3.3 Molecularly imprinted solid phase extraction

Turner *et al.*, [228], employed DMF as a porogen for the imprinting of ochratoxin A. They expected that the use of DMF as porogen would be compatible with subsequent rebinding under aqueous conditions. The NMR data above shows that there is a π-π interaction between ibuprofen and pyridine in DMF. However, as discussed this type of interaction is comparatively weak and at best augments the rebinding due to geometric fit. Furthermore, it is also possible that under aqueous conditions rebinding is driven by hydrophobic interactions between ibuprofen and the binding cavity. To test the ability of the MIPs IBU 2 and IBU 3 to specifically extract ibuprofen under aqueous conditions SPE was used. Given the results obtained for the preliminary rebinding studies, the solid phase extraction procedure was designed as follows. The analyte was loaded in 10:90 ACN: water, washed with 1% TEA in ACN and eluted with methanol. Figure 4.9 shows the recovery on elution for the two MIPs studied, IBU 2 and IBU 3.

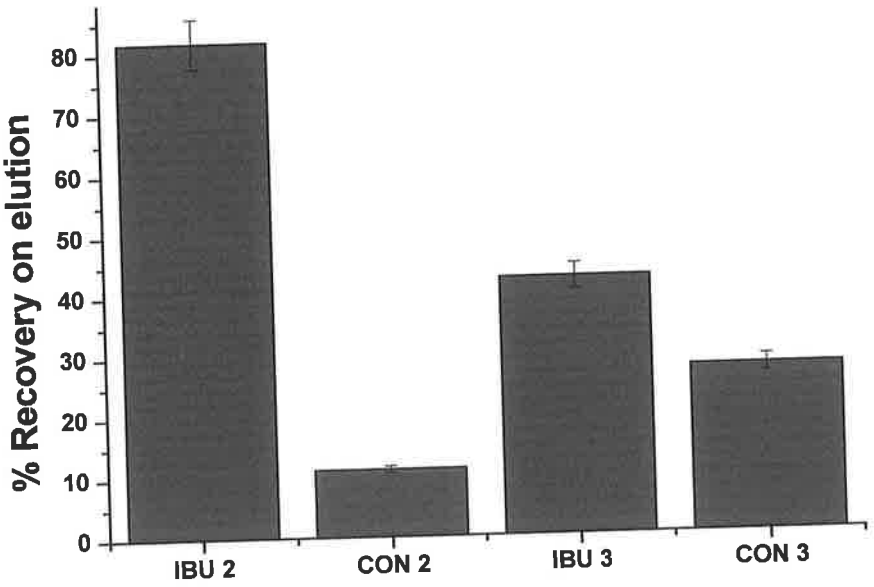

Figure 4.9: Comparison of the recovery of ibuprofen by MIPs IBU 2 and IBU 3 by solid phase extraction along with the corresponding controls.

Both MIPs were made using DMF as porogen however, the functional monomer was different in each case. When 2-vinylpyridine was replaced with methacrylic acid significant reduction in specific recovery on elution was observed. Furthermore it was also observed that with the MAA MIP, a higher level of non-specific binding was seen. This validates the initial modelling studies (table 4.1 and figure 4.2) which had predicted using energy minimisation calculations that a MIP for ibuprofen prepared with vinylpyridine would give a stronger interaction than one prepared with methacrylic acid as monomer. In addition, as described previously, the rationale supporting the significantly higher binding score of vinylpyridine over methacrylic acid is the nature of the specific interaction and orientation of the pre-polymerisation complex.

Several other approaches to the SPE studies were undertaken. It was found that loading in greater ratios of acetonitrile: water led to a reduction in the % recovery on elution. Loading in methanol was found to result in non-retention of the ibuprofen. This was attributed to the high degree of solubility of ibuprofen in methanol leading to a large degree of elution (or non-retention) during the loading phase.

4.3.4 Real sample analysis

To investigate the ability of the SPE method to extract ibuprofen from a pharmaceutical preparation, a Nurofen™ liquid caplet containing 200 mg ibuprofen (in gel form) was used. The liquid ibuprofen was dissolved in a minimum volume of acetonitrile and made up to a concentration of 20 μg/ml. SPE was conducted with loading in 10:90 ACN: water. Figure 4.10 shows the recovery of ibuprofen from the liquid Nurofen™ capsule.

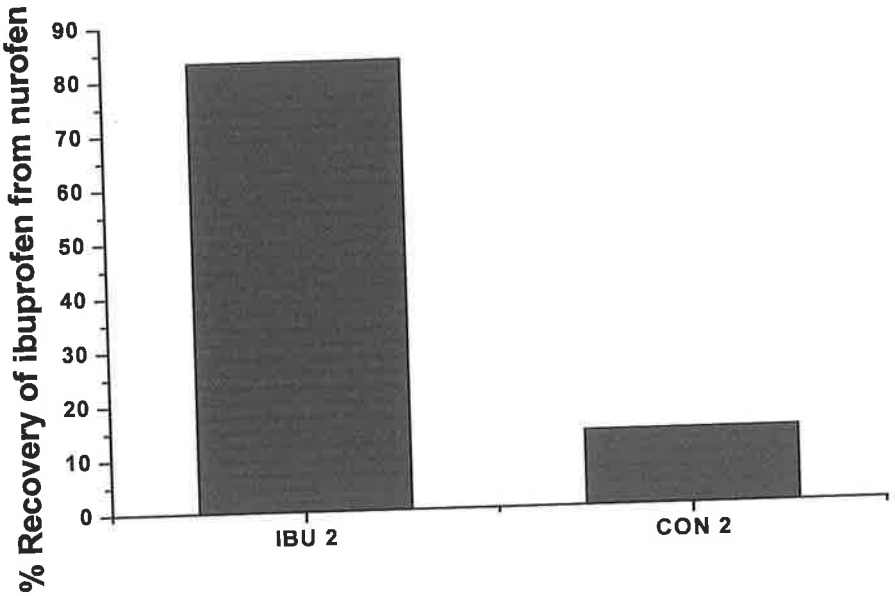

Figure 4.10: The specific recovery of ibuprofen from a Nurofen™ caplet by MIP IBU 2 alongside the corresponding control polymer

As can be seen the % recovery on elution was high in comparison to the control. The MIP has thus shown to bind ibuprofen very strongly. A highly efficient clean up system for extraction of ibuprofen from pharmaceutical preparations has been demonstrated using MIP technology.

4.3.5 Selectivity in MISPE

The selectivity of the MIP for ibuprofen over the ibuprofen analogues ketoprofen and naproxen was investigated using solid phase extraction. Table 4.2 shows the recovery on elution of each of the three compounds:

Table 4.2 Recoveries of ibuprofen and analogues on MIPs IBU 2 and IBU 3 along with the corresponding controls (CON 2 and CON 3)

Compound	IBU 2	CON 2	IBU 3	CON 3
	% Recovery	% Recovery	% Recovery	% Recovery
Ibuprofen	83.34	2.81	21.20	2.51
Naproxen	30.96	3.25	14.32	2.57
Ketoprofen	17.94	1.44	4.52	1.08

The structures of both ketoprofen and naproxen contain two aromatic rings. However, the molecular volume (as calculated by Accerlys) for ketoprofen is significantly larger than that of naproxen (ketoprofen having a molecular volume of 178.4 Å and naproxen being 151 Å). The molecular volume of ibuprofen has been calculated to be 149.8 Å. The study by Haginaka *et al.*, [233] found a similar trend in terms of specific binding in HPLC studies. Given the probability of both ketoprofen and naproxen forming π–π interactions with vinylpyridine, there are three possible explanations for the selectivity of the MIP for ibuprofen over the analogues. In the first case, the incorporation of the pre-polymerisation complex into the cross-linked matrix leads to cavities with structural memory as well as specific functional groups. Secondly, the nature and strength of the π–π interaction(s) with the analogues will be different. Ketoprofen contains a carbonyl group in between the two aromatic rings. This group will change the electron density of the ketoprofen molecule affecting its potential π stacking arrangement. A similar situation applies to naproxen. Two adjoined aromatic rings will have different π electron resonance to a single ring and will lead to changes in the nature of the interaction. Thirdly, as Erzöz *et al.*, [222] pointed out, an aromatic functionality within the binding cavity may have the ability

Table 4.3 Data obtained from nitrogen porosimetry analysis for both MIPs and the corresponding control polymers

Polymer	Surface area (m^2/g)	Total pore volume (cm^3/g)	Avg pore diameter (nm)
IBU 2	316.67	0.638	7.60
CON 2	213.39	0.144	2.62
IBU 3	270.77	0.179	2.56
CON 3	174.36	0.152	3.32

A point of note from table 4.3 is the larger average pore diameter of the MIP compared with the pore size of the control. The IBU 2 has an average pore size of almost three times that of CON 2. Given that the relative ratio of template: functional monomer may be 1:2 or greater, the molecular volume of the complex will be quite large. Preliminary studies indicate a value in the region of 500–600 Å (data not shown). This will invariably lead to polymers with larger sized cavities allowing easier access of template during rebinding. Thus, the cavities formed by removal of the template may contribute to the larger pores of the MIP.

Particle size studies were carried out to investigate the effect of solvents on MIP particles. Turner *et al.*, [228] have demonstrated that swelling of MIPs has a detrimental effect on their performance in terms of rebinding finding that a MIP with a higher average particle size performed poorly in terms of rebinding relative to a MIP with a smaller average particle size. Here it is shown that exposure of the IBU 2 MIP to different solvents significantly affects the particle size distribution (table 4.4 left column). The MIP (IBU 2) showed that exposure to water caused the least increase in particle size, whereas exposure to methanol caused the greatest. The particle size study compares well with the simple swelling analysis study (table 4.4).

to interact by non-specific hydrophobic interactions with hydrophobic compounds. The solubility of ibuprofen in water is $1.74x10^{-4}$ mol/L [236]. Naproxen is significantly less soluble in water ($6.31x10^{-5}$ mol/L). However ketoprofen is slightly more soluble than ibuprofen ($5.58x10^{-3}$ mol/L) [236]. Hence, it is most likely that there are combined effects that are responsible for the specific and selective uptake of ibuprofen from solution. These effects are primarily, shape complimentarity, hydrophobic effects and π electron interactions. It is important to note that the mechanism of selectivity of the MIP for ibuprofen over ketoprofen and naproxen may be different (in terms of π interactions and hydrophobic interactions) but in either case it is dominated by geometric effects. The possibility of structural memory of the MIP warranted a further investigation of the polymer morphologies, and this is described in section 4.3.6.

4.3.6 Morphological characterisation of the imprinted polymers

To further probe the nature of the structural selectivity, morphological studies were conducted on the ibuprofen MIPs. The results of these studies are presented in tables 4.3 and 4.4. The pore structure and surface area were studied using the nitrogen porosimetry adsorption method (table 4.3) and the particle size distribution was studied using Malvern instruments light scattering technology (table 4.4). As reported [201], MIPs tend to have higher surface areas than the corresponding controls. A result of this phenomenon is that the MIP will have more binding sites that are better distributed throughout the cavity. A greater total pore volume is indicative of the MIP having a superior sample load capacity. As can be seen from table 4.3, the MIP IBU 2 expresses over 4 times the total pore volume of its corresponding control polymer (CON 2).

Table 4.4 Data obtained from particle size and swelling studies

Solvent of exposure	d50 (μm)[1]	Swelling Ratio[2]
Water	63.260 ±2.4	1.325
Acetonitrile	69.525 ±6.1	1.815
Methanol	71.859 ±8.2	2.090
Dimethylformamide	*	1.414

[1]defined as the size (in μm) below which 50% of the particles (sample) lie

[2] defined as $(M_w-M_d)/M_d$, where, M_w is the mass of the wet polymer and M_d is the mass of the dry polymer

*Particle size data not available

From this study it can be seen that exposure to water causes the smallest increase in weight ratio whereas exposure to acetonitrile and methanol significantly enhance the swelling. Referring to figure 4.5, it can be seen that rebinding was significantly better in water (with 10% acetonitrile) than in acetonitrile alone. In addition, exposure of the MIP to DMF causes only marginally more swelling than exposure to water. In general MIPs perform better in the solvent in which they are prepared. The results suggest that swelling in water: ACN (90:10) may be closer to that observed in DMF under the conditions in which the MIP was prepared. The aim of this study was to design a MIP for ibuprofen capable of rebinding under aqueous conditions and to rationally explain the physico-chemical nature of this. This study reiterates the importance of an aqueous environment for rebinding of ibuprofen. In this environment both hydrophobic interactions and π electron interactions will be pronounced.

4.4 Conclusion

The aim of this study was to rationally design a molecularly imprinted polymer for ibuprofen capable of being used in an aqueous environment. This was successfully synthesised. This MIP is capable of recognising ibuprofen in aqueous samples with acceptable selectivity over the structurally related analogues naproxen and ketoprofen. A non-imprinted polymer (NIP or control), constructed in parallel with the MIP did not possess this recognition ability. A further aim was to investigate the chemical and physical nature of the recognition. For this, studies were carried out into the nature of the pre-polymerisation complex formation. NMR and molecular modelling software were used for this purpose. Data attained by these methods were used to construct the MIPs in a rational design approach. A contribution to the complex formation between ibuprofen and 2-vinylpyridine is understood to be a π–π stacking arrangement between the aromatic rings of monomer and template. In DMF or under aqueous conditions this interaction may be more important that a H bonded or ion pair interaction

The rationale for the ability of this MIP to work effectively in an aqueous environment lies with the polar aprotic nature of the porogen DMF. Since the stacking interaction is electrostatic in nature it would be as strong in a nonpolar solvent (e.g. chloroform) or in a more polar solvent (e.g. MeOH). A detailed molecular dynamics simulation study of the nature of π-π stacking complexes in explicit solvent is performed in chapter 5. It is of course entirely plausible that a successful MIP against ibuprofen could be generated in either non-polar or polar solvents. However the fundamental nature of the PPC will be different under these conditions and 2-vinylpyridine may or may not be the most suitable monomer for that particular porogen.

Following construction of the MIP, the percentage rebinding was evaluated and selectivity assessed by solid phase extraction. The MIP, IBU 2–made using 2-vinylpyridine as a monomer–showed high selectivity for ibuprofen over structurally related analogues. It was furthermore capable of quantitatively extracting ibuprofen from a pharmaceutical preparation.

Physical characterisation of the polymer was performed by analysis of the porous environment and by particle size analysis. The surface area and pore volume were significantly higher for the MIPs over the controls and for IBU 2 in comparison to IBU 3. This is indicative of better accessability of functional sites within the pores. The higher total pore volume is suggestive of the MIP having a higher load capacity. Swelling was investigated using particle size studies on exposure of the MIP to different solvents. A higher degree of swelling corresponded to poorer rebinding results in the same solvents. The implication again is that the pre-polymerisation environment can act to stabilise secondary (or weak) interactions but interactions that can exist in aqueous systems and hence this is the mechanism of recognition in the aqueous system.

Chapter 5

Optimising selectivity in MIPs – molecular dynamics simulations and the preparation of uniform beads

5.1 Introduction

Modelling of a system resembling the pre-polymerisation mixture with solvated template, functional monomer and cross-linker is a complex task that requires extensive computational resources. The AMBER strategy aims at simulating complexation events between template molecules and selected functional monomers in the pre-polymerisation mixture using molecular dynamics simulations in the nanosecond (ns) timeframe. These models are based on an accurate physical representation of the solvent environment by explicitly including the solvent molecules. This approach focuses on obtaining a fundamental insight into complex formation and behaviour with time. In addition, the influence of solvent molecules on the complexation events and types of occurring molecular interactions are investigated. So far, computational approaches based on combinatorial libraries or molecular modelling are limited to few applications. However, their importance in elucidating the mechanisms of binding site formation and molecular recognition of MIPs is undoubted.

Recently, significant improvements in the morphology of MIPs have been achieved an example of which being Weng et al., [237] and based on the morphological nature of the polymer, MIP technology is being incorporated into and ever increasing array of analytical methodologies. The work presented in this thesis so far has focused on the two contributing factors to the rebinding of the template - the physical shape and dimensions of the pores and the distribution and strength of the functionalities contained within the pores. To elucidate the true nature of the PPC in terms of understanding the factors that drive the MIP firstly to rebind to a particular template and secondly to selectively discriminate between the template and structurally and functionally similar compounds, a more fundamental knowledge of the development of the pre-polymerisation complex and its interaction with its immediate environment i.e. solvent (or porogen) is required. This can be achieved in a number of ways, namely molecular spectroscopy and NMR as already discussed [23,103,106] or by the employment of computational analysis based on molecular modelling.

Molecular modelling itself has achieved significant attention throughout the history of the rational design approach to MIPs. One area already dealt with in this thesis is the ability of MIPs to recognise targets in aqueous media. One of the most important criteria affecting this ability is the choice of imprinting solvent. This point further emphasises the importance of including solvent in molecular modelling and MD simulations. Indeed the importance of solvent in subsequent recognition ability of MIPs has been the subject of several studies. In the literature, both functional and morphological effects of different porogens on MIPs have been investigated. A comparative study on the influence of porogens on the rebinding ability and selectivity of a MIP towards nicotinamide was performed [113]. The results of the study found that the properties of the porogen namely hydrogen bond capacity and dielectric constant had significant effects on the interaction energies (ΔE) of the template-monomer interactions. Aprotic solvents were predicted to lead to MIPs with better affinity and selectivity. In this study a morphological approach using SEM on imprinted polymers (and volumes of porogens) was undertaken [79]. It was demonstrated that MIPs generated in acetonitrile produced better defined spherical polymer microparticles. Importantly, it was observed that the MIPs prepared with acetonitrile showed greater specific % rebinding than MIPs prepared with the more non-polar dichloromethane. This is further proof of polar aprotic solvents (e.g. acetonitrile, DMF) enhancing subsequent rebinding in resultant MIPs. Molecular dynamics (MD) simulations using AMBER have also been explored. AMBER comprises numerous programs for modelling and MD simulations. Furthermore, hydrogen bonding interaction was confirmed between 2,4-dichlorophenoxyacetic acid and 4-vinylpyridine in chloroform, while in water the dominant interaction in complex formation was shown to be a π-π stacking arrangement. From this study it is again evident that the solvent used has a significant effect on the nature of the interaction of template and monomer in the formation of the PPC.

Wu *et al.*, [238], have performed complex simulations employing sequential modelling methods – the PM3 semi-empirical quantum method and the *ab initio* method (Hartree-Fock method with a 6-31G basis set). These approaches, allow the determination of the energy of a system (pre-polymerisation complex) based on quantum mechanical explanations of molecular systems which approximate the Schrödinger wave function. The Hartree-Fock method creates numerous wave

functions and works on the assumption the wave function of minimum energy will approximate the true wave function. Approximate molecular orbital theories (also known as semi-empirical quantum methods) are less computationally expensive yet produce results of comparable accuracy to *ab initio* quantum methods. This is allowed because of the system of approximations rather than intricate detailed calculations of integrals – recognised as the most computationally intensive aspect of *ab initio* methods. Furthermore, only valence electrons are considered for calculation.

Both *ab initio* and semi-empirical methods are superior methods of incorporating aspects of atomic behaviour compared to mechanical force fields describing processes as bond stretching, rotation and torsion. These relatively simple models will not describe important complexation events such as π-π stacking or hydrophobic interactions [141]. The major disadvantage of the *ab initio* and semi-empirical approaches is that the model systems are studies *in vacuo*. As pointed out throughout this thesis and in the literature, the porogen has a major impact on both the formation and the stability of the pre-polymerisation complex. Considering this point, the above disadvantage is quite considerable.

The importance of the porogen is vital in this regard. If the matrix effects are not taken into account then potential interactions of the PPC with the matrix such as H bonding and van der Waals interactions are not incorporated into the model leading to a distorted representation of the complex formation. As a result of this, energy calculation values can be somewhat different when solvent effects are considered.
Molecular Dynamics (MD) simulations are now increasingly being used for the purposes of gaining a greater appreciation of the intermolecular forces (interactions) involved in the formation of the PPC. Data produced from MD simulations include interaction energies (binding scores), closest approach distances and active site groups between molecular systems and different ligands.

In terms of the overall approach of optimising MIP performance in rebinding, a suspension polymerisation procedure was adopted for generation of the MIPs. Production of beaded MIPs has been shown to be superior in contrast to monolith MIPs in terms of ease of preparation, time costs and can be applied to systems using commonly used functional monomers and porogens. Furthermore, given that

suspension polymerisation can produce beads of given size, the technique is highly applicable to applications such as solid phase extraction and HPLC column packing. In this study, suspension polymerisation based on liquid fluorocarbon as the suspending medium based on the method of Perez-Moral and Mayes [239] has been employed. It is a fast and reliable methodology that synthesises particles by UV irradiation in 10–20 min (for easily-polymerising monomers). The beads obtained have a diameter that can vary between 5 and 50 μm depending on the stirring speed and the amount of surfactant. It employs a perfluorocarbon solvent (perfluoro-(1,3-dimethylcyclohexane) (PMC)) in the continuous phase, which allows the establishment of the same interactions that occur in "bulk" polymers (each particle acts like a mini-bulk reactor). The fluorocarbon-suspending medium can be easily recycled by distillation. The technique has not been widely adopted however despite its many advantages. This is possibly due to misconceptions that it is complex, needs extensive re-optimisation of the process or stabilising surfactant for each new system or suspicion that it produces polymers with unusual properties or higher non-specific binding than conventionally produced materials as reported by Ansell and Mosbach [53].

5.1.1 Aims and objectives

With the above studies taken into consideration, the aim of this work was to fully investigate by molecular dynamics simulations in explicit solvent the nature of the stability of a PPC for naproxen and the functional monomer – 4-vinylpyridine. Three solvents of differing properties were selected for the modelling studies; DMF, chloroform and methanol. These three solvents along with the monomer mentioned are commonly used in molecular imprinting. Importantly, it was an objective of this work that data obtained from the MD simulations is verified by NMR spectroscopic studies. Furthermore, based on the MD simulation data, corresponding MIPs (using suspension polymerisation based on liquid fluorocarbon as the suspending medium) have been produced and their rebinding to naproxen has been investigated thoroughly by uptake and displacement studies. In addition, the final objective was to demonstrate the selectivity of the optimum MIP for naproxen over the closely related structural (and functional) analogues ketoprofen and ibuprofen.

5.2 Experimental

5.2.1 Materials

Naproxen, ibuprofen, ketoprofen, deuterated DMF and phosphoric acid were purchased from Sigma-Aldrich (Dublin, Ireland). Methacrylic acid, 4-vinylpyridine, 2,2'-dimethoxy-2-phenylacetophenone (DMAP) were obtained from Sigma-Aldrich (Poole, U.K.). EDMA was washed with 1M NaOH and dried with anhydrous $MgSO_4$ and stored over molecular sieve. 4-VP was vacuum distilled and stored in freezer. Deuterated methanol was obtained from Apollo Scientific, Bredbury, U.K. All other solvents were purchased from Labscan, Dublin, Ireland. Perfluoro-(1,3-dimethylcyclohexane) (PFDMC) was obtained from Fluorochem (Old Glossop, U.K.)

5.2.2 NMR studies

All ^{1}H NMR spectra were recorded on a Brucker 400 MHz instrument at room temperature. The volume of each sample tube was kept constant at 750 µl and the concentration of naproxen and pyridine was 0.04 M. Typically, naproxen was dissolved in the appropriate deuterated solvent and the monomer was then added at naproxen: monomer ratios 1:1, 1:2, 1:4, 1:10. For the purposes of spectral clarity, 4VP was replaced with deuterated pyridine. All data processing was performed using the MESTREC ^{1}H NMR software program (www.mestrec.com). All peaks were referenced to the appropriate deuterated solvent peak.

5.2.3 Preparation of molecularly imprinted polymers

Suspension polymerisation with the following procedure was carried out. PFDMC (25 mL) was saturated with the porogenic solvent. Typically, 1-3 drops of solvent were added and the mixture shaken. Saturation was achieved when a few very small droplets were seen floating on top of the PFDMC. A 100 mg quantity of surfactant was then dispersed in the fluorocarbon by shaking and then stirring. The imprinting mixture in 3.18 mL of porogen was then added and stirred. A 1:4:20 ratio of

naproxen: 4VP: EGDMA with 1% mol of initiator (DMAP, UV initiator) was used for the process. The above mixture was placed into a reactor comprised of a straight tube with a side arm for Ar purging. The tube was surrounded by a water jacket for temperature control. An overhead stirrer (IKA Eurostar digital, IKA, Werke, Stanten, Germany) equipped with a stainless steel paddle was used for agitation. Water at 60^0C was recirculated through the water jacket. The two phases were mixed by stirring at 2000 rpm for 5 minutes. Then Argon was purged through the mixture for 5 min to removed dissolved oxygen. The Ar supply was removed and the mixture stirred at 500 rpm and held at this speed for the duration of the polymerisation which was performed using a UV light (Black ray lamp from Ultraviolet products ltd). The lamp was placed very close to the apparatus and the polymerisation was continued for 15 min. Following polymerisation, the contents of the reactor were emptied into a sintered glass funnel and filtered from the excess continuous phase. The beads were washed several times in acetone to remove excess surfactant.

Dried polymer particles were imaged using a light microscope following polymerisation at 10x and 40x to verify that the procedure had been successful.

5.2.4 Scanning Electron Microscopy (SEM)

For SEM, fine polymer particles were placed (sprinkled) onto aluminium pegs and then gold coated. Imaging was performed using a Hitachi S3000N scanning electron microscope (tungsten filament).

5.2.5 Rebinding studies

5.2.5.1 Optimisation of polymer amount

In order to determine the weight of polymer for use in the rebinding assay, a 10 μg/mL concentration of naproxen was used. A 4 mg quantity of MIP (or control) was suspended in the appropriate solvent (DMF, MeOH or buffer (1mL)) in 1.5 mL microcentrifuge tubes and serially diluted (2x) to 0.032 mg by suspending the polymer by vortexing and removing 0.5 mL for further dilution. 0.5 ml of a 20 μg/mL concentration of naproxen (giving a final volume of 1ml and concentration of 10

μg/mL per tube) was added. The tubes were incubated by shaking at room temperature for 16 h. Following this, the tubes were centrifuged at 12,000 rpm for 10 min and the supernatant removed. The concentration of naproxen in the supernatant was determined by HPLC with reference to a standard curve. The % naproxen adsorbed onto the polymer was defined as total naproxen concentration minus supernatant concentration. A logarithmic plot of bound/total naproxen versus polymer concentration revealed the optimum polymer amount for use in future binding assays.

5.2.6 Naproxen displacement study

A displacement study was performed to investigate the selectivity of the naproxen MIP towards naproxen over the analogues ibuprofen and ketoprofen and also over the non-related compound caffeine. Given the necessity to measure concentrations of naproxen below the optimum concentration deduced (above), 200 ng/mL was selected for the study. Hence 200 ng/mL naproxen, along with ibuprofen or ketoprofen or caffeine in the range 50 ng/mL to 2000 ng/mL was added to 0.5 mg of MIP or control and left shaking for 16 h at room temperature. Following this, the tubes were centrifuged at 12,000 rpm for 10 min and the supernatant removed. The concentration of naproxen in the supernatant was determined by HPLC with reference to a standard curve. The initial % uptake of naproxen at the amount of MIP use (0.5 mg) had previously been determined. For this purpose, extra naproxen found in the supernatant was deemed to have been displaced from the MIP. A plot was generated of % naproxen bound to the MIP versus the concentration of displacer.

5.2.7 HPLC determinations

High performance liquid chromatography (HPLC) was performed on a Hewlett Packard 1050 system (pump, autosampler and vwd). For fluorescence measurements the detector was a HP1100 FLA. Chemstation software was used for instrument control. The VWD was operated at 220 nm for detection of naproxen, ibuprofen and ketoprofen. Caffeine was detected a 276 nm. For fluorescence studies (naproxen only) the excitation wavelength was set to 220 nm and the emission to 330 nm. A 10μl injection volume was used for all assays and separations were performed on an

Alltech bravda BDS C18 column 250 x 4.6 mm i.d. 5 μm internal diameter. The mobile phase was a mixture of acetonitrile and 0.05 M aqueous phosphoric acid (50:50 v/v) and the flow was maintained at 1.0 ml/min with isocratic elution.

5.2.8 Characterisation by HPLC

For HPLC characterisation in this study, the MIPs were mechanically slurry packed into empty 4.6 x 100 cm stainless steel HPLC columns. A 1.5g quantity was weighed out, suspended in acetonitrile by sonicating, and packed at a pressure of 200 bar. Columns were conditioned using acetonitrile until a stable baseline was reached. The mobile phase used for characterisation was acetonitrile (1% HOAc) at a flow rate of 1.0 ml/min. For performance evaluation, naproxen and ibuprofen were used, both at a concentration of 10 μg/ml. Methanol was used as the void marker. HPLC analysis was performed at room temperature.

5.3 Molecular dynamic simulations

5.3.1 Pre-modelling considerations

The following modelling procedure of the naproxen/4VP system is discussed as a sequence of several processing steps required for molecular dynamics calculations of these molecules in explicit solvent.

5.3.1.1 Generation of the molecular structure files

Topology files of naproxen and 4VP were created in Brookhaven protein data bank (PDB) format. These file types contain information such as atom type, charge, connectivity and starting Cartesian co-ordinates (see Appendix B). A drawback with AMBER 7 is depending on the origin of the files, the PDB structures (files) may require modification as AMBER may not recognise the file type. For each input file a force field description is generated which is compatible with the AMBER force fields. The template and functional monomer were defined as two residues within a unit (the

system of interest) with the solvent molecules as further residues. Each residue must be defined as such a unit. Therefore in the respective 'prepin' files Naproxen was defined as NAP, and 4-VP as 4VP. The program *Parmchk* was then used to read in the 'prepin files' as well as the forcefield files generating two output files ('frcmod') for any missing parameters. The individual PDB structures were both opened simultaneously in the same *Viewerlite* file (DS Viewer pro) and the molecules positioned in the desired starting configuration. The new pdb file for the relevant 'complex' was then saved and inspected for compatibility with the *LeaP* program.

Note: All molecular structures were initially drawn with Chemsketch 5.0 (www.acdlabs.com). The structures were drawn in 2D option, molecules elected and changed with 3D structure optimisation. This was found to be the most convenient way of generating molecular structures for conversion to PDB format in a way acceptable to AMBER. Furthermore, each molecule could be treated in the same way.

LEaP allowed solvation of the complex creating an AMBER co-ordinate and parameter/topology input file for the main MD program *Sander*. The following starting configurations were selected for Naproxen and 4-VP (figure 5.1 below)

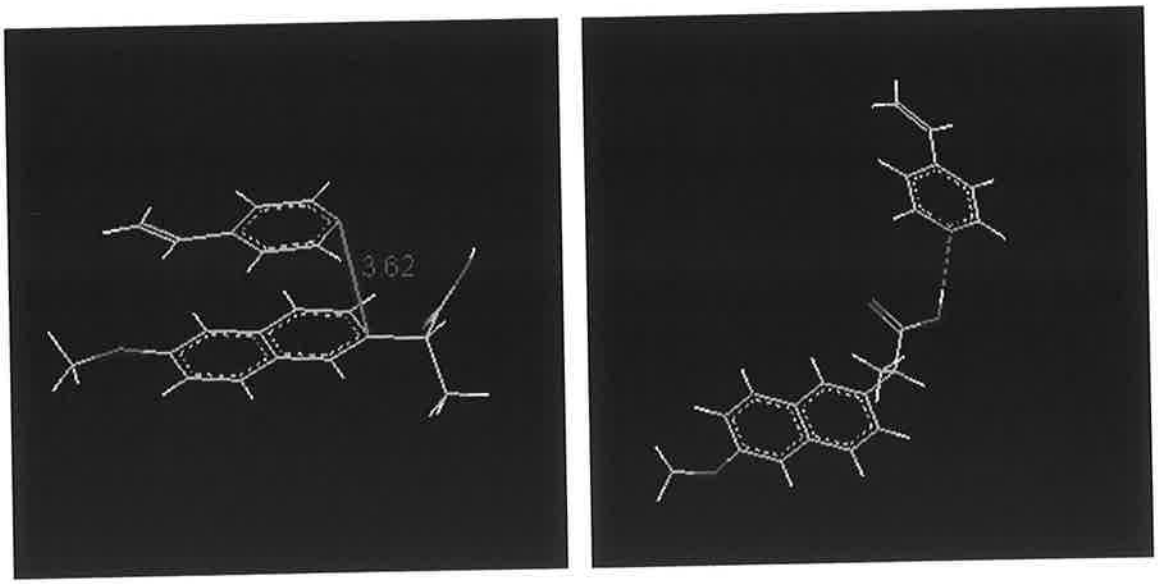

(a) (b)

Figure 5.1 Initial configurations (a) model of π-π stacking configuration and (b) hydrogen bonding/electrostatic interaction between Naproxen and 4-VP. Residue 1 (NAP 1): Naproxen Residue 2 (4VP 2): 4-VP

5.3.1.2 Solvation and preparation of structural files

Periodic boundary conditions were defined and the molecules placed in a solvent box (methanol, chloroform or DMF) with 10 Å of solvent added around the complex in each direction. For example, residues 3 to x of the solvent molecules in the box e.g. DMF molecules, DMF 1 to DMF x

5.3.1.3 Energy minimisation

Energy minimisation involved the following steps before starting the system equilibration prior to molecular dynamics runs:

- Energy minimisation with restrained solvent;
- Short MD run;
- Energy minimisation with restrained solute;
- Short MD run;
- Energy minimisation of solute and solvent without restraint;

First, the positions of the atoms were relaxed to remove any corrupt van der Waals (non-bonded) contacts without causing substantial changes to the structures. Prior to executing molecular dynamics simulations it was necessary that any large steric overlaps or electrostatic inconsistencies were minimised. Large steric overlaps lead to initially large forces and subsequent velocities frequently resulting in distortion of the structure or localised areas of distortion. During solvent energy minimisation, the solute molecules are restrained to their initial positions in order not to distort their structure. A force constant of up to 5000 kcal/mol can be selected for the restraint. For minimisation any value is possible, however, the force constants should not be too large since the frequency of the bond vibration increases with increasing force constant. This may lead to MD integration failures unless the time step for the simulation is short enough to represent the high frequency motions. A force constant of 100 kcal/mol was selected for the restrained minimisation steps. To conclude the minimisation procedure, the whole system energy was minimised with no restraints applied. Constant pressure dynamics were used allowing the box size to change. If only constant volume simulations are executed vacuum bubbles may appear in the box. The minimisation steps as well as the applied restraints were written into one text input file (see Appendix B) from where *Sander* reads all commands and applies them to the system.

5.3.1.4 Equilibration of the system

Since during longer equilibration times (e.g. 250 ps) the molecules (naproxen and 4VP) slowly drifted apart, the following distance restraints were introduced between the two molecules to prevent drifting during the equilibration step.

-Naproxen/4VP (1:1) in DMF
-Naproxen/4VP (1:1) in MeOH
-Naproxen/4VP (1:1) in $CHCl_3$

Atoms defining the ring are treated as a group and the distance between the two rings was restrained. The restraint was placed on the distance between a pair of matched atoms and was incorporated into the energy function as an additional penalty term. A distance restraint of 3.6 Å was placed between the rings. A restraint of 3 Å was placed

between the nitrogen of the pyridine ring and the proton of the naproxen molecule for the hydrogen bonded configuration (figure 5.1 a).

5.3.1.5 MD simulation (production run)

For the production run of 1 ns, all restraints were removed and the system was allowed to freely evolve. The following properties were monitored:

- Density: For chloroform the density of 1.49 g/mL should be reached and remain stable after the equilibration step. For methanol it should be 0.791 and for DMF is should be 0.944 g/mL.
- Eptot: Total potential energy should be stable after the equilibration step. If the conformation of the molecule is not in a stationary phase the potential energy is subject to drift.
- Temperature: The temperature ramping is defined in the input file for the MD calculations in *Sander* (mdin). The default starting temperature is 0 K. The reference temperature at which the system is to be kept through a weak coupling scheme is 300 K. The time constant for heat bath coupling is set between 0.5 and 5.
- RMSd: The RMSd values (in Å) are calculated and plotted using ptraj and provide information on whether the conformation has reached a stationary state. The RMS deviation of each frame in the trajectory to the first frame in the trajectory is calculated. This is useful in determining how far the structures have drifted during the MD run.

Molecular Dynamics simulations were performed on the Amber 7 molecular modelling package. The forcefields applied to production simulations were ffpp and GAFF. The conformations of naproxen/4VP and (Figure 5.1) were placed in a periodic box (periodic boundary conditions) of methanol (MEOHBOX10), chloroform (CHCL3BOX10) or DMF (DMFBOX10). DMF itself is not included in the solvent library of molecules accompanying Amber and had to be generated manually by obtaining a pdb file of DMF. The complex was placed in a box containing minimised DMF molecules. Energy minimisations were performed on the

DMF BOX until the density reached the known value for DMF. Regarding periodic box boundary conditions, 10Å of appropriate solvent was added surrounding the complex in every direction.

5.4 Results and discussion

5.4.1 Molecular Dynamics simulations of Naproxen/4-VP π-π complex conformation in explicit solvent.

The Amber 7 program allowed the observation of the interactions between naproxen and 4-vinylpyridine in three explicit solvents, namely, methanol (MeOH) and *N*,*N*'-dimethylformamide (DMF) and chloroform ($CHCl_3$) over a 1 ns trajectory. Hence, the distances between selected centered atoms on both naproxen and the functional monomer in question can be analysed throughout the duration of the simulation. This provides critical information on the proximity of interacting functional groups over time and is directly related to the length of time that the complex remains intact. Furthermore, the total time (in terms of percentage of the simulation run time) that the molecules lie in close proximity and are able to form hydrogen bonds or participate in π-π delocalisation interactions can be calculated.

As discussed in the introduction, the solvent employed for solvation of the pre-polymerisation complex can enhance or hinder complex formation. Recent studies have shown polar aprotic solvents sometimes to be superior to nonpolar or polar protic solvents in this regard. However, many systems have been imprinted using nonpolar solvents such as chloroform or polar solvents such as methanol. For the molecular dynamics studies three solvents were selected for study. Important characteristics of the solvents are shown in table 5.1.

Table 5.1: Properties of the three solvents used for the study

Solvent	Template solubility	Density (g/mL)	Snyder polarity index	Polarity	H bond forming [174]
MeOH	YES	0.791	6.6	Polar protic	Strong
DMF	YES	0.944	6.4	Polar aprotic	Medium-weak
CHCl3	YES	1.494	3.4-4.4	Non-polar	Weak

The solvents listed in the table were selected due to their ability to dissolve all components of the polymerisation mixture and because they are all solvents which have previously been employed in the generation of MIPs. In this respect it was important to show applicability of the modelling systems to common solvents used for imprinting. An important difference between the solvents is their respective hydrogen bond forming abilities. A solvent with a higher propensity to form hydrogen bonds is more likely to form hydrogen bond interactions with either the template or the monomer and as such obstruct efficient PPC formation. It is important to note that AMBER does not include effects of either initiator or cross linker in the energy calculations or molecular dynamics simulations. Given the fact that the initiator is usually present at levels not exceeding 1 mol % it is a valid assumption to ignore its effects via interaction with either the template or monomer or solvent. Regarding, cross linker, a decrease of 4.5% in the strength of the functional monomer – template complex on addition of cross-linker to the template – monomer solution has been demonstrated [60]. Hence it is a valid assumption to omit the effects of cross-linker from the energy calculation. Given that the probability of cross-linker inhibiting the complex formation is small, the only potential effect is by changing the density of the solution (in real terms) and this is not taken into account by the model. However within AMBER – before the simulation - a series of energy minimisations are performed and the system is equilibrated until conditions of constant temperature, pressure and total potential energy are met. Furthermore the density of the system is monitored until it reaches that of the experimentally verified density of the porogen in question. For example the DMF system was minimised until the density of DMF – 0.944 g/mL was met.

All three porogens chosen for the process are also commonly used in molecular imprinting and figure 5.1 shows the starting configurations simulated between naproxen and the monomers.

5.4.1.1 MD simulation of the π-π complex in DMF

Figure 5.1a, is the π-π stacking arrangement between naproxen and 4-VP. This was selected as the starting configuration for the molecular dynamics simulation. Here the distance between the mass centered rings of naproxen and 4-VP was monitored throughout the production run. An initial distance of 3.62Å was chosen. This is within the range at which π-π stacking interactions occur [103]. The stacking interaction is shown to remain intact for the duration of the run with the distance varying between 3 and 6Å as shown in figure 5.2

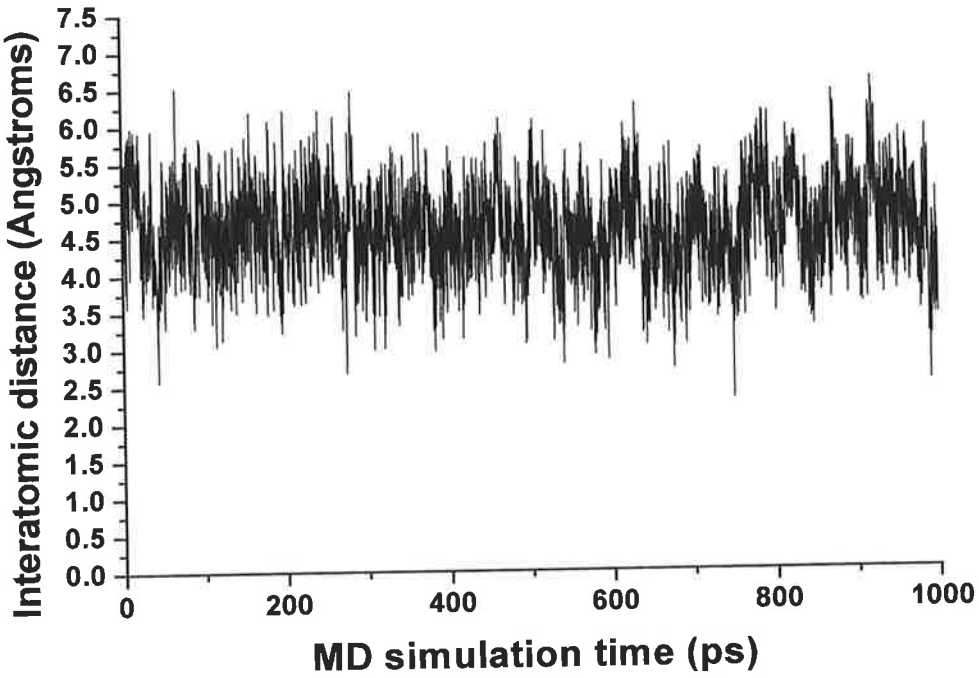

Figure 5.2 The results of the MD simulations for both the π-π stacking arrangement in DMF

The average distance of the molecules is ~4.5 Å. Calculations performed in MS excel for this study show that the molecules of the complex remain within 5 Å of each other for 72.3% of the duration of the simulation and that the intermolecular distance does not extend beyond 7 Å. These data are indicative of the relative stability of the complex in DMF. The 1 ns MD simulation of the system in DMF then has modelled aromatic π-π stacking interactions demonstrating that this is a stable interaction

between the molecules. The existence of the stacking interaction was subsequently studied by ^{1}H NMR spectroscopy.

5.4.1.2 NMR analysis of the π-π complex

To provide empirical evidence of the stacking complex formation further NMR experiments were performed. If a π-π stacking interaction occurs between two molecules both containing aromatic rings then this will be reflected in an upfield shift of the relevant aromatic protons. This is due to the fact that during electron delocalisation they will be deshielded and hence will resonate further upfield. The magnitude of the observed chemical shift however is not as strong as with other known effects e.g. hydrogen bonding. Figure 5.3 designates the protons for the aromatic peaks of naproxen in $CDCl_3$. The aromatic protons are identified as P1-P6.

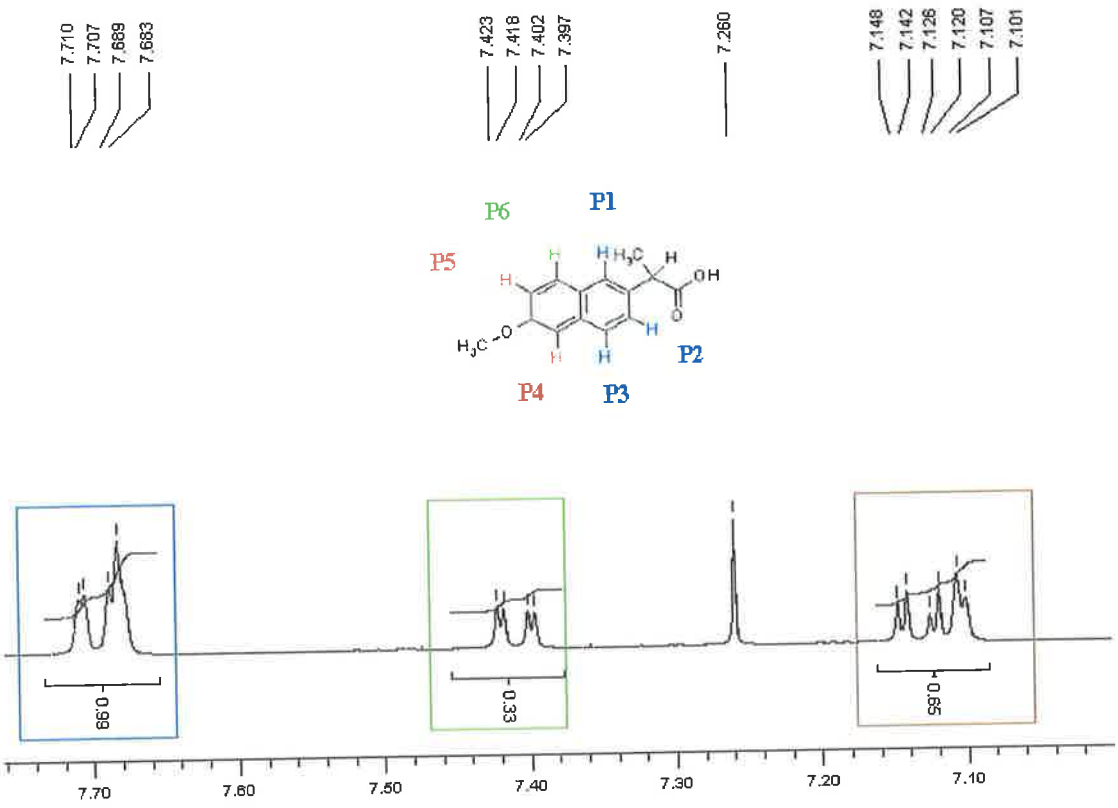

Figure 5.3: shows the 1H NMR assignment of the aromatic protons on the naproxen molecule for titration studies

On addition of an equimolar concentration of deuterated pyridine to a solution of naproxen in d_7-DMF slight upfield shifts of protons P1-P3 were observed (figure 5.4). This shift increased upon further addition of deuterated pyridine at ratio of 1:2, 1:4 and 1:10.

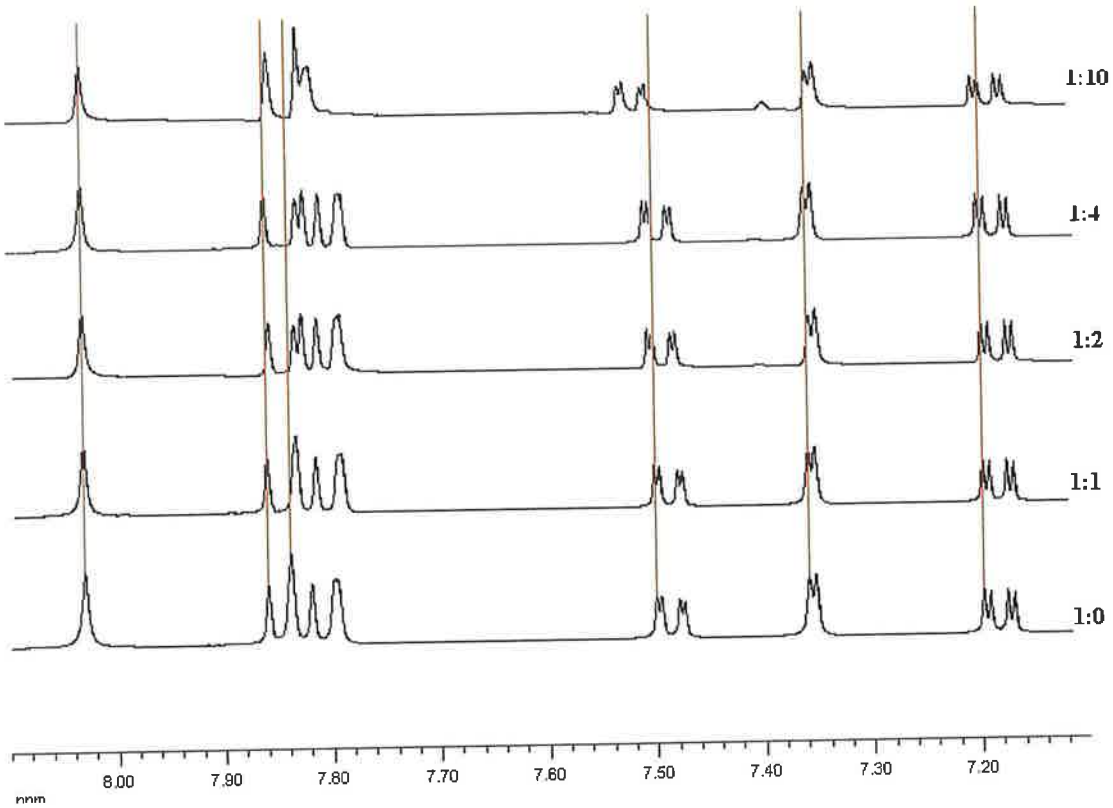

Figure 5.4: shows the chemical shifts observed when a solution of naproxen is titrated with d-pyridine in d_7-DMF for the aromatic protons of naproxen.

At ratios of 1:2 and higher, it was noticed that peaks corresponding to protons P1-P3 began to split. At a ratio of 1:10 peak merging was observed possibly reflecting the solvation of the molecule in deuterated pyridine rather than the d_7-DMF. The upfield shift indicated in figure 5.4 increased when the molar ratio was increased to 1:2 naproxen: pyridine for protons P1–P3. A downfield shift was observed for P6 at ratios of 1:2 and 1:4. This becomes significant at a ratio of 1:10. Furthermore, for P4 and P5 slight downfield shifts were detected. This is indicative of the pyridine in fact being closer to P1-P3 and away from P4-5 and may indicate that the approximate stacking angle is shifted i.e. the stacking is not in the edge on or face to face arrangement. Different orientations have been observed for aromatic dimers, ranging

from face to face structures to edge on (T shaped) structures with several proposed models for aromatic interactions [240-242]. As discussed by Jorgensen and Severance, [233], shifted stacked structures are preferred to face-to-face configurations. Furthermore, since the magnitude of the shift increases with the further addition of deuterated pyridine, it is possible that higher order complexes are formed. Ansell and Kuah [107] have shown increased shifts of ephedrine protons upon further addition of methacrylic acid to a solution of ephedrine indicating the formation of 1:1 and 1:2 complexes. It is also possible that it is a weak 1:1 interactyion and as such on further addition of pyridine a continued change in shift would be observed. The continued upfield shift of the peaks for the aromatic protons, P1, P2, and P3 is shown in figure 5.5

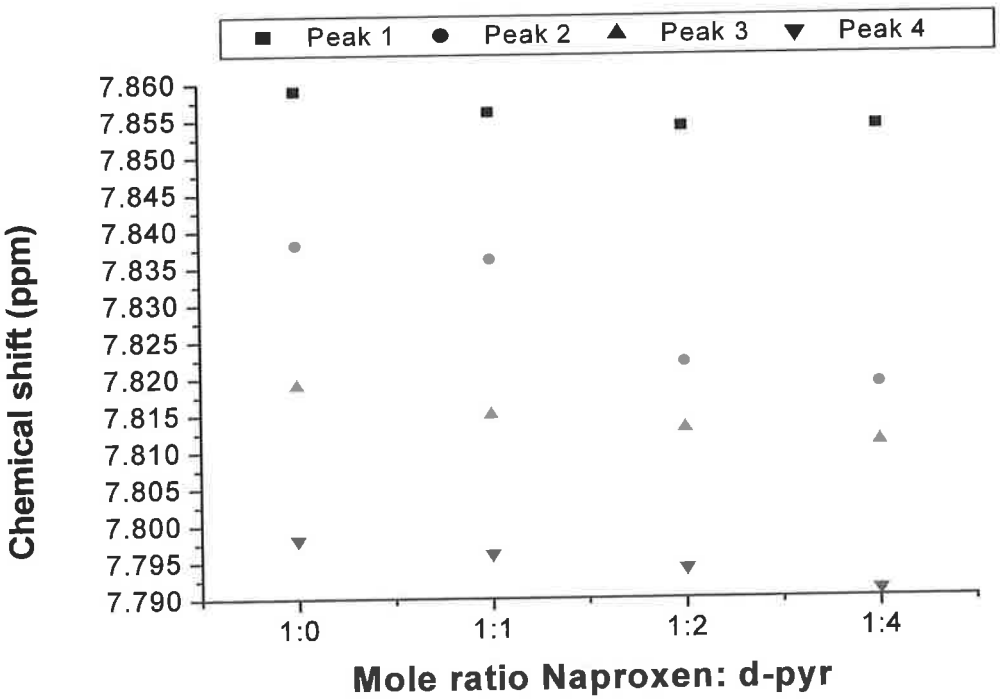

Owing to the nature of the π electron distribution in the naproxen molecule it is possible that the delocalisation interactions with 4VP are transient and are continually breaking up and reforming in solution. Hence the magnitudes of the observed changes in chemical shifts are small and the interaction is likely to be weak in nature. However, no changes in chemical shift of the protons were observed when d_7-DMF

was replaced with MeOD or $CDCl_3$ indicating the specific nature of the naproxen-4VP interaction in DMF.

5.4.1.3 MD simulation of π-π complex in MeOH

In order to study the effect of a change in solvent on the characteristics of the conformation of the pre-polymerisation complex, the molecular dynamic simulation was repeated with MeOH in place of DMF. The 1 ns trajectory between the mass centered rings of naproxen and 4-VP is shown in figure 5.6

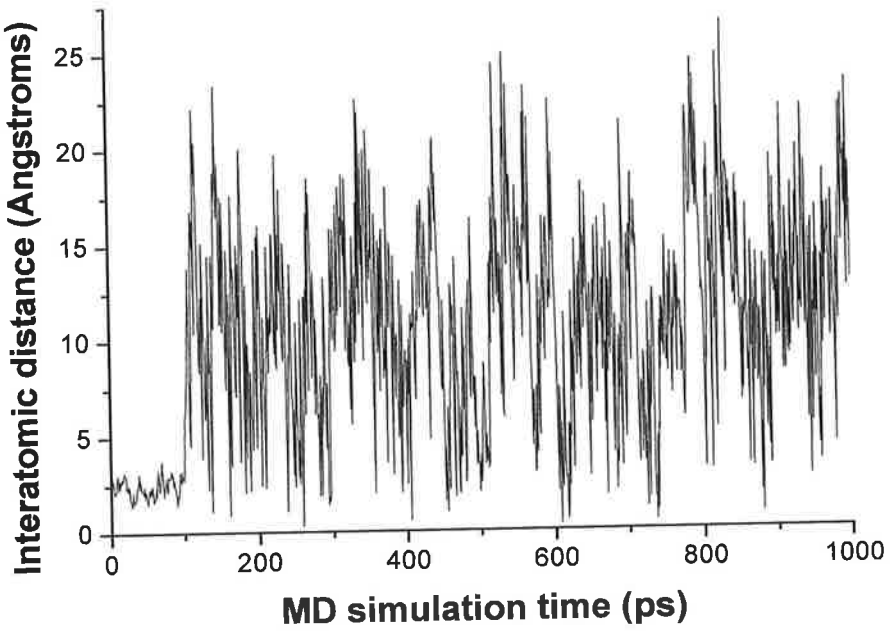

Figure 5.6 The results of the MD simulations for both the π-π stacking arrangement in MEOH

From this study, it is apparent that the complex remains intact for the first 100 ps of the simulation. However, following this the complex is broken up (and for 22.6% of the simulation is at a distance of less that 5 Å). There is a proportion of the simulation in which the molecules are in close proximity to potentially form π-π stacking interactions. However, this is likely to be caused by random close proximity as the molecules drift apart and move around the MeOH box in an apparent arbitrary fashion. Since the distance between the molecules ranges from below 1Å to

approximately 30Å it can be stated that the molecules drift apart without reasonable chance of the complex reforming. Moreover, it can be seen that the molecules are not in close proximity for a significant amount of time to allow reformation of the stacking interaction. A rationale for the observed difference in PPC conformation in DMF and MeOH is the hydrogen bond forming ability of the solvents. As discussed in chapter 4 (4.3.1.2), the nature of π interactions is that they are weak. Hence since they can contribute towards specific rebinding in the polymer it is important that they are preserved in solution. π-π interactions can contribute towards specific rebinding in two ways as already discussed. They can contribute towards the spatial configuration of the PPC and they can add an augmentory interaction in terms of functionality. Lübke *et al.*, [243] performed an investigation to determine whether relatively weak interactions involving aromatic π electrons could be exploited for the generation of MIPs. 2,3,7,8-tetrachlorodibenzodioxin (TCDD) was used as the template. A recognition element was introduced into the binding sites by the inclusion of a polymerizable, electron-rich, aromatic ether capable of forming π-π interactions with the electron-deficient dioxin molecule. The MIP produced showed significantly higher uptake of TCDD than the corresponding non-imprinted controls, even at concentrations as low as 2 nM. Lübke *et al.*, [243] then have underlined the importance of choosing a suitable monomer to enhance π-π interactions. In this chapter, the importance of solvent is emphasised in preserving the nature of weak interactions in self-assembled solutions.

Given that MeOH has a higher propensity to form hydrogen bonds than DMF, it is probable that both naproxen and 4-VP form hydrogen bonded interactions with methanol and each becomes surrounded by MeOH molecules. This would preclude the reformation of the π-π interaction. The hydrogen bond forming ability of the solvents is in part related to their densities. Hydrogen bonding is more likely to occur - or at least stronger hydrogen bonds will form - between a species and a solvent of lower density. Hence, with methanol having a lower density than DMF (0.781 and 0.944 g/mL respectively) it is proposed that MeOH will preferentially form hydrogen bonds with both naproxen and 4-vinylpyridine with the result being the formation of a weakened pre-polymerisation complex. The ^{1}H NMR studies show no observable shifts of any of the aromatic protons of naproxen in MeOD upon addition of deuterated pyridine from ratios of 1:1 to 1:20 (figure 5.5). Furthermore, Xu *et al.*,

[110] state that methanol can efficiently compete with the functional monomer for the functional groups of the template. Thus, it can weaken or block the formation of hydrogen bonding between the functional monomer and the template.

5.4.1.4 MD simulation of π-π complex in Chloroform

Given that chloroform allows the formation of hydrogen bonds between naproxen and 4-VP it was tested by NMR titration. Nomachi *et al.*, [109] have demonstrated that $CHCl_3$ performed better in terms of the stabilisation pf the PPC for a melatonin-MAA complex than either THF or ACN. However, in this experiment no observable shifts of any of the naproxen aromatic protons was observed by NMR. It is proposed that chloroform, as a nonpolar solvent would reduce the likelihood the formation of interactions such as π-π stacking. The stability of the complex in chloroform was examined by MD simulation and the result is shown in figure 5.7.

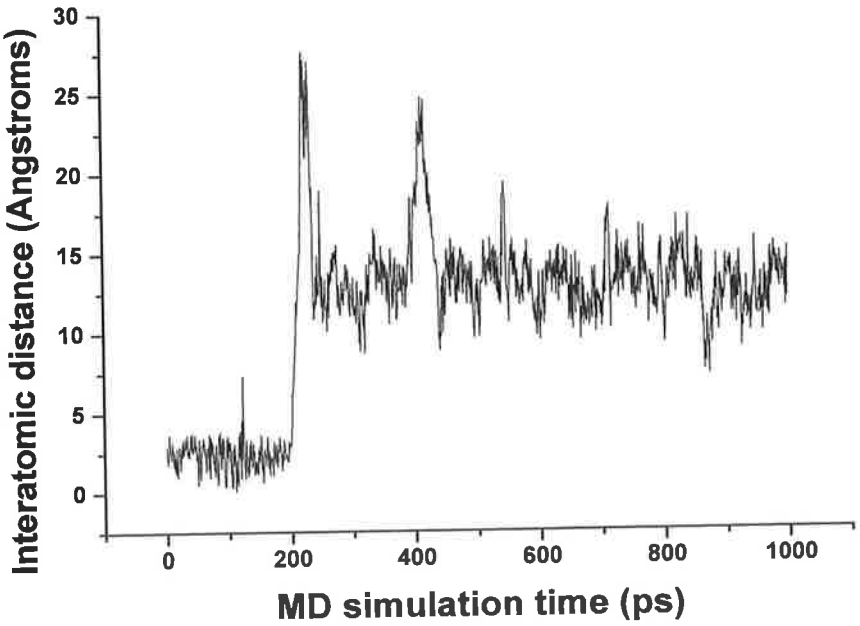

Figure 5.7: The results of the MD simulations for both the π-π stacking arrangement in $CHCl_3$.

From this study, as expected, the π-π stacking conformation was shown not to be stable in chloroform. After ~200 ps the complex is broken up and the two separate molecules remain isolated drifting about the box. The data suggests that there is no

possibility of re-complexation between the molecules throughout the duration of the simulation as the molecules do not approach the minimum distance necessary for π-π stacking to occur. It was concluded that the most favourable conditions for the fidelity of the stacking arrangement arise when DMF (polar aprotic solvent) is used as the solvent as the stacking arrangement is unstable in MeOH or $CHCl_3$.

What the MD simulations of the π-π stacking experiments reveal is that in the rebinding solvent these interactions can reform more readily than in another solvent. In these experiments and for the template naproxen it is proposed that the stacking interaction plays a contributory role towards the stabilisation of the PPC. This interaction augments a shape induced thermodynamic fit rebinding. It is likely that other electrostatic interactions or hydrophobic effects contribute towards the stabilisation of the PPC also. This is particularly true in aqueous rebinding media. In this system only the π-π interaction has been modelled. However it is expected that energy calculations such as those performed by Hyperchem in chapters 2 and 3 performed in the explicit solvents would reveal important energy differences in this regard. In order to investigate the potential of hydrogen bonding or electrostatic interactions to contribute towards complex stability, the complex was rearranged into a position to allow interaction between the –OH of naproxen and the N of the 4VP ring. This takes into account the potential for hydrogen bonding between the aforementioned atoms. This was also performed in the three solvents DMF, MeOH, $CHCl_3$.

5.4.2 Molecular Dynamics simulations of naproxen/4VP hydrogen bonded complex conformations in explicit solvent.

5.4.2.1 MD simulation of hydrogen bonded / electrostatic interaction complex in DMF

In order to investigate the stability of alternate configurations under molecular dynamics simulation conditions the hydrogen bonding arrangement of naproxen/4VP was also studied by MD simulation. For this configuration the -OH of naproxen was set at a distance of 3Å from the N of the pyridine ring. As DMF had provided good

results previously for the stacking configuration it was selected as the first solvent to study. The MD simulation result is shown in figure 5.8.

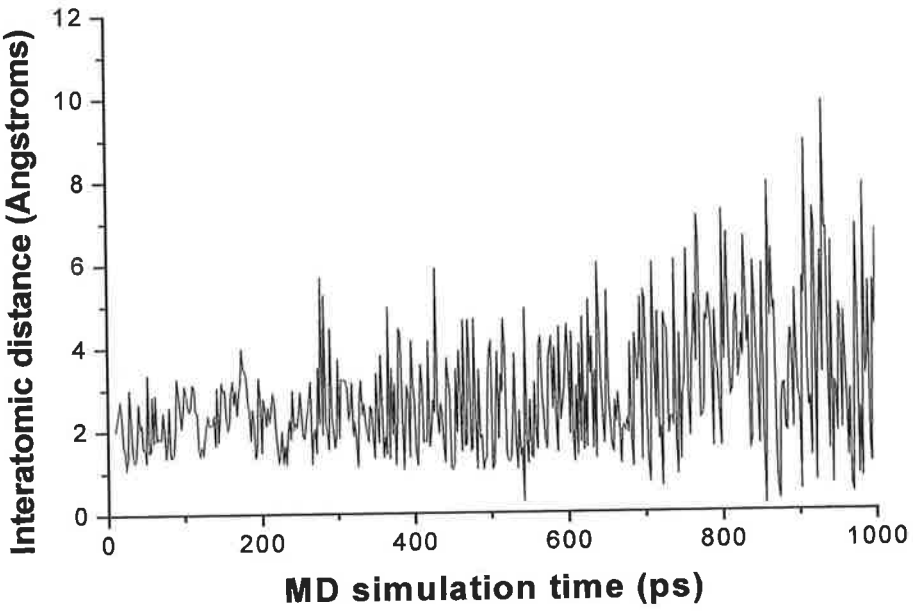

Figure 5.8: The results of the MD simulations for the electrostatic configurations in DMF

When DMF is employed as the explicit solvent it can be observed that the two molecules remain in sufficiently close contact to participate in hydrogen bonding until approximately 300 ps of the production run. After this stage it was noted that the interaction became less stable with the distance oscillating between 1 and 6Å. By 1000 ps of the production run the distance had reached over 10Å. It was calculated that over the duration of the run that the two molecules remain at a distance below the proximity of 3.0 Å or less for 31.4% of the time It is probable that in DMF, hydrogen bonding and electrostatic interactions between naproxen and 4-VP is likely provide an augmentory interaction in addition to stacking for the stabilisation of the complex. This result also provides an insight into the complex stoichiometry, which, given the functionalities on both template and monomer is likely to be greater than a 1:1 ratio. In addition, for MIPs prepared using non-covalent interactions (hydrogen bonding, ionic interactions, hydrophobic interactions, etc.) the extent of template complexation in the pre-polymerization mixture is a consequence of a series of equilibria. Being a

system in equilibrium, the stronger interactions between the template and the functional monomer(s), the more stable template–monomer complex being formed. This results in an increase in the concentration of the complex.

5.4.2.2 MD simulation of hydrogen bonded / electrostatic complex in MeOH

In order to assess the effect of a change of solvent on the electrostatic interaction MeOH was employed as the explicit solvent and the complex solvated as before except in MeOH. The plot of distance between the –OH of naproxen and the N of pyridine in MeOH is shown in figure 5.9:

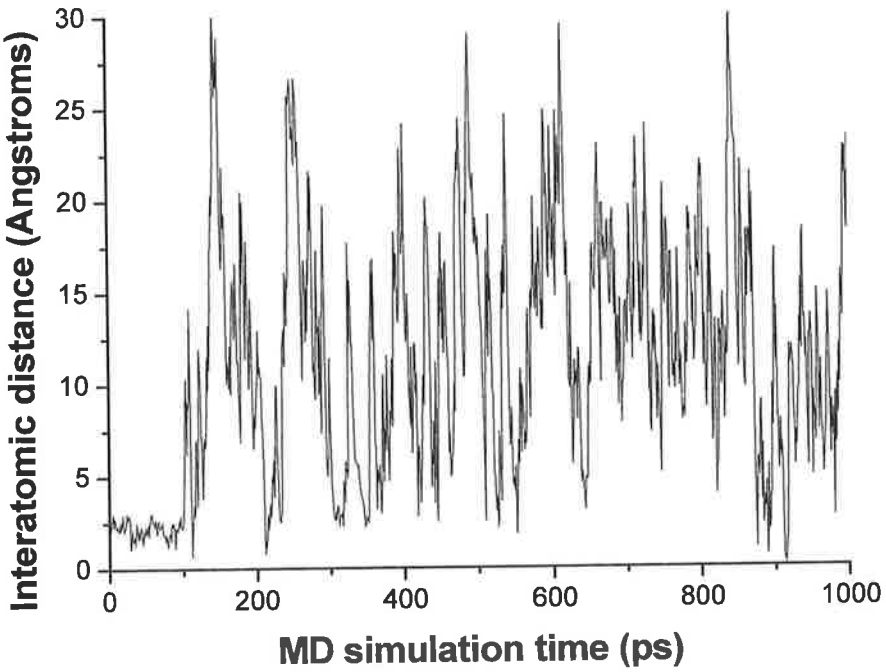

Figure 5.9: The results of the MD simulations for the hydrogen bonded configurations in MeOH

As can be seen from figure 5.9, the complex is not stable in methanol and following 100 ps of the run, naproxen drifts away from 4-VP and similar to the effect seen with the π-π stacking interaction in MeOH, the recombination of the molecules is based on probability given that the molecules rotate freely around the periodic box with

apparent randomness. In fact the complex remains at an intermolecular distance of less that 3.0 Å for less than 15% of the simulation time. The hydrogen bonding strength is very much modulated by the medium, in the case of methanol used as the solvent, the hydrogen bonding between naproxen and 4VP does not exist or is very weak. It is therefore unlikely that that this complex would self assemble in a solution of methanol.

5.4.2.3 NMR analysis of hydrogen bonded complex configuration

To support the molecular dynamics prediction again ^{1}H NMR was used. In this study, the chemical shift of the –OH proton of naproxen on complexation with deuterated pyridine was observed in d_7-DMF, MeOD and $CDCl_3$. Figure 5.10 shows the magnitude of the shift observed for the –OH proton when the complex is solvated in d_7-DMF. This effect is not observed when d_7-DMF is replaced with MeOD. A change in shift was observed for the proton in $CDCl_3$. This is indicative of complex formation in this medium also.

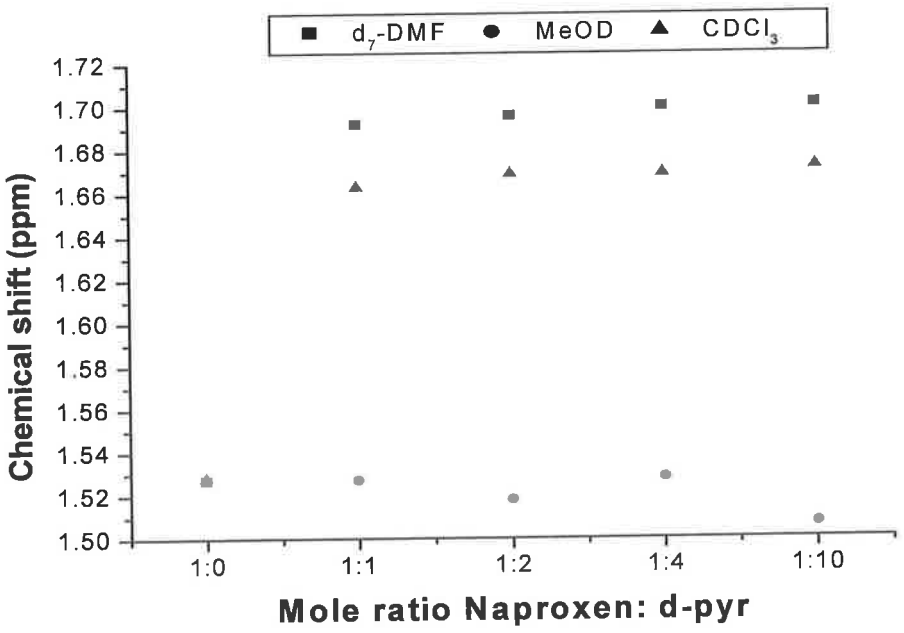

Figure 5.10: shows the shifts of the P-OH proton when titrated as above in d_7-DMF, MeOD and $CDCl_3$

This result shows further evidence of the importance of the porogen in enhancing the formation of the pre polymerisation complex. The magnitude of the shift does not significantly increase beyond a 1:1 ratio of naproxen to pyridine indicating that this is the complex stoichiometry for this configuration. Figure 5.10 indicates that one molecule of pyridine can interact strongly with one molecule of naproxen in DMF and chloroform. In particular this demonstrates the advantage of employing a polar aprotic solvent as both types of interaction are stabilised in DMF in contrast to MeOH and $CHCl_3$. Referring to table 5.1, the Snyder polarities of both MeOH and DMF are similar and the difference lies within the hydrogen bonding capacity of the solvents. When 4VP was used as the functional monomer, it cannot effectively interact with the template in the pre-polymerization mixture in MeOH, thus the template–monomer complex is not formed. It would be expected then that a polymer generated for naproxen using 4VP as functional monomer and methanol as porogen would have little affinity for the template. A further point of note is that no changes in shift for the aliphatic CH_3 and CH protons were observed in the NMR titration study. This is important because as these protons do not move the conclusion of separate π-π aromatic and Hydrogen bond formations is much more likely.

5.4.2.4 MD simulation of hydrogen bonded / electrostatic complex in Chloroform

As the NMR showed interaction between the –OH proton of naproxen and the nitrogen of pyridine, for completeness, the MD simulation was repeated in chloroform and the result is shown in figure 5.11

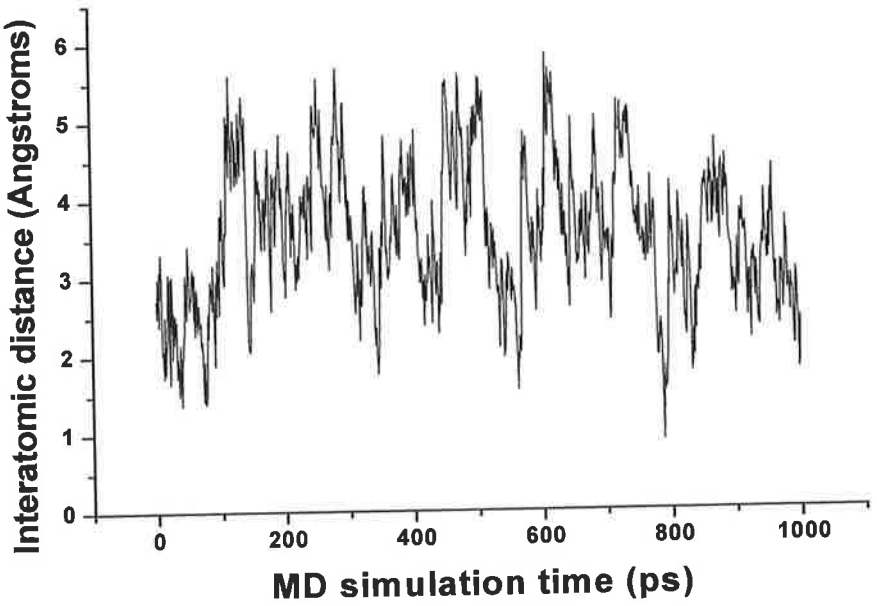

Figure 5.11: The results of the MD simulations for the hydrogen bonded configurations in $CHCl_3$.

This trajectory demonstrates that the molecules are in relatively close proximity for the duration of the production run and the furthest point that the complex drifts apart to is 6 Å. Importantly, NMR studies are again in agreement with the MD simulation data for chloroform indicating the relative stability of a complex. Hence, the presence of electrostatic interactions or hydrogen bonding in $CHCl_3$ is demonstrated by the MD simulation since the molecules do not rotate freely about the box (as observed for methanol in figure 5.9). Since the distances are more stable i.e. average distance of 3.5Å it is highly likely that hydrogen bonding contributes towards a complex formation in $CHCl_3$.

Numerous researchers, for instance Jie *et al.*, [118], have selected chloroform as solvent citing the reason that this porogen will not interfere with hydrogen bond formation. This study did indeed show a change in chemical shift of the amino protons of Apy in $CDCl_3$ when titrated with MAA. This observation suggests that the hydrogen and/or nitrogen of the amino group of Apy were involved in hydrogen-bonding formation and the pyridine nitrogen could also be involved in hydrogen bonding as a hydrogen bond acceptor. The same authors also stated that the nitrogen and the side-chain amino hydrogen cause cooperative hydrogen bonding formation

with acetic acid and deduced that the cooperative interaction is much stronger than single hydrogen bonding and can provide interacting binding sites of higher selectivity in the resulting polymer. This was confirmed by a spectrophotomtetric method.

From the modelling and NMR data in this study it was concluded that there was a potential complex formation between naproxen and 4VP in chloroform and the probability is that the interaction is based on a hydrogen bonding interaction. It is expected however that the MIP prepared in DMF with 4VP as monomer would show enhanced rebinding in aqueous media in contrast to MIPs prepared in MeOH and $CHCl_3$.

5.4.3 Modelling outlook

The examination of the applicability of molecular modelling techniques to the elucidation of the structure and nature of pre-polymerisation complexes yielded encouraging results. From the studies conducted the following statements can be made from observations of the molecular dynamics simulations of the naproxen/4VP system in DMF, methanol and chloroform:

The H bonding interactions between naproxen and 4VP in a polar solvent (methanol) do not play an important role in complex formation and it is probable that highly polar solvents in fact disrupt effective formation of hydrogen bonds

It was expected that π-π stacking would be more stable in polar solvents. This is indeed the case for polar solvents relative to nonpolar solvents. However, the model has shown that it is in fact more stable in an aprotic solvent (DMF) than in methanol.

Hydrogen bonding interactions play a further augmentory role in complex formation and stabilisation between naproxen and 4-VP in DMF helping to stabilise the π-π stacking interactions. Hydrogen bonding interaction is also important in development of a complex in chloroform

It was found that the behaviour of template and functional monomer could be followed in explicit solvent in these studies, which modelling based on docking studies and energy calculations does not fully allow.

5.4.4 Generation of molecularly imprinted polymers

In order to test the results obtained in the modelling studies a number of MIPs were prepared. The MIPs correspond to the systems studied by MD simulations. Two of the solvents – DMF and methanol - used for the molecular modelling studies were employed as porogens for the development of the molecularly imprinted polymers and 4-vinylpyridine was used as the functional monomer. It was found that the polar aprotic solvent DMF produced larger sized beads (typically over 25 μm in diameter) but with a narrow size distribution (optical observation). Figure 5.12 a shows a representative field view of the bead sizes produced by the use of DMF as porogen. Figure 5.12b shows a zoom of typical sized beads produced. The highly porous interior of the beads is demonstrated in figure 5.12c. A damaged bead was used to analyse the interior and shows the large surface area available for adsorption. When methanol was employed as the porogen the beads were generally smaller but with a significantly greater size distribution range. Furthermore a greater level of aggregate formation was observed (figure 5.12d). Representative SEM images of both the DMF polymer and the MeOH polymer are shown in figure 5.12.

(a)
200um
(b)
23.65um
24.54um
26.45um
20um
(c)
2um
(d)
20um

Figure 5.12:The SEM images obtained for the polymers made in DMF (a) (b) and (c) while a representative sample of the MIP generated in MeOH is shown in (d). (a) shows a representative field view of the size distribution obtained using DMF as porogen. (b) shows a close up of the morphology and size of the DMF beads. (c) was obtained by focusing on an area of a damaged bead and shows the highly porous internal of the bead.

Difficulties had been previously observed for the generation of beaded polymers using DMF and 4-vinylpyridine together [244]. However, rather than a fundamental problem with the applicability of the technique when using DMF, it was discovered that a higher rate of agitation produced the MIP beads in the desired format. The use of DMF did produce beads with a greater average diameter than had been observed with other polar aprotic solvents such as ACN and DMSO however it was noted from both SEM images and light microscopy that the average size distribution of the DMF beads was significantly smaller [244].

An attempt was made to reduce the bead size of the DMF polymeric material. For this purpose the amount of surfactant was varied. Reducing the amount to 10 mg led to the inhibition of bead formation while increasing the amount to 40 and 50 mg did not reduce the bead size.

5.4.5 Morphological and physical characterisation of the polymers

The two MIPs (along with the corresponding controls) were prepared by the liquid fluorocarbon suspension method. They were termed the DMF MIP and MeOH MIP. 4-Vinylpyridine was used as the functional monomer for both polymers. The porosity of the polymers was studied by nitrogen adsorption analysis and the average pore diameters and surface areas for all of the polymers generated (along with the corresponding control non-imprinted polymers) are shown in table 5.2.

Table 5.2: The BET data obtained for both MIPs and corresponding controls by BET analysis

Polymer	Surface area (m^2/g)	Total pore volume (cm^3/g)	Average pore diameter (nm)
DMF MIP	337.3681	0.9100	10.3913
DMF Control	168.7155	0.3926	2.1493
MeOH MIP	223.5857	0.5203	5.1768
MeOH Control	77.0131	0.2894	1.2742

A distinguishing feature of the polymers in this study is the significantly larger surface area for the beaded polymer generated in DMF in contrast to the MeOH beads indicating a higher area available for rebinding with the DMF beads. From this investigation the greater average pore diameter and total pore volume of the DMF polymer is notable. Given that the same ratio of cross-linker (EGDMA) is employed for both polymerisations, that there was no variation in temperature and that the volume of porogen was constant, the divergence in the above data is a direct result of the type of porogen employed i.e. polar aprotic (DMF) opposed to polar (MeOH).

While the AMBER data has generated information relating to the stability of a complex in either porogen, the BET analysis has provided data that shows directly the morphological effect that the different porogens have on the structure and porosity of the resultant polymers. This result is directly related to their adsorption capacity. Furthermore, given the increased average pore size of the DMF MIP - 10.39 Å, it is demonstrated that there are two components vital to the memory of a MIP exclusive of the choice of optimal functional monomer. The stability of the pre-polymerisation complex in the porogen and the physical structure of the resultant polymer. These criteria are controlled by the type of porogenic solvent used for the polymerisation.

5.4.6 Rebinding studies

In order to test the functioning of the polymers in terms of their relative percentage rebinding in comparison to control polymers a series of rebinding experiments were performed. Initially, a binding curve as a function of polymer amount was determined in order to select the most suitable quantity of polymer required for further binding studies. This was performed for both the DMF and MeOH MIPs and controls in organic and aqueous media.

5.4.6.1 Rebinding with the DMF MIP

The results for the rebinding to the DMF MIP under organic conditions are presented in figure 5.14.

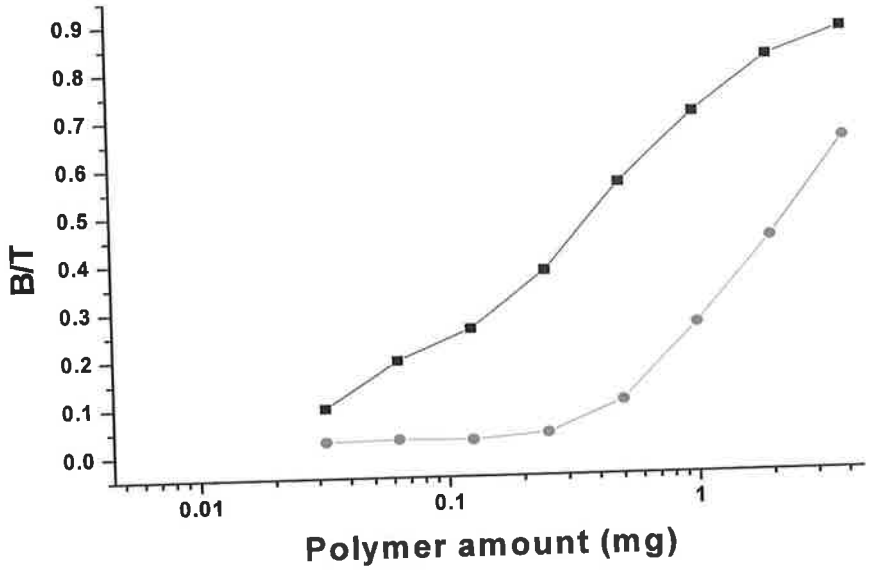

Figure 5.14 The binding of naproxen to the beaded MIPS under organic conditions polymers generated in DMF. For organic conditions, the rebinding was assessed in DMF. Key black line MIP rebinding, Red line control rebinding.

Here it was found that the optimum amount of polymer for use in rebinding is 0.25-0.5 mg since above this amount a large increase in non-specific binding is observed. On the basis of results in chapter 4, the optimum solution to use for rebinding is probably DMF (figure 5.14a). It is a well established fact that MIPs perform well (in terms of rebinding) in the polymerisation solvent relative to other solvents. Importantly, this is most likely due to a a swelling effect as when the rebinding was assessed in acetonitrile no specific uptake was observed. This is a notable point as acetonitrile is also a polar aprotic solvent with a low propensity to form hydrogen bond interactions. Other polar aprotic solvents such as THF were not tested. When uptake was assessed in methanol no rebinding beyond control levels was observed. Rebinding was also observed under aqueous conditions and is shown in figure 5.15.

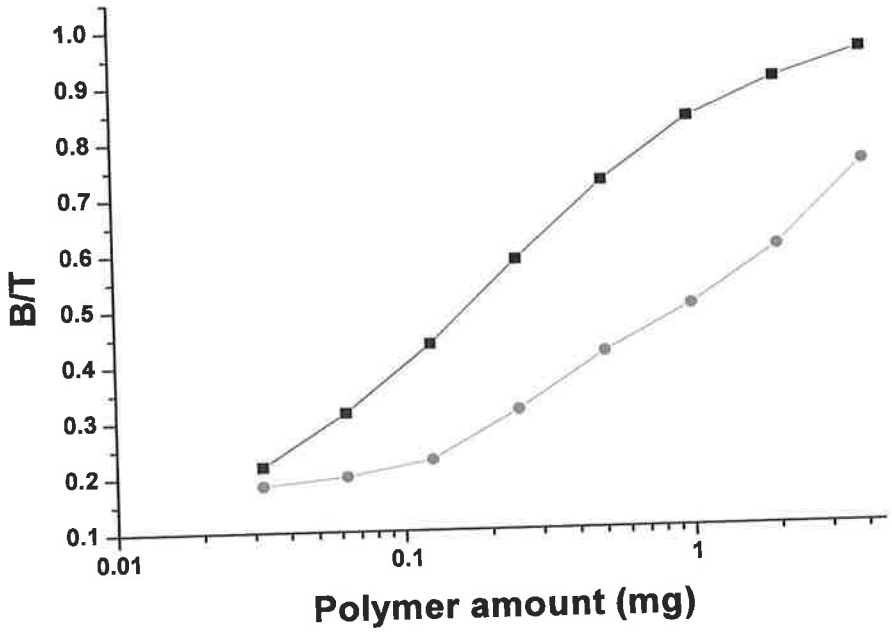

Figure 5.15 the binding of naproxen to the beaded MIPS under aqueous conditions for polymer generated in DMF. For aqueous conditions, the rebinding was assessed in 0.1M citrate buffer pH 6.8 containing 10% ethanol and 0.05% Tween 20. Key black line MIP rebinding, Red line control rebinding

At higher amounts of polymer it was noted there is an increase in non-specific binding, however the specific uptake remains high at 0.25-0.5 mg and is evidence that this MIP could be employed in an aqueous based rebinding assay. As discussed earlier one of the outstanding advantages of MIPs is their ability to be applied to binding assays in organic or aqueous media. This is a significant advantage over antibodies which do not perform well in organic conditions.

5.4.6.2 Rebinding with the MeOH MIP

Regarding the MIP prepared in methanol, only low levels of rebinding were observed methanol - figure 5.16

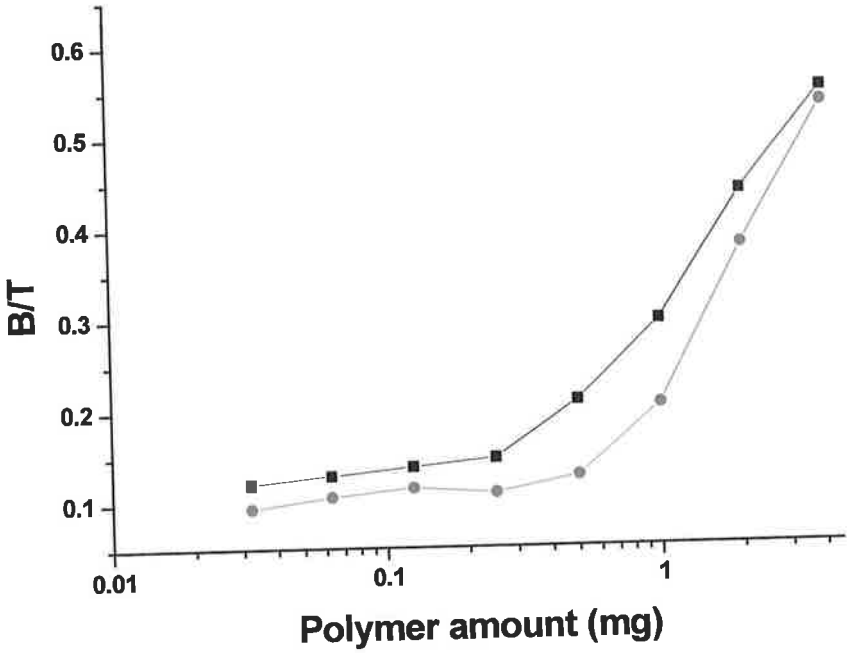

Figure 5.16 the binding of naproxen to the beaded MIPS under organic conditions and for polymers generated in MeOH. For organic conditions, the rebinding was assessed in MeOH

Some specific rebinding (in the region of 10% above control levels) was noted when methanol was used as the rebinding solvent. This only occurred at quantities of polymer between 0.25 and 1mg. Below this amount no specific rebinding was seen and above this amount non-specific adsorption increased steadily. The uptake was also assessed under aqueous conditions and the rebinding is shown in figure 5.17

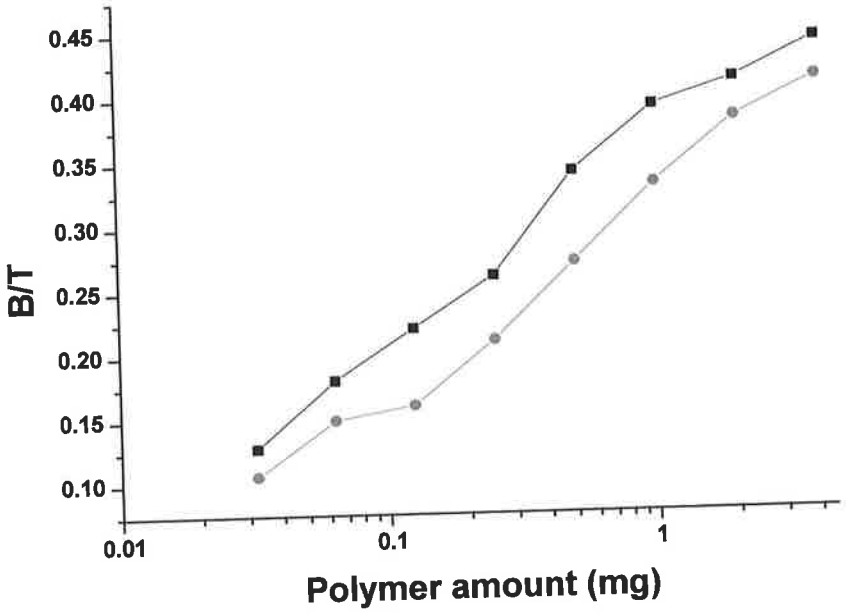

Figure 5.17 The binding of naproxen to the beaded MIPS under aqueous conditions for polymers generated in MeOH. For aqueous conditions the rebinding was assessed in 0.1M citrate buffer pH 6.8 containing 10% ethanol and 0.05% Tween 20. Key black line MIP rebinding, Red line control rebinding.

The molecular dynamics simulations and ^{1}H NMR titrations had predicted that the DMF MIP would be superior to the MeOH MIP and this has shown to be the case in terms of rebinding. The DMF MIP has outperformed the MeOH MIP in that it has proved effective for specific naproxen uptake in both aqueous and organic conditions. The influence of the judicious selection of porogen is directly demonstrated in this study showing that electrostatic interactions can be preserved (enhanced) under the correct solvation conditions. The MeOH MIP showed only marginal specific uptake under organic conditions (MeOH) and less under aqueous conditions.

5.4.6.3 Naproxen displacement study.

In order to examine the cross reactivity of the DMF MIP for naproxen towards similar compounds, a displacement study was performed. This was done using two of the structural analogues of naproxen namely ibuprofen and ketoprofen along with the non-structurally related compound caffeine. Rebinding in MIPs is dependent on two events - namely, the functionality imparted to the polymer by the incorporated functional groups and the spatial complementarity imparted by the shape of the template. It was expected that the MIP would discriminate between naproxen and its analogues. The result of the displacement assay is presented in figure 5.18.

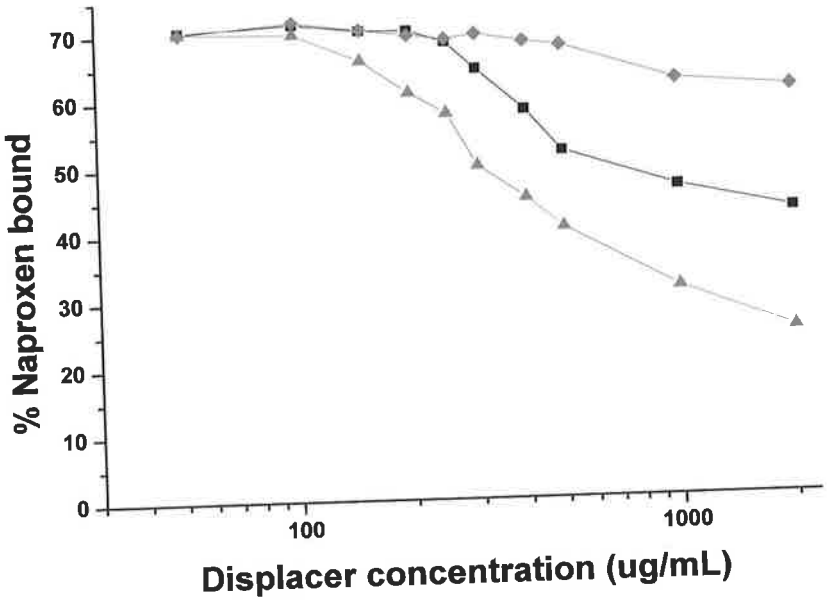

Figure 5.18: Figure 7: The % naproxen bound as a function of increasing concentrations of displacer from an original 200 mg/L solution in 0.1M citrate buffer pH 6.8 containing 10% ethanol and 0.05% Tween 20. Key

From the study, it can be seen the unrelated compound caffeine leads to negligible displacement of naproxen until a concentration of 1000 µg/mL caffeine is reached and even at a concentration of 2000 µg/mL caffeine a decrease of only 10% from the original bound naproxen concentration is observed. It is notable that ibuprofen displaces a significantly greater amount of naproxen from the MIP than ketoprofen,

this is particularly evident at concentrations lower than that of naproxen (200 μg/mL). This is attributed to a size exclusion effect, given that ibuprofen has a similar molecular volume to naproxen and ketoprofen is a more bulky molecule with a significantly different shape. Interestingly at an ibuprofen concentration of 2000 μg/mL approximately 45% of the originally bound naproxen has been displaced indicating the potential for cross reactivity between naproxen and ibuprofen. Furthermore, since the modelling data indicates that the nature of the specific interactions are π-π stacking and a contribution from other sources of electrostatic interaction and potentially hydrogen bonding, ibuprofen will form a stronger interaction with 4VP than ketoprofen. The ketoprofen the molecule contains an electron withdrawing carbonyl group between the two aromatic rings. This will serve to also reduce the level of interaction with 4VP. The "optimal spatial fit" theory (see chapter 6 – next chapter) has been developed for analysis of the role of shape complementarity in selective rebinding in MIPs and the results presented here suggest a similar effect is in operation. Essentially, ketoprofen will not fit into the cavity generated by naproxen because of its extra size and bulk, but also because of its shape and it is excluded from the cavity by steric hindrance. Ibuprofen being of similar molecular volume will fit into the nanocavity and can indeed manoeuvre within the cavity. However, as its spatial distribution is significantly different to that of naproxen rebinding will have to overcome an extra thermodynamic barrier hence a lower level of rebinding is observed. The molecule exhibiting the optimal spatial fit, in this case naproxen, will demonstrate a better fit to the shape of the binding cavity.

5.4.7 Naproxen MIP properties – chromatographic evaluation

For chromatographic evaluation of the polymers, both of the naproxen MIPs were slurry packed into HPLC columns of dimensions 100 x 4.6 mm i.d. The aim of the study was to compare the chromatographic performance of the MIP prepared in DMF and that prepared in MeOH in terms of resolution between naproxen and ibuprofen. Ibuprofen was chosen as it showed a greater potential for cross reactivity in the naproxen displacement study than ketoprofen. 10 µl of a 10 µg/mL mixture of both naproxen and ibuprofen was injected on to the column. The mobile phase was acetonitrile (1% acetic acid) and methanol was used as a void marker. The flow rate was 1.0 ml/min. The retention times of the compounds are summarised in table 5.3.

Table 5.3 Retention times of compounds on imprinted and control polymer columns for both the DMF and MeOH imprinted polymers

Polymer	Analyte	R_t (min)
DMF MIP	Void	1.87
	Naproxen	13.30
	Ibuprofen	7.30
DMF CON	Void	1.41
	Naproxen	5.01
	Ibuprofen	3.08
MeOH MIP	Void	2.81
	Naproxen	4.59
	Ibuprofen	~7.20
MeOH CON	Void	2.19
	Naproxen	2.67
	Ibuprofen	~4.90

The imprinted polymer prepared in DMF shows significantly better retention of both ibuprofen and naproxen than the corresponding non-imprinted polymer. Figure 5.19 below shows the chromatograms obtained when a mixture containing 10 µg/mL of

naproxen and 10 µg/mL of ibuprofen were injected onto the DMF MIP column. For the control (non-imprinted polymer), 10 µl of 2 µg/mL concentrations of each were injected. The determination of retention times indicates the improved retention of the analyte of interest (naproxen) in the DMF MIP over the MeOH MIP and the improved retention of the MIPs in contrast to the controls.

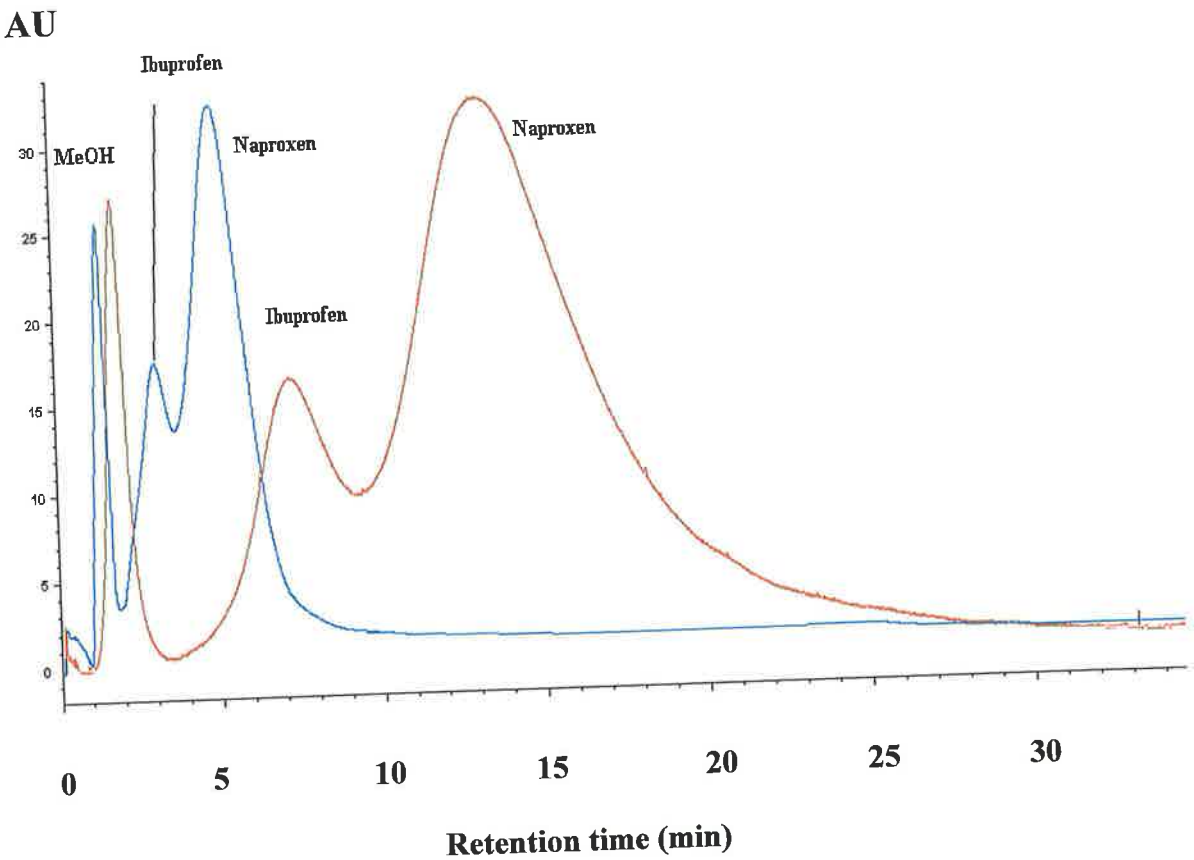

Figure 5.19: shows the separation of naproxen and ibuprofen using ACN;AcOH (99:1) mobile phase on the MIP imprinted with 4VP in DMF alongside the control non-imprinted polymer.

——— DMF MIP Column ———DMF Control column

In order to assign the peaks, ibuprofen and naproxen were injected individually as shown in figure 5.20 a (naproxen) and b (ibuprofen)

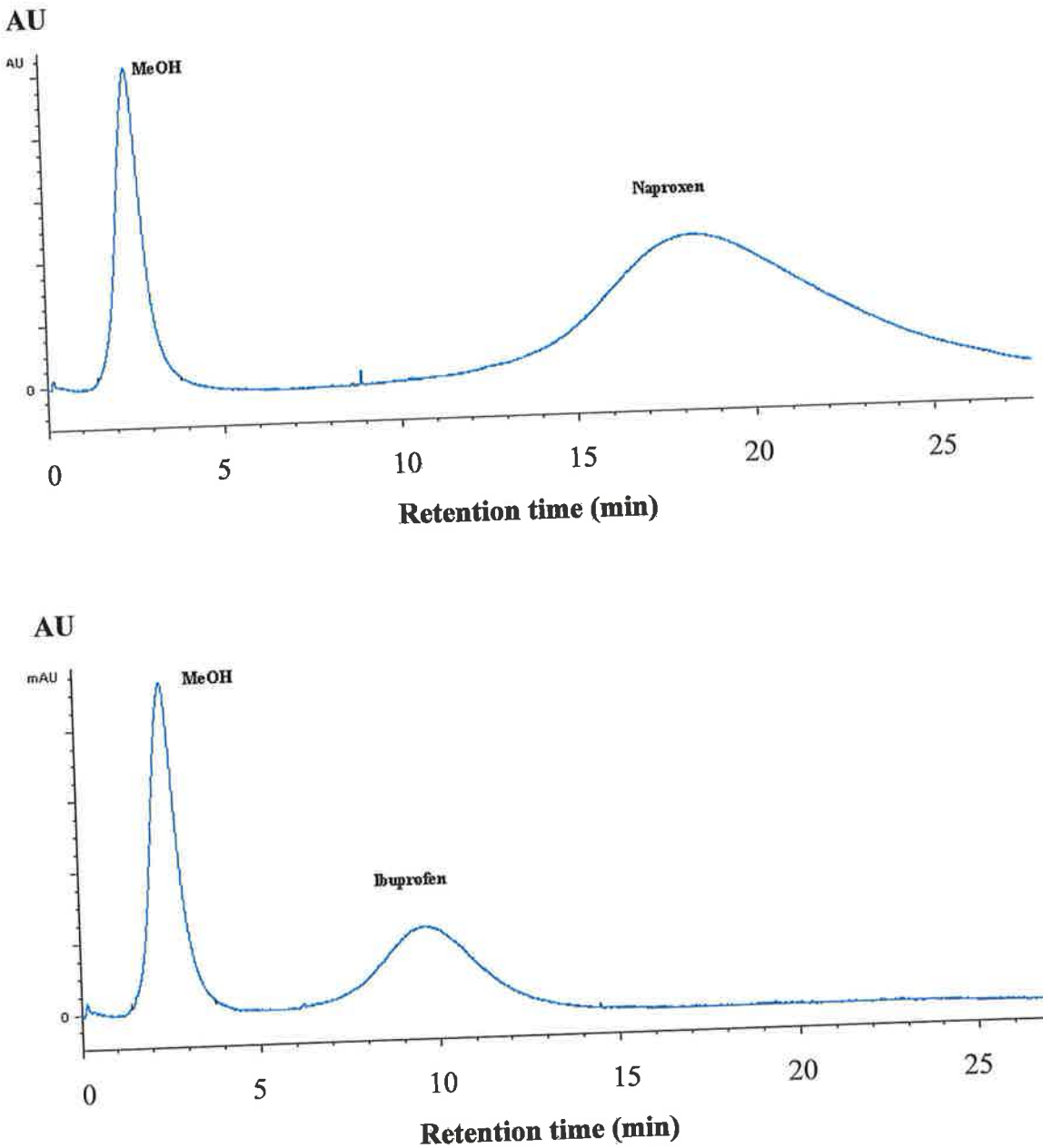

Figure 5.20 shows the single injection of naproxen (a) and ibuprofen (b) on the MIP imprinted with 4VP in DMF using ACN (100) as mobile phase

Note the difference in retention time between the separation and the single injections. This is a result of the application of 1% AcOH to the ACN to reduce the tailing. The separation of ibuprofen and naproxen on the same MIP without the addition of acetic acid can be seen in figure 5.21

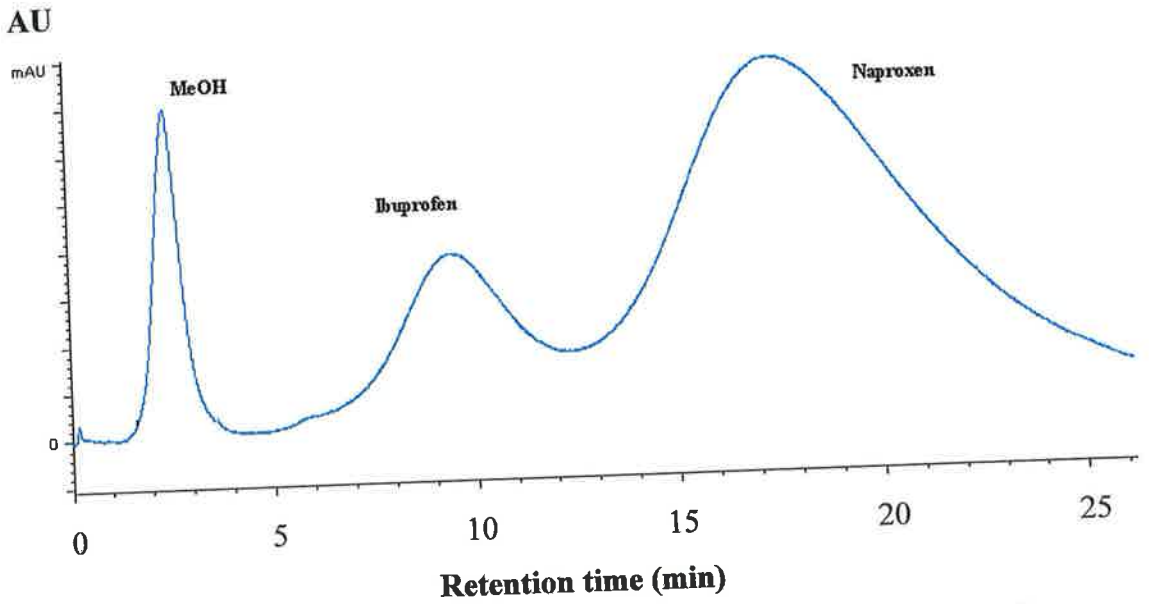

Figure 5.21: shows the separation of naproxen and ibuprofen using 100% ACN mobile phase on the MIP imprinted with 4VP in DMF

It is obvious then that the addition of 1% acetic acid reduces tailing probably by masking non-specific binding and inhibiting weak interactions.

The HPLC analysis was also conducted on the MIP prepared in MeOH. The conditions were as described and the result is shown in figure 5.22 below.

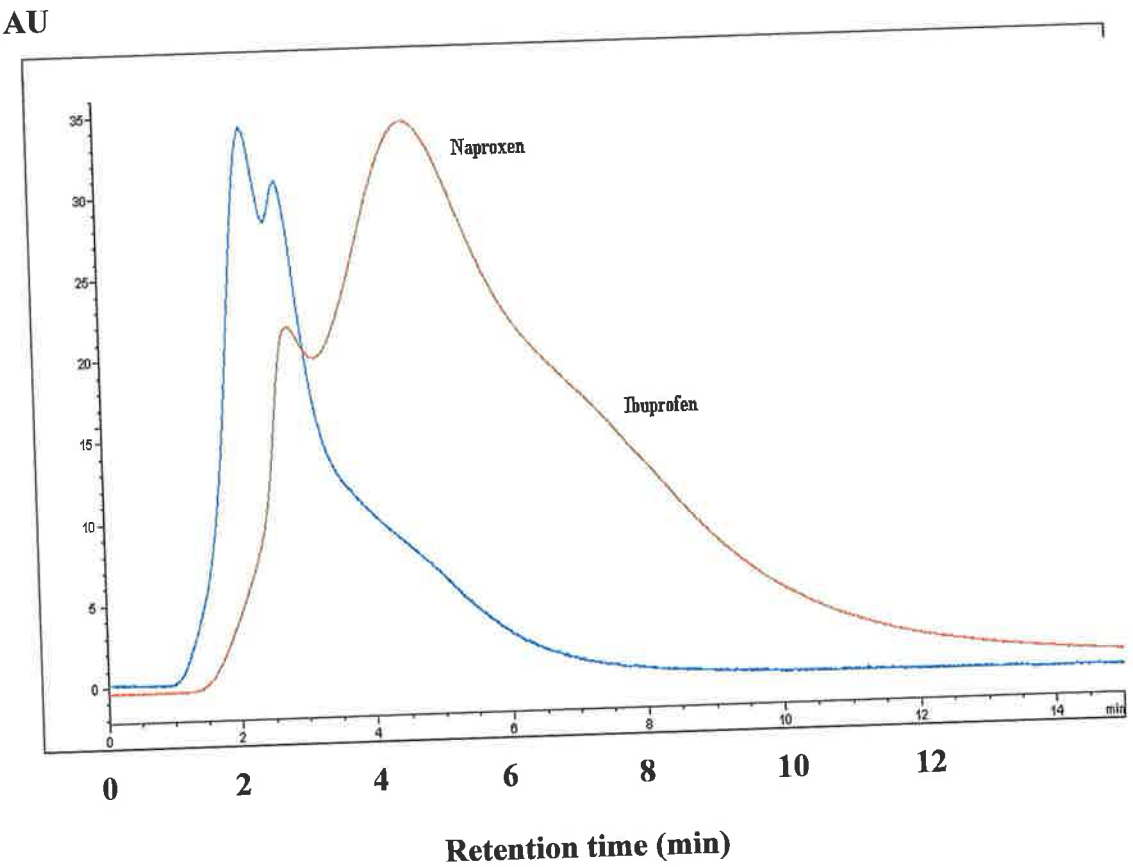

Figure 5.22: shows the separation of naproxen and ibuprofen on the MIP imprinted with 4VP in MeOH using ACN: AcOH (99:1) as the mobile phase alongside the control non-imprinted polymer.

Note in figure 5.22 identification of naproxen was identified by as the greater of the peaks due to its higher molar extinction coefficient and single injections were not performed. The control polymer showed no retention of either analyte

It is apparent from figures 5.19 and 5.22 that the MIP prepared in DMF displayed greater affinity for naproxen that that prepared in MeOH. This is shown by the greater retention time seen for naproxen (table 5.17 and the above figures). Using the parameters for evaluation – capacity factor (k'), separation factor (α) and retention

index (RI) the results were further processed to facilitate a simple comparison of MIP properties. These calculated parameters are shown in table 5.4

Table 5.4 Summary of capacity factors, separation factors and retention indices for the chromatographic study of the naproxen MIP prepared in DMF. Values obtained from figure 5.19

	Analyte	t_{ctl}	k'_{ctl}	t_{imp}	k'_{imp}	α_{ctl}	α_{imp}
DMF	MeOH	1.2		1.4			
	Naproxen	5.2	3.33	13.1	8.36	2.22	2.02
	Ibuprofen	3.0	1.5	7.2	4.14	-	-

In the analysis of the values in this study the imprinted polymers displayed greater affinity for the template molecule, naproxen over the analogue ibuprofen. This is evident in that the retention indices for ibuprofen are less than one.

The values from the HPLC studies corroborate the findings of the NMR studies and AMBER modelling in showing that the use of DMF as porogen induces a greater imprinting efficiency than MeOH. It is probable that the π-π stacking interactions are stabilised in DMF whereas the MeOH environment has been shown to be incompatible with the conformation.

5.5 Conclusion

The aim of this study was to investigate using molecular dynamics (with explicit solvent) and physical measurements the effect of porogenic solvents on MIP rebinding and retention behaviour. A significant achievement was in demonstrating directly that the stabilisation of a PPC interaction in a particular solvent could considerably affect the later rebinding. The results reported in this work have shown the potential for the use of molecular dynamics simulations in enhancing the understanding of the nature of the pre-polymerising complex. It was found that the type of porogen employed is of vital importance to the generation of a successful imprint. There are two reasons for the importance of porogen. Firstly, the stability of the interactions of the pre-polymerisation complex in the porogen will directly affect the affinity of the resultant polymer for the template. Secondly, the type of porogen used will govern the adsorption capacity in terms of the porosity and surface area of the polymer. Recent data suggests that polar aprotic solvents such as DMF and acetonitrile can enhance the development of a strong complex by having a low propensity to form hydrogen bonds with the template or monomer and by allowing the formation of hydrophobic interactions. However other solvents such as methanol and nonpolar solvents like chloroform and toluene have received much attention in the literature. This study has selected DMF (polar aprotic) and methanol (polar protic) and shown that template monomer complex is more stable in DMF. Furthermore it has been shown that the nature of the interaction is a π-π stacking effect and that it is this complex that is broken up in methanol more easily than in DMF.

In addition the MD simulation, ^{1}H NMR titration studies show upfield shifts of naproxen aromatic protons in d_7-DMF and not in MeOD consistent with a π-π electron delocalisation effect reducing the shielding on the aromatic protons and hence resonating further upfield. MIPs were produced non-covalently in beaded form using a suspension polymerisation employing a perfluorocarbon as a continuous phase. This method was shown to be compatible with both solvents employed. DMF produced beads which, while large (c.25 μm) in diameter had a smaller size distribution in comparison to the beads produced using methanol, which displayed a large size distribution. Furthermore, it was demonstrated that it is possible to adapt the

suspension polymerisation technique with minimum work to include both DMF and 4-Vinylpyridine in the polymerisation mixture. In terms of rebinding studies, the DMF MIP was shown to be selective in comparison to control non-imprinted polymers with non-specific binding increasing with both increased amounts of polymer used in the binding assay and an increase concentration of naproxen. In addition the selectivity of the DMF MIP for naproxen over the structurally related compounds ibuprofen and ketoprofen has been demonstrated.

The overall significance of this work is that computational predictions are now in agreement with experimentally derived data. There is also room for significant future development of the MD technique as applied to modelling PPC interactions. The above results represent a much-simplified approach in that each solvent box contains just one complex. Future work could model the interaction of higher order complexes. It is very possible that ratios such as 2:2 rather than 1:1 could exist. Experimental support for this phenomenon might be provided by X-ray cryatallography. The combination of modelling and X-ray provides an interesting opportunity to actually deduce not only the ratio but also the structure of the PPC.

Further developments in molecular modelling are allowing the simulation of more than one box at a time. For instance, in the data presented here the molecules are not permitted to leave the box. If a "multi-box" approach was employed then a molecule could leave a box but automatically enter from the other side thus maintaining the total number of molecules. This would increase the probability of self-assembly recombinations. Finally and returning to the situation of just one complex, it is entirely possible that a box could contain many complexes. Hence if a complex breaks up, a molecule would be free to interact with either a second molecule of functional monomer or another template molecule. In this way it would be possible to model the potential for co-operative type binding or the creation of specific binding cavities towards dimers or trimers etc.

Chapter 6

A molecularly imprinted sol gel for ibuprofen: An analytical study of the factors influencing selectivity

6.1 Introduction

The recent developments in molecularly imprinted sol gels have been discussed in section 1.9. As reviewed by Alexander *et al.*, [245], the majority of reported molecularly imprinted silica systems have been in bulk form utilising a single functionalised monomer. An example of this approach is that of Mizukami *et al.*, [246] where TEOS was hydrolysed in the presence of optically active organic compounds. Optical resolution of tris(pentane-2,4-dinato)metal complexes was achieved using sol gel derived composites. Furthermore, NMR results disclosed that an optically active organic compound in the sol gel is highly dispersed. This is most likely because it bonds to silicon atoms. In a review by Collinson [247], the importance of careful selection of the synthetic conditions for a general sol–gel preparation, such as silicon to water ratio, pH and type of silane monomer used is explained. Through variations in the sol-gel processing conditions (silicon-to-water ratio, pH, type of silicon alkoxide), materials with optimal porosity and/or hydrophobicity can be prepared for separations and facilitated transport applications.

The basic sol–gel process involves the sequential hydrolysis and polycondensation of alkoxy silicon derivatives (e.g. tetraethyl orthosilicate (TEOS), or tetramethyl orthosilicate (TMOS)), in aqueous acid or base with a mutual cosolvent. Sol–gel precursors are mainly silicon alkoxides, which can be obtained in a high degree of purity. Tetramethoxysilane (TMOS) undergoes a more rapid hydrolysis than tetraethoxysilane (TEOS). TMOS was used by Nakanishi *et al.*, [248] to produce a well-defined macroporous structure in a monolithic wet gel. Wagh *et al.*, [249] compared the aerogels obtained from three different precursors: TEOS, TMOS and PEDS. They concluded that TMOS yields narrow and uniform pores and higher surface area than TEOS. The sol–gel precursors may include a mixture of alkoxysilanes, one of them being a functionalized moiety such as aminopropyltriethoxysilane (APTES). A study by Mansur *et al.*, [250] inserted different chemical functionalities, both organic and inorganic in a silica glass based sol–gel derived network to create specific chemical activities. Modified silica glass networks were prepared by reacting alkoxysilanes with different chemical functionalities, such as tetraethoxysilane, aminopropyl triethoxysilane, and

mercaptopropyl triethoxysilane (MPTS). The chemical activity of the created multifunctional surfaces was evaluated by the ability of the incorporated proteins to remain adsorbed onto the different gels. Porcine insulin and bovine serum albumin were impregnated into modified networks and desorption of those proteins was monitored. Results showed that gels with multifunctionalities regularly dispersed can be successfully produced by optimizing some of the processing parameters of the gels, such as pH and concentration of reactants. The data also revealed that the type and concentration of chemical functionalities within the gels regulate the ability of incorporated proteins to remain adsorbed on them, suggesting that chemically patterned surfaces and interfaces can be prepared which regulate protein–substrate interactions. To prepare monolithic sol–gel columns with surface bonded ligands, Malik and Hayes [251] utilized two sol–gel precursors and a deactivation reagent (phenyldimethylsilane) to produce a monolith.

The starting silicon derivative is dissolved in a solvent, an aqueous solution (acid or base) reacts and gelation is produced within a certain period of time. TEOS, TMOS or other silicon alkoxides are not soluble in water. They are dissolved in alcohol to produce a homogeneous solution and water is then added. Hydrolysis of silicon alkoxides is a versatile technique that can produce different materials according to the different parameters and to the acid catalysis or base catalysis reaction. It may produce silica spheres or silica gels depending upon the experimental conditions [252]. As Siouffi [252] also states, Another critical point is the ratio Si:water, i.e. the proportions of TMOS (or TEOS) and water which yields different products. Hydrolysis is performed with a catalyst. Three procedures are possible: acid catalysis, base catalysis and two-step catalysis. Acid catalysis is generally performed with HCl or H_2SO_4. Gelation times are generally longer when the pH of the sol is low [252]. Base catalysis usually involves dilute ammonia [253]. Under base catalysis condensation kinetics are faster than hydrolysis kinetics. The two-step procedure was proposed by Brinker *et al.*, [254]. In a typical procedure [253] TMOS, ethanol, H_2O and HCl are combined and this first solution is then mixed with H_2O and ammonia. The addition of NH_4OH as a second catalyst to a sol initially catalyzed by HCl can increase the rate of condensation reactions and reduce the gelation time.

6.1.1 Aims and objectives

This chapter describes the study of the individual and combined factors that are responsible for selectivity in sol gels. The template chosen was ibuprofen. In order to gain an enhanced understanding of factors affecting selectivity, three sol gels each of differing complexity and functionality were prepared and their ability to selectively discriminate between ibuprofen and its structural and functional analogues, naproxen and ketoprofen have been studied. In the choice of functionalised siloxanes (analogous to functional monomers in MIPs) important functionalities such as hydrogen bond forming ability, electrostatic interactions and potential π-π stacking interactions have been considered. In numerous sol–gel publications, a two-monomer polymerisation approach is adopted an example of which being the study of Yu *et al.*, [255]. Furthermore, the two and three monomer systems offer an increased complexity in terms of the molecular size and shape of the resultant nanocavities in the sol gel. It is proposed that the major determinant of selectivity is the spatial complementarity of the cavity; however, there is a significant contribution from functional interactions within the cavity.

To study the specific criteria affecting selectivity in sol gels three sol gels were prepared for ibuprofen utilising two and three functional silane systems. The relative rebinding of each of the three compounds to the sol gels was assessed by % recovery in solid phase extraction and by spin coating of thin films onto a glass substrate.

6.2 Experimental

6.2.1 Materials

Tetraethoxysilane (TEOS), 3-Aminopropyltriethoxysilane (APTES) and phenyltrimethoxysilane (PTMOS) were purchased from Sigma Aldrich, Dublin and used as received. Ibuprofen, naproxen and ketoprofen were also purchased from Sigma Aldrich, Dublin. All organic solvents were of HPLC grade and were purchased from Labscan, Dublin, Ireland.

6.2.2 Preparation of sol gels

All of the sol gels generated contained TEOS and one or both of APTES / PTMOS. The preparation consisted of two stages: firstly the hydrolysis without ibuprofen (template) and secondly condensation in the presence of ibuprofen. A 12 ml aliquot of 2-ethoxyethanol was mixed with 12 ml of TEOS. A 400 μL quantity of PTMOS or 600 μL of APTES or both were then added. Following this 400 μL of concentracetd HCl followed by 4 ml of water were then added and the mixture left stirring for 2 h at RT. After 2 h, 206.28 mg of ibuprofen in 20 ml water (min vol. ethanol – enough to completely dissolve the quantity of ibuprofen) was added to 16 ml of the imprinting mixture and stirred for 10 min. A non-imprinted sol gel was prepared under the same conditions but with the omission of ibuprofen. Condensation was allowed to progress at 80°C for 16 h and then for 1 week at room temperature. Following this the sol gel was crushed with a mortar and pestle and sieved. Particles between 45 and 25 μm diameter were collected by sieving. The crushed sol gels were then washed to remove the template by continuous stirring in a solution of hot methanol containing 10% acetic acid. Washing was repeated until no trace of ibuprofen could be detected by HPLC. Table 6.1 shows the components of each sol gel.

Table 6.1 Components of each of the sol gels

Sol Gel 1	Sol Gel 2	Sol Gel 3
2-EtOH (12 ml)	2-EtOH (12 ml)	2-EtOH (12 ml)
TEOS (12 ml)	TEOS (12 ml)	TEOS (12 ml)
APTES (600 µl)		APTES (600 µl)
	PTMOS (400µl)	PTMOS (400 µl)
HCl (400 µl)	HCl (400 µl)	HCl (400 µl)
H_2O (24 ml)	H_2O (24 ml)	H_2O (24 ml)

6.2.3 Physical characterisation of sol gels

The infrared absorption spectra of the sol gels were obtained on a Perkin Elmer GX FTIR system. Particle size measurements were performed on a Malvern mastersizer particle size instrument by the light scattering technique. A 25 mg quantity of the sol gel was exposed to 5 ml of a range of solvents for 4 h in order to examine changes in the average particle sizes of the particles.

6.2.4 Rebinding analysis

To assess the effect of different solvents on the % uptake of ibuprofen by the sol gels a1 ml solution of ibuprofen at 1 µg/mL was added to 50 mg of the sol gels (and controls) in a 1 ml microcentrifuge tube in the solvents as shown in figure 6.3. The solutions were shaken for 4 h at room temperature and then centrifuged. The presence of ibuprofen in the supernatant was assayed by HPLC and the amount bound was calculated as:

Total ibuprofen - free (supernatant) = bound ibuprofen

6.2.5 Solid phase extraction studies

Empty solid phase extraction cartridges were washed with methanol before use. The cartridges were then dried and 200 mg of the dry sol gel (or corresponding control) was placed between two frits. The cartridge was washed with 10% acetic acid in methanol and then with methanol 4 times until no trace of ibuprofen could be detected by HPLC. All SPE experiments were performed on a VacMaster SPE processing station manifold. Before analyte loading, the polymer was conditioned with 1 ml methanol, 1 ml acetonitrile and 1 ml water and then conditioned to the appropriate pH (pH 4-8) with water adjusted with dilute HCl or dilute NaOH. In the loading step, 1 μg/ml ibuprofen, naproxen and ketoprofen was loaded in water at pH 4-8. For the washing step, 1 ml of 1% triethylamine (TEA) or 1% pyridine in acetonitrile or a 50:50 ratio of toluene: acetonitrile was used. Specifically bound material was eluted with 2 ml of methanol. The experiments were repeated in triplicate. After each experiment the cartridge was regenerated by washing with 3 ml of water and 3 ml of methanol.

6.2.6 HPLC studies

HPLC was performed on a Hewlett Packard 1050 (HP 1050) LC system (pump, injector, detector) employing Chemstation software. The variable wavelength detector was operated at 220nm for ibuprofen determinations. For fluorescence applications the excitation wavelength was set at 290 nm and the emission at 350 nm. A 10 μl injection volume was used. Separations were performed on a 25 cm X 4.6 mm, 5 μm Alltech Bravda BDS C18 column.

6.2.7 HPLC measurements

For the ibuprofen/naproxen/ketoprofen selectivity studies the mobile phase used was a 52:28:20 ratio of water: acetonitrile: methanol. The mobile phase was adjusted to pH 3.2 with phosphoric acid. For urine analysis, the mobile phase used was a 50:50 ratio of 50 mM phosphoric acid: acetonitrile.

6.2.8 Real sample analysis

A volunteer was given a single dose of ibuprofen (200 mg) contained in a Nurofen™ tablet. Urine samples were collected at a 6 h interval. A 1 ml aliquot of each urine sample was passed through the sol gel SPE cartridge and washed and eluted as described in section 2.6. Free ibuprofen was quantified with reference to a standard curve. The presence of ibuprofen was shown at the correct retention time by spiking with a known concentration of the compound. To examine conjugated ibuprofen and ibuprofen metabolites, the urine samples were hydrolysed according to the methods of de Oliveira *et al.*, [256] and Tan *et al.*, [257].

6.2.9 Spin coating studies

Pre-condensation sol gel mixtures were spin coated onto clean glass microscope slides using a spin coater at different speeds. A 1000 µl aliquot (enough to cover the entire slide) was used. For a direct UV assay, the sol gel (400 µl) was coated onto a single side of a quartz cuvette. Typically, the slide was spun for 30 s at varying speeds (ranging from 1000 rpm to 4000 rpm). The slide was dried for 48 h at room temperature and stored at 4°C. The selective adsorption of ibuprofen from both aqueous standard solutions and urine was analysed. Initially a time study was performed to determine the minimum incubation time necessary and also the optimum concentration for use in the assay. For this the glass slide was immersed in a 1 µg/mL solution of ibuprofen in 50 mM sodium phosphate for 1, 2, 4, 16, and 24 h time periods. Following removal from the ibuprofen solution, the slides were washed in the same solution before bound material being removed from the slide by immersion in methanol. Ibuprofen in the solution was quantified by HPLC.

6.2.10UV measurements

UV measurements were performed on a Varian 50 Scan UV visible spectrophotometer equipped wit Cary UV software. The analytes were detected at 220 nm

6.3 Results and discussion

6.3.1 Physical and morphological characterisation of the sol gels

Three sol gels were prepared for this study. Sol Gel 1 contained APTES as the functional monomer. Sol gel 2 contained PTMOS as the functional monomer and Sol gel 3 contained a mixture of APTES and PTMOS. The three sol gels prepared were analysed by IR spectroscopy post washing. Figure 6.1 shows the most distinctive infrared absorption bands related to the generation of sol gels.

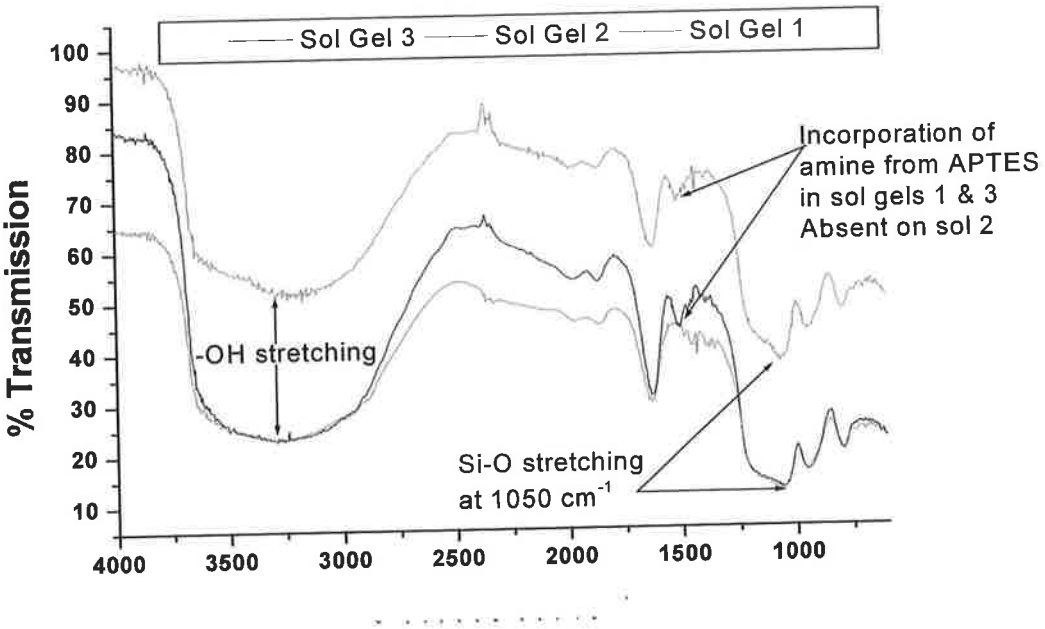

Figure 6.1 FTIR absorption spectra for the three sol gels. Notable bands include the –OH at ~3250 cm^{-1} and Si-O stretching at 1050 cm^{-1}.

The spectra shown are those of the imprinted sol gels post washing. No differences were observed between imprinted and non-imprinted sol gels i.e. no evidence of residual temlate could be observed by FTIR analysis. In the 3400-3200 cm^{-1} region, the stretching due to residual water and Si-OH stretching is observed. The band observed in all three samples at ~1050 cm^{-1} is indicative of Si-O stretching [258] stretching while those at 930 cm^{-1} and 780 cm^{-1} can be attributed to methyl C-H

stretching. Sol gels 1& 3 both contain a small band at ~ 1500 cm^{-1} and this is absent in sol gel 2. This can be attributed to the incorporation of the amine group from the APTES silane (functional monomer) into the former sol gels and not the latter. Furthermore as has been described, [259], the spectral features are consistent with organic modified silicas and also given the similarity between the imprinted and non-imprinted sol gels, the presence of the template did not alter the physical nature of the sol gel.

In contrast to MIPs, sol gels do not exhibit significant swelling [170]. In order to examine the potential degree of swelling, particles of sol gel 3 were placed in equal volumes of a range of organic and aqueous solvents and the average particle size of sol gel 3 was measured by particle size light scattering technology. The lack of swelling is an important characteristic in sol gels and will act to preserve the integrity of the binding cavity. Sol gels have been reported to shrink [260] with an associated loss of sorption capacity. Figure 6.2 shows the shrinkage observed when sol gel 3 was dispersed in different solvents for 4 h (stirring) followed by measurement of particle size.

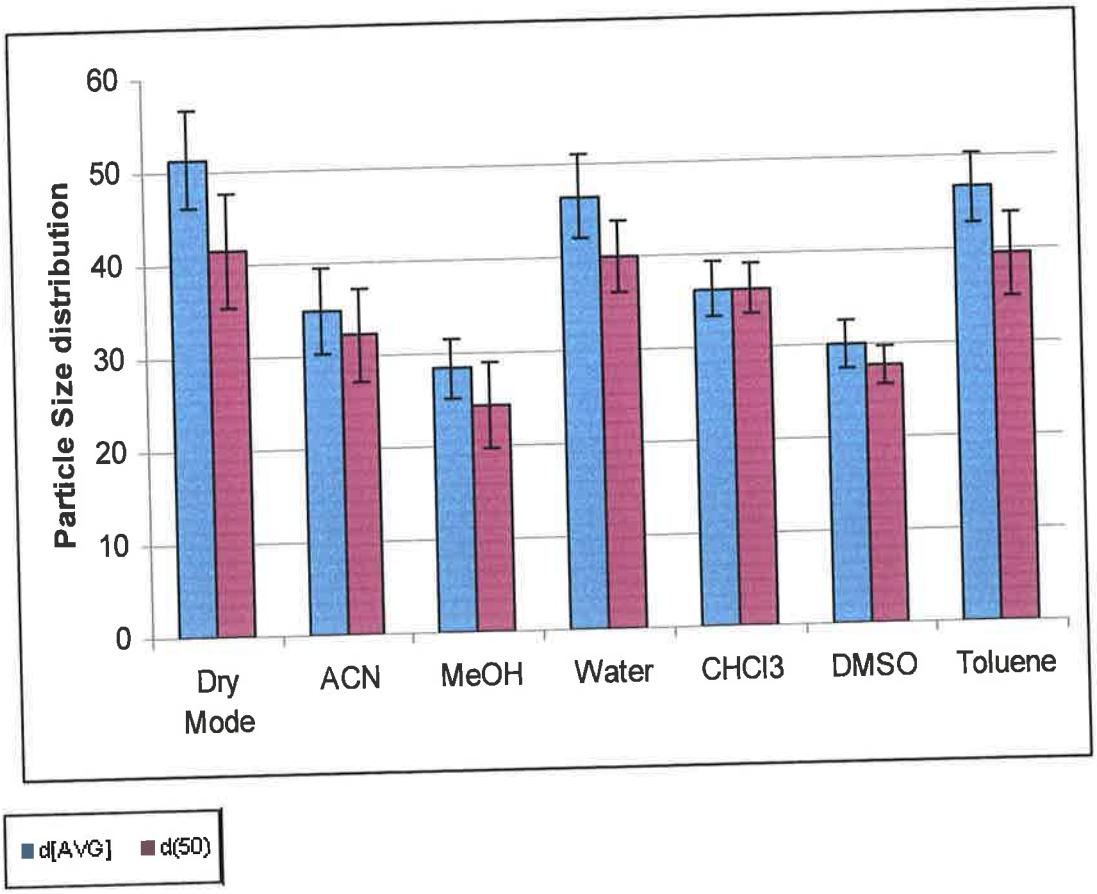

Figure 6.2: The percentage shrinkage associated with particle size distribution measurements for sol gel 3. The sol gel was exposed to the solvents shown and the shrinking (relative to dry mode) is illustrated. Errors are based on the standard deviation of two experiments. The value d(50) is the value at which 50% of the particles in the solution lie while the value d[AVG] is the average particle size. Both can be interpreted as the mean of the particle sizes in a sample.

It was found that water caused the least reduction in average particle size and nonpolar solvents lead to only minimal shrinkage. Both polar protic (methanol) and polar aprotic (ACN and DMSO) cause greater observed shrinkage of the sol gel. It is somewhat surprising that the more polar solvents are observed to lead to greater shrinkage of the sol gel than the nonpolar solvents. Collinson [247] has reported that during drying, alcohol evaporates from the pores causing the sol gel to shrink. In this instance it is likely that the polar solvents diffuse into the pores and cavities of the sol gel replacing residual water and evaporate during the measurements leading to continued shrinking of the material. The nonpolar solvents may not diffuse into the

pores as efficiently and hence their loss through evaporation has less of a shrinking effect on the pores.

6.3.2 Rebinding studies

In order to assess the performance of the imprinted sol gels, a study of the rebinding abilities was carried out as described in 6.2.4. A variety of rebinding solutions were prepared for the study. Figure 6.3 shows the relative specific uptake i.e. % rebinding in the sol gels minus that in the control sol gels.

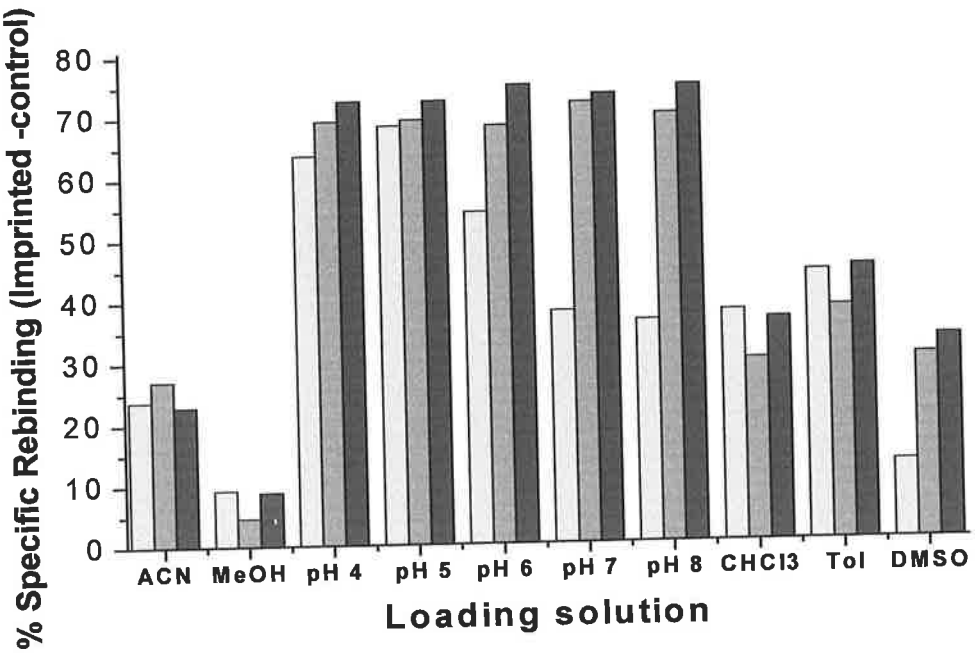

Figure 6.3: Shows the specific rebinding (uptake in imprinted sol gels minus that in non-imprinted) for the three sol gels under a range of organic and aqueous conditions. pH 4-8 are aqueous solutions of ibuprofen.

Key: Sol gel 1 Sol gel 2 Sol gel 3

The pH was adjusted to the relevant value by addition of concentyrated HCl or concentrated NaOH.

6.3.2.1 Effect of solvent on rebinding

It was found that all three of the sol gels demonstrated enhanced specific rebinding of ibuprofen in aqueous conditions. The sol gels perform best in aqueous conditions followed by nonpolar (chloroform, toluene) polar aprotic (acetonitrile, DMF) and then polar protic (methanol and ethanol) solvents. A similar trend has been noted by Marx and Liron [164]. In this study, it was pointed out that the increased rebinding of propanolol to the sol gel could result from the preferred solubility of the molecule in organic media relative to aqueous and this is in part justified by the partition coefficient of propanolol in the octanol/water system. Nonpolar solvents such as chloroform would not be expected to interfere with hydrogen bonding whereas more polar solvents will form strong hydrogen bonds with the template thus precluding the formation of specific interactions with the functionalities in the pores [32]. This is can be directly related back to the shrinking study in figure 6.2 where the least shrinking was found in water followed by nonpolar solvents. Thus, the highest level of shrinking and the lowest level of specific rebinding were observed in the polar solvents.

6.3.2.2 Effect of pH on rebinding

The effect of pH on rebinding of ibuprofen to the 3 sol gels was studied. In the case of sol gel 1 (prepared with the APTES monomer) figure 6.3 shows that at pH 4 and 5 the rebinding is significantly greater than at pH 4-5 (>60% specific rebinding as opposed to 40-50%). The pK_a of ibuprofen is reported to be 4.8 [281]. Since a significant method of complex formation of ibuprofen with APTES or with the silanol –OH's may be hydrogen bonding, a negatively charged molecule will be unable to participate in hydrogen bonding and hence this type of interaction will be reduced. Some rebinding will still occur to the sol gel at higher pH's because of the presence of van der Waals, electrostatic forces along with interactions of ibuprofen with the silanols of the sol gel. Furthermore, it could also be explained by the increased preference of the molecule for the aqueous phase above the pK_a. For these reasons an abrogation of rebinding is not observed. This is further exemplified by the rebinding in aqueous conditions to sol gels 2 (and 3) also shown in figure 6.3 and importantly, the

rebinding to sol gels 2 and 3 is not pH dependent. Here the monomer used was PTMOS (sol gel 2), which will possibly form π-π stacking interactions with ibuprofen and the nature of these interactions will not be significantly altered by changes in pH in the region 4-8. As such, considerable rebinding of ibuprofen to sol gels 2 and 3 is observed at all pH's examined. Sol gel 3 contains both APTES and PTMOS. As part of the three monomer system, the significance of the hydrogen bonding interaction with APTES is reduced relative to other determinants of selectivity such as shape complementarity, electrostatic and π-π interactions and hence these interactions can to a large extent compensate for the loss of the hydrogen bonding at higher pH's.

It was found that the rebinding decreased slightly when toluene was used as the rebinding solvent between sol gel 1 (43.9%) and sol gel 2 (38.1%). This is shown in figure 6.3. As toluene contains an aromatic ring, the probability of forming a π-π complex with ibuprofen is somewhat increased. This may hinder the ability of the ibuprofen molecule to form stacking complexes with the functional groups on the inside of the sol gel cavities and further the increased molecular volume may also inhibit entry of the molecule into the cavity. However it is likely that any π-π stacking between ibuprofen and toluene will be extremely weak. The interpretation of rebinding studies indicates that there are a significant array of factors that combine to reach optimum binding conditions for all of the sol gels. It is in fact likely that these factors – hydrogen bonding between ibuprofen and the amine groups (at pH 4-5), and electrostatic interactions at a pH greater than 6 between a deprotonated ibuprofen and the amine groups all contribute to the rebinding.

6.3.3 Molecularly imprinted solid phase extraction: Contribution of π-π stacking interactions to selectivity

Sol gel 2 contains PTMOS as the functional monomer with the concomitant ability to form π-π stacking complexes with ibuprofen. However, both naproxen and ketoprofen also contain aromatic rings, which could increase the probability of cross reactivity. Pyridine was chosen as a component of the washing solution. This is due to that fact that the aromatic ring of pyridine would disrupt non-specific interactions by forming π-π interactions with weakly bound material i.e. naproxen and ketoprofen. Furthermore, it will act as a competing amine for material, which may be non-specifically bound to the surface silanol groups. This is because the nitrogen of the pyridine ring will form a complex with the carboxylic –OH of each molecule. It was found that when 1% pyridine in acetonitrile was used as the washing solution, a large portion of the ibuprofen was removed from all of the sol gels. It was noticeable however that a larger proportion of the analogues were removed also. There are two reasons for this. Acetonitrile is a powerful eluting solvent and moreover, the nature of π-π stacking is that it is a weak interaction (weaker than hydrogen bonding). Hence it is vital that conditions are suitable so as to augment the stacking interactions.

Referring to figure 6.3, it is observed that chloroform may be a suitable solvent for enhancing specific π-π interactions yet disrupting non-specific binding of naproxen and ketoprofen. This is because as a nonpolar solcvent CHCl3 will disrupt any non-specifically bound material. Hence only ibuprofen undergoing strong specific interactions will stay bound. It was expected that competition would occur for ibuprofen and its analogues between the functional sites on the sol gel and the pyridine. As π-π stacking interactions are electrostatic in nature, it was expected that only specifically bound material undergoing π-π stacking and also in correct spatial configuration would be retained on the sol gel otherwise the interaction would not survive in chloroform. Figure 6.4 shows the results of this approach.

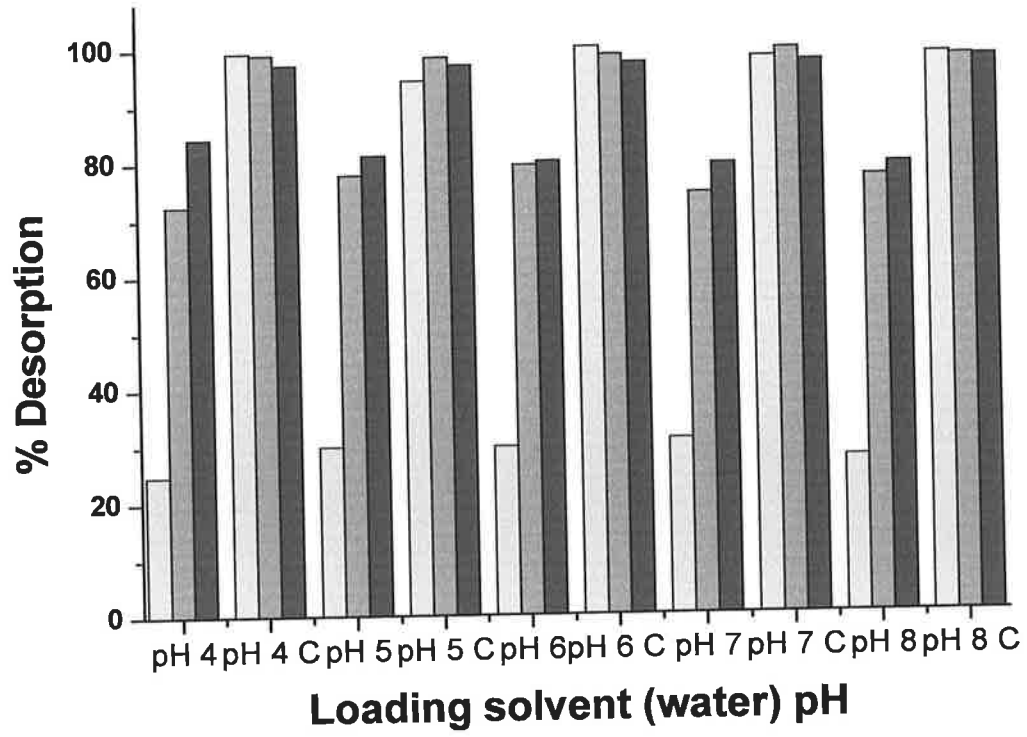

Figure 6.4: Selectivity study on sol gel 2. The % desorption was studied on washing with 1% pyridine in 50:50 acetonitrile: chloroform under loading conditions ranging from pH 4-pH 8.

To fully appreciate this result the discussion on the nature of the π-π stacking mechanism in this context needs to be furthered. Figure 6.5 shows the 3-dimensional structure of the three molecules.

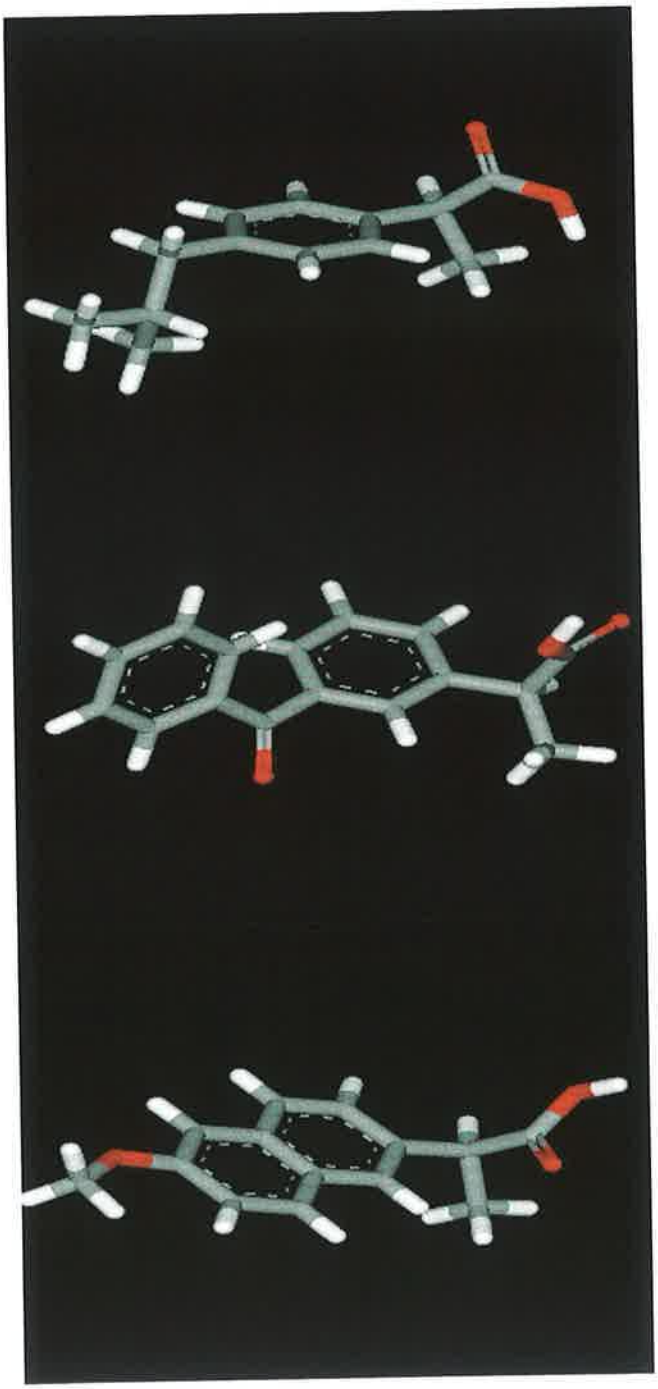

Figure 6.5: The three dimensional structures of the molecules used in the study ibuprofen (above) ketoprofen (middle) and naproxen (below).

Figure 6.5 shows the three molecules in the study that contain aromatic groups and are capable of undergoing stacking interactions with a functional aromatic group. However, the relative strength of the interaction will differ considerably between the molecules. Ibuprofen contains a single aromatic ring with no electron withdrawing substituents directly on the ring. The shape of the molecule also affords steric manoeuvrability to a potential aromatic ring coming into close contact and allowing the formation of the π-π electron delocalisation necessary. Regarding ketoprofen, the molecule possesses a carbonyl group between the two aromatic rings. The nature of this substituent will affect the charge transfer ability of the ketoprofen aromatic rings in forming π-π stacking arrangements with PTMOS. Naproxen contains a naphthyl group which will be higher in electron density. Since it will be mostly excluded from the specific ibuprofen binding cavities, it will be subject to π electron charge transfer formation with the pyridine in the washing solution and can be removed from the MIP column. Hence, the strength of π-π stacking interactions between the PTMOS ring and each of the analogues will differ. Figure 6.4 also shows significant removal of naproxen and ketoprofen. The desorption of these molecules is attributed to a shape exclusion effect and to the ability of the pyridine to form π electron interactions with ketoprofen and naproxen and remove them from the specific binding cavities.

6.3.4 Shape complementarity

A major component of selectivity of the sol gels for ibuprofen is shape complementarity. From the 3 dimensional structures of the analogues shown in figure 6.5, it can be seen that there are considerable differences in shape. The Acceryls program calculates the molecular volume of ibuprofen to be 149.8 $Å^3$ with that of naproxen at 151.0 $Å^3$. Ketoprofen has a molecular volume of 174.8 A^3.In the field of molecularly imprinted polymers, the work of Spivak and co-workers have shown the importance of shape selectivity in non-covalently imprinted polymers. For sol gels, it has been demonstrated that imprinted silica could act as a shape selective base catalyst. To study this further a third sol gel (sol gel 3) was prepared using both APTES and PTMOS. It was expected that the resultant nanocavity would be even more size and shape selective for ibuprofen. As is shown in figure 6.6, the selectivity for ibuprofen over naproxen and ketoprofen showed a marked increase over using APTES or PTMOS alone as the functional monomer.

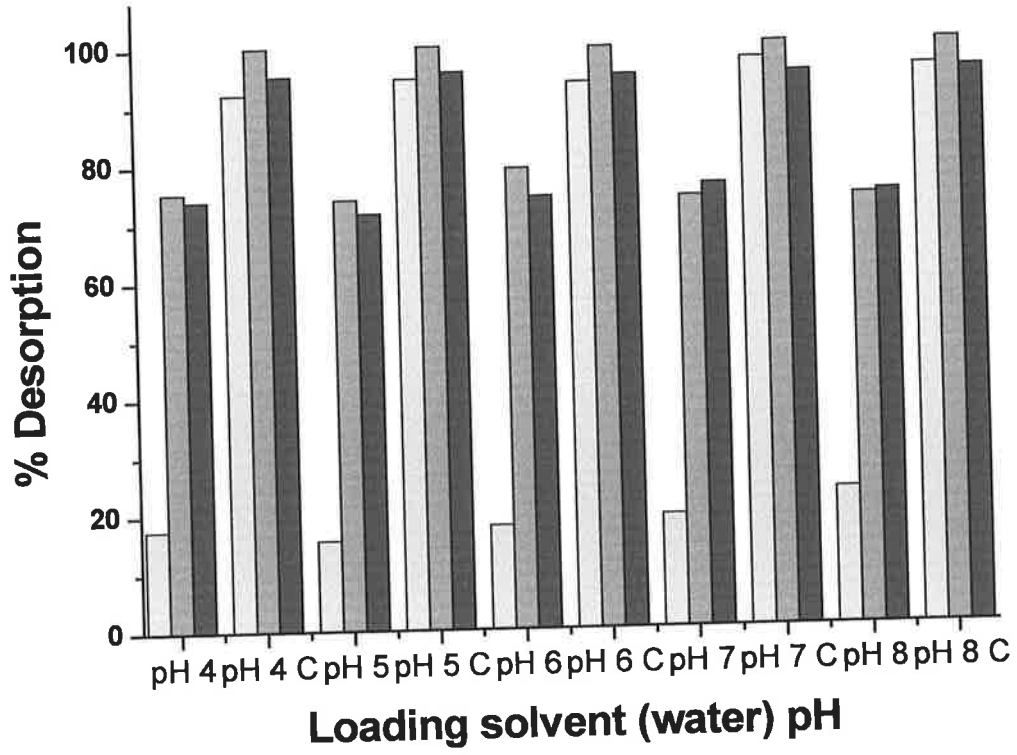

Figure 6.6: Selectivity study on sol gel 3. The % desorption of each drug (from % of each drug applied) loaded in 1 ml water (at appropriate pH) from sol gel 3 was studied on washing with 1% pyridine in 50:50 acetonitrile: chloroform.

The binding of catecholamines on imprinted on silica–alumina gel shows a size selective effect [262]. Compared to norepinephrine and epinephrine, the small size of dopamine imprinted cavities only allowed rebinding to dopamine itself. The selectivity of the MIP receptor prepared with different ratios of template to functional silane was examined with seven analytes: dopamine, epinephrine, norepinephrine, ascorbic acid, homovanillic acid, uric acid, and l-tyrosine. The results showed a size selective effect for the receptors with respect to the recognition of the catecholamines. Some factors affecting the recognition ability were the solution pH of analytes and surface capping on the MIP. Based on the results obtained and exhibited in figure 6.6, a fourth sol gel was prepared this time using naproxen as template. It was expected that this sol gel would show an increased level of cross reactivity towards ibuprofen than the ibuprofen imprinted material had towards naproxen since the smaller size of

ibuprofen would be better able to fit in to the cavity generated by naproxen. These results are presented in figure 6.7.

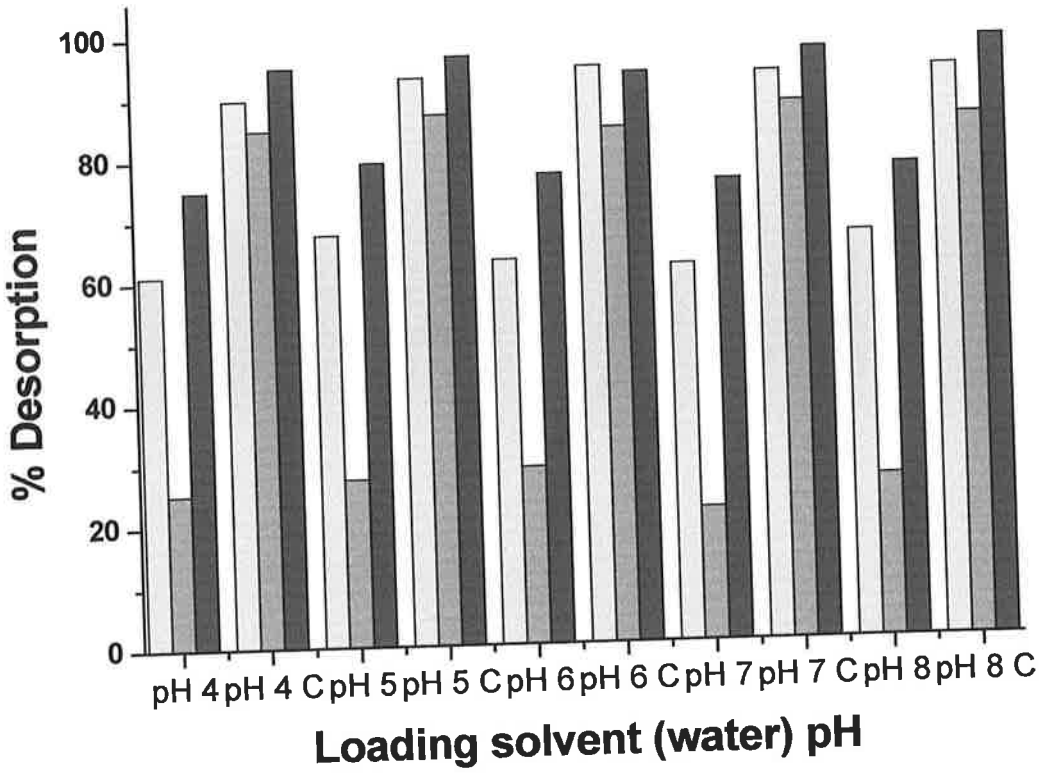

Figure 6.7 Selectivity study on sol gel 4. The % desorption from sol gel 4 was studied on washing with 1% pyridine in 50:50 acetonitrile: chloroform.

A degree of cross reactivity was observed but the level was lower than expected. This phenomenon has been attributed to shape selectivity and the concomitant thermodynamically unfavourable conditions for ibuprofen binding to a larger cavity. Shape complementarity assumes an increased significance when a competing molecule to the analyte of interest is smaller in size or bulk (or at least of similar size). If the competing molecule was larger then it would be excluded from the binding cavity due to steric hindrance as is evident from the high level of desorption of ketoprofen. This is illustrated in figure 6.7.

Essentially, a molecule of similar size but different shape i.e. ibuprofen will be allowed to manoeuvre within the naproxen sol gel binding cavity but with sub-maximal binding. The phenomenon is described as a "non-optimal spatial fit" [64] with reference to MIPs. In effect, if a molecule lacks optimal shape complementarity to the spatial organisation of the binding cavity, the number of potential contact interaction points will be reduced. Since the optimal spatial fit is not achieved, rebinding will have to overcome an extra thermodynamic barrier, hence a lower level of rebinding will be observed. The molecule exhibiting the optimal spatial fit, in the case of sol gel 4, naproxen, will demonstrate a better fit to the shape of the binding cavity and thus the sol gel showed enhanced selectivity towards naproxen. Despite the similar molecular volumes of ibuprofen and naproxen, the shapes of the molecules are significantly different. Hence, a molecularly imprinted sol gel prepared against ibuprofen demonstrates selective rebinding on the order of ibuprofen >> naproxen> ketoprofen and a molecularly imprinted sol gel prepared against naproxen showed naproxen >> ibuprofen> ketoprofen.

6.3.5 Application to sample analysis

To demonstrate the applicability of the molecularly imprinted ibuprofen sol gel (sol gel 3) it was employed in a solid phase extraction procedure. A urine sample was taken from a volunteer at 6 h post ingestion of a single dose of 200 mg of ibuprofen contained in a Nurofen™ tablet. Ibuprofen undergoes extensive conjugation in the human body with the kidney being the main source of excretion. Only 1% of an ingested dose of ibuprofen is excreted as the free i.e. unconjugated molecule. Two major metabolites of ibuprofen are produced – carboxyibuprofen and hydroxyibuprofen for each of which stereoisomers exist.

A 1 ml volume of urine at the above time point was loaded independently onto the sol gel column without pH adjustment. Although, selective clean up of the urine sample was achieved, a small recovery of ibuprofen and the analogues carboxyibuprofen and hydroxyibuprofen was obtained. This was attributed to the significant glucuronidation of ibuprofen. Given the large size of this molecule it will not be compatible with the spatial complementarity afforded by the sol gel cavity. In order to free the ibuprofen, the urine sample was subjected to a hydrolysis reaction as described [276]. This led to greatly increased peak areas for ibuprofen and the metabolites for the same sample. The above procedure was repeated using the same loading and washing conditions as before. As can be seen from figure 6.8 (below), good clean up of the urine sample was achieved. The quantity of non-metabolised ibuprofen in the sample at 6 h post ingestion was quantified at 7.07 μg/mL. The excellent selectivity and sensitivity has further been demonstrated with a recovery of 102.31%.

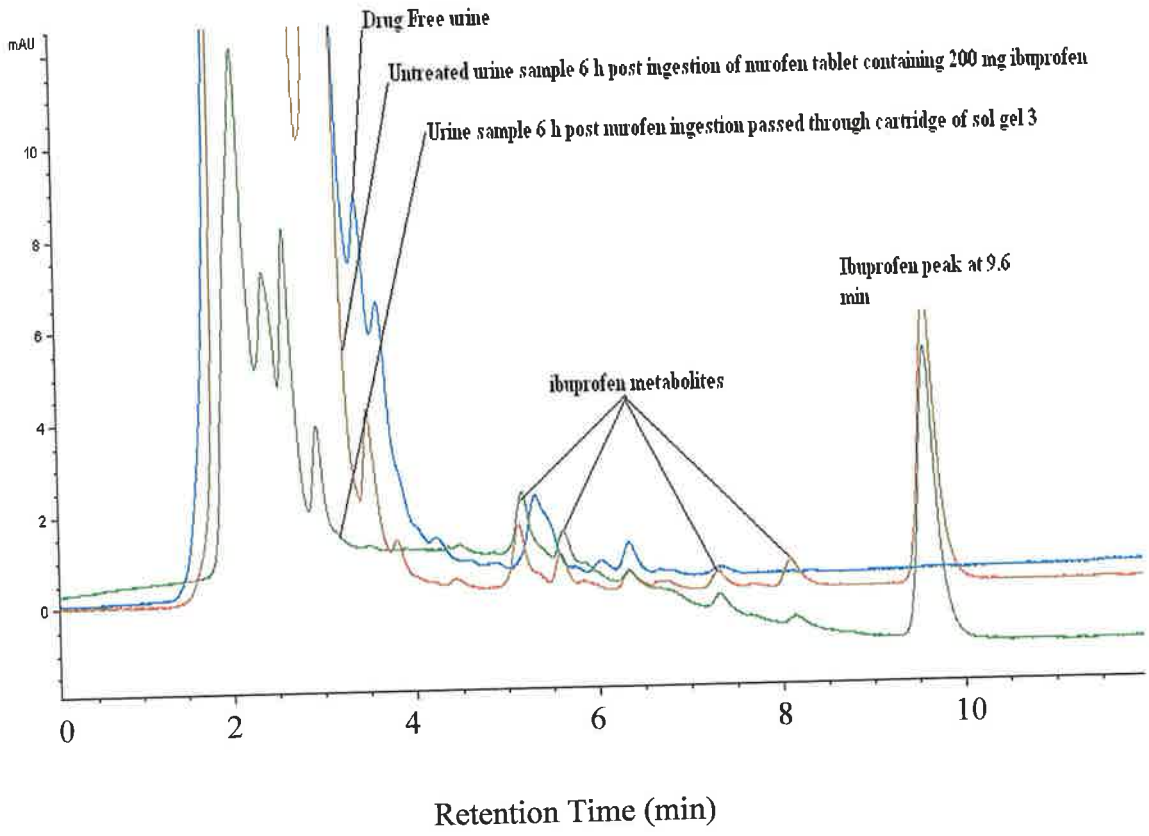

Figure 6.8: HPLC chromatograms obtained following solid phase extraction of a urine sample (with hysrolysis) 6 h post ingestion of 200 mg ibuprofen using 200 mg of sol gel 3. Ibuprofen eluted at 9.6 min with the more polar metabolites between 5.0 and 8.5 min.

Given the close structural similarity between ibuprofen and the two major metabolites (figure 6.9 below), the sol gel did not discriminate significantly between the metabolites of ibuprofen.

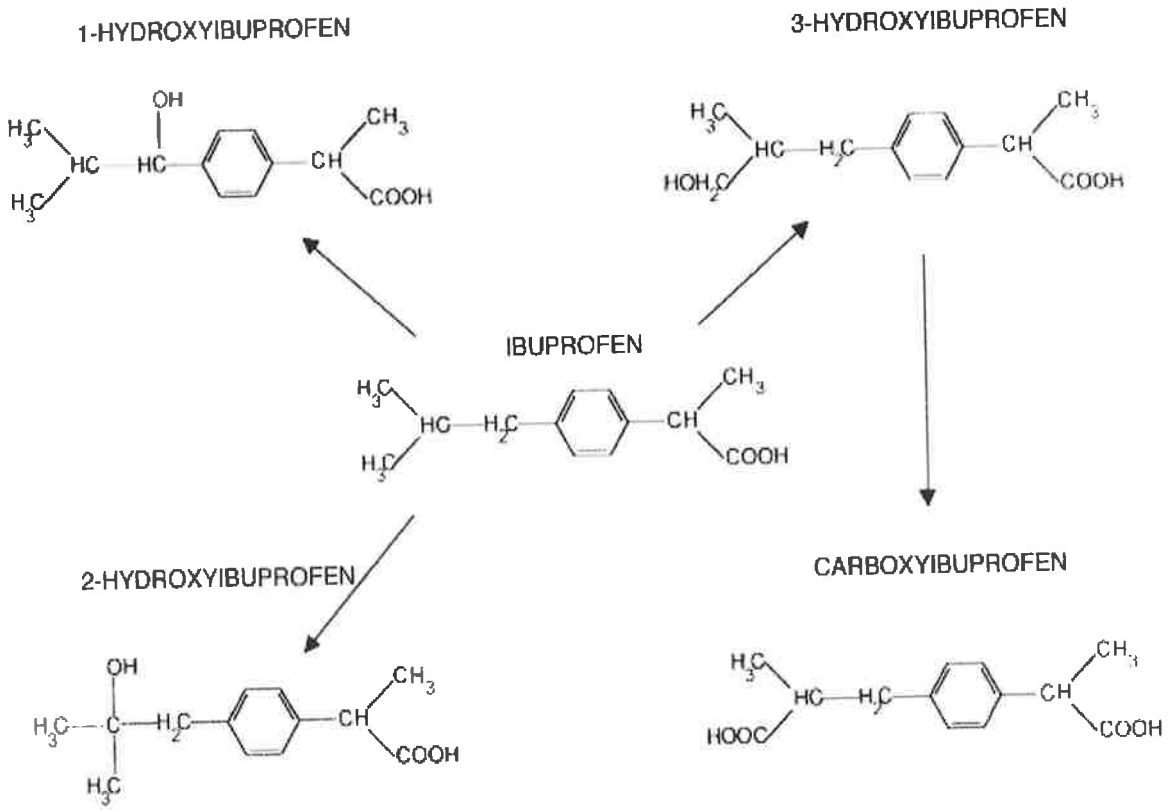

Figure 6.9 Oxidative route of ibuprofen metabolism. Reproduced without modification from de Oliveira *et al.*, [276]

It is probable that the sol gel displayed significant retention of metabolites in addition to ibuprofen. This is likely due to the fact that all of the metabolites contain an extra hydroxyl group and will still be capable of undergoing hydrogen bonding with the APTES functionality while ibuprofen will be fully deprotonated at the pH of urine. This is the most likely working hypothesis as the spatial differences between ibuprofen, carboxyibuprofen and hydroxyibuprofen are minimal. The contribution of specific electrostatic interactions towards selectivity is evident here. Essentially, both in MIP and imprinted sol gel systems the major determinant of the memory effect is shape complementarity however relatively subtle interactions such as electrostatic, stacking or hydrogen bonding can act to augment the and strengthen the binding. It is important then that these interactions are preserved during the production of imprinted materials.

6.3.6 Coating of sol gels

A number of physical characteristics of sol gels and the sol gel process itself render them suitable for coating onto surfaces. These characteristics include optical transparency and the ability to form thin layers. Furthermore, the condensation process can be performed in air and does not require an isolated system e.g. polymerisation of acrylate monomers must be performed in an inert atmosphere with the exclusion of oxygen vital to the process.

When a thin layer of an imprinted sol gel is coated onto a surface, a specific, fast and direct sensing element can be generated. This is because diffusion effects are delayed (see introduction for discussion on diffusion in MIPs).

6.3.6.2 Study of speed of spin coating

In order to study the effect of coating speed, 1000 µl of pre-condensation sol gel 3 (including template) was spin coated at the following speeds, 1000, 2000, 3000, 4000 onto glass microscope slides (75 x 12 mm). The slides were allowed to air dry for 24 h. Following this the template (ibuprofen) was removed by repeatedly passing methanol over the slide until no trace of ibuprofen could be detected by HPLC. For this purpose, the washings were evaporated to dryness and resuspended in a 1 ml volume. The slides were then laced in a solution of ibuprofen at 1 µg/ml (200 ml) overnight (24 h) at room temperature. The slides were removed and washed by placing in a bath of sodium phosphate 50 mM (200 ml) for 16 h. Specific material was eluted by placing the slides in methanol (200 ml) overnight (sealed). The amount of ibuprofen desorbed from the slides was quantified by HPLC. The amount of ibuprofen in the methanol was plotted against the speed of spin coating in rpm. This is shown in table 6.2:

Table 6.2: The concentration of ibuprofen determined by the coated sol gel expressed as a % of the original known concentration eluted with methanol

Speed of spin coating (rpm)	% Desorbed from Imprinted sol gel	% Desorbed from control sol gel
1000	8.96	0.17
2000	17.27	0.21
3000	21.47	0.22
4000	16.27	0.19

The initial amount of ibuprofen in μg in the 200 ml solution is

$$1 \times 200 = 200\ \mu g$$

The amount of ibuprofen in the methanol (post desorption from the slide) was calculated in μg and presented as a percentage of the initial concentration. Given the high solubility of ibuprofen in methanol along with its ability to disrupt hydrogen bonding and π-π stacking interactions it was deemed to be a suitable solvent for this purpose. The results indicated that the slides had reached saturation levels of binding by 24 h. The relatively low % rebinding is indicative of the coated sol gel having a low capacity i.e. the binding sites are quickly saturated. Noteworthy is the excellent specificity exhibited with negligible levels of non-specific adsorption to the control sol gel. Furthermore, there is an optimum speed for spin coating with reference to this sol gel. The amount of rebinding reaches a peak at 3000 rpm. This suggests that at 1000 and 2000 rpm, the coating is too thick to allow ibuprofen to diffuse into the binding sites. At 3000 rpm, the layer thickness is smaller and ibuprofen molecule can diffuse more readily. At 4000 rpm or higher, a decrease in rebinding was observed. This is attributed to a greater than desired quantity of the sol gel being removed from the slide and hence coverage may not be complete. Also a layer that is too thin will not possess the significant quantity of binding sites required to maximise ibuprofen binding.

6.3.6.3 A direct UV assay for ibuprofen

The outside of a quartz cuvette was coated with the same mixture as section 6.3.5.1, (30 s at 3000 rpm). Washing was performed by iimmersing the slide in sodium phosphate 50 mM overnight at RT. The rebinding and washing conditions were as described. On consecutive days an increasing concentration of ibuprofen was assayed by direct UV reading at 220 nm. The linearity is demonstrated below in figure 6.10:

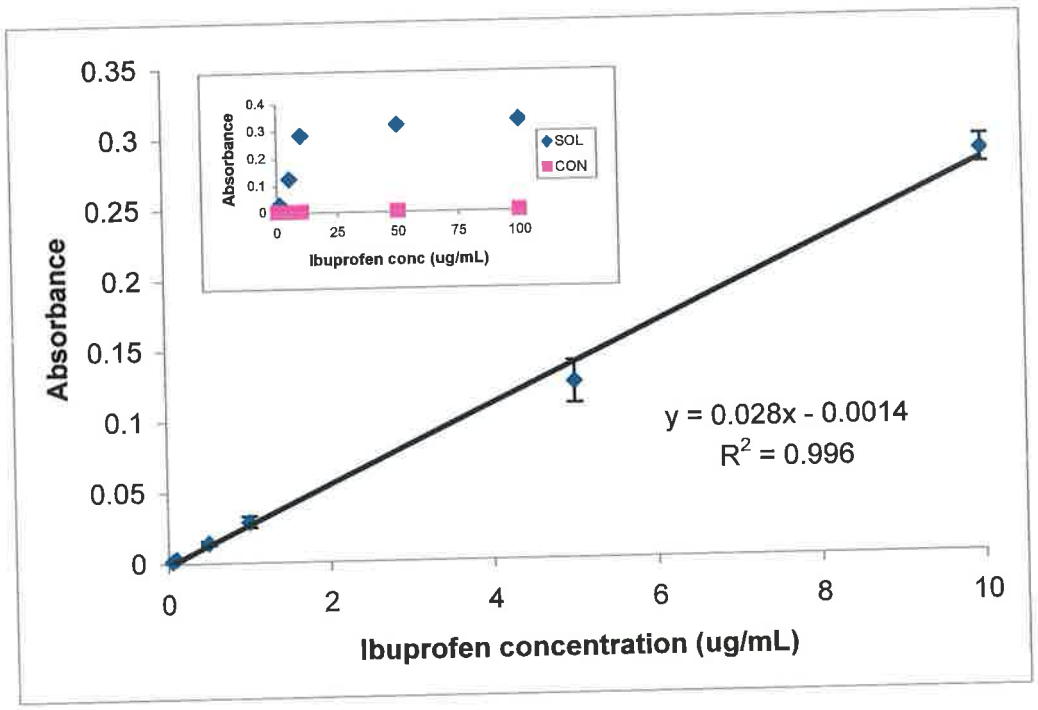

Figure 6.10: Linearity of the sol gel response to increasing concentrations of ibuprofen.

Above 10 µg/ml, linearity was lost as the binding pockets on the sol gel became saturated. Again, note the negligible non-specific adsorption to the control (inset). The sol gel coating technology offers an attractive alternative to MIPs. The advantage of optical transparency is particularly useful. Their ease of coating (without inconvenient problems such as degassing may mean they are more applicable than MIPs in sensor type applications.

6.4 Conclusion

The objective of this study was to enhance the understanding of the nature of selectivity in molecularly imprinted sol gels. This was achieved in two ways. Firstly, the physical characterisation of sol gels generated using different functional silanes and secondly by probing the selective rebinding abilities of each of the sol gels by varying experimental rebinding conditions and determining the optimum solid phase extraction procedure to extract ibuprofen from a mixture of ibuprofen, ketoprofen and naproxen whilst not extracting the latter two molecules. It was proposed that there are two determinants of selectivity in these sol gels. Firstly specific geometric binding cavities which through spatial complementarity serve as highly selective shape based exclusion cavities which allow entry of the analyte of interest (template) whilst refusing access to even analogues of the template depending on the level of spatial similarity of the analogue(s) with the template. Secondly, there is the chemical functionality imparted to the sol gel by the functional silane e.g. APTES, PTMOS.

The potential applications of such highly selective sol gels have been demonstrated by solid phase extraction clean up and preconcentration of ibuprofen (and metabolites) from urine and by demonstrating the efficiency of sol gel coatings in specific analyses. The applications of this type of material are many and can be performed easily and economically. It was demonstrated that by understanding the nature of sol gel chemistry, specific and selective materials can be produced that can easily be used as solid phase sorbents or incorporated into analytical devices.

The results of the experiments indicate that along with the functionality imparted to the sol gel by the development of template-monomer complexes a major determinant of selectivity is shape selective memory. The utilisation of a three monomer system affords recognition in the cavities based on the formation of π-π stacking interactions, hydrogen bonding, van der Waals forces, electrostatic interactions and shape complementarity and minimises cross reactivity. In addition real sample analysis has been performed on urine samples containing ibuprofen and metabolites showing specific preconcentration.

Chapter 7

Conclusion

7.1 General

The self-assembly approach for the synthesis of molecularly imprinted polymers has demonstrated significant potential for producing selective, highly cross linked polymeric biomimetic materials in a straightforward method. However as is evident from this thesis, it is evidently a multi-disciplinary task. The usual schematic employed in figure 1.1 is too simplistic to accurately represent the myriad of processes acting in concert to produce the molecular specificity associated with MIPs. Nevertheless, many examples throughout the literature demonstrate the successful application of MIPs as synthetic recognition materials in sample preparation, chromatographic separation and as antibody substitutes in binding assays. Numerous factors, in particular, the choice of functional monomer, cross-linker and porogenic solvent as well as the ratio between template and functional monomer will affect the resulting imprinting efficiency as demonstrated by the example of the imprinting of the chemotherapeutic agent methotrexate. Molecularly imprinted solid phase extraction allowed solid phase extraction clean up of caffeine from spiked soft drink samples without preceding clean up steps.

Despite the general advantages of MIPs including thermal, chemical and mechanical stability, non-covalently imprinted polymers are characterised by substantial binding site heterogeneity with a low percentage of high affinity binding sites which has limited their practical application. Based on these considerations, improving the binding characteristics of MIPs b developing highly optimised imprinted polymers is necessary. Consequently this thesis aimed at a rational understanding of the principles underlying formation of binding sites investigating molecular level interactions between the components involved in imprinting at the pre-polymerisation stage. For this purpose ibuprofen and naproxen were used as model templates. The interactions between the templates and the commonly used functional monomers (2 and 4-vinylpyridine and methacrylic acid were investigated by ^{1}H-NMR studies and by molecular dynamics simulations. An lternative molecular imprinting method was investigated by sol gel chemistry.

7.2 Chapter 2

In chapter 2, the generation of a specific MIP for caffeine is approached by screening caffeine against 2-VP and MAA. MAA showed the highest binding energy scores. The molar ratio as examined by further energy minimisation calculations, NMR spectroscopy and UV mole ratio plots. An initial appreciation of the importance of the porogen was observed when MIPs produced with the same template: functional monomer ratio showed different rebinding efficiencies during SPE studies. Furthermore, increasing the volume of the optimal solvent can improve rebinding by increasing the surface area and pore sizes leading to better flow characteristics and mass transfer in SPE.

7.3 Chapter 3

When using expensive or toxic compounds such as methotrexate a trial and error approach to MIP optimisation is a limiting option unless a "dummy" template can be used. Particularly useful in this regard is epitope imprinting. Essentially, a portion of the molecule of interest (preferably a portion of particular molecular structure and unique functionality) is imprinted. Analogous to antibody binding to the epitope of an antigen, the MIP will recognise the template based on the rebinding to the imprinted portion. In the solid phase extraction studies demonstrated in chapter 3, it is shown that imprinting of a substructure can lead to comparable extraction efficiencies to imprinting the entire molecule. Furthermore, given the limited template solubility exhibited by methotrexate a compromise needed to be made regarding porogenic solvent. It is expected that imprinting the glutamic acid substructure in a less severe solvent to DMSO would lead to greater recoveries. A similar approach was adopted by Quaglia showing just such an effect.

7.4 Chapter 4

The recognition of a substructure of a molecule evidently involves a contribution from shape or spatial organisation in the rebinding. This phenomenon was investigated further in chapter 4. Ibuprofen was selected as a model template molecule due to the fact that its analogues – ketoprofen and naproxen both have a similar anti-inflammatory effect in animals. Both act to repress expression of COX 1 and COX 2 in animal cells. All three molecules possess similar functionalities however the shape of each molecule is considerably different. Molecular modelling and ^{1}H-NMR studies indicated the presence of π-π stacking interactions between the aromatic rings of ibuprofen and 2-vinylpyridine. These interactions are also likely to be present with 2-VP and both of the analogues to differing extents. In addition, ibuprofen was imprinted in DMF – a molecule previously shown to be compatible for rebinding of the template to the polymer under aqueous conditions. In order to determine the effect of changing solvents on % uptake of template, the polymer was exposed to different solvents. Changes in the particle size were measured. Importantly, these can be indicative of swelling of the polymer and hence distortion of the binding sites.

7.5 Chapter 5

In order to model the effect of solvents of differing properties (polarity) on the stability of conformations of pre-polymerisation complexes of naproxen with 4-Vinylpyridine were analysed by molecular dynamics simulations in explicit solvent (DMF, methanol and chloroform). These studies have revealed that MD are an effective and highly promising tool following molecular level interactions. The simulations resulted in a trajectory of the molecules at a nanosecond timescale directly visualising the interacting groups. Furthermore, factors known to affect imprinting such as solvation effects may be assessed with MD simulations e.g. calculation of solvation free energies of selected conformations. The incorporation of empirical data (e.g. NMR) into simulations would significantly improve the control of the starting configurations rendering MD simulations a useful tool for investigating physical and chemical phenomena. Thereby appropriate candidate molecules with

high selectivity for a particular candidate analyte can be identified in a predictive process.

As part of an overall approach to optimising MIP performance, chapter 5 also demonstrated the feasibility of generating beaded MIPs with previously untested porogens such as DMF. The compatibility of the suspension polymerisation technique with 4-VP and DMF was proved. The differences in the morphology are apparent from the SEM images further emphasising the effect that the solvent can have both on the nature of the pre-polymerisation complex and on the morphology of the resulting polymer.

7.6 Chapter 6

Alternative approaches to molecular imprinting technology were investigated namely by the development of molecularly imprinted sol gel specific for ibuprofen. The development of molecularly imprinted sol gels is in its infancy however certain physical characteristics make them highly suitable as selective layers for incorporation into sensors. Chapter 6 investigated the nature of selective recognition in imprinted sol gels by studying solid phase extraction and spin coating applications. It was shown that the sol gel could selectively extract ibuprofen from standard solutions with minimal extraction of the related analogues ketoprofen and naproxen. Furthermore, undiluted urine samples could be passed through a column for the highly efficient extraction of ibuprofen. In addition, glass slides and cuvettes spin coated with an imprinted sol gel could be used in a binding assay type application. One of the greatest advantages of sol gels is optical transparency making them very suitable for use in sensing applications also they do not require difficult polymerisation conditions and can be produced directly on surfaces easily.

7.7 Final statement

From the present body of work it can be concluded that monitoring and understanding the non-covalent interactions responsible for complex formation and complex stability in the pre-polymerisation solution (and ideally during the polymerisation) will lead to enhanced imprints. The effects resulting from variation of the polymerisation components and conditions are key towards developing optimised imprinted polymers as these factors directly affect the binding site heterogeneity. Furthermore, the importance of simultaneous multiple site interactions for increased complex stability was discussed. It is vital that these multiple site interactions are stabilised or maintained during the polymerisation process for subsequent maximum specific and selective rebinding to the template of interest. Much further work needs to be performed to ascertain the individual contribution of each identified interaction towards complex formation. In essence, this requires more empirical measurements which modelling software can take into account during simulations. It is too early a stage in the development of molecular modelling to state that modelling and computational approaches can predict optimum conditions for maximum MIP rebinding efficiency. However, it can be concluded that in this thesis, modelling is in general agreement with the empirical data, which augers well for its development as a tool in the predictive approach the development of biomimetic receptors based on molecular imprinting technology.

Bibliography

[1] Kempe, M., Mosbach, K., J. Chromatogr. A. (1995) 694, 3

[2] Vidyasankar, S., Arnold, F., Curr. Opin. Biotech. (1995) 6, 218

[3] Andersson, L., J. Chromatogr. B. (2000) 745, 1

[4] Nicholls, I., Ramström, O., Mosback, K., J. Chromatogr. A., (1995) 691, 349

[5] Ferrer, I., Barcelo, D., TrAC, (1999) 18, 180

[6] Sergeyeva, T.A., Piletsky, S.A. Brovko, A.A., Slinchenko, E.A., Sergeeva, L.M., El'skaya, A.V. Anal. Chim. Acta (1999) 392, 105

[7] Yu, C., Mosbach, K., J. Chromatogr. A (2000) 888, 63

[8] Karlsson, J.G, Andersson, L.I., Nicholls, I.A., Anal. Chim. Acta (2001) 435, 57

[9] Rathbone, D.L., Adv. Drug Del. Rev. (2005) 57, 1854

[10] Van Nostrum, C.F., Drug Discovery Today: Technologies (2005) 2, 119

[11] Ramström, O., Mosbach, K., Curr. Opin. Chem. Biol. (1999) 3, 759

[12] O'Mahony, J., Nolan, K., Smyth. M.R., Mizaikoff, B., Anal. Chim. Acta (2005) 534, 31

[13] Baggiani, C., Giovannoli, C., Anfossi, L., Tozzi, C., J. Chromatogr. A., (2001) 938, 35

[14] Urraca J.L, Marazuela, M.D., Merino, E.R., Orellana, G., Moreno-Bondi, M.C., J. Chromatogr. A., (2006) 1116, 127

[15] Kochkodan, V., Weigel, W., Ulbricht, M., Desalination (2002) 149, 323

[16] Caro, E., Masqué, N., Marcé, R.M., Borrull, F., Cormack, P.A.G., Sherrington, D.C., J. Chromatogr. A (2002) 163, 969

[17] Taranekar, P., Huang, C., Advincula, R.C., Polymer (2006) 47, 6485

[18] Mayes, A.G. Mosbach, K., TrAC, (1997) 16, 321

[19] Tóth, B, Pap, T., Horvath, V., Horvai, G., Anal. Chim. Acta, 2007, in press

[20] Cormack, P.A.G., Zurutuza Elorza, A., J. Chromatogr. B (2004) 804, 173

[21] Kugimiya, A., Takei, H., Anal. Chim. Acta (2006) 564, 179

[22] Schmidt, R.H., Belmont, A-S., Haupt, K., Anal. Chim. Acta (2005) 542, 118

[23] O'Mahony, J., Molinelli, A., Nolan, K., Smyth, M.R. Mizaikoff, B., Biosens. Bioelectron. (2005) 20, 1884

[24] Sellergren, B., Shea, K.J., J. Chromatogr. A (1993) 654, 17

[25] Zhu, X., Yan, J., Su, Q., Cai, J., Gao, Y., J. Chromatogr. A (2005) 1092, 161

[26] Takeuchi, T., Minato, Y., Takase, M., Shinmori, H., Tetrahedron Letters (2005) 46, 9025

[27] Tanabe, K., Takeuchu, T., Matsui, J., Ikebukuro, K., Yano, K., karube, I., J. Chem. Soc. Chem. Commun., (1995) 2303

[28] Spivak. D., Shea, K.J., J. Org. Chem. (1999) 64, 4627

[29] Steinke, J.H.G., Dunkin, I.R., Sherrington, D.C., Trends Anal. Chem. (1999) 18, 159

[30] De Benedetto, G., Malitesta, C., Palmisano, F., Giorgio Zambonin, P., Anal. Chim. Acta (1999) 389, 197

[31] Sree, U., Yamamoto, Y., Deore, B., Shiigi, H., Nagaoka, T., Synthetic Metals (2002) 131, 161

[32] Olwill, A., Hughes, H., O'Riordain, M., McLoughlin, P., Biosens. Bioelectron. (2004) 35, 688

[33] Corton, E., García-Calzón, J.A., Díaz-García, M.E., Journal of Non-Crystalline Solids (2007) 353, 974

[34] Hu, X., Hu, Y, Li, G., J. Chromatogr. A (2007) 1147, 1

[35] Lin, J.M., Nakagama, T., Uchiyama, K., Hobo, T., J. Pharm.Biomed. Anal. (1997) 15, 1351

[36] Theodoridis, G., Konsta, G., Bagia, C., J. Chrmatogr. B (2004) 804, 43

[37] Allender, C.J., Brain, K.R., Ballatore, C., Cahard, D., Siddiqui, A., McGuigan, C., Anal. Chim. Acta (2001) 435, 107

[38] Dong, H., Tong, A., Li, L., Spectrochimica Acta Part A: Molecular and Biomolecular Spectroscopy (2003) 59, 279

[39] Parmpi, P., Kofinas, P., Anal. Chim. Acta (2004) 25, 1969

[40] Rachkov, A., Minoura, N., J. Chromatogr. A (2000) 889, 111

[41] Bossi, A, Bonini, F., Turner, A.P.F., Piletsky, S.A., Biosens. Bioelectron. (2007) 22, 1131

[42] Alexander, C., Vulfson, E.N., Adv. Mat., (1997) 9, 751

[43] Dickert, F.L., Hayden, O., Anal. Chem. (2002) 74, 1302

[44] Karim, K., Breton, F., Rouillon, R., Piletska, E.V., Gurreiro, A., Chianella, I., Piletsky, S.A., Adv. Drug. Del. Rev. (2005) 57, 1795

[45] Guyot, A., Synthesis and structure of polymer supports. In: D.C. Sherrington and P. Hodge, Editors, *Syntheses and Separations Using Functional Polymers*, Wiley, Chichester (1988), pp. 1–42.

[46] Mayes, A.G., Whitcombe, M.J., Adv. Drug. Del. Rev., (2005) 57, 1742

[47] Andersson, L.I., J. Chromatogr. B (2000) 887, 3

[48] Tamayo, F.G., Casillas, J.L., Martin-Esteban, A., Anal. Chim. Acta (2003) 482, 165

[49] Sambe, H., Hoshina, K., Moaddel, R., Wainer, I.W., Haginaka, J., J. Chromatogr. A (2006) 1134, 88

[50] Ye, L., Cormack, P.A.G., Mosbach, K., Anal. Chim. Acta (2001) 435, 187

[51] Zeng, F., Zimmerman, S.C., Kolotuchin, S.V., Reichert, D.E.C., Ma, Y., Tetrahedron (2002) 58, 2002

[52] Zimmerman, S.C., Wendland, M.S., Rakow, N.A., Zharov, I., Suslick, K.S., Nature (2002) 418, 399

[53] Mayes, A.G., Mosbach., K., Trends in Analytical Chemistry (1997) 16, 321

[54] Bruggemann, O., Haupt, K., Ye, L., Yilmaz, E., Mosbach, K., J. Chromatogr. A (2000) 889, 15

[55] Perez-Morales, N., Whitcombe, M., Vulfson, E., Marcomol. (2001) 34, 830

[56] Haginaka, J., Sakai, Y., J. Pharm. Biomed. Anal., (2000) 22, 899

[57] Yoshimatsu, K., Reimhult, K., Krozer, A., Mosbach, K., Sode, K., Ye, L., Anal. Chim. Acta (2004) 587, 112

[58] García-Calzón, J.A., Díaz-García, M.E., Sensors & Actuators B: Chemical (2006) in press

[59] Oral, E., Peppas, N.A., Polymer (2004) 45, 6163

[60] Andersson, H.S., Nicholls, I.A., Bioorganic Chemistry (1997) 25, 203

[61] Lu, Y., Li, C., Liu, X., Huang, W., J. Chromatogr. A (2002) 950, 89

[62] Lei, J.D., Tong, A.J., Spectrochimica Acta Part A: Molecular and Biomolecular Spectroscopy (2005) 61, 1029

[63] Baggiani, C., Anfossi, L., Baravalle, P., Giovannoli, C., Tozzi, C., Anal. Chima. Acta (2005) 531, 199

[64] Spivak, D.A., Simon, R., Campbell, J., Anal. Chim. Acta (2004) 504, 23

[65] Ohkubo, K., Sawakuma, K., Sagawa, T., J. Mol. Cat. A: Chemical (2001) 165, 1 1

[66] Lavignac, N., Brain, K.R., Allender, C.J., Biosens. Bioelectron. (2006) 22, 138

[67] Hwang, C.C., Lee, W.C., J. Chromatogr. A (2002) 962, 69

[68] Diñeiro, Y., Isabel Menéndez, M., Carmen Blanco-López, M., Lobo-Castañón, J., Miranda-Ordieres, A.J., Tuñón-Blanco, P., Biosens. Bioelectron. (2006) 22, 364

[69] Physical Chemistry, Atkins, P.W., VCH: Weinheim, 1996

[70] Supramolecular chemistry; Steed, J.W., atwood, J.L., Wiley & Sons: England, 2000

[71] Perrin, C.L., Nielson, J.B., "Strong hydrogen bonds in chemistry and biology" Annu. Rev. Phys. Chem. 48, 511, (1997)

[72] Nicholls, I.A., Ramström, O., Mosbach, K., J. Chromatogr. A (1995) 691, 349

[73] Liu, Y., Wang, F., Tan, T., Lei, M., Anal. Chim. Acta (2007) 581, 137

[74] Chapuis, F., Pichon, V., Lanza, F., Sellergren, B., Hennion, M-C., J. Chromatogr. A (2003) 999, 23

[75] Janotta, M., Weiss, R., Mizaikoff, B., Bruggemann, O., Ye, L., Mosbach, K., Intern. J. Environ. Anal. Chem., (2001) 80, 75

[76] Jodlbauer, J., Maier, N.M., Linder, W., J. Chromatogr. A (2002) 945, 45

[77] Theodoridis, G., Konsta, C., Bagia, C., J. Chromatogr. B (2004) 804, 43

[78] Haupt, K., Dzgoev, A., Mosbach, K., Anal. Chem. (1998) 70, 628

[79] Sergeyeva, T.A., Brovko, O.O., Piletska, E.V., Piletsky, S.A., Goncharova, L.A., Karabanova, L.V., Sergeyeva, L.M., El'skaya, A.V., Anal. Chim. Acta (2007) 582, 311

[80] Silvestri,, D., Barbani, N., Cristallini, C., Giusti, P., Ciardelli, G., J. Memb. Sci., (2006) 282, 284

[81] Ansell, R.J., J. Chromatogr. B (2004) 804, 151

[82] http://library.thinkquest.org/03/oct/00520/gallery/photos/Bclonalselection.jpg

[83] Legido-Quigley, C., Oxelbark, J., De Lorenzi, E., Zurutuza-Elorza, A., Cormack, P.A.G., Anal. Chim. Acta (2007) in press

[84] Yin, J., Wang, S., Yang, G., Yang, G., Chen, Y., J. Chromatogr. B (2006) 844, 142

[85] Svenson, J., Nicholls, I.A., Anal. Chim. Acta (2001) 435, 19

[86] Zhang, Z., Li, H., Liao, H., Nie, L., Yao, S., Sensors and Actuators B: Chemical (2005) 105, 182

[87] Lu, Y., Li, C., Wang, X., Sun, P., Xing, X., J. Chromatogr. B (2004) 804, 53

[88] Joshi, V.P., Kulkarni, M.G., Mashelkar, R.A., Chemical Engineering Science (2000) 55, 1509

[89] Kim, H., Kaczmarski, K., Guiochon, G., Chemical Engineering Science (2006) 61, 5249

[90] Hu, S.G., Li, L., He, X.W., Anal. Chim Acta (2005) 537, 215

[91] Chassaing, C., Stokes, J., Venn, R.F., Lanza, F., Sellergren, B., Holmberg, A., Berggren, C., J. Chromatogr. B (2004) 804, 71

[92] Monolithic materials: Preparation, properties and applications; Svec, F., Ed., Tennikova, T.B., Ed., Deyl, Z., Journal of Chromatography library, 64, Elsevier, Amsterdam, 2003

[93] Viklund, C., ponten, E., Glad, B., Irgum, K., Horstedt, P, Svec, F., Chem. Mater. (1997) 9, 463

[94] Chianella, I., Karim, K., Piletska, E.V., Preston, C., Piletsky, S.A., Anal. Chim. Acta (2006) 559, 73

[95] Syu, M.J., Nian, Y.M., Chang, Y.S., Lin, X.Z., Shiesh, S.C., Chou, T.C., J. Chromatrgr. A (2006) 1122, 54

[96] Suedee, R., Seechamnanturakit, V., Canyuk, B., Ovatlarnporn, C., Martin, G.P., J. Chromatogr. A (2006) 1114, 239

[97] Nicholls, I.A., Adbo, K., Andersson, H.S., Andersson, P.O., Ankarloo, J., Hedin-Dahlström, J., Jokela, P., Karlsson, J.G., Olofsson, L., Rosengren, J., Shoravi, S., Svenson, J., Wikman, S., Anal. Chim. Acta (2001) 435, 9

[98] Carabias-Martínez, R., Rodríguez-Gonzalo, E., Herrero-Hernández, E., Anal. Chim. Acta (2006) 559, 186

[99] Batra, D., Shea, K.J. Cur. Opin. Chem. Biol. (2003) 7, 434

[100] Lanza, F., Hall., A.J., Sellergren, B., Bereczki, A., Horvai., G., Bayoudh, S., Cormack, P.A.G., Sherrington, D.C. Anal. Chim. Acta, (2001) 435, 91

[101] Cederfur, J., Pei, Y., Zihui, M., Kempe, M., J. Comb. Chem., (2003) 5, 67

[102] Xu, Z., Liu, L., Deng, Q., J. Pharm. Biomed. Anal., (2006) 41, 701

[103] O'Mahony, J., Molinelli, A., Nolan, K., Smyth, M.R., Mizaikoff, B., Biosens. Bioelectron. (2006) 21, 1383

[104] NMR Spectroscopy. 2nd Ed.; H. Gunther, John Wiley and Sons, Chichester, 1995

[105] Introduction to NMR Spectroscopy; R.J. Abraham, J. Fisher, and P. Loftus, John Wiley & Sons, Chichester, 1988

[106] Idziak, I., Benrebouh, A., Deschamps, F., Anal. Chim. Acta (2001) 435, 137

[107] Ansell, R.J., Kuah, K.L., Analyst (2005) 130, 179

[108] Dong, W., Yan, M., Zhang, M., Liu, Z., Li, Y., Anal. Chim. Acta (2005) 542, 186

[109] Nomachi, M., Kubo, T., Hosoya, K., kaya, K., Anal. Bioanal. Chem. (2006) 384, 1291

[110] Xu, Z., Liu, L., Deng, Q., J. Pharm. Biomed. Anal. (2006) 41, 701

[111] Job, P., Ann. Chim. (1928) 9, 113

[112] Poe, A., J. Phys. Chem., (1963) 67, 1070

[113] Wu, L., Zhu, K., Zhao, M., Li, Y., Anal. Chim. Acta (2005) 549, 39

[114] Matsui, J., Kubo, H., Takeuchi, T., Anal. Chem., (2000) 72, 3286

[115] Wulff, G., Knorr, K., Bioseparation (2002) 10, 257

[116] Lancelot, J., J. Am. Chem. Soc., (1977) 99, 7037

[117] Hawley, J., Bampos, N., Aboitiz, N., Jiminez-Barbero, J., Lopez de la Paz, M., Sanders, J.K.M., Carmona, P., Vicent, C., Eur. J. Org. Chem. (2002) 1925

[118] Jie, Z., Xiwen, H., Anal. Chim. Acta (1999) 381, 85

[119] Whitcombe, M., Martin, L., Vulfson, E.N. Chromatographia (1998) 47, 457

[120] Lu, Y., Li, C., Zhang, H, Liu, X., Anal. Chim. Acta (2003) 489, 3

[121] Svenson, J., Andersson, H.S., Piletsky, S.A., Nicholls, I.A., J. Mole. Recognition. (1998) 11, 83

[122] Liu, Y., Liu, X., Wang, J., Anal. Lett. (2003) 36, 1631

[123] Piletsky, S.A., Andersson, H.S., Nicholls, I.A., J. Mol. Recognit. (1998) 11, 94

[124] Piletsky, S.A., Andersson, H.S., Nicholls, I.A., Macromolecules (1999) 32, 633

[126] Chen, H., Weiner, W.S., Hamilton, A.D., Cur. Opin. Chem. Biol., (1997) 4, 458

[128] Haginaka, J., Tabo, H., Ichitani, M., Takihara, T., Sugimot, A., Sambe, H., J. Chromatogr. A (2006) in press

[129] Piletsky, S.A., Karim, K., Piletska, E.V., Day, C.J., Freebairn, K.W., Legge, C., Turner, A.P.F., Anal. Chem. (2002) 74, 1288

[130]http://www.tripos.com/index.php?family=modules,SimplePage,comp_informatics

[131] Chianella, I., Karim. K., Piletska, E.V., Preston, C., Piletsky, S.A., Takeuchi, T., Dobashi, A., Kimura, K., Anal. Chem. (2000) 72, 2418

[132] Monti, S., Cappelli, C., Bronco, S., Giusti, P., Ciardelli, G., Biosens. Bioelectron.(2006) 22, 153

[133] Chen, Y.C., Brazier, J.L., Yan, M., Bargo, P.R., Prahl, S.A., Sensors and Axctuators B : Chemical (2004) 102, 107

[134] Pavel, D., Lagowski, J., Polymer (2005) 46, 7278

[135] Paniagua-Gonzalez, G., Fernandez Hernando, P., Durand Alegría, J.S., Anal. Chim. Acta (2006) 557, 179

[136] Wu, L., Zhu, K., Zhao, M., Li, Y., Anal. Chim. Acta (2005) 549, 39

[137] Wei, S., Jakusch, M., Mizaikoff, B., Anal. Chim. Acta (2006) 578, 50

[138] Bartko, A.P., Dickson, .M., J. Phys. Chem. B (1999) 103, 3053

[139] Shea, K.J., Sasaki, D.Y., J. Am. Chem. Soc., (1991) 113, 4109

[140] Skogsberg, U., Meyer, C., Rehbein, A., Fischer, G., Schauff, S., Welsch, N., Albert, K., Hall, A.J., Sellergren, B., Polymer (2007) 48, 229

[141] Simon, R., Collins, M.E., Spivak, D.A., Anal. Chim. Acta (2007) in press

[142] Ohkubo, K., Sawakuma, K., Sagawa, T., Journal of Molecular Catalysis A: Chemical (2001) 165, 1

[143] John O'Mahony, PhD Thesis. Dublin City University, 2004

[144] Alex Molinelli, PhD Thesis. Georgia Institute of Technology, 2004

[145] Molecular modelling, Principles and applications> Leach, A.R., Pearson education, 2nd edition, 2001

[146] Verlet, L., Physical Review (1967) 165, 201

[147] Rodger, P.M., Mol. Sim., (1989) 3, 263

[148] Hockney, R.W., Methods in computational physics (1970) 9, 136

[149] Bolton, K., Nordholm, S.J., Comput. Phys. (1994) 113, 320

[150] Case, D.A., Pearlman, D.A., Caldwell, J.W., Cheatham, III, T.E., Wang, J., Ross, W.S., Simmerling, C.L., darden, T.A., Merz, K.M., Stanton, R.V., Cheng, A.L., Vincent, J.J., Crowley, M., Tsui, V., Gohlke, H., Radmer, R.J., Duan, Y., Pitera, J., Massova, I., Seibel, G., Singh, U.C., Weiner, P.K., Kollman, P.A., (2002) AMBER 7, University of California, San Francisco

[151] Wang, J., Cieplak, P., Kollman, P.A., J. Comput. Chem. (2000) 21, 1049

[152] Pearlman, D.A., case, D.A., Caldwell, J.W., Ross, W.S., Cheatham, III, T.E., DeBolt, S., Ferguson, D., Siebel, G., Kollman, P., Comp. Phys. Commun. (1995) 91, 1

[153] Jorgensen, W.L., Chandrasekhar, J., Madura, J., Klein, M.L., J. Chem. Phys. (1983) 79, 926

[154] Ewald, P., Annaken der Physik (1921) 64, 253

[155] Liu, X., Yang, J., Wang, L., Yang, X., Lu, L., Wang, X., Materials Science and Engineering A (2000) 289, 241

[156] Tursiloadi, S., Imai, H., Hirashima, H., Journal of Non-Crystalline Solids (2004) 350, 271

[157] Krebs, J.K., Brownstein, J.M., *Journal* of Luminescence (2007) 124, 257

[158] Baklanova, N.I., Zima, T.M., Naimushina, T.M., Kosheev, S.V., Journal of the European Ceramic Society (2004) 24, 2139

[159] Tezuka, T., Tadanaga, K., Tadanaga, A., Tatsumisago, M., Solid State Ionics (2007) in press

[160] Shapiro, L., Marx, S., Mandler, D., Thin Solid Films, (2007) 515, 4624

[161] Tiwari, A., Mishra, A.P., Dhakate, S.R., Khan, R., Shukla, S.K., Mat. Lett., (2007) in press

[162] Øye, G., Glomm, W.R., Vrålstad, T., Volden, S., Magnusson, H., Stöcker, M., Sjöblom, J., Advances in Colloid and Interface Science (2006) 123, 1

[163] http://www.psrc.usm.edu/mauritz/solgel.html

[164] Pauling, L., J. Am. Chem. Soc. (1940) 62, 2643

[165] Dickey, F.H., Proc. Natl. Acad. Sci, (1949) 35, 227

[166] Zhang, Z., Nie, L., Yao, S., Talanta, (2006) 69, 435

[167] Han, D-M., Fan, G-Z., Yan, X-P., J. Chromatogr. A. (2005) 1100, 131.

[168] Marx, S., Liron, Z., Chem. Mater. (2001) 13, 3624.

[169] Leung, M.K.P., Chow, C-F., Lam. M-H., J. Mater. Chem. (2001) 11, 2985.

[170] Fernandez-Gonzalez, A., Badia Laino, R., Diaz Garcia, M-E., Guardia, L., Viale, A., J. Chromatogr. B. (2004) 804, 247

[171] da Costa Silva, R.G., Augusto, F., J. Chromatogr. A. (2006) 1114, 216

[172] Zhang, Z., Long, Y., Nie, L., Yao, S., Biosens. Bioelectron. (2006) 21, 1244.

[173] Zhang, Z., Liao, H., Li, H., Nie, L., Yao, S., Anal. Biochem. 336 (2005) 336, 108.

[174] B. Sellergren, Editor, *Molecularly Imprinted Polymers: Man-Made Mimics of Antibodies and Their Applications in Analytical Chemistry*, Elsevier, Amsterdam (2001).

[175] Cichna-Markl, M., J. Chromatogr. A (2006) 1124, 167

[176] Hunnius, M., Rufiska, A., Maier, W.F., Microporous Mesoporous Mater. (1999) 29, 389.

[177]Cummins, W., Duggan, P., McLoughlin, P., Anal. Chim. Acta, 542 (2005) 542, 52

[178] A. Katz, A., Davis, M.E., Nature, (2000) 403, 286

[179] Kühl, M., Jauch, K., Rauch, J., Engemann, B., Riedelsheimer, C., Schalhorn, A., Wilmanns, W., Eur. J. Cancer (1995) 31, S153

[180] Maria Rubino, F., J. Chromatogr. B (2001) 764, 217

[181] Kempe, M., Mosbach, K., Tetrahedron Lett. (1995) 36, 3564

[182] Hosoya, K., Yoshizako, K., Shirasu, Y., Kimata, K., Araki, T., Tanaka, N., Haginaka, J., J. Chromatogr. A (1996) 728, 139

[183] Mullet, W.M., Lai, E.P.C., J. Pharm. Biomed. Anal., (1999) 21, 835

[184] Baggiani, C., Trotta, F., Giraudi, G., Moraglio, G., Vanni, A., J. Chromatogr. A (1997) 786, 23

[185] Ye, L., Cormack, P.A.G., Mosbach, K., Anal. Chim. Acta (2001) 435, 187

[186] Theodoridis, G., Manesiotis, P., J. Chromatogr. A (2002) 948, 163

[187] Zougagh, M., Ríos, A., Valcárcel, M., Anal. Chim. Acta (2005) 539, 117

[189] Tunc, Y., Hasirci, N., Yesilada, A., Ulubayram, K., Polymer, (2006) 47, 6931

[190] Rückert, B., Kolb, U., Micron, (2005) 36, 247

[191] Liu, X., Ouyang, C., Zhao, R., Shangguan, D., Chen, Y., Liu, G., Anal. Chim Acta (2006) 571, 235

[192] Davies, M.P., De Biasi, V., Perrett, D., Anal. Chim. Acta (2004) 504, 7

[193] Delaunay-Bertoncini, **N.,** Pichon, V., Hennion, M.C., J. Chromatogr. A (2003) 999, 3

[194] Chapuis, F., Pichon, V., Lanza, F., Sellergren, B., Hennion, M.C., J. Chromatogr. B (2004) 804, 93

[195] Stuart, J.J.P., J. Comput. Chem.(1989) 209, 221

[196] Zheng, Y.J., Merz Jr, K.M., J. Comput. Chem. (1992) 13, 1151

[197] Deng, Y., Huang, M.J., Int. J. Quantum Chem.(2004), 100, 746

[198] He, J.F., Zhu, Q.H., Deng, Q.Y., Spectrochimica Acta Part A: Molecular and Biomolecular Spectroscopy (2006) in press

[199] Berggren, C., Bayoudh, S., Sherrington, D., Ensing, K., J. Chromatogr. A (2000) 899 105.

[200] Puoci, F., Garreffa, C., Iemma, F., Muzzalupo, R., Spizzirri, U.G., Picci, N., Food. Chem. (2005) 93, 349

[201] Brüggemann, O., Anal. Chim. Acta (2001), 435, 1

[202] Quaglia, M., Chenon, K., Hall, A.J., De Lorenzi, E., Sellergren, B., J. Am. Chem. Soc., (2001) 123, 2146

[203] Rachkov, A., Minoura, N., Biochimica et Biophysica Acta (BBA) - Protein Structure and Molecular Enzymology (2001) 1544, 455

[204] Chianella, I., Piletsky, S.A., Tothill. I.E., Chen, B., Turner, A.P.F., Biosens. Bioelectron., (2003) 18, 119

[205] Dong, W., Yan, M., Liu, Z., Wu, G., Li, Y., Separation and Purification Technology (2007) 53, 183

[206] Hall, A.J., Achilli, L., Manesiotis, P., Quaglia, M., De Lorenzi, E., Sellergren, B., J. Org. Chem. (2003) 68, 9132

[207] Chow, C.F., Lam, M.H.W., Leung, M.K.P., Anal. Chim. Acta (2002) 21, 17

[208] Le Moullec, S., Truong, Montauban, C., Begos, A., Pichon., Bellier, B., J. Chromatogr. A (2007) 1139, 171

[209] Castell. O.K., Allender, C.J., Barrow, D.A., Biosens. Bioelectron. (2006) 22, 526

[210] Lavine, B.K., Westover, D.J., Kaval, N., Mirjankar, N., Oxenford, L., G.K., Talanta (2007) In press

[211] Carabias-Martínez, R., Rodríguez-Gonzalo., E., Herrero-Hernández, E., J. Chromatogr. A (2005) 1085, 199

[212] Suedee, R., Intakong, W., Dickert, F.L., Talanta (2006) 70, 194

[213] Ramanaviciene, A., Ramanavicius, A., Biosens. Bioelectron. (2004) 20, 1076

[214] Dżygiel, P., O'Donnell, E., Fraier, D., Chassaing, C., Cormack, P.A.G., J. Chromatogr. B (2007) In press

[215] Caro, E., Marce, R.M., Cormack, P.A.G., Sherrington D.C., Borrull, F., J. Chromatogr. B (2004) 813, 137

[216] Haginaka, J., Trends in Analytical Chemistry, (2005) 24, 407

[217] Jiang, X., Tian, W., Zhao, C., Zhang, H., Liu, M., Talanta (2007) 72, 119

[218] Strikovsky, A., Hradil, J., Wulff, G., Reactive and Functional Polymers (2003) 54, 49

[219] Zhang, L., Cheng, G., Fu, C., Reactive and Functional Polymers (2003) 56, 167

[220] Araki, K., Goto, M., Furusaki, S., Anal. Chim. Acta (2002) 469, 17
[221] Belmont, A.S., Jaeger, S., Knopp, D., Niessner, R., Gauglitz, G., Haupt, K., Biosens. Bioelectron. In press, 2007

[222] Erzöz, A., Denizli, A., Şener, İ, Atilir, A., Diltemiz, S., Say, R., Sep. Pur. Technol. (2004) 38, 173

[223] Schirmer, C., Meisel, H., J. Chromatogr. A (2006) 1132, 325

[224] Chapuis, F., Mullot, J.U., Pichon, V., Tuffal, G., Hennion, M.C., J. Chromatogr. A (2006) 1135, 127

[225] Sambe, H., Hoshina, K., Moaddel, R., Wainer, I.W., Haginaka, J., J. Chromatogr. A (2006) 1134, 88

[226] Baggiani, C., Anfossi, L., Baravalle, P., Giovanolli, C., Tozzi, C., J. Chromatogr. A (2005) 531, 199

[227] Zhang, T., Liu, F., Chen, W., Wang, J., Li, K., Anal. Chim. Acta (2001) 450, 53

[228] Turner, N.W., Piletska, E.V., Karim, K., Whitcombe, M., Malecha, M., Magan, N., Baggiani, C., Piletsky, S.A., Biosens. Bioelectron. (2004) 20, 1060

[229] Lübke, C., Lübke, M., Whitcombe, M.J., Vulfson, E.N., Macromolecules (2000) 33, 5098

[230] Maier, N., Buttinger, G., Welhartizki, S., Gavioli, E., Linder, W., J. Chromatogr. B (2004) 804, 103

[231] Haginaka, J., Sanbe, H., Takehira, H., J. Chromatogr. A (1999) 857, 117

[232] Chen, W.Y., Chen, C.S., Lin, F.Y., J. Chromatogr. A (2001) 923, 1

[233] Jorgensen, W.L., Severence, D.L., J. Am. Chem. Soc., (1990) 112, 4768

[234] Joshi, V.P., Karode, S.K., Kulkarni, M.G., Mashelkar, R.A., Chem. Eng. Sci. (1998) 53, 2271

[235] Kim, H., Spivak. D.H., Org. Lett. (2003) 18, 3415

[236] Perlovich, G.L., Kurkov, S.V., Kinchin, A.N., Bauer-Brandl, A., AAPS Pharm. Sci. (2004) 6, Article 3

[237] Weng, C.H., Yeh, W.M., Ho, K.C., Lee, G.B., Sensors and Actuators B: Chemical (2001) 121, 576

[238] Wu, L., Li, Y., Anal. Chim. Acta (2003) 482, 175

[239] Pérez-Moral, N., Mayes, A.G., Anal. Chim. Acta (2004) 504, 15

[240] Hunter, C.A., Saunders, J.K.M., J. Am. Chem. Soc. (1990), 112, 5525
[241] Martin, C.B., Mulla, H.R., Willis, P.G., Cammers-Goodwin, A., J. Org. Chem. (1999) 64, 7802

[242] Sinnokrot, M.O., Sherrill, C.D., J. Am. Chem. Soc. (2004) 126, 7690

[243] Lübke, M., Whitcombe, M.J., Vulfson, E.N., J. Am. Chem. Soc., (1998) 120, 13342

[244] Mayes, A., Farrington, K., Personal Communication (2007)

[245] Alexander, C., Andersson, H.S., Andersson, L.I., Ansell, R.J., Kirsch, N., Nicholls, I.A., O'Mahony, J., Whitcombe, M.J., J. Mol. Recognit. (2006) 19, 106

[246] Mizukami F., Akiyama, Y., Izutsu, H., Supramol. Sci. (1998) 5, 433

[247] Collinson, M.M., Cirt. Rev. Anal. Chem. (1999) 29, 289

[248] Nakanishi, N., Soga, J., J. Non-Cryst. Solids (1992) 139, 1

[249] Wagh, P.B., Begag, R., Pajonk, G.M., Venkasteswara Rao, A., Haranath, D., Mater. Chem. Phys. (1999) 57, 214

[250] Mansur, H.S., Vasconcellos, W.L., Lenza, R.S., Orefice, R.L., Reis, E.F., Lobato, Z.P., J. Non-Cryst. Solids (2000) 273, 109

[251] Malik, A., Hayes, J.D., PCT/USO1/04271, August 16th, 2001

[252] Siouffi, A., J. Chromatogr. A (2003) 1000, 801

[253] Dieudonne, P., Hafidi Alaoui, A., Delord, P., Phalippou, J., J. Non-Cryst. Solids (2000) 162, 155

[254] Brinker, C.J., Keefer, K.D., Schaefer, D.W., Assink, R.A., Kay, B.D., Ashley, C.S., J. Non-Cryst. Solids (1984) 63, 45

[255] Yu, J., Dong, L., Wu, C., Wu, L., Xing, J., J. Chromatogr. A (2002) 978, 37

[256] de Oliveira, A.R.M., de Santana, F.J.M., Sueli Bonato, P., Anal. Chim. Acta (2005) 538, 25

[257] Tan, S.C., Jackson, S.H.D., Swift, G.C., Hutt, A.J., J. Chromatogr. B (1997) 701, 53

[258] Silverstein, R.M., Webster, F.X., Spectrometric identification of organic compounds, sixth edition Wiley, New York, 1997.

[259] da Costa Silva, R.G., Augusto, F., J. Chromatogr. A (2006) 1114, 216

[260] Guardia, L., Badia, R., Diaz-Garcia, M.E., Biosens. Bioelectron. (2006) 21, 1822

[261] Janjikhel, R. K., Moji Adeyeye, C., Pharm. Dev. Technol. (1999) 4, 9

[262] Ling, T.R., Syu, Y.Z., Tasi, Y.C., Chou, T.C., Liu, C.C., Biosens. Bioelectron. (2005) 21, 901

Appendix A

The AMBER 7 package

The AMBER 7 package consists of over 60 programs with the most important (and relevant) described below:

- *Antechamber*: This program suite automates the process of developing force field descriptions for most organic molecules. *Antechamber* generates from the respective pdb files (pdb format) new 'prepin' files with a format that can be read into LEaP for use in molecular modelling. The force filed description that is generated is designed to be compatible with the usual AMBER force fields.
- *Parmchk*: This reads in an 'ac' file or a 'prep' input file as well as a force field file. It writes out a 'frcmod' file for the missing parameters.
- *LEap*: An X windows based program that provides for basic model building and AMBER co-ordinate and parameter/topology input file creation. It includes a molecular editor that allows for building residues and manipulating molecules.
- *Sander*: (Simulated Annealing with NMR Derived Energy Restraints). This is the main program used for molecular dynamics simulations. The program relaxes the structure by iteratively moving the atoms down the energy gradient until a sufficiently low average gradient is obtained. The molecular dynamics portion generates configurations of the system by integrating Newtonian equations of motion. MD will sample more configurative space than minimisation and will allow the structure to cross over small potential energy barriers.
- *Ptraj* and *Carnal*: Programs to analyse MD trajectories, computing (e.g. RMS deviation) from a reference structure, hydrogen bonding analysis, time co-ordination functions, diffusional behaviour etc.

AMBER 7 parameter/topology file formats

The basic files necessary to run Sander are:

- 'prmtop': A description of the molecular topology, force field parameters, periodic box type, atom and residue names.
- 'prmcrd': (or a 'restrt' file from a previous run): a description of the co-ordinates and optionally the velocities and current box dimensions.
- 'mdin': the Sander input file which is a series of namelists and control variables.
- 'mdout': output format, user readable state informationa nd diagnostics
- 'restrt': final co-ordinates, velocity and box dimensions; file used

Preparation of structure files for use in *LEaP* with *Antechamber* and *Parmchk*

AMBER 7 is supplied with applications (*Antechamber and Parmchk*) designed to modify and rectify flaws in imported structural files. The first step in th egeneration of the Naproxen/4-VP system for molecular dynamics simulation was therefore to prepare the input in a suitable format. Having created the 'prepin' input file required by *LEaP* for energy minimisation, the program *Parmchk* was used to investigate whether the 'prepin' file violates the requirements for application of the force field at th enext stage. For this type of application the 'gaff' (general amber force field) was used. *Parmchk* identifies missing parameters in the 'prepin' file and also creates any necessary focefield modifications in an 'frcmod' file.

Solvation and preparation of structural files for use in *Sander*, *xLEap* and *tLEaP*

The structures prepared with *Antechamber* and *Parmchk* were introduced into *LEaP* for visualisation. The *LEaP* program is also necessary to generate two types of file required for the actual minimisation run – a list of Cartesian co-ordinates of all atos in th efile ('prmcrd' file) and a topology file ('prmtop' file). These two files are the only

format accepted by *Sander*, employed in energy minimisation and molecular dynamics.

Energy minimisation

The minimisation steps as well as restraints are written into one text input file, from where *Sander* reads all commands and applies them to the system. *Sander* also reports on the energy state of the system at regular intervals (the frequency of which is determined by the user) by writing an 'mdinfo' file, which tells the user the energy state of the system at the last step recorded. The coordinates of the atoms at each step recorded are output to a coordinate file ('mdcrd'), permitting the user to later examine the movements of the complex during minimisation using MD visualisation programs (such as the *VMD* package). The final coordinates of the system at the end of the run are written to a file called restart file. The trajectory saved as 'md.crd' file and can be viewed with *VMD*, associated with the 'restrt' file as starting frame and contains five frames per ps. However, of greatest interest to the user will be the 'mdout' files created by *Sander* which documents the parameters of interest for the duration of the minimisation run.

Equilibration

In MD simulations, atoms of the molecules and of the surrounding solvent undergo a relaxation that usually lasts for tens or hundreds of picoseconds before the system reaches a stationary state. Thermodynamic properties such as temperature, energy and density are monitored until the values are stable. The initial non-stationary segment of the simulated trajectory is discarded in the calculation of equilibrium properties. Before running long MD runs, the system must be equilibrated using volume, pressure and temperature control to adjust e.g. the solvent to experimental values. For a periodic system, constant pressure is the only way to equilibrate the density if the starting state is not correct. Another potential problem is small gaps at the edges of the box. Every system must be equilibrated first at constant volume to something close to the final temperature before turning on constant pressure (ntb=2, ntp>0) to reach a proper density. The pressure may be maintained at a constant defined value by e.g.

scaling the volume. In AMBER, the system is coupled to an external bath of constant pressure and/or temperature.

Appendix B

Starting configurations (pdb) and 'mdin' input files for MD runs in Sander

- **PDB file of Naproxen/4-VP complex, π-π stacking starting configuration**

```
ATOM   1  O    NAP  1    3.357   1.423   0.000
     1.00 0.00
ATOM   2  H    NAP  1    3.544   1.733   0.950
     1.00 0.00
ATOM   3  C    NAP  1    4.764   0.871  -0.315
     1.00 0.00
ATOM   4  O    NAP  1    4.963   0.424  -1.452
     1.00 0.00
ATOM   5  C    NAP  1    5.851   0.742   0.797
     1.00 0.00
ATOM   7  H    NAP  1    6.066   1.662   1.128
     1.00 0.00
ATOM   8  C    NAP  1    5.465   0.200   1.544
     1.00 0.00
ATOM   9  H    NAP  1    7.109   0.105   0.372
     1.00 0.00
ATOM   10 H    NAP  1    7.234  -1.346   0.448
     1.00 0.00
ATOM   11 H    NAP  1    8.513  -1.907  -0.081
     1.00 0.00
ATOM   12 C    NAP  1    9.733  -3.611  -0.629
     1.00 0.00
ATOM   13 H    NAP  1    8.700  -3.236  -0.128
     1.00 0.00
ATOM   14 C    NAP  1    9.533  -3.611  -0.492
     1.00 0.00
ATOM   15 C    NAP  1    7.625  -4.149   0.367
     1.00 0.00
ATOM   16 H    NAP  1    7.821  -5.842   0.262
     1.00 0.00
ATOM   17 C    NAP  1    6.498  -3.649   0.889
     1.00 0.00
ATOM   18 H    NAP  1    5.792  -4.263   1.243
     1.00 0.00
ATOM   19 C    NAP  1    6.305  -2.196   0.939
     1.00 0.00
ATOM  20  O    NAP  1    5.468  -1.824   1.342
     1.00 0.00
ATOM  21  C    NAP  1    5.031  -1.261   1.639
     1.00 0.00
ATOM   22 H    NAP  1    4.520  -0.849   1.984
     1.00 0.00
```

```
ATOM     23 H    NAP  1     4.009  -0.215   2.600
1.00 0.00
ATOM     24 H    NAP  1     3.520   0.468   2.839
     1.00 0.00
ATOM     25 C    NAP  1     3.287   0.887   3.267
     1.00 0.00
ATOM     26 H    NAP  1     3.755   1.362   2.541
     1.00 0.00
ATOM     27 C    NAP  1     4.029   2.001   1.862
     1.00 0.00
ATOM     28 C    NAP  1     4.508   1.528   2.387
     1.00 0.00
ATOM   29  H    NAP  1     5.681   1.029   2.922
     1.00      0.00
ATOM     30 C    NAP  1     6.012   0.551   3.015
     1.00      0.00
ATOM     31 H    NAP  1     6.328  -0.102   3.213
     1.00 0.00
TER
ATOM     1  C    4VP  2     1.242   1.098  -2.107
     1.00 0.00
ATOM     2  H    4VP  2     0.249   1.005  -2.035
     1.00 0.00
ATOM     3  C    4VP  2     2.019   1.162  -0.965
     1.00 0.00
ATOM     4  H    4VP  2     1.590   1.110  -0.063
     1.00 0.00
ATOM     5  N    4VP  2     3.392   1.289  -1.709
1.00       0.00
ATOM     6  C    4VP  2     3.998   1.358  -2.321
     1.00 0.00
ATOM   7    H    4VP  2     4.990   1.452  -2.394
     1.00 0.00
ATOM     8  C    4VP  2     3.221   1.297  -3.464
     1.00 0.00
ATOM     9  H    4VP  2     3.650   1.346  -4.364
     1.00 0.00
ATOM     10 C    4VP  2     1.847   1.168  -3.352
     1.00 0.00
ATOM     11 C    4VP  2     1.023   1.102  -4.572
     1.00 0.00
ATOM     12 H    4VP  2     1.086   0.378  -5.258
     1.00 0.00
ATOM     13 C    4VP  2     0.112   2.052  -4.824
     1.00 0.00
ATOM     14 H    4VP  2    -0.444   2.003  -5.654
     1.00 0.00
ATOM     15 H    4VP  2    -0.010   2.811  -4.185
     1.00 0.00
```

- **PDB file of Naproxen/4-VP complex, hydrogen bonding starting configuration**

```
ATOM      1  O   NAP  1      2.814   1.259  -0.367  1.00
      0.00
ATOM      2  H   NAP  1      3.267   1.046  -0.678  1.00
      0.00
ATOM      3  C   NAP  1      3.982   1.679  -0.992  1.00
      0.00
ATOM      4  O   NAP  1      4.501   2.019  -0.028  1.00
      0.00
ATOM      5  C   NAP  1      4.019   2.611  -0.225  1.00
      0.00
ATOM      7  H   NAP  1      4.223   2.661  -0.526  1.00
      0.00
ATOM      8  C   NAP  1      4.817   3.021  -0.002  1.00
      0.00
ATOM      9  H   NAP  1      5.021   2.666  -0.418  1.00
      0.00
ATOM     10  H   NAP  1      4.201   2.413  -0.236  1.00
      0.00
ATOM     11  H   NAP  1      4.135   2.039  -0.697  1.00
      0.00
ATOM     12  C   NAP  1      3.789   2.367  -1.258  1.00
      0.00
ATOM     13  H   NAP  1      3.552   2.691  -0.359  1.00
      0.00
ATOM     14  C   NAP  1      3.014   2.228   0.120  1.00
      0.00
ATOM     15  C   NAP  1      2.392   2.039   0.367  1.00
      0.00
ATOM     16  H   NAP  1      2.147   1.264   0.991  1.00
      0.00
ATOM     17  C   NAP  1      2.829   2.001   1.026  1.00
      0.00
ATOM     18  H   NAP  1      2.457   1.060   1.843  1.00
      0.00
ATOM     19  C   NAP  1      2.972   1.469   1.316  1.00
      0.00
ATOM     20  O   NAP  1      3.436   1.991   0.642  1.00
      0.00
ATOM     21  C   NAP  1      3.260   1.243   0.967  1.00
      0.00
ATOM     22  H   NAP  1      3.842   1.846   0.392  1.00
      0.00
ATOM     23  H   NAP  1      4.019   2.231   0.647  1.00
      0.00
ATOM     24  H   NAP  1      4.267   2.684   0.252  1.00
      0.00
```

```
ATOM     25  C    NAP   1      4.657   2.785   0.684   1.00
      0.00
ATOM     26  H    NAP   1      4.575   2.540   0.757   1.00
      0.00
ATOM     27  C    NAP   1      5.039   2.996   1.024   1.00
0.00
ATOM     28  C    NAP   1      5.391   2.105   0.617   1.00
      0.00
ATOM   29   H    NAP   1      5.937   1.209   0.343   1.00
      0.00
ATOM     30  C    NAP   1      5.173   1.369   0.642   1.00
      0.00
ATOM     31  H    NAP   1      4.116   0.842   1.227   1.00
      0.00
TER
ATOM     1   C    4VP   2      6.878   6.357   1.229   1.00
      0.00
ATOM     2   H    4VP   2      7.315   6.974   1.943   1.00
      0.00
ATOM     3   C    4VP   2      6.414   4.237   0.374   1.00
      0.00
ATOM     4   H    4VP   2      7.325   4.347   1.468   1.00
      0.00
ATOM     5   N    4VP   2      5.023   4.329   0.871   1.00
      0.00
ATOM     6   C    4VP   2      4.003   4.917  -0.753   1.00
      0.00
ATOM   7     H    4VP   2       3.339   4.647  -1.280   1.00
      0.00
ATOM     8   C    4VP     2 4.456   6.341  -0.973   1.00
      0.00
ATOM     9   H    4VP   2      3.874   6.039  -0.098   1.00
      0.00
ATOM     10  C    4VP   2      5.336   6.709   0.451   1.00
      0.00
ATOM     11  C    4VP   2      5.684   8.337   0.734   1.00
      0.00
ATOM     12  H    4VP   2      5.530   8.104   1.601   1.00
      0.00
ATOM     13  C    4VP   2      6.231   9.674   0.487   1.00
      0.00
ATOM     14  H    4VP   2      6.397   10.781  0.676   1.00
      0.00
ATOM     15  H    4VP   2      7.124   8.746  -0.354   1.00
      0.00
```

- **Ibuprofen 'PREPIN' file for use in *LEaP* and *Parmchk***

```
molecule.res
IBU     INT  0
CORRECT      OMIT DU   BEG
  0.0000
    1  DUMM  DU    M    0   -1   -2      0.000      .0        .0
.00000
    2  DUMM  DU    M    1    0   -1      1.449      .0        .0
.00000
    3  DUMM  DU    M    2    1    0      1.522   111.1        .0
.00000
    4  C10   c3    M    3    2    1      1.540   111.208   180.000  -
0.09207
    5  H11   hc    E    4    3    2      1.090   109.062   -41.301
0.03295
    6  H12   hc    E    4    3    2      1.090   111.463  -162.154
0.03450
    7  H13   hc    E    4    3    2      1.090   108.346    77.549
0.03611
    8  C9    c3    M    4    3    2      1.542     1.804  -147.619  -
0.06398
    9  C11   c3    3    8    4    3      1.543   109.540  -105.178  -
0.09094
   10  H14   hc    E    9    8    4      1.091   109.726   -62.788
0.03251
   11  H15   hc    E    9    8    4      1.090   109.883   176.921
0.04073
   12  H16   hc    E    9    8    4      1.090   109.511    57.240
0.03387
   13  H10   hc    E    8    4    3      1.091   109.031    14.228
0.04926
   14  C8    c3    M    8    4    3      1.544   109.486   133.784  -
0.03753
   15  H8    hc    E   14    8    4      1.090   109.405   -58.631
0.05227
   16  H9    hc    E   14    8    4      1.090   109.690    60.929
0.04889
   17  C2    ca    M   14    8    4      1.514   109.804  -178.360  -
0.06555
   18  C3    ca    B   17   14    8      1.399   120.428  -101.191  -
0.12833
   19  C4    ca    S   18   17   14      1.399   120.278   178.204  -
0.11328
   20  H3    ha    E   19   18   17      1.089   118.743  -179.752
0.13470
   21  H2    ha    E   18   17   14      1.090   119.990    -1.046
0.13382
   22  C1    ca    M   17   14    8      1.399   119.885    77.151  -
0.12971
   23  H1    ha    E   22   17   14      1.090   120.098     1.287
0.13401
   24  C     ca    M   22   17   14      1.399   119.973  -178.166  -
0.10816
   25  H     ha    E   24   22   17      1.091   119.621   179.758
0.13210
   26  C5    ca    M   24   22   17      1.400   120.557     0.143  -
0.08615
```

```
  27  C6     c3     M    26   24   22      1.514    117.906   179.736  -
0.05376
  28  C7     c3     3    27   26   24      1.542    113.418  -171.051  -
0.08979
  29  H5     hc     E    28   27   26      1.091    109.835    56.664
0.04939
  30  H6     hc     E    28   27   26      1.090    110.029   -64.379
0.04951
  31  H7     hc     E    28   27   26      1.091    109.208   176.165
0.05525
  32  H4     hc     E    27   26   24      1.091    108.497   -50.384
0.08442
  33  C12    c      M    27   26   24      1.502    108.727    67.632
0.63498
  34  O1     oh     S    33   27   26      1.344    119.874     4.784  -
0.59772
  35  H17    ho     E    34   33   27      0.980    109.472  -109.040
0.44239
  36  O      o      M    33   27   26      1.203    119.965  -172.149  -
0.55469


LOOP
   C5   C4

IMPROPER
   C8   C3   C2   C1
   C2   C4   C3   H2
   C3   C5   C4   H3
   C2    C   C1   H1
   C1   C5    C    H
   C6   C4   C5    C
   C6    O  C12   O1

DONE
STOP
```

- **Naproxen 'PREPIN' file for use in *LEaP* and *Parmchk***

```
molecule.res
IBU     INT  0
CORRECT     OMIT DU   BEG
  0.0000
   1  DUMM  DU     M    0   -1   -2      0.000      .0        .0
.00000
   2  DUMM  DU     M    1    0   -1      1.449      .0        .0
.00000
   3  DUMM  DU     M    2    1    0      1.522    111.1       .0
.00000
   4  C10   c3     M    3    2    1      1.540    111.208   180.000  -
0.09207
   5  H11   hc     E    4    3    2      1.090    109.062   -41.301
0.03295
   6  H12   hc     E    4    3    2      1.090    111.463  -162.154
0.03450
   7  H13   hc     E    4    3    2      1.090    108.346    77.549
0.03611
```

```
   8  C9     c3    M     4    3    2      1.542     1.804  -147.619  -
0.06398
   9  C11    c3    3     8    4    3      1.543   109.540  -105.178  -
0.09094
  10  H14    hc    E     9    8    4      1.091   109.726   -62.788
0.03251
  11  H15    hc    E     9    8    4      1.090   109.883   176.921
0.04073
  12  H16    hc    E     9    8    4      1.090   109.511    57.240
0.03387
  13  H10    hc    E     8    4    3      1.091   109.031    14.228
0.04926
  14  C8     c3    M     8    4    3      1.544   109.486   133.784  -
0.03753
  15  H8     hc    E    14    8    4      1.090   109.405   -58.631
0.05227
  16  H9     hc    E    14    8    4      1.090   109.690    60.929
0.04889
  17  C2     ca    M    14    8    4      1.514   109.804  -178.360  -
0.06555
  18  C3     ca    B    17   14    8      1.399   120.428  -101.191  -
0.12833
  19  C4     ca    S    18   17   14      1.399   120.278   178.204  -
0.11328
  20  H3     ha    E    19   18   17      1.089   118.743  -179.752
0.13470
  21  H2     ha    E    18   17   14      1.090   119.990    -1.046
0.13382
  22  C1     ca    M    17   14    8      1.399   119.885    77.151  -
0.12971
  23  H1     ha    E    22   17   14      1.090   120.098     1.287
0.13401
  24  C      ca    M    22   17   14      1.399   119.973  -178.166  -
0.10816
  25  H      ha    E    24   22   17      1.091   119.621   179.758
0.13210
  26  C5     ca    M    24   22   17      1.400   120.557     0.143  -
0.08615
  27  C6     c3    M    26   24   22      1.514   117.906   179.736  -
0.05376
  28  C7     c3    3    27   26   24      1.542   113.418  -171.051  -
0.08979
  29  H5     hc    E    28   27   26      1.091   109.835    56.664
0.04939
  30  H6     hc    E    28   27   26      1.090   110.029   -64.379
0.04951
  31  H7     hc    E    28   27   26      1.091   109.208   176.165
0.05525
  32  H4     hc    E    27   26   24      1.091   108.497   -50.384
0.08442
  33  C12    c     M    27   26   24      1.502   108.727    67.632
0.63498
  34  O1     oh    S    33   27   26      1.344   119.874     4.784  -
0.59772
  35  H17    ho    E    34   33   27      0.980   109.472  -109.040
0.44239
  36  O      o     M    33   27   26      1.203   119.965  -172.149  -
0.55469


LOOP
```

```
   C5    C4

IMPROPER
   C8    C3    C2    C1
   C2    C4    C3    H2
   C3    C5    C4    H3
   C2     C    C1    H1
   C1    C5     C     H
   C6    C4    C5     C
   C6     O   C12    O1

DONE
STOP
```

- **4-vinylpyridine 'PREPIN' file for use in *LEaP* and *Parmchk***

```
molecule.res
4VP     INT  0
CORRECT      OMIT DU   BEG
  0.0000
    1  DUMM  DU     M     0   -1   -2      0.000      .0        .0
.00000
    2  DUMM  DU     M     1    0   -1      1.449      .0        .0
.00000
    3  DUMM  DU     M     2    1    0      1.522    111.1       .0
.00000
    4  C8    c2     M     3    2    1      1.540   111.208   180.000  -
0.19127
    5  H14   ha     E     4    3    2      1.111   100.111  -177.012
0.11810
    6  H15   ha     E     4    3    2      1.108    22.508    31.705
0.11513
    7  C7    ce     M     4    3    2      1.343   138.656   -12.767  -
0.12450
    8  H13   ha     E     7    4    3      1.111   118.782  -162.175
0.12714
    9  C1    ca     M     7    4    3      1.485   122.304    18.169  -
0.01667
   10  C2    ca     M     9    7    4      1.389   121.706    -6.806  -
0.23875
   11  H9    ha     E    10    9    7      1.110   120.632    -0.319
0.14276
   12  C6    ca     M    10    9    7      1.383   119.857   179.642
0.39296
   13  H12   h4     E    12   10    9      1.111   120.092  -179.965
0.02158
   14  N5    nb     M    12   10    9      1.383   119.794     0.150  -
0.66375
   15  C4    ca     M    14   12   10      1.384   120.579    -0.081
0.39211
   16  H11   h4     E    15   14   12      1.111   120.194  -179.951
0.02176
   17  C3    ca     M    15   14   12      1.383   119.626     0.081  -
0.23930
   18  H10   ha     E    17   15   14      1.112   119.909   179.978
0.14269


LOOP
```

```
   C3   C1

IMPROPER
   C7  H14   C8  H15
   C8   C1   C7  H13
   C3   C2   C1   C7
   C6   C1   C2   H9
   C2  H12   C6   N5
   C3  H11   C4   N5
   C4   C1   C3  H10

DONE
STOP
```

- **Energy minimisation, no restraints**

```
minimisation
&cntrl
   imin=1,
   ntc=1, ntb=1,
   maxcyc=500, npr=25,
& end
```

- **Energy minimisation, restraints e.g. DMF or methanol or chloroform restrained**

```
minimisation
 &cntrl
    imin=1,
    ntr=1,
    ntc=1,
    ntb=1,
    maxcyc=500, ntpr=25,
&end
group input for restrained DMF atoms
100.0
DMFBOX 10
END
END
DISANG=RST.dist
```

- **Energy minimisation, restraints, e.g. complex**

```
minimisation
 &cntrl
    imin=1,
    ntr=1,
    ntc=1,
    ntb=1,
    maxcyc=500, ntpr=25,
&end
group input for restrained complexdmf atoms
100.0
RES 1 45
END
END
IBU 1
4VP 2
```

- **Distance restraint for energy minimisation/MD equilibration**

```
#
#    1 IBU C13      2 4VP N4       3.5
  &rst
     ixpk= 0,  nxpk= 0,  iat= 18,   24,    r1= 1.30,
     r2= 1.80, r3= 3.00, r4=3.50,
          rk2= 20.0,     rk3= 20.0,     ir6= 1,   ialtd=
0,
&end
```

- **mdin for energy minimisation no restraint**

```
minimisation run
 &cntrl
    imin=1,
    ntb=1,
    ntc=1,
    maxcyc=500, ntpr=25,
&end
DISANG=RST.dist
```

- **Equilibration of the system pre-MD run, constant volume**

```
MD run
&cntrl
imin=0,
nmropt=1,
ntx=1,
iwrap=1,irest=0,
tempi=0,
temp0=300,
tautp=0.2,
ntt=1,
ntb=1,
ntp=0,
ntslim=5000,
ntwe=100,
ntwx=100,
ntpr=25,
&end
&wt
   type='REST',
   istep1=1,
   istep2=5000,
   value1=1
   value2=2
&end
&wt type 'END'    &end
LISTIN=POUT
```

```
LISTOUT=POUTDISANG=RST.dist
```

- **Equilibration of the system pre-MD run, constant pressure**

```
MD run
&cntrl
imin=0,
nmropt=1,
ntx=7,
iwrap=1,irest=0,
temp0=300,
tautp=0.2,
ntt=1,
ntb=2,
ntp=1, tautp=0.05,
ntc=2, ntf=2,
ntslim=250000,
ntwe=100,
ntwx=100,
ntpr=50,
&end
&wt
   type='REST',
   istep1=1,
   istep2=5000,
   value1=1
   value2=2
&end
```

NOTE:1

For cP2 and cP3 'taup' was changed to 0.5 an 5 respectively. After energy minimisation, cV1, cP1, cP2 and cP3, a long equilibration run cP4 was performed. The runs cV1, cP1, cP2 and cP3 were performed with 50000 steps. For cP4, 'taup@ was changed t 1 and 'ntslim' to the required run time e.g. 250000 steps (250ps with 0.001 ps per step)

- **Equilibration run with distance restraint**

```
MD run
&cntrl
imin=0,nmropt=1,
ntx=7, iwrap=1,
irest=1, temp0=300,
tautp=0.2,ntt=1,
```

```
ntb=2, ntp=1,taup=0.05,
ntc=2, ntf=2,
ntslim=250000,
ntwe=100, ntxw=100, ntpr=25,
&end
&wt
type='REST'
istep1=1
istep2=5000,
value1=1,
value2=1,
&end
&wt type='END' %& end
LISTIN=POUT
LISTOUT=POUT
DISANG=RST.dist
```

Note 2:

The file 'RST.dist' has to be defined with the 'mdin' file

Distance restraint between the Ibuprofen aromatic ring and the 4-VP ring (atoms of a ring defined as a group)

```
& rst
&rst
     ixpk= 0,  nxpk= 0,  iat= 18,    24,     r1= 1.30,
     r2= 1.80, r3= 3.00, r4=3.50,
          rk2= 20.0,     rk3= 20.0,     ir6= 1,    ialtd=
0,
&end
&rst
  iat=0,0,0,0
&end
```

Note: 3

'Make DIST_RST' gives the default value of 20.0 kcal/mol.A for rk2 and rk3 (if rk2=0 kcal/mol.A, there will be no lower bond between two atoms. This is reasonable with molecular mechanics refinement because the van der Waals parameters in the force field will not allow two non-bonded atoms to get closer than they should be). In the command line IAT(1) to IAT(4) are the atoms defining the restraint. If IAT (3) $\leq$ 0, it is a distance restraint. If IAT(4) $\leq$ 0, it is an angle restraint. Otherwise it is a torsional restraint. If a distance restraint is chosen, and IAT(1) < 0, then a group of

atoms is defined as well, and the co-ordinate averaged position of this group will be used in place of the co-ordinates of atom 1 [(IAT 1)]. Similarly if IAT (2) < 0, a group of atoms will be defined below whose co-ordinate averaged position will be used in place of the co-ordinates for atom 2 [(IAT 2)].

Appendix C

List of publications arising from this thesis

I. Peer reviewed articles

1. **Predicting the performance of molecularly imprinted polymers: Selective extraction of caffeine by molecularly imprinted solid phase extraction**
   Analytica Chimica Acta, Volume 566, Issue 1, 27 April 2006, Pages 60-68
   Keith Farrington, Edmond Magner and Fiona Regan

2. **Investigation of the nature of MIP recognition: The development and characterisation of a MIP for Ibuprofen**
   Biosensors and Bioelectronics, Volume 22, Issue 6, 15 January 2007, Pages 1138-1146
   Keith Farrington and Fiona Regan

3. **A molecularly imprinted sol gel for ibuprofen: An analytical study of the factors influencing selectivity**
   Keith Farrington and Fiona Regan
   Article in preparation

4. **Optimising selectivity in MIPs – molecular dynamics simulations and the preparation of uniform beads based on liquid fluorocarbon suspension**
   Keith Farrington, Andrew Mayes, Boriz Mizaikoff and Fiona Regan
   Article in preparation

II Oral presentations

1. **Graduate student symposium on molecular imprinting**
   INFU, University of Dortmund,
   December 2-5, 2004

2. **Royal Society of Chemistry, Analytical Research Forum, 2005**
   University of Plymouth, England
   June 14-16, 2005

3. **Advanced Polymeric Materials**
   Polymer Institute of the Slovak Academy of Sciences
   Slovak Chemical Society
   Bratislava, Slovakia,
   June 11-15, 2006

4. **MIP 2006**
   Cardiff University,
   Cardiff, Wales,
   10-14 September 2006

III Poster presentations

1. **Royal Society of Chemistry, Analytical Research Forum,**
   University of Preston, England
   June 14-16, 2006

2. **Second World Congress on Synthetic Receptors,**
   Salzburg, Austria,
   September 2005